CORA Cork Open Research Archive
Cartlann Taighde Oscailte Chorcaí

Title	Drug dissolution from mesoporous silica systems
Authors	McCarthy, Carol A.
Publication date	2018
Original Citation	McCarthy, C. A. 2018. Drug dissolution from mesoporous silica systems. PhD Thesis, University College Cork.
Type of publication	Doctoral thesis
Rights	© 2018, Carol A. McCarthy. - http://creativecommons.org/licenses/by-nc-nd/3.0/
Download date	2026-11-01 07:00:34
Item downloaded from	https://hdl.handle.net/10468/8571



UCC
University College Cork, Ireland
Coláiste na hOllscoile Corcaigh

University College Cork, Ireland
Coláiste na hOllscoile Corcaigh

Drug Dissolution from Mesoporous Silica Systems

Carol McCarthy BPharm MPharm MPSI

A thesis submitted to the National University of Ireland, Cork for the degree of Doctor of Philosophy in the School of Pharmacy

December 2018

Head of School

Prof. Stephen Byrne

Supervisor

Dr. Abina M Crean

Table of Contents

Table of Contents ..... **ii**

Declaration ..... **viii**

List of Tables ..... **ix**

List of Figures ..... **xi**

Glossary ..... **xvii**

Publications ..... **xxi**

Peer-Reviewed Publications xxi

Submitted for Publication in Peer-Reviewed Journals xxi

Presentations ..... **xxii**

Oral Presentations xxii

Poster Presentations xxiii

Abstract ..... **xxv**

Acknowledgements ..... **xxviii**

Chapter 1: Introduction **33**

1.1. Oral Drug Delivery 34

1.1.1. Biopharmaceutical Classification System (BCS) 34

1.2. Drug Dissolution 36

1.2.1. Dissolution Theory 36

1.2.2. Dissolution Process 38

1.2.3. Dissolution Rate 39

1.2.4. Wettability of the Solid Surface during Dissolution 40

1.3. Dissolution Enhancing Formulations 41

1.3.1. Amorphous Drug Formulations 43

1.3.2. Supersaturating Drug Delivery Systems (SDDS) 45

1.4. *In Vitro* Dissolution Experimental Set-Up 46

1.4.1. Sink vs Non-Sink Conditions 47

1.4.2. Dissolution Media 47

1.4.3. Dissolution Apparatus 49

1.4.4. *In Vitro In Vivo In Silico* Relationships 51

1.5. Adsorption at Solid/Liquid Interface 52
1.5.1. Theory of Adsorption at the Solid/Liquid Interface 53
1.5.2. Adsorption Isotherms 54
1.5.2.1. Langmuir Isotherm 55
1.5.2.2. Freundlich Isotherm 56

1.6. Adsorption/Desorption Behaviour of Mesoporous Silica Systems: Current Knowledge 57

1.7. Hypothesis, Aims and Objectives 59
1.7.1. Hypothesis 59
1.7.2. Aim 59
1.7.3. Objectives 59

Chapter 2: Mesoporous Silica Formulation Strategies for Drug Dissolution Enhancement: A Review 62

2.1. Abstract 63

2.2. Introduction 64

2.3. Silica for Drug Delivery (Non-Porous and Porous) 66
2.3.1. Non-Porous Silica 66
2.3.2. Mesoporous Silica 69

2.4. Drug Loading Processes 71
2.4.1. Melt Process 71
2.4.2. Solvent Loading Methods 72
2.4.2.1. Solvent Immersion Processes 72
2.4.2.2. Incipient Wetness Impregnation Process 73
2.4.2.3. Loading using Supercritical Fluid Technology (SCF) 75
2.4.3. Large Scale Drug Loading Techniques 76

2.5. Mesoporous Silica Characteristics Influencing Drug Loading and Release 76
2.5.1. Silica Pore Architecture and Particle Properties 77
2.5.2. Surface Functionalization 80

2.6. Physical and Chemical Stability of Drug Loaded Silica System 83

2.7. Drug release 86
2.7.1. Release Mechanism Studies 86
2.7.2. Role of Supersaturation 91

2.8. Conclusion 93

Chapter 3: Role of Drug Adsorption onto the Silica Surface in Drug Release from Mesoporous Silica Systems 94

3.1 Abstract 95

3.2 Introduction 97
3.3 Materials and Methods 99
3.3.1 Materials 99
3.3.2 Surface Tension Measurements 99
3.3.3 Solubility Measurements 100
3.3.4 Adsorption Studies 100
3.3.5 Preparation of Sulphamethazine Loaded Silica Formulations 102
3.3.6 Drug Content Quantification 102
3.3.7 Dissolution Studies 103
3.3.8 HPLC Analysis of Sulphamethazine and Sodium Dodecyl Sulphate 104
3.3.9 Pore Size Analysis of Mesoporous Silica Systems Before and After Dissolution 105
3.3.10 Statistical Analysis 106
3.4 Results 107
3.4.1 Sulphamethazine (Sz) Loading Efficiency 107
3.4.2 Solubility Studies 107
3.4.3 Adsorption Studies 108
3.4.3.1 Sulphamethazine Adsorption onto Silica in 0.1 M HCl Medium 108
3.4.3.2 SDS Adsorption onto Silica in 0.1 M HCl Medium 111
3.4.3.3 Sulphamethazine Adsorption onto Silica in 0.1 M HCl/SDS Media 113
3.4.4 Dissolution Studies 115
3.4.4.1 Sulphamethazine Loaded Silica Systems in 0.1 M HCl Medium 117
3.4.4.2 Sulphamethazine Loaded Silica Systems in 0.1 M HCl/SDS Media. 119
3.4.5 Porosity Analysis of Recovered SBA-15 Following Dissolution 119
3.4.6 Relating Dissolution Release Profiles to Adsorption Isotherms 120
3.5 Discussion 123
3.6 Conclusions 128

Chapter 4: Drug Release from Mesoporous Silica Systems: The Influence of Dissolution Media Composition 129

4.1 Abstract 130
4.2 Introduction 131
4.3 Materials and Methods 133
4.3.1 Materials 133
4.3.2 Solubility Measurements 133
4.3.3 Surface Tension Measurements 134
4.3.4 Adsorption Studies 135
4.3.5 Preparation of Sulphamethazine Loaded Silica Formulations 135
4.3.6 Drug Content Quantification 136
4.3.7 Dissolution Studies 136
4.3.8 HPLC Analysis of Sulphamethazine 137

4.3.9 UV-Vis Spectroscopy Analysis of Pepsin Adsorption 137
4.3.10 Statistical Analysis 138
4.4 Results 139
4.4.1 Solubility Studies 139
4.4.2 Surface Tension Measurements 140
4.4.3 Sulphamethazine (Sz) Loading Efficiency 141
4.4.4 Adsorption Isotherm 141
4.4.4.1 Simulated Gastric Fluid (SGF) 142
4.4.4.2 FaSSIF-V2 144
4.4.5 Dissolution Studies 146
4.4.5.1 Simulated Gastric Fluid 146
4.4.5.2 FaSSIF-V2 149
4.4.6 Relating Dissolution Release Profiles to Adsorption Isotherms 152
4.5 Discussion 154
4.6 Conclusion 157

Chapter 5: Mechanism of Drug/Silica Interaction and its Influence on Drug Adsorption and Release Under Supersaturating Conditions 158

5.1. Abstract 159
5.2. Introduction 160
5.3. Materials and Methods 163
5.3.1. Materials 163
5.3.2. Crystalline and Amorphous Solubility Measurements 163
5.3.3. Fourier Transform Infrared Spectroscopy (FTIR) 165
5.3.4. Fluorescence Spectroscopy 165
5.3.5. Adsorption Experiments 166
5.3.6. Estimation of IND and INDME Molecular Dimensions 167
5.3.7. Preparation of Drug Loaded SBA-15 Systems 168
5.3.8. X-Ray Powder Diffraction (XRPD) Analysis 169
5.3.9. *In vitro* dissolution experiments 169
5.3.10. High Performance Liquid Chromatography (HPLC) 170
5.3.11. Statistical Analysis 170
5.4. Results 171
5.4.1. Crystalline and Amorphous Solubility 171
5.4.2. Mechanism of Interaction 172
5.4.2.1. FTIR Spectroscopy 172
5.4.2.2. Fluorescence Spectroscopy 174
5.4.3. Adsorption Studies 176
5.4.3.1. Adsorption Isotherms 176
5.4.3.2. Desorption Studies 179
5.4.3.3. Competitive Adsorption 180

5.4.3.4. Influence of Urea on Adsorption 181
5.4.3.5. Influence of Ionic Strength 182
5.4.4. Preparation of Drug Loaded SBA-15 Systems 183
5.4.5. *In Vitro* Release under Supersaturating Conditions 186
5.5. Discussion 191
5.6. Conclusion 200

Chapter 6: *In Vitro* Dissolution Models for the Prediction of *In Vivo* Performance of an Oral Mesoporous Silica Formulation 201

6.1 Abstract 202
6.2 Introduction 204
6.3 Material and Methods 206
6.3.1. Materials 206
6.3.2. Preparation of Fenofibrate Loaded Silica Formulation 206
6.3.3. Drug Content Quantification 207
6.3.4. Solubility Measurements 207
6.3.5. *In Vitro* Dissolution Experiments 208
6.3.6. *In Vivo* Oral Bioavailability Study 209
6.3.7. Quantitative Analysis of Fenofibrate 211
6.3.8. *In Vitro* and *In Vivo* Data Analysis 212
6.3.9. *In Silico* Predictive Modelling 213
6.4 Results 214
6.4.1. Drug Content Quantification 214
6.4.2. Fenofibrate Solubility 214
6.4.3. *In Vitro* Dissolution 214
6.4.3.1. USP Type II (Paddle) Apparatus 214
6.4.3.2. USP Type IV (Flow-Through Cell) Apparatus 219
6.4.3.3. Transfer Model in USP Type IV (Flow-Through Cell) Apparatus 220
6.4.4. *In Vivo* Oral Bioavailability 222
6.4.5. *In Silico* IVIVR Modelling 226
6.5. Discussion 231
6.6 Conclusion 236

Chapter 7: Discussion 237

7.1. Introduction 238
7.2. Interpretation and Implications of Findings 238
7.2.1. Dynamic Equilibrium between Drug Adsorption on Silica and Free Drug in Solution 239
7.2.2. Dissolution Experimental Set-Up for Mesoporous Silica Formulations 241

7.3. Strengths and Limitations 244
7.4. Recommendations for Future Work 247
7.5. Conclusions 249

References 251

Declaration

I declare that the work contained within this thesis has not been previously submitted for a degree at this or any other university. All the work contained within this thesis is entirely my own work, apart from due acknowledgements. I give my permission for the library to lend or copy this thesis upon request.

Signed: _____

Carol McCarthy

List of Tables

Table 1.1 Dissolution enhancing formulations 43

Table 1.2 Linearized forms of Langmuir and Freundlich isotherms.....56

Table 2.1 Characteristics of a selection of porous and non-porous silica materials .68

Table 2.2 Examples of drug incorporated into functionalised mesoporous silica materials.....82

Table 3.1 Properties of silica materials obtained from suppliers 99

Table 3.2 Linearized forms of Langmuir and Freundlich isotherms 101

Table 3.3 Isotherm parameters obtained by fitting Sz and SDS adsorption data (mmol/m^2) onto SBA-15 and Aerosil®200 to Langmuir and Freundlich isotherms (SDS adsorption data only produced an acceptable fit with Freundlich isotherm).....111

Table 3.4 Solubility and dissolution parameters for unprocessed Sz and Sz loaded silica formulations in the three dissolution media investigated.....116

Table 4.1 Composition of Simulated Gastric Fluid (SGF) and Fasted State Simulated Intestinal Fluid Version 2 (FaSSIF-V2) 134

Table 4.2 Surface tension measurements for SGF, FaSSIF-V2 and individual components of both biorelevant media 141

Table 4.3 Cumulative drug dissolution (%) for unprocessed drug and drug-loaded silica formulation at 24 h in SGF, FASSIF and their respective components 149

Table 5.1 Equilibrium and amorphous solubility values for IND and INDME 172

Table 5.2 Ratio of the intensity of the first and third peaks (I_1/I_3) for pyrene in the presence of various additives in McIllvaine buffer pH 2.2 containing HPMC 100 µg/ml at 37 ^oC.....175

Table 5.3 Binding affinity parameters (K_L and K_F) and R^2 values obtained by fitting drug adsorption onto SBA-15 to Langmuir and Freundlich isotherm linear equations 177

Table 5.4 SBA-15 formulations with loaded IND and INDME at specific theoretical monolayer coverage levels 184

Table 5.5 Amount of drug and silica present (mg) and supersaturation ratios (*S*) attained during original dissolution and dissolution of precipitate 190

Table 6.1 Summary of *in vitro* dissolution parameters.....218

Table 6.2 Summary of *in vivo* pig model parameters 223

Table 6.3 Summary of *in vitro/in vivo* relationship parameters. Observed and predicted C_{max} and AUC values and the correlation (R^2) between the observed and predicted plasma profiles generated by the Gastroplus™ IVIVCPlus® software are displayed. 230

List of Figures

Figure 1.1 The Biopharmaceutical Classification Scheme.....35

Figure 1.2 Schematic representation of the dissolution process 37

Figure 1.3 Schematic representation of the dissolution process 38

Figure 1.4 Spreading of a liquid on a solid surface 40

Figure 1.5 Supersaturating drug delivery system profile.....46

Figure 1.6 Schematic of USP II (paddle) apparatus.....50

Figure 1.7 Schematic of USP IV (flow-through cell) apparatus.....51

Figure 1.8 Adsorption at the solid/liquid interface.....53

Figure 1.9 Langmuir Isotherm.....55

Figure 1.10 Freundlich Isotherm 57

Figure 1.11 Graphical thesis outline 61

Figure 2.1 TEM image of SBA-15 mesoporous silica.....70

Figure 2.2 Schematic illustration of potential sites for drug distribution throughout the silica matrix.....88

Figure 2.3 Fenofibrate release profiles from mesoporous silica formulations 89

Figure 3.1 TGA profiles for degradation of (a) sulphamethazine and (b) SBA-15 over a temperature range of 100 – 900 ^{o}C.....102

Figure 3.2 Adsorption isotherms for Sz adsorption 110

Figure 3.3 Adsorption isotherms for SDS adsorption 112

Figure 3.4 Adsorption isotherms for Sz adsorption 114

Figure 3.5 Dissolution profiles of Sz loaded SBA-15 (♦), Aerosil®200 (Δ) and unprocessed Sz (□) in (a) 0.1 M HCl, (b) 0.1 M HCl SDS 10 mM and (c) 0.1 M HCl SDS 50 mM 118

Figure 3.6 (a) Pore size distribution of unprocessed SBA-15 (dashed line with dot) and recovered SBA-15 samples after drug loading and dissolution in 0.1 M HCl (black line), 0.1 M HCl 10 mM SDS (dotted line) and 0.1 M HCl 50 mM SDS (dashed line); (b) recovered SBA samples after drug loading and dissolution in 0.1 M HCl 10 mM SDS (dotted line) and in 0.1 M HCl 50 mM SDS (dashed line) 120

Figure 3.7 Comparison of (a) Sz and (b) SDS bound both predicted (from adsorption isotherm data) and experimentally determined after dissolution in 0.1 M HCl 122

Figure 3.8 Comparison of the actual bound Sz fraction (mmol/m^2 silica) after dissolution in the three media investigated for (a) SBA-15 and (b) Aerosil®200 122

Figure 4.1 Solubility of sulphamethazine in (a) SGF and solutions of its individual components and (b) FaSSIF-V2 and solutions of its individual components (TCA = sodium taurocholate) at 37 ^oC. 140

Figure 4.2 Adsorption isotherms for Sz adsorption (mmol Sz /m^2 silica) onto SBA-15 in dilute HCl (●), NaCl (▲), pepsin (◇) and SGF (■) at 37 ^oC. 143

Figure 4.3 Adsorption isotherms for Sz adsorption (expressed as Log Quantity Adsorbed (mg Sz /m^2 silica)) onto SBA-15 in dilute HCl (●) and pepsin (◇) at 37^oC. The adsorption isotherm for pepsin adsorption (mg pepsin/m^2 silica) onto SBA-15 in dilute HCl (■) (in the absence if Sz) at 37 ^oC is also displayed.....144

Figure 4.4 Adsorption isotherms for Sz adsorption (mmol Sz /m^2 silica) onto SBA-15 in dilute NaOH (●), NaCl (▲), TCA (□) and FaSSIF-V2 (♦) at 37^oC. 145

Figure 4.5 Dissolution profiles of (a) unprocessed Sz and (b) Sz loaded SBA-15 in specific dissolution media ((♦) represents SGF, (●) pepsin, (☐) NaCl and (▲) 0.1 M HCl). 148

Figure 4.6 Dissolution profiles of (a) unprocessed Sz and (b) Sz loaded SBA-15 in specific dissolution media ((♦) represents FaSSIF, (Δ) TCA, (☐) NaCl and (●) dilute NaOH). 151

Figure 4.7 Comparison of % drug adsorbed (mmol/m^2 silica) during adsorption and dissolution studies in components of (a) SGF and (b) FaSSIF-V2 media.....153

Figure 5.1 Molecular structure and estimated molecular dimensions for (a) IND and (b) INDME 168

Figure 5.2 IR spectra of blank SBA-15, IND and INDME ((a) and (b) respectively) amorphous forms and drug loaded SBA-15 systems in the region of 1600 to 1800 cm^{-1} 173

Figure 5.3 Adsorption isotherm of (a) IND and (b) INDME on SBA-15 from McIllvaine buffer pH 2.2 containing HPMC 100 µg/ml at 37 °C. The dashed lines indicate theoretical monolayer coverage of IND and INDME 176

Figure 5.4 Adsorption isotherm of IND (●) and INDME (Δ) in McIllvaine buffer pH 2.2 containing HPMC 100 µg/ml at 37 ^oC based on solute activity in solution 178

Figure 5.5 Desorption of IND and INDME after adsorption onto SBA-15 in McIllvaine buffer pH 2.2 containing HPMC 100 µg/ml at 37 ^oC 179

Figure 5.6 Adsorption of IND and INDME onto SBA-15 during individual isotherm experiments and competitively (with the alternate drug in solution) 180

Figure 5.7 Adsorption data for (a) IND and (b) INDME (at the same activity level) in McIllvaine buffer pH 2.2 containing HPMC 100 µg/ml at 37 °C in the absence and presence of 0.1 M urea 181

Figure 5.8 Adsorption data for (a) IND and (b) INDME at two initial drug concentrations (2 µg/ml and 8 µg/mL) in three media of varying ionic strength: distilled water, 0.1 M NaCl and 0.5 M NaCl containing HPMC 100 µg/ml at 37 °C 182

Figure 5.9 Comparison of % drug loading efficiency for IND and INDME.....185

Figure 5.10 p-XRD diffractograms of (a) IND loaded SBA-15 and (b) INDME loaded SBA-15 at specified loading levels in the range 25 – 150% monolayer coverage ...185

Figure 5.11 Dissolution of (a) IND and (b) INDME loaded SBA-15 systems in McIllvaine buffer (pH 2.2) containing HPMC 100 µg/ml at 37 °C dosed at amorphous solubility levels.....187

Figure 5.12 p-XRD diffractorgrams of (a) IND and (b) INDME formulations before and after dissolution 188

Figure 5.13 Dissolution of recovered precipitate of (a) IND and (b) INDME loaded SBA-15 systems in McIllvaine buffer (pH 2.2) containing HPMC 100 µg/ml at 37 °C dosed at amorphous solubility levels. 189

Figure 6.1 Fenofibrate release profiles for Lipantil Supra® in SGF at 37 °C; (▲) indicates Type IV apparatus, (●) indicates Type II (paddle) apparatus. 216

Figure 6.2 Fenofibrate release profiles from mesoporous silica formulation (■) and Lipantil Supra® (◆) in FaSSIF-V2 media at 37 °C for Type II (paddle) apparatus. ...217

Figure 6.3 Fenofibrate release profiles from mesoporous silica formulation (■) and Lipantil Supra® (◆) in FaSSIF-V2 media at 37 °C for Type IV (flow through cell) apparatus. 220

Figure 6.4 Fenofibrate release profiles from mesoporous silica formulation (■) and Lipantil Supra® (◆) in USP IV Transfer Model at 37 °C (incorporating SGF to FaSSIF-V2 transfer) 221

Figure 6.5 Plasma concentration of fenofibric acid vs. time profiles after oral administration of 67 mg fenofibrate to fasted pigs, (■) indicates mesoporous silica formulation, (◆) indicates Lipantil Supra®, (▲) indicates intravenous preparation 223

Figure 6.6 Extent of release (AUC) and oral bioavailability of fenofibrate from mesoporous silica and Lipantil Supra® formulations. A = extent of release using Type II apparatus, B = extent of release using FaSSIF-V2 media in a Type IV apparatus, C = extent of release using Type IV Transfer model, D = oral bioavailability determined using an *in vivo* pig model. (Graphs show AUC over 240 min for Type II and Type IV, 360 min for Transfer and 24 h for *in vivo* pig model). 225

Figure 6.7 Ratio of extent of release of fenofibrate from the silica formulation vs. the commercial product, Lipantil Supra®, for the *in vitro* dissolution experiments and the *in vivo* pig study. Graphs display ratio of AUC release of silica formulation: Lipantil Supra® over 240 min for Type II and Type IV, 360 min for Transfer and 24 h for *in vivo* pig model). 226

Figure 6.8 Plasma concentration profiles for observed data (designated by the markers – (■) indicates mesoporous silica formulation, (◇) indicates Lipantil Supra®) and predicted plasma concentration-time profiles based on Type IV apparatus ...227

Figure 6.9 Plasma concentration profiles for observed data (designated by the markers – (■) indicates mesoporous silica formulation, ◇) indicates Lipantil Supra®)

and predicted plasma concentration-time profiles based on USP IV Transfer model 228

Glossary

λ_{max}	Lamda Max
%PE	Average Absolute Percentage Error
ANOVA	Analysis of Variance
ASD	Amorphous Solid Dispersion
AUC	Area Under the Curve
B	Concentration of Drug Adsorbed to the Silica Surface
BCS	Biopharmaceutical Classification System
BJH	Barrett Joyner Halenda Adsorption Correlation
BMM	Bimodal Mesoporous Silica
C_b	Concentration in Bulk Solution
C_{max}	Peak Plasma Concentration that a Drug Achieves in a Specified Compartment or Test Area of the Body
CMC	Critical Micellar Concentration
C_s	Saturated Solubility
CO_2	Carbon Dioxide
DAD	Photo Diode Array Detector
DMA	Dimethylacetamide
DMF	Dimethylformamide
DMSO	Dimethylsulfoxide
DSC	Differential Scanning Calorimetry
ELSD	Evaporating Light Scattering Detector
F	Concentration of Free Substrate in Solution
F_{abs}	Absolute Bioavailability
FaSSIF-V2	Fasted State Simulated Intestinal Fluid Version 2
Fb	Fenofibrate

FDA	Food and Drug Administration
FT-IR	Fourier Transform Infrared Spectroscopy
GI	Gastro-intestinal
GIT	Gastro-intestinal Tract
HPMC	Hydroxypropylmethylcellulose
HMPCAS	Hydroxypropylmethylcellulose acetate succinate
HMS	Hollow Mesoporous Spheres
HPLC	High Performance Liquid Chromotography
HPMC	Hydroxypropylmethylcellulose
ICH	International Conference on Harmonisation
IND	Indomethacin
INDME	Indomethacin Methyl Ester
IR	Immediate Release
i.v.	Intravenous
IVIVC	*In Vitro In Vivo* Correlation
IVIVR	*In Vitro In Vivo* Relationship
K_F	Freundlich Binding Affinity Parameter
K_L	Langmuir Binding Affinity Parameter
LLPS	Liquid-Liquid Phase Separation
LP	Large Pore
m	Surface Heterogeneity Index (Freundlich Isotherm)
mM	Millimolar
M	Molar
MCF	Mesoporous Cellular Silica Foam
MCM-41	Mobil Composition of Matter No. 41
NaCl	Sodium Chloride

NaOH	Sodium Hydroxide
NCE	New Chemical Entity
N_t	Number of Binding Sites (Langmuir Equation)
PAA	Polyacrylic Acid
PBPK	Physiologically Based Pharmacokinetic
P_{eff}	Permeability
PEG	Polyethylene Glycol
PVP	Polyvinylpyrrolidone
pXRD	Powder X-Ray Diffraction
S	Supersaturation Ratio
SBA-15	Santa Barbara Amorphous Material
SC-CO_2	Supercritical Carbon Dioxide
SCF	Supercritical Fluid Technology
SD	Standard Deviation
SDDS	Supersaturating Drug Delivery Systems
SDNA	Spray-Dried Nanoadsorbate Technology
SDS	Sodium Dodecyl Sulphate
SEM	Scanning Electron Microscopy
SGF	Simulated Gastric Fluid
SLS	Sodium Lauryl Sulphate
Sz	Sulphamethazine
TCA	Sodium Taurocholate
T_g	Glass Transition Temperature
T_{max}	Time after Administration of a Drug when the Maximum Plasma Concentration is Reached
TEM	Transmission Electron Microscopy
TGA	Thermogravimetric Analysis

IVIVC	*In Vitro/In Vivo* Correlation
IVIVR	*In Vitro/In Vivo* Relationship
USP	United States Pharmacopeia

Publications

Peer-Reviewed Publications

McCarthy CA, Ahern RJ, Devine KJ, Crean AM. Role of Drug Adsorption onto the Silica Surface in Drug Release from Mesoporous Silica Systems. Molecular Pharmaceutics. 2018;15(1):141-9.

doi: https://doi.org/10.1517/17425247.2016.1100165

McCarthy CA, Faisal W, O'Shea JP, Murphy C, Ahern RJ, Ryan KB, Griffin BT, Crean AM. *In vitro* dissolution models for the prediction of *in vivo* performance of an oral mesoporous silica formulation. Journal of Controlled Release. 2017;250:86-95.

doi: https://doi.org/10.1016/j.jconrel.2016.12.043

McCarthy CA, Ahern RJ, Dontireddy R, Ryan KB, Crean AM. Mesoporous silica formulation strategies for drug dissolution enhancement: a review. Expert Opinion on Drug Delivery. 2016;13(1):93-108.

doi: 10.1021/acs.molpharmaceut.7b00778

Submitted for publication in peer-reviewed journals

McCarthy CA, OMahony T, Devine KJ, Crean AM. Drug release from mesoporous silica systems: The influence of dissolution media composition. Submitted to *International Journal of Pharmaceutics, November 2018.*

Presentations

Oral Presentations

McCarthy CA, Crean AM. Factors influencing drug *in vitro* dissolution performance from drug-mesoporous silica systems. SSPC Scientific Advisory Board Meeting, Trinity College Dublin, 7th June 2017.

McCarthy CA, Faisal W, O'Shea JP, Murphy C, Ahern RJ, Ryan KB, Griffin BT, Crean AM. *In vitro* dissolution models for the prediction of *in vivo* performance of an oral mesoporous silica formulation. 39th All Ireland Schools of Pharmacy Conference, University College Cork, 24th – 25th April 2017.

McCarthy CA, Crean AM. Can *in vitro* dissolution models predict *in vivo* performance of mesoporous silica formulations? SSPC Technical Meeting, University College Dublin, 7th September 2016.

McCarthy CA, Crean AM. Investigation of *in vitro* drug dissolution from silica carriers; can we predict drug release using equilibrium adsorption isotherms for porous and non-porous silica systems? SSPC Technical Meeting, University College Cork, 30th March 2016.

McCarthy CA, Crean AM. Investigation of *in vitro* drug dissolution from silica carriers; can we predict drug release using equilibrium adsorption isotherms for porous and non-porous silica systems? 38th All Ireland Schools of Pharmacy Conference, Royal College of Surgeons in Ireland, Dublin, 21st – 22nd March 2016.

McCarthy CA, Crean AM. Outline of Project Aims and Objectives. Face-to-Face P9 Meeting, Trinity College Dublin, 25th August 2015.

Poster Presentations

McCarthy CA, Crean AM, Taylor LS. Mechanism of drug/silica interaction and its influence on drug adsorption and release. SSPC Technical Meeting, University of Limerick, 10th -- 11th October 2018.

McCarthy CA, Ahern RJ, Devine KJ, Crean AM. Role of drug adsorption onto the silica surface in drug release from mesoporous silica systems. SFI Review, University of Limerick, 10th November 2017.

McCarthy CA, Ahern RJ, Devine KJ, Crean AM. Investigation of drug adsorption/desorption behaviour onto the mesoporous silica surface during dissolution; can surfactants influence this process? 44th Annual Meeting & Exposition of the Controlled Release Society, Boston, Massachusetts, USA, 16 – 19th July 2017.

McCarthy CA, Faisal W, O'Shea JP, Murphy C, Ahern RJ, Ryan KB, Griffin BT, Crean AM. *In vitro* dissolution models for the prediction of *in vivo* performance of a mesoporous silica formulation. 8th pan-European Science Conference (EUPAT 8), University College Cork, 3rd – 4th October 2016.

McCarthy CA, Ryan KB, Crean AM. Can equilibrium adsorption isotherms be used as a predictor for *in vitro* drug dissolution from silica carriers? UKICRS Symposium, Cardiff University, Wales, 21st – 22nd April, 2016.

McCarthy CA, Crean AM. Drug adsorption/desorption behaviour onto the silica surface during dissolution; can surfactants influence this process? SSPC Technical Meeting, University College Cork, 11th April 2017.

McCarthy CA, Crean AM. Investigation of drug-silica interactions to increase understanding of drug loading and release from silica materials. SFI Review, University of Limerick, 10th December 2015.

Abstract

Mesoporous silica materials have been investigated as novel formulation aids for oral drug delivery due to their drug solubility enhancing characteristics. However, the mechanism of drug release from these systems is not well understood. Several studies have reported unexplained incomplete release from mesoporous silica carriers. It has been reported, in other research fields, that passive drug adsorption onto the silica surface is possible. However, the implications for this behaviour on drug release from silica systems has not been considered to date. Dissolution studies involving these formulations are generally conducted using Type II dissolution apparatus under sink conditions with traditional simple buffer media. In this thesis, the suitability of this dissolution approach for mesoporous silica systems is considered. The overall aim of this thesis was to investigate factors influencing drug adsorption and release from mesoporous silica systems to enhance understanding of their drug release profiles.

This thesis began with a comprehensive overview of the literature which identified the gaps in knowledge in this area. Based on these findings, the hypothesis, aims and objectives were developed. The four research chapters were each dedicated to factors which could potentially affect drug release; formulation excipients, dissolution medium, drug/silica interactions and dissolution apparatus. The role of drug adsorption on the silica surface was explored across several of the chapters using adsorption isotherms, adsorption models and spectroscopic techniques. Several aspects of dissolution experimental design were investigated including sink and supersaturating conditions, traditional simple buffer media *versus* biorelevant

media and Type II (paddle) apparatus *versus* Type IV (flow-through cell) and a Transfer model (incorporating an SGF to FaSSIF-V2 media transfer). Finally, the results of *in vitro* dissolution studies were compared to *in vivo* performance in a fasting pig model.

The literature review demonstrated the gap in knowledge concerning the mechanism of drug release from mesoporous silica systems. This informed the central themes of the thesis which were explored in four research chapters. In Chapter 3, it was determined that formulation excipients which can reduce surface tension of the dissolution media (e.g. surfactants) can significantly increase drug release from mesoporous silica carriers. Passive drug adsorption and competitive adsorption involving drug and surfactant molecules on the silica surface was also observed. Chapter 4 built on work from the previous chapter and demonstrated that components of biorelevant media that reduced surface tension can also enhance drug release from silica systems. This chapter established that the influence of biorelevant media extends beyond its impact on drug supersaturation promotion and that its use should also be recommended under sink conditions. In Chapter 5, the focus was placed on investigating drug/silica interactions under supersaturating conditions. It was determined these interactions occur through a hydrogen bonding process and not *via* non-specific hydrophobic interactions. It was determined that the dynamic equilibrium which exists between adsorbed and free drug during passive adsorption and dissolution can be related to the drug's activity in solution. Finally, in Chapter 6, it was observed that dissolution experimental design can influence *in vitro* drug release from mesoporous silica systems. It was established that the Type IV

apparatus incorporating an SGF -> FaSSIF-V2 transfer is the best predictor of *in vivo* performance.

The findings of this thesis have made a significant contribution to enhancing knowledge on drug release from mesoporous silica systems. It provides robust recommendations for the design of *in vitro* dissolution studies involving mesoporous silica formulations including choice of dissolution media, drug supersaturation level and dissolution apparatus. Interesting results concerning the influence of drug activity in solution on the equilibrium process observed during drug adsorption and dissolution from mesoporous silica materials were documented. These findings open up interesting new avenues for future research in the field of mesoporous silica carriers for oral drug delivery.

Acknowledgements

The PhD journey is not one that is taken alone. I wish to thank the colleagues, friends and family whose advice, help and encouragement was instrumental in getting me to the finish line.

Firstly, I would like to thank my supervisor, Dr. Abina Crean, for her incomparable support and guidance throughout every step of this process. She was always so generous in sharing her time, advice, knowledge and expertise with me. Her warmth, positivity and interest in her student's development made the PhD journey a very enjoyable one.

I would like to thank the Synthesis and Solid-State Pharmaceutical Centre (SSPC) for providing funding for this research, including my time as a Visiting Scholar in Purdue. I am grateful to Debbie for all her help and patience with the extensive paperwork for my Purdue visit and would like to thank Louise and Sarah for the fun and chats during technical meetings and Ploughing Championships! A special mention must go to Sarah for involving me in so many outreach projects which kept me sane at various stages of the PhD!

Over the last four years, I have had the privilege to work with fantastic colleagues in the School of Pharmacy. I would particularly like to mention Aisha, Kathleen, Eimear, Noreen, Áine, Ken, Tom, Michael, Sonja, Katie, Brendan, Caitriona and Karen. A special mention must go to the technicians – it was during my time in Purdue (where they have no technical support!!) that I realised just how lucky we are to have four outstanding technicians, without whom the PhD would be a struggle for most. Some

of these colleagues have become firm friends whose conversations in the lab or over tea would always brighten my day. Thank you to Tom for your kindness and your readiness to help with every problem, big or small. Thank you to Ken for all the good advice (PhD related and not!) and the fun times in Aseptic labs. Finally, a special thank you to Sonja for your friendship over the last few years. I have such good memories of spending time with you, Dusan and Marko both in Cork and in Banja Luka. Looking forward to plenty more Serbian parties in the future!

I was very lucky to have wonderful colleagues and friends in the Chemistry, Clinical and Pharmaceutics Departments in UCC that made my PhD so enjoyable. In particular, I would like to mention a number of those whose PhD journeys coincided with my own and have now become great friends. To Valeria, for your optimism and enthusiasm; to Raghu, for the PhD pep-talks; to Jamie, for all the laughs in the lab; to Joey, (my SOP neighbour), for your eternal positivity and for the long chats when we should have been working; to Christina, for the fond memories of a great trip to Copenhagen and to Maria for all the chats over cups of tea in Daybreak. There are two people that deserve a special mention. To (Lady) Elena and Elaine (my Twitter buddy), your friendship brightened up my days in the lab and filled them with lots of laughter, fun and so many coffees. You are both fantastic researchers and inspired me every day with your intelligence, work ethic and determination. I will never forget our trip to Boston and Cape Cod – I know there will be many more adventures in the years to come!

I could not have imagined getting through the PhD process without my best friend, Aoife, who has been with me every step of the way. It is wonderful to reflect on all

the lovely memories and good times we shared together over these last four years – the countless dinners and cups of tea, nights out, adventures races, the half-marathon and the many trips and holidays (including one epic adventure in New Zealand!). I will always be forever grateful we undertook this journey together, that we shared the laughter and the tears, the highs and the lows and everything in-between. It wouldn't have been the same without you Aoife!

To all my friends outside of the PhD bubble, for their support and encouragement. I would like to thank everyone in Mayfield Pharmacy where I spent many happy Saturdays over the last four years. To Gwen, Norma, Emma, Emma G, Chloe, Fiona, Robert, Emmett, Shane, Joe and Seamus, thank you for all the fun, cake and great memories. A special thanks to Seamus for your support and friendship, which I am truly grateful for. I would also like to thank Claire, Seamus, Laura, Chailu and Abhijit. To Claire – thank you for the strong friendship which has survived 5 years in Australia, looking forward to seeing you much more often in the years to come.

To the Allen family (Tom, Joan, John, Sarah, Philip, John, James, Eoin and Alanna) – thank you for welcoming a Kerry girl so warmly into your home!

To my own family, thank you so much for everything! To Mom and Dad, I am truly grateful for the constant love, support and encouragement you provide in my life. You have instilled in me the importance and value of education and hard work which has been instrumental in guiding me to this point. This thesis is as much your achievement as my own. To my three amazing sisters, Emma, Shauna and Nicole, thank you so much for all the fun and laughter over the last four years. It has been a

xxx

source of inspiration to me to see you all achieve so much in your own lives during this time, through your own hard work, intelligence and determination.

My final thanks are saved for Evin – meeting you during the PhD means I will always look back on this time in my life with the fondest of memories. Your support and encouragement over the last few years has allowed me to aim higher and reach farther than I would have ever thought possible. I truly appreciate your sense of perspective, your sound advice, intelligence, motivation, kindness and sense of adventure. The last few years are filled with so many great memories and I look forward to many more adventures with you in the future. *'Do not go where the path may lead, go instead where there is no path and make a trail'.*

“All life is an experiment.

The more experiments you make the better.”

Ralph Waldo Emerson

Chapter 1: Introduction

1.1. Oral Drug Delivery

Drug delivery *via* the oral route is the most widely used and patient acceptable dosage form (1). For an orally administered drug to be absorbed into the bloodstream, it must first undergo dissolution in the gastrointestinal tract (2). In 2000, it was reported that the introduction of combinatorial chemistry and high throughput screening had resulted in the properties of new chemical entities shifting towards higher molecular weight and increasing lipophilicity, resulting in decreased aqueous solubility (3, 4). This trend continues in drug discovery today and has become a significant challenge for the pharmaceutical industry as novel formulations are required to deliver these poorly water-soluble drug molecules (5, 6).

1.1.1. Biopharmaceutical Classification System (BCS)

To assist in formulation development, a scientific framework, the Biopharmaceutical Classification System, was developed by Amidon *et al* (Figure 1.1) (7). Under this system, drugs can be categorized into four basic groups according to their solubility properties and their ability to permeate the gastrointestinal mucosa. Physicochemical limitations of the drug as a source of incomplete release from the formulation are recognised. This classification is based on the solubility properties of the drug substance throughout the upper GI tract and is defined as the minimum solubility of a drug across a pH range of 1 to 8 at a temperature of 37 ± 0.5 °C. High-solubility drugs are categorized as those with a ratio of dose to solubility volume that is less than or equal to 250 ml. Permeability (P_{eff}, expressed in units of 10^4 cm per second) is defined as the effective human jejunal wall permeability of a drug. High-

permeability drugs are generally those with an extent of absorption greater than or equal to 90 %. Below this figure, the drug is considered poorly permeable (8).

It was reported in 2002 that more than 40 % of drug candidates discovered using combinatorial chemistry have poor aqueous solubility, a number which has only increased in recent years (5, 9). These BCS Class II and IV drugs pose an industry-wide challenge as a result of their poor dissolution behaviour *in vivo*.

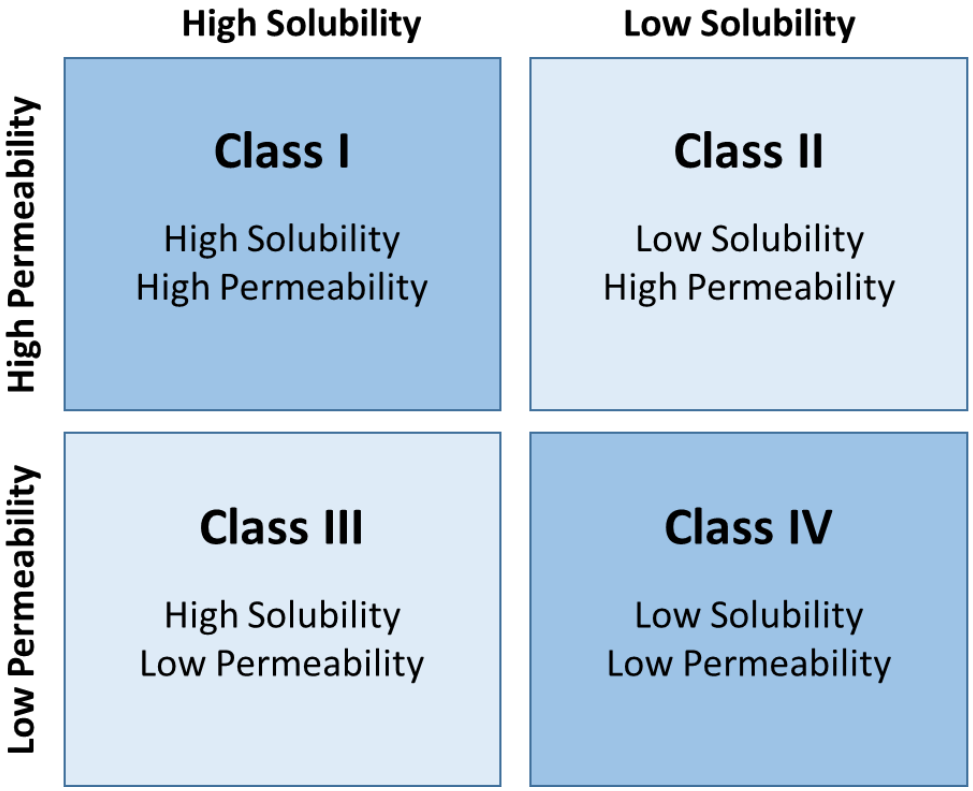


Figure 1.1 The Biopharmaceutical Classification Scheme (adapted from Amidon *et al* (7)).

1.2. Drug Dissolution

Dissolution is the process of a solute dispersing/dissociating in a solvent, forming a molecular-level chemically and physically homogenous dispersion (10). In oral drug delivery, the drug generally exists in a solid phase initially and dissolves in the dissolution medium to transition to a liquid phase (solution). This is an essential step before the drug can be absorbed across the intestinal wall. Absorption from poorly water-soluble drugs, falling into the BCS Class II category, is typically dissolution rate-limited (11).

1.2.1. Dissolution Theory

Dissolution occurs spontaneously when a negative free-energy difference exists between the free energy of the drug molecules in the solid phase (G_{solid}) and the liquid phase (G_{liquid}) (12). Molecules will move from the solid to the liquid phase until the free-energy gradient is eliminated and equilibrium is reached ($G_{solid} = G_{liquid}$). This free-energy difference (ΔG) can be described in Equation 1.1,

$$\Delta G = \Delta H - T\Delta S \qquad Equation\ (1.1)$$

where ΔH and ΔS are the enthalpy and entropy of mixing, respectively. It is dependent on temperature, physicochemical properties of the drug and composition of the dissolution medium (13). Dissolution of a drug molecule from a solid phase to a liquid phase in solution involves three stages (Figure 1.2). Drug particles are wetted by the solvent which results in the breakdown of solid-state bonds. The solvent medium generates a cavity to accommodate the individual drug molecules released. Finally, the drug molecules enters the solvent cavity, resulting in dissolution (14).

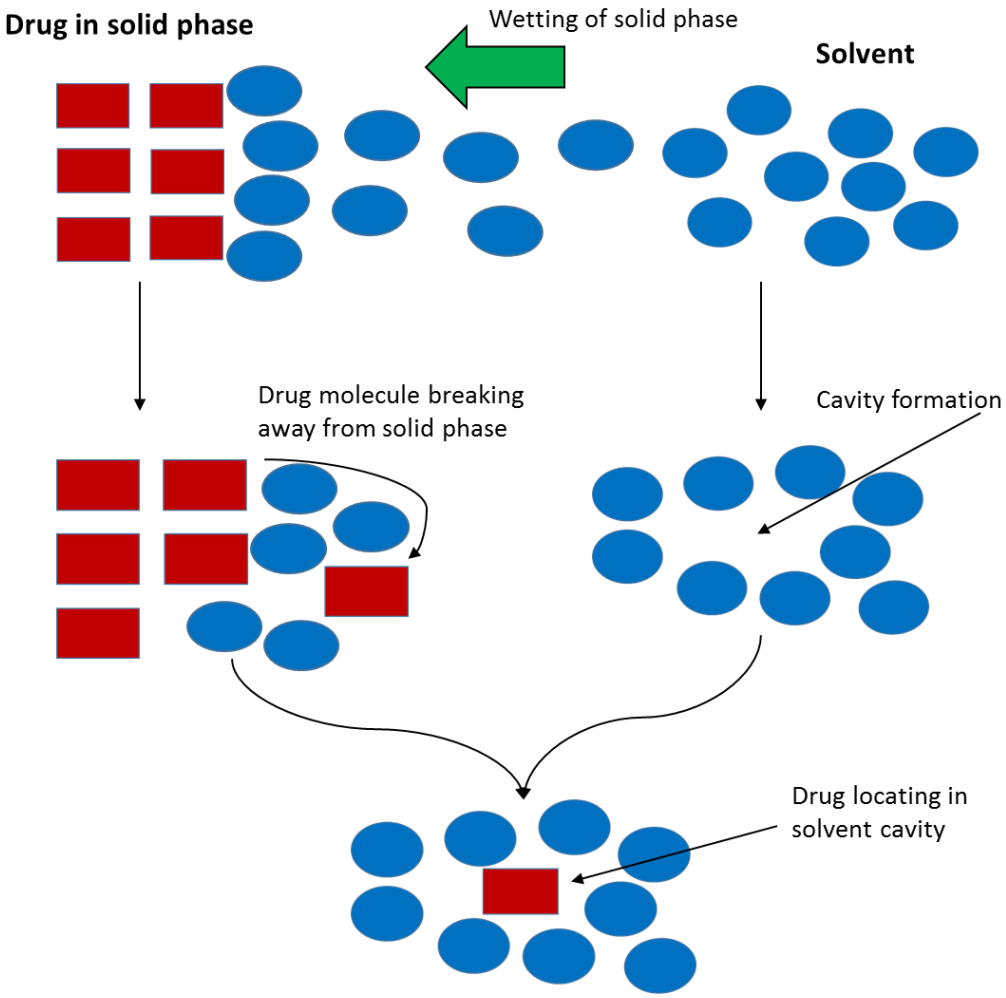


Figure 1.2 Schematic representation of the dissolution process

1.2.2. Dissolution Process

Drug dissolution occurs in a two-step process. The drug molecules first undergo a solid-liquid phase transition in the interfacial region where the drug quickly reaches a saturated concentration (C_s). The concentration gradient which exists between this saturated layer and the bulk solution (C_b) drives the diffusion of the drug molecules into the bulk liquid (2). This diffusion is the second stage of the dissolution process (Figure 1.3). The movement of drug into the bulk solution allows for more drug molecules in the solid phase to undergo phase transition and enter the interfacial region, maintaining its saturated drug concentration (12).

The boundary layer is an area of low flow movement adjacent to the interfacial region existing as a result of adhesional forces between the solute and solvent. Drug molecules must first diffuse through this layer before reaching the bulk solution (12, 15).

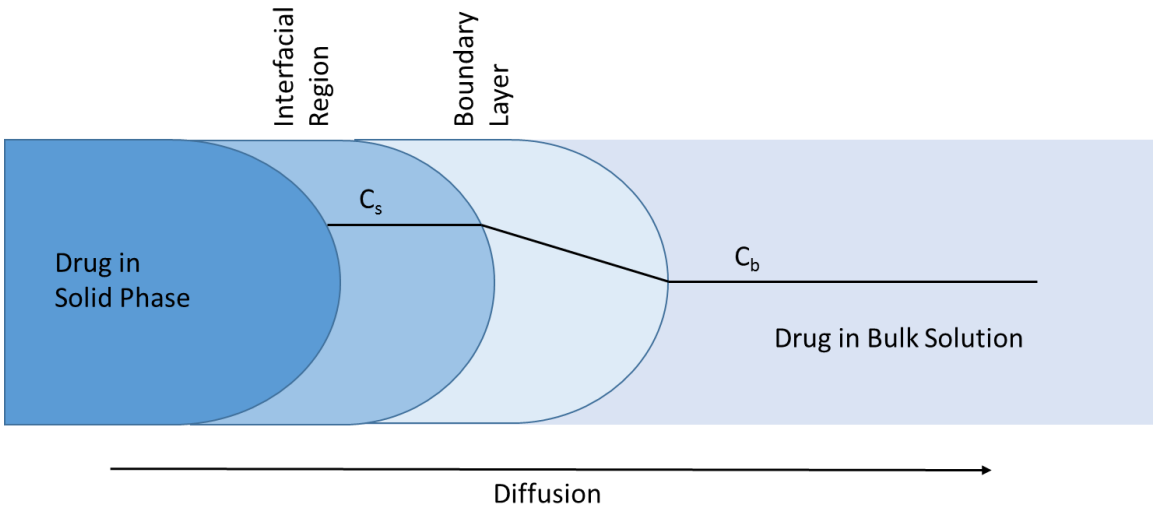


Figure 1.3 Schematic representation of the dissolution process

1.2.3. Dissolution Rate

Dissolution rate is the movement of mass from a solid phase to a liquid phase per unit time (d*m*/d*t*). It can be represented mathematically by the Noyes-Whitney equation (Equation (1.2)) (16)

$$\frac{\mathrm{d}m}{\mathrm{d}t} = -k(C_s - C_b) \qquad Equation\ (1.2)$$

The rate of dissolution is proportional to both the concentration gradient between the interfacial region and the bulk solution in addition to a second factor, the constant *k.*

Nernst and Brunner developed this equation further by incorporating the diffusion layer concept and Fick's second law to derive the Nernst-Brunner equation (Equation (1.3)) (17, 18)

$$\frac{\mathrm{d}C}{dt} = \frac{DS}{Vh}(C_s - C) \qquad Equation\ (1.3)$$

where *D* is the diffusion coefficient, *S* is the surface area of the solid in contact with the dissolution medium, *h* is the thickness of the diffusion layer and *V* is the volume of the dissolution medium.

The thickness of the boundary layer can be influenced by the chemical composition of the drug and the dissolution medium, the temperature of the system and dissolution medium agitation (14, 15). The solid/liquid interfacial surface area can be increased by reducing particle size, increasing particle porosity and increasing the wettability of the surface (2, 19-21).

1.2.4. Wettability of the Solid Surface during Dissolution

The process of wetting the drug's solid surface during drug delivery is a key step in the dissolution process (Section 1.2.2). Wetting of drug particles by the dissolution medium occurs when the surface of the drug solid is covered by liquid on immersion in the dissolution medium. A decrease in the contact angle between the drug surface and liquid medium is observed as the contact area between the two phases increases (Figure 1.4).

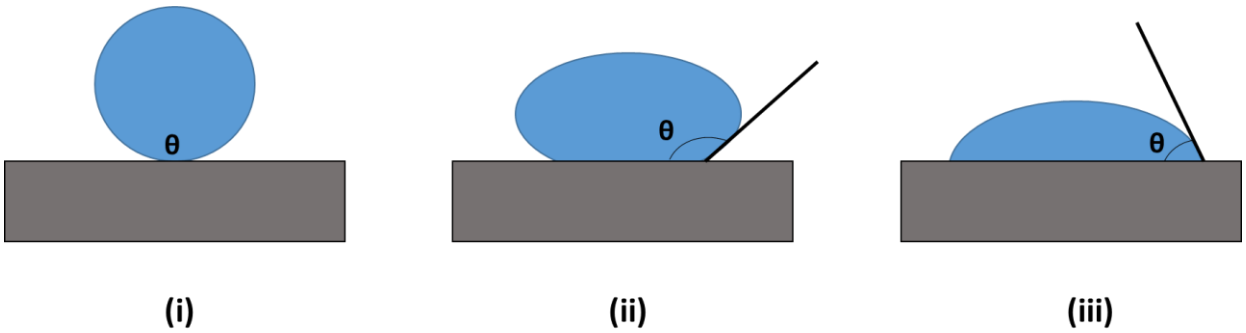


Figure 1.4 Spreading of a liquid on a solid surface

Wettability can be defined as the tendency for a liquid to spread on a solid substrate. It describes the extent of intimate contact between the liquid and solid phases (22). Increasing the wettability of the solid surface can increase drug dissolution rate. Two parameters have a significant influence on the wettability of a liquid on a solid surface – the degree/extent of wetting and the rate of wetting. The degree of wetting is generally indicated by the contact angle formed at the interface between solid and liquid and is dependent on surface and interfacial energies at the solid/liquid interface. The rate of wetting is a measure of how fast the liquid wets the surface

and subsequently spreads over it. This is influenced by a number of factors including temperature, capillary forces, viscosity of the liquid and chemical reactions occurring at the interface (23).

Liquid properties are one of the most significant factors influencing both the extent and rate of wetting. Viscosity, surface tension and density affect spreading of a liquid drop over a solid substrate. Based on Young's equation (24), a lower contact angle or better wetting is expected when the liquid interfacial tension is low. This is most commonly achieved through the addition of surfactants to the dissolution media. High viscosity of the liquid phase can impede surface wetting. It has been reported that a droplet with higher viscosity produces a smaller maximum spread, because the higher viscous dissipation decreases the rate of spread (25). These factors need to be considered when choosing an appropriate dissolution medium for *in vitro* release studies (Section 1.4.2).

1.3.Dissolution Enhancing Formulations

Where solubility or dissolution has been identified as the rate-limiting step for absorption, a strategic decision is usually made to progress the drug candidate via the use of enabling formulations (26). Numerous formulation approaches have been developed to enhance drug dissolution. These can be divided into physical and chemical modifications (27). Chemical modifications encompass the use of soluble pro-drugs and conversion of the compound of interest to a more soluble salt form. These strategies are not preferred as they result in the pharmaceutical company

performing further clinical testing as these products represent NCEs (new chemical entities) (21).

Many approaches have been developed which physically modify the drug. These include particle size reduction, modification of the crystal habit, complexation, solubilisation and the use of drug loading carriers (Table 1.1). This thesis focused on the use of inorganic carriers as drug delivery systems, specifically silica carriers. Drug loaded onto these carriers exists in an amorphous form, thus enhancing dissolution (Section 1.3.1) (28) Both non-porous and mesoporous systems were investigated. These materials are discussed, in detail, in Chapter 2 where a detailed literature review of their use as novel oral drug delivery formulations is presented.

Table 1.1 Dissolution enhancing formulations

PHYSICAL MODIFICATION	
Particle Size Reduction	
Micronization	(20, 29, 30)
Nanosuspensions	(31-33)
Modification of the Crystal Habit	
Polymorphs	(34-36)
Co-Crystals	(37-39)
Complexation/Solubilisation	
Surfactants	(40-42)
Cyclodextrins	(43, 44)
Drug-Loading Carriers	
Lipid-Based Systems	(45-48)
Polymeric Carriers	(49-51)
Inorganic High Surface Area Carriers	
Non-Porous Carriers	(52, 53)
Mesoporous Carriers	(54-56)
CHEMICAL MODIFICATION	
Soluble Prodrugs	(57, 58)
Salts	(59, 60)

1.3.1. Amorphous Drug Formulations

Poorly water-soluble, crystalline drugs exhibit an increase in solubility in their amorphous form (21, 61). One method utilised to generate the amorphous state is to cool melted crystalline drug below its T_g (glass transition temperature), while avoiding crystallization, to the point at which it becomes a supercooled liquid (62). Material in this glassy state behaves like a brittle solid, but without crystalline structure and possessing short-range order. Other approaches to produce the amorphous form include vapor condensation, precipitation from solution (solvent

evaporation, freeze drying and spray drying) and milling (21, 63-65). The amorphous state of a drug has a higher enthalpy, entropy, free energy and volume compared to its crystalline form, resulting in higher apparent drug solubility. Amorphous drug delivery systems are developed to take advantage of the favourable solubility characteristics of the amorphous drug form.

Drug loaded onto polymeric carriers can exist in its amorphous state and these amorphous solid dispersions (ASDs) have been the focus of much research over the last decades (49, 66-68). Examples of commonly used polymers include hydroxypropylmethylcellulose (HPMC), polyvinylpyrrolidone (PVP), polyethylene glycol (PEG) and polyacrylic acid (PAA). Formulations incorporating this approach have proven useful for enhancing drug dissolution (63, 69, 70). One challenge for ASDs is to ensure long-term stability of the drug in the amorphous form through prevention of drug recrystallization (27, 49). The amorphous solid state is one of high free energy and thus it is thermodynamically favourable to return to the crystalline form (61).

Alternative carriers to polymers are also under investigation to assess their usefulness in formulation development. These include inorganic silica carriers, which are the focus of this thesis. Drug loaded onto the silica surface can also become amorphous in nature, resulting in enhanced drug release (54, 55, 71). Silica materials possess many favourable characteristics for use as carriers in oral drug delivery. They boast high surface areas, ordered pore networks and surface functionalization capabilities for controlled drug release (72-74). Long-term stability of amorphous drug in the mesopores has also been reported (75, 76). Silica-based drug carriers are

more resistant to heat, pH, mechanical stress, and hydrolysis-induced degradations than many polymer materials used to enhance drug dissolution (77). Drug-loaded silica formulations are discussed in more detail in Chapter 2.

1.3.2. Supersaturating Drug Delivery Systems (SDDS)

Dissolution enhancing formulations such as ASDs and drug-loaded silica systems can result in drug supersaturation in the intestinal environment. This is advantageous as it can overcome the limitations of equilibrium solubility levels for BCS Class II drugs (78). During dissolution of these formulations, drug concentrations exceed their equilibrium solubility in the intestinal fluids producing a thermodynamically unstable drug supersaturation that has the tendency to return to the equilibrium state by precipitation (Figure 1.5). However, if the metastable state exists for a time sufficient for drug adsorption, it can result in an enhanced flux across the intestinal wall (79). Therefore, the benefit of these formulations is dependent on the stability of the saturated state and the kinetics of drug precipitation.

In this thesis, the supersaturation potential of drug-loaded silica systems and the relationship of supersaturated drug release with drug adsorption behaviour are investigated.

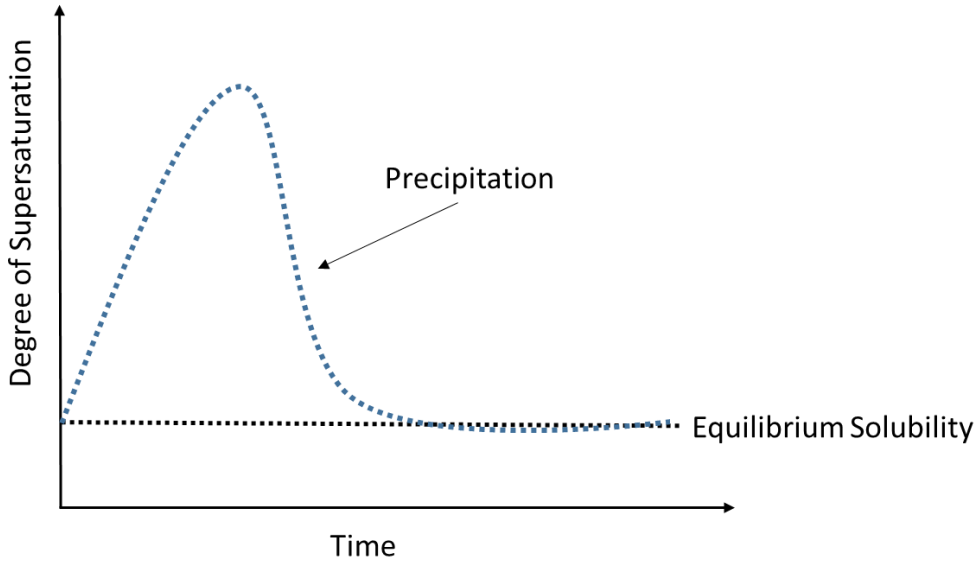


Figure 1.5 Supersaturating drug delivery system profile

1.4. *In Vitro* Dissolution Experimental Set-Up

In vitro drug dissolution experiments are an essential part of formulation pre-screening. While many innovative drug delivery systems have been developed for BCS Class II drugs, traditional dissolution experiments have not changed radically since the 1970s. Experiments involving the standard basket (Type I) and paddle apparatus (Type II) and simple dissolution media have limitations which are of significance to BCS Class II drugs with their challenging biopharmaceutical properties. The development of more biorelevant *in vitro* dissolution experiments could improve the quality of data generated and lead to better prediction of *in vivo* behaviour and bioavailability (80).

1.4.1. Sink vs Non-Sink Conditions

When the concentration, $C_{b,}$ (the concentration gradient which exists between this saturated layer and the bulk solution) is not more than 33 % of the saturated solubility value (C_s), it is considered negligible (81, 82). This is the definition of 'sink' conditions for a dissolution study. These low drug concentrations attempt to model what occurs in the gastrointestinal tract when drug is absorbed rapidly from solution across the intestinal barrier (83, 84). Under sink conditions, (C_s – C_b) becomes constant such that the rate of dissolution is directly proportional to the saturated solubility, C_s. Most dissolution studies reported in the literature are conducted under sink conditions. However, non-sink conditions are now recommended for *in vitro* dissolution of novel BCS Class II formulations which adopt a supersaturating drug delivery approach (85).

1.4.2. Dissolution Media

The composition of the gastrointestinal tract can significantly affect drug solubility, an important parameter in the Noyes-Whitney and Nernst-Brunner equations (Section 1.2.3). For ionisable drugs, buffer capacity and pH are pertinent factors whereas for lipophilic drugs, fat level and bile salt concentration should be considered (86). Physiological parameters such as surface tension (Section 1.2.4) and volume of the luminal contents can also play an important role (87). A significant proportion of dissolution experiments in the literature investigating drug release from dissolution enabling formulations utilise traditional dissolution media such as 0.1 M HCl and phosphate buffer (pH 6.8) (88-92). These simple media do not mimic

the contents of the gastrointestinal tract and therefore cannot adequately simulate the *in vivo* environment. Over the last decade, the development of biorelevant media has aimed to better replicate conditions in the stomach and the proximal small intestine in both the pre- and postprandial states (including Fasted-State Simulated Intestinal Fluid (FaSSIF-V2), which is utilised in this thesis) (87, 93-95). This has improved the relationship between *in vitro* dissolution studies and *in vivo* performance. However, many studies continue to use traditional media rather than their more biorelevant counterparts, which is potentially inappropriate for BCS Class II drug formulations.

1.4.3. Dissolution Apparatus

The basket (Type I) and paddle (Type II) apparatus were the first dissolution tests introduced into the US Pharmacopeia. They are useful for quality control testing and for product development of immediate release (IR) oral drug products belonging to BCS Class I and Class III. However, these *in vitro* dissolution methods are not as successful at predicting *in vivo* behaviour of formulations delivering poorly water-soluble drugs (80).

Paddle and basket apparatus require dissolution media volumes in the range of 500-1000 ml (Figure 1.6). These volumes are utilised to generate sink conditions, which are useful to demonstrate complete drug release from a dosage form. However, this overestimates the gastric volume in the fasted stomach which is unlikely to exceed 250 ml (96). The hydrodynamics of these apparatus are also problematic as they do not consider *in vivo* conditions and vary substantially within the dissolution vessel (97, 98). Another concern is the potential development of a coning effect in the apparatus during the experiment (99). Granules or particles with sufficiently high density form a mound, inhibiting dissolution in the stagnant zone below the paddle/basket.

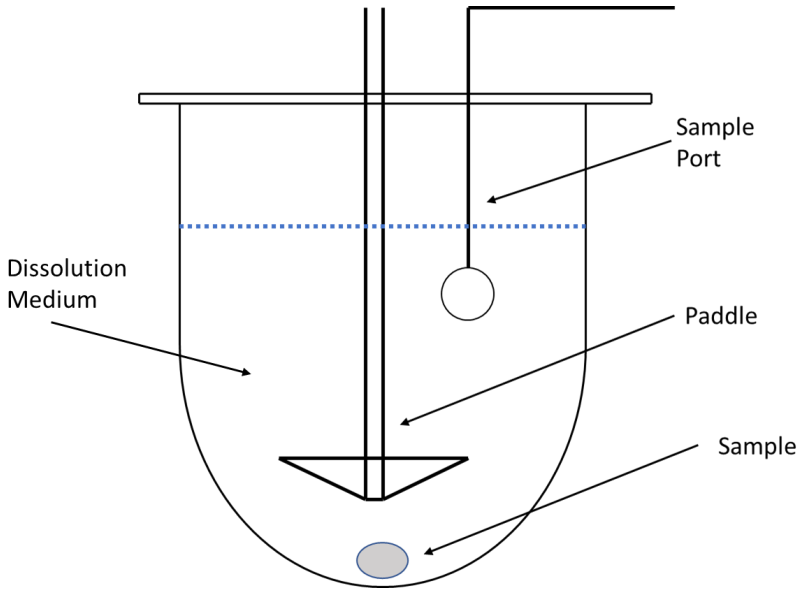


Figure 1.6 Schematic of USP II (paddle) apparatus

In recent years, two additional dissolution apparatus have been added to the US Pharmacopeia, the reciprocating cylinder (Type III) and the flow-through cell (Type IV). In this thesis, the biorelevance of the flow-through cell is compared to the paddle apparatus (Figure 1.6 and Figure 1.7).

The USP Type IV apparatus consists of a reservoir containing the dissolution medium, a water bath that maintains the dissolution medium at 37 ± 0.5 ^{o}C and a pump that forces it upwards through the cell at a specific flow rate (4, 8 or 16 ml/min) (Figure 1.7). The flow-through cell is fitted with a filter to prevent the escape of dissolved particles from the top of the cell. The bottom cone of the cell is filled with small glass bead (~ 1 mm) to produce a laminar fluid flow and one bead (~ 5 mm) to protect the fluid entry tube (80). It can operate as an open system with fresh dissolution medium continuously flowing through the cell or as a closed system where a fixed volume of dissolution medium is recycled (100). The USP IV has the potential to operate at

lower agitation rates than the paddle apparatus, resulting in lower fluid velocities which are considered more biorelevant (101, 102). However, data regarding the superiority of the USP Type IV over traditional dissolution apparatus are not in agreement (103, 104). Further investigation is warranted to determine whether the USP Type IV is superior at predicting *in vivo* behaviour compared to the basket and paddle apparatus.

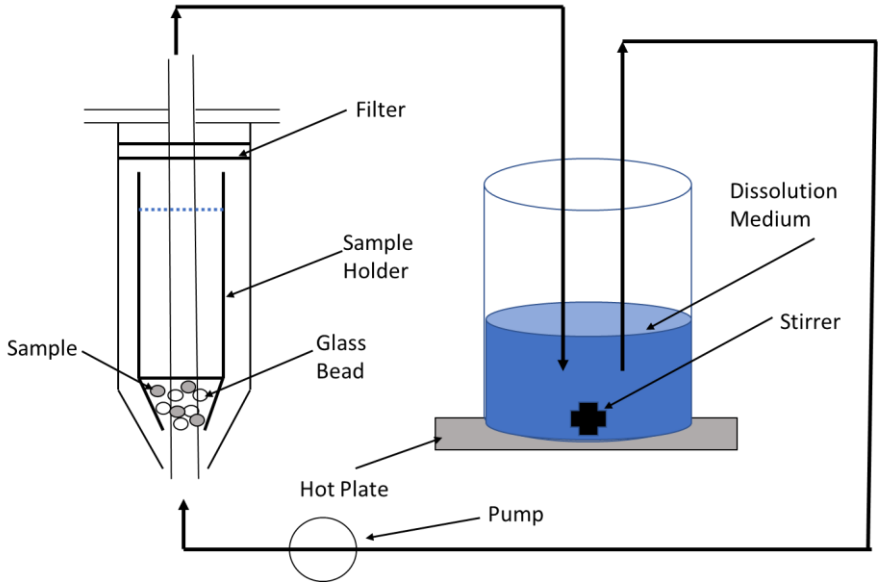


Figure 1.7 Schematic of USP IV (flow-through cell) apparatus

1.4.4. *In Vitro In Vivo In Silico* Relationships

In vitro biorelevant dissolution testing has proved useful in qualitatively, and in some cases quantitatively, predicting *in vivo* performance. However, these *in vitro* methods cannot capture the full picture of what is happening in the *in vivo* environment. For example, gastric emptying, permeability through the intestinal membrane, transit time, pH and fluid volume in each segment of the GI tract, first pass metabolism and excretion can all play a role in drug bioavailability. To better predict *in vivo* behaviour,

in vitro test results can be combined with physiologically based pharmacokinetic (PBPK) models using *in silico* software (80). An *in vitro in vivo* correlation (IVIVC) is traditionally defined as a predictive mathematical relationship between *in vitro* drug dissolution and an *in vivo* experiment, covering either the entire absorption curve (Level A) or an individual parameter associated with the rate or extent of absorption (as in Level C correlations) (105). Linear IVIVC's have been derived for modified release preparations but are unlikely in the case of immediate release products for which absorption is not dissolution rate limited (106). However, the non-linear models produced by *in silico* software can be useful – here the term *in vitro in vivo* relationship (IVIVR) is preferred to IVIVC. The development and implementation of *in silico* models to predict IVIVRs for use in novel immediate release formulation development is still in its infancy. Working to increase understanding of the link between *in vitro* dissolution and *in vivo* performance could help streamline the drug development process.

1.5. Adsorption at Solid/Liquid Interface

While dissolution has been the subject of extensive research in the drug delivery field, significantly less is reported relating to drug adsorption at the solid-liquid interface. This adsorption could have a role in determining the extent of drug release from particular novel drug delivery formulations such as inorganic carriers. This gap in knowledge requires further investigation and is a central focus of this thesis.

1.5.1. Theory of Adsorption at the Solid/Liquid Interface

Adsorption results from energetically favourable interactions between the solid adsorbent and the solute species. It is often a complex process as it can be influenced by a combination of solid, solvent and solute components of the system (107). Interactions between the adsorbent and adsorbate species can take the form of various electrostatic interactions, including Van der Waals forces and hydrogen bonding, or stronger interactions such as covalent bonding. Lateral interaction between molecules of the adsorbed species can also contribute to the adsorption and desorption processes.

These interactions between adsorbate species (in solution) and adsorbent material result in the selective partitioning of the adsorbate species to the interface in preference to the bulk medium (Figure 1.8).

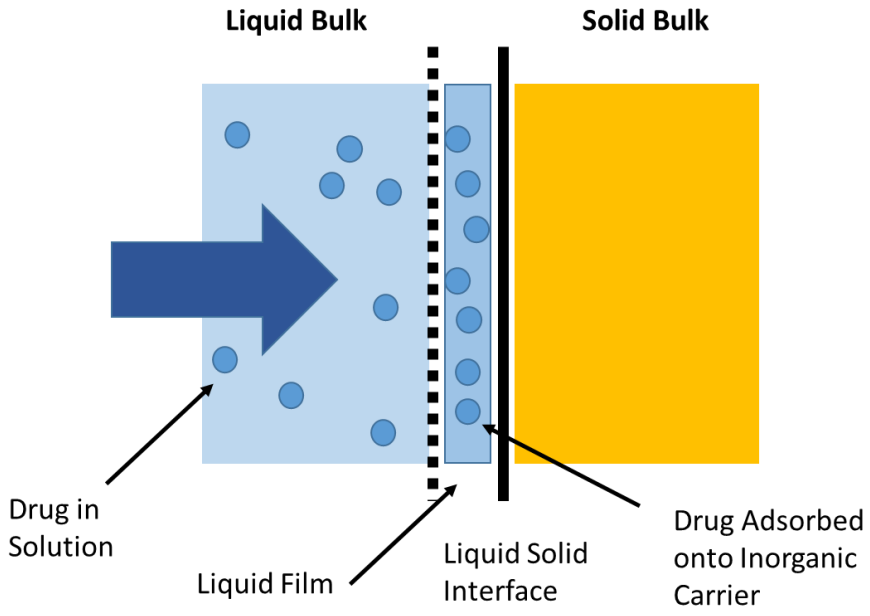


Figure 1.8 Adsorption at the solid/liquid interface

Adsorption can be broadly classified into two categories, physical adsorption and chemical adsorption (108). Physical adsorption is usually weak, generally reversible and involves small energy changes. Van der Waals forces and electrostatic forces such as hydrogen bonding are primarily responsible for physical adsorption which is also characterized by a high rate of adsorption and the formation of multilayers (109). Chemical adsorption occurs through covalent bonding between the adsorbate and the solid surface. Chemical adsorption normally involves an activation stage and is characterized by relatively high energy changes and a low rate of adsorption. Such adsorption is usually strong, irreversible and limited to a monolayer. However, this distinction between physical and chemical adsorption has been proven to be arbitrary and in many cases an intermediate character of adsorption exists, for example, adsorption involving strong hydrogen bonds or weak charge transfer (110).

1.5.2. Adsorption Isotherms

Adsorption isotherms are used to describe adsorption processes and represent a functional relationship between the amount adsorbed and the activity of the adsorbate at equilibrium under constant temperature conditions (107). A number of isotherm models have been developed to describe this relationship based on varying fundamental approaches (111). Two of the most commonly applied isotherms are discussed below.

1.5.2.1. Langmuir Isotherm

The Langmuir isotherm is an empirical model which assumes monolayer adsorption (the adsorbed layer is one molecule in thickness). Under the conditions of this model, adsorption only occurs at a finite number of definite localized sites which are identical and equivalent. There is no lateral interaction or steric hindrance between the adsorbed molecules, even on adjacent sites (112). Homogeneous adsorption exists where each molecule possesses constant enthalpies and sorption activation energy (all sites possess equal affinity for the adsorbate) (113).

Graphically, it is characterized by a plateau, an equilibrium saturation point where no further adsorption can take place (Figure 1.9) (114). The Langmuir linear equation is displayed in Table 1.2.

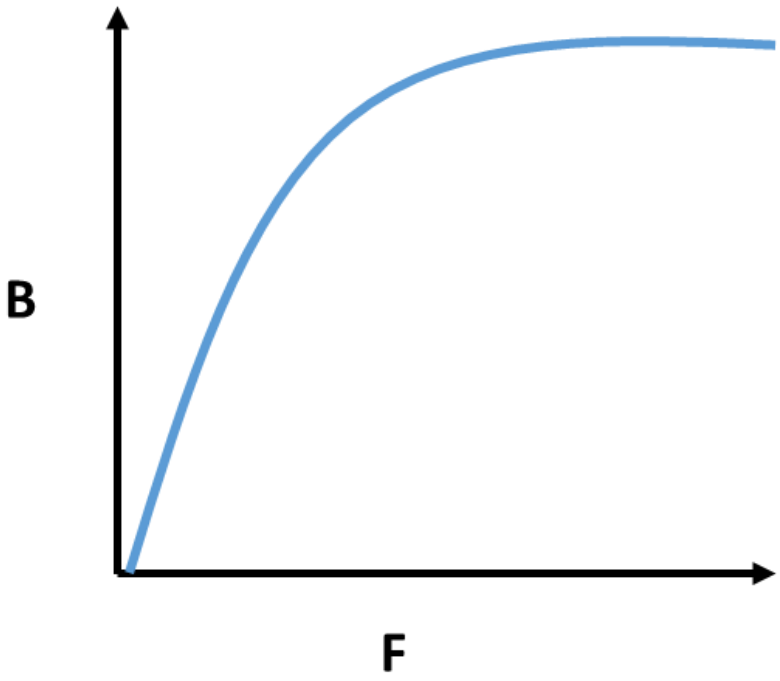


Figure 1.9 Langmuir Isotherm (B represents the concentration of drug adsorbed to the silica surface, F represents the concentration of free substrate in solution at equilibrium conditions)

Table 1.2 Linearized forms of Langmuir and Freundlich isotherms

NAME	LINEARISED FORM
Langmuir	$F/B = (1/K_L.Nt) + F/Nt$
Freundlich	$mlogF = logB + K_F$

where *B* is the concentration of drug adsorbed to the silica surface, *F* is the concentration of free substrate in solution at equilibrium, N_t is the total number of binding sites and K_L *and* K_F are related to the average binding affinity.

1.5.2.2. Freundlich Isotherm

In contrast to the Langmuir isotherm, the Freundlich empirical model can be applied to multilayer adsorption, with non-uniform distribution of adsorption heat and affinities over the heterogeneous surface (Figure 1.10) (115). At present, the Freundlich isotherm is widely applied in heterogeneous systems especially for organic compounds or highly interactive species on activated carbon and molecular sieves. The slope of the line, determined from the linear equation, is a measure of adsorption intensity or surface heterogeneity, becoming more heterogeneous as its value gets closer to zero. The Freundlich linear equation is displayed in Table 1.2.

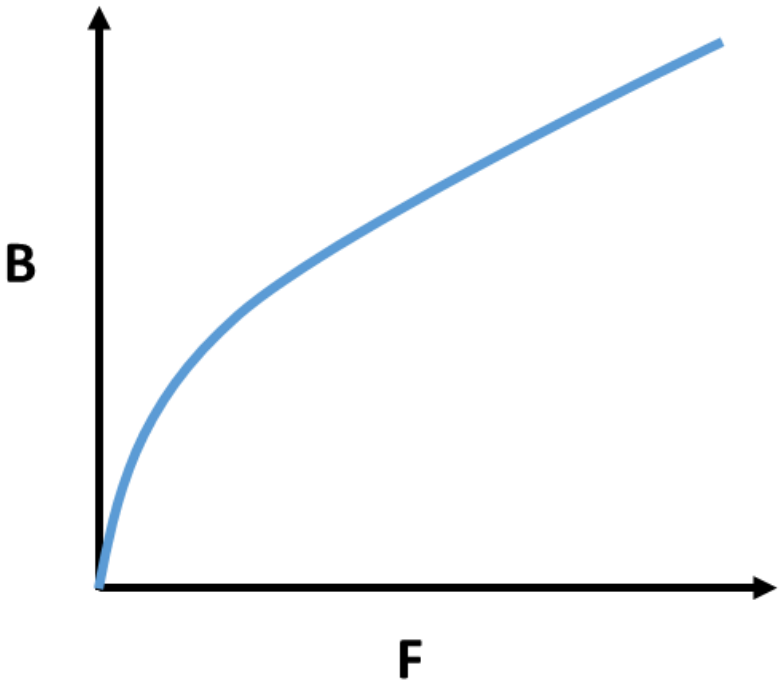


Figure 1.10 Freundlich Isotherm (B is the concentration of drug adsorbed to the silica surface, F is the concentration of free substrate in solution at equilibrium)

1.6. Adsorption/Desorption Behaviour of Mesoporous Silica Systems: Current Knowledge

Mesoporous silica systems have been extensively investigated as novel formulations for BCS Class II drugs (see Chapter 2). However, there remains a gap in knowledge concerning the mechanism of drug release from these carriers. An initial 'burst' release of drug is generally observed in their dissolution profile. However, while most of the drug is released here, full drug dissolution from the silica surface is not achieved in many cases (54, 55, 116). This incomplete release profile is not well understood.

It has been suggested that drug release rate can be controlled by the equilibrium between drug molecules bonding with silica surface *versus* free drug in solution in the aqueous medium (117). This was suggested by Xue *et al* as an explanation for the slower drug release rate observed after initial 'burst' release from a mesoporous silica formulation. It may also play a role in understanding the basis of incomplete release from mesoporous silica systems but this has not been investigated to date.

Outside of its use in drug delivery, mesoporous silica has been investigated as an adsorbent for chemical removal from wastewater of pharmaceutical industrial manufacturers (118). Bui *et al* reported that drug molecules could adsorb both reversibly and irreversibly onto the silica surface. This could have implications for drug release from when these materials are utilized as drug delivery systems.

Furthermore, a comprehensive review on adsorption of organic molecules onto the silica surface has been published by Parida *et al* (119). They presented an overview of studies which reported passive adsorption of numerous organic adsorbates onto the silica surface including surfactants, dyes, polymers and proteins.

Based on these reports and knowledge of the fundamentals of adsorption at the solid/liquid interface discussed above (Section 1.5), it would be of interest to examine adsorption/release behaviour from mesoporous silica systems during dissolution. This could enhance understanding of the mechanism of drug release from these carriers and thus aid in formulation development.

1.7. Hypothesis, Aims and Objectives

1.7.1. Hypothesis

The mechanism of drug dissolution from mesoporous silica systems is not well understood. Investigation of factors that influence drug adsorption, retention and release from these formulations can help address this gap in current knowledge.

1.7.2. Aim

Investigate factors influencing drug adsorption and release from mesoporous silica systems to enhance understanding of their drug release profiles.

1.7.3. Objectives

A number of specific objectives were identified to achieve this aim.

1. Compile a literature review to examine current knowledge of drug loading and release from mesoporous silica
2. Exploration of drug and surfactant adsorption/release behaviour on the silica surface with a view to determining factors influencing these processes
3. Ascertain factors which play a role in drug adsorption and dissolution from mesoporous silica formulations in the presence of biorelevant media (SGF and FaSSIF-V2)

4. Probe the mechanism of drug/silica interactions and whether these interactions are influenced by a dynamic equilibrium process under supersaturating conditions
5. Investigate the potential for *in vitro* dissolution experimental design to affect drug dissolution from a mesoporous silica formulation

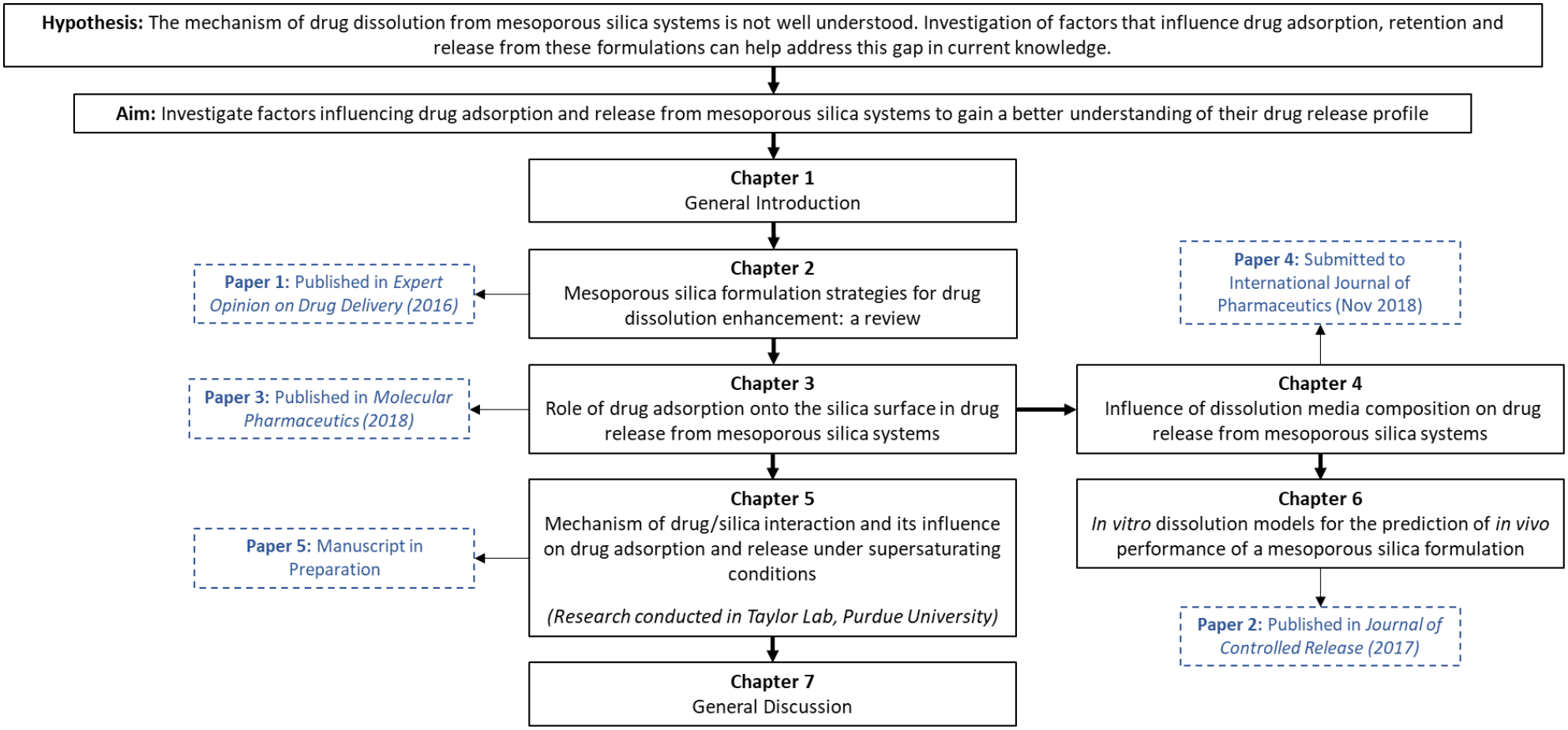


Figure 1.11 Graphical thesis outline

Chapter 2: Mesoporous Silica Formulation Strategies for Drug Dissolution Enhancement: A Review

Modified Version of Publication

McCarthy CA, Ahern RJ, Dontireddy R, Ryan KB, Crean AM. Mesoporous silica formulation strategies for drug dissolution enhancement: a review. Expert Opinion on Drug Delivery. 2016;13(1):93-108.

2.1. Abstract

Mesoporous silicas have demonstrated excellent properties to enhance the oral bioavailability of poorly water-soluble drugs. This review provides an overview of different methods utilised to load drugs onto mesoporous silica carriers. The influence of silica properties and silica pore architecture on drug loading and release are discussed. The kinetics of drug release from mesoporous silica systems are examined and the manufacturability and stability of these formulations are reviewed.

2.2. Introduction

As discussed in Chapter 1, loading drugs onto a mesoporous silica substrate has been considered as a formulation strategy to overcome the limitations of drugs classified as Biopharmaceutics Classification System (BCS) II, whose bioavailability is said to be dissolution rate limited. Adsorption of drugs onto porous and non-porous silica materials has been described in the literature since the early 1970's (120, 121). In 2001, Vallet-Regi *et al* identified the potential of mesoporous silica as a controlled release system (72). Its ability to enhance the delivery of poorly soluble drugs was subsequently investigated (55, 122, 123). Mesoporous silica carriers have a number of attractive features for enhancing drug dissolution such as high surface area, large pore volume and ordered pore networks (74). They can also provide an adjustable drug release profile as their surface hydroxyl groups can be functionalized to control release. Mesoporous silica materials have also displayed structural stability on storage (124). This provides an advantage over solid dispersions composed of biodegradable polymeric materials which can demonstrate solid-state phase separation on storage due to their hygroscopic nature (125). Silica-based drug carriers are more resistant to heat, pH, mechanical stress, and hydrolysis-induced degradations than many polymer materials used to enhance drug dissolution. A range of silica materials are commonly used as excipients in numerous oral drug products and are considered non-toxic and biocompatible (126). There is limited evidence to describe the safety of ordered mesoporous silica grades, especially when they are administered in larger quantities required to enhance drug delivery (127, 128). Hudson *et al* reported that ordered mesoporous silicas (MCM-41, SBA-15 and

MCF) have the potential to be toxic when delivered by certain routes (intravenous and intra-peritoneal) (128). Recently, a number of animal studies have been conducted using oral mesoporous silica formulations, suggesting the oral route is more biocompatible (56, 129, 130). Several publications have considered the issues relating to mesoporous silica potential toxicity, including an extensive review by Manzano *et al* (127, 131, 132).

The aim of this review is to summarise the progress made in the development of mesoporous silica carriers to enhance drug dissolution rate. A particular focus will be placed on the factors that influence drug loading and release in mesoporous silica systems. The mechanism and kinetics of drug release in such formulations will be discussed.

2.3. Silica for Drug Delivery (Non-Porous and Porous)

A wide range of silicon dioxide (silica) materials exist. However, amorphous hydrophilic silica has been the focus for researchers in the oral drug delivery field. It can be divided into two categories, porous and non-porous.

2.3.1. Non-Porous Silica

The most common non-porous fumed silica is colloidal silicon dioxide (hydrophilic fumed silica). Examples of commercial varieties include, Cab-O-Sil® (Cabot Corporation), Aerosil ® (Evonik Industries) and HDK® (Wacker)(Table 2.1). Colloidal silicon dioxide has been utilised for many years in the pharmaceutical industry as a glidant to improve dry powder flowability in powder tableting processes.

The relatively large surface area of silicon dioxide allows for a poorly water-soluble drug to be deposited onto its surface which enhances the drug's dissolution rate as the loaded drug is present in its amorphous form (53). In contrast to mesoporous silica, there is a history of regulatory acceptance of these non-porous silicon dioxides as pharmaceutical excipients for oral drug delivery which is advantageous for formulation development. Fumed silicon dioxide is employed in Bend Research Inc.'s Spray-Dried Nanoadsorbate Technology (SDNA) (133). The SDNA process consists of a solid amorphous drug or drug/excipient dispersion adsorbed to the surface of the silica. This approach greatly increases the surface area of the drug dispersion, relative to normal solid dispersion particles, which leads to rapid drug dissolution resulting in improved bioavailability relative to crystalline drug. The physical stability of this drug/silica system is also superior to pure amorphous formulations. However, the

majority of published research on the use of silica as a carrier for poorly water-soluble drugs has centred on mesoporous silica, which is the focus of this thesis.

Table 2.1 Characteristics of a selection of porous and non-porous silica materials

Silica	Type	Pore structure	Pore volume (cm^3/g)	Pore size (nm)	Surface area (m^2/g)	Reference
Colloidal SiO_2	Aerosil®	N/A	N/A	N/A	50 – 300	(134)
Colloidal SiO_2	Cab-O-Sil®	N/A	N/A	N/A	200	(134)
Colloidal SiO_2	HDK	N/A	N/A	N/A	150 – 200	(134)
Mesoporous	MCM-41	Hexagonal	0.5 – 1.5	1.5 – 10	800 – 1000	(74)
Mesoporous	MCM-48	Cubic	1.05	1.5 – 10	1000	(135, 136)
Mesoporous	SBA-15	Hexagonal	0.50 –0. 65	5 – 8	400 – 800	(137)
Mesoporous	FSM-16	Honeycomb	0.28 – 0.83	1.5 – 4	680 – 1000	(138)
Mesoporous	TUD-1	Foam-like	0.5 – 1.7	4 – 18	400 – 1000	(139)
Mesoporous	Sylysia®350	Disordered	1.6	21	300	(140)
Mesoporous	Syloid®244	Disordered	1.42	19.0	311	(90)

2.3.2. Mesoporous Silica

Mesoporous silica (pore size range 2-50 nm) can enhance the dissolution rate of poorly water-soluble drugs as drug loaded on the surface also exists in an amorphous state (55). However, it possesses an important advantage over non-porous materials in that it has a significantly larger surface area and it is possible to control its porous architecture during manufacture (Table 2.1) (74). Due to its porous nature, drug molecules can be confined and stabilised within the silica pores in a non-crystalline form (75, 141-143). The ratio of drug molecule size to silica pore width and the interaction of the drug molecules with the silica substrate prevents recrystallization of the drug by nano-confinement (124, 144, 145).

There are many varieties of mesoporous silica, the most widely investigated in the literature are listed in Table 2.1. Researchers have developed both ordered and non-ordered mesoporous silicas which vary in final architecture due to differences in conditions during manufacture, for example, temperature and surfactant concentration. Examples of non-ordered mesoporous silicas include Syloid® and Sylysia® materials which have been investigated as drug carriers (140, 146-148). Ordered mesoporous silica materials with a uniformity in pore shape, size and volume have also been developed. Examples of ordered materials include the Mobil crystalline material (MCM) range of mesoporous silicas which was developed by researchers of the Mobil Corporation in 1992 and is part of the M41S family of molecular sieves. They possess a well ordered stable hexagonal unidirectional mesoporous network (74). MCM-48 is a modification of MCM-41

with a cubic array of pores (135). It has been reported that a cubic structure with space group *Ia3d* can increase molecular accessibility and displays potential for the development of controlled release systems (136). The Santa Barbara Amorphous type mesoporous silica (SBA-15) was developed by researchers at the University of California, Santa Barbara in 1998 (137). The pore sizes of SBA-15 are larger than MCM-41 (149); this property facilitates faster release from SBA-15 than MCM-41. The highly ordered pore structures of mesoporous silica MCM-41 and SBA-15 are demonstrated in the transmission electron microscopy (TEM) image below (Figure 2.1).

In recent years, a number of commercial mesoporous silicas marketed for pharmaceutical formulation have been developed. Parteck®SLC is a silica formulation by Merck Millipore Corporation, Syloid® silicas have been produced by Grace Pharmaceuticals and Sylysia® by Fuji Sylysia Chemical Ltd. (146, 147, 150).

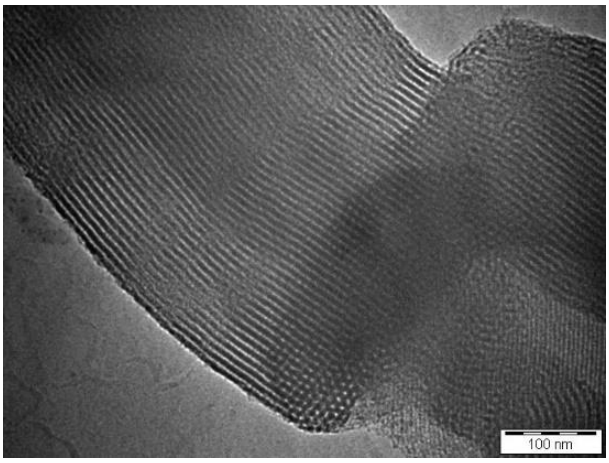


Figure 2.1 TEM image of SBA-15 mesoporous silica

2.4. Drug Loading Processes

Numerous methods to load drug onto mesoporous silica substrates have been developed. These include melt processes, various organic solvent processes and methods involving supercritical fluid (SCF) technology. The extent of drug loading depends on surface area and the affinity of the drug for the silica substrate (151, 152). The internal silica pore volume and the concentration of drug in solution are also important considerations (153). The choice of loading process can also affect the quantity of drug loaded, drug distribution in the silica and drug physiochemical properties in the mesoporous structure (54, 55, 142).

2.4.1. Melt Process

Mellaerts *et al* utilised a melt method to load ibuprofen and itraconazole onto SBA-15 (154). The melt process involves heating the drug loaded mesoporous system above the drug's melting point which could result in potential drug degradation (154). Itraconazole was not successfully loaded onto SBA-15 at any of the drug loading ratios investigated. It was not homogeneously distributed throughout the silica surface and remained somewhat crystalline. Whereas, ibuprofen was successfully loaded onto SBA-15 in a non-crystalline state and achieved rapid *in vitro* release (154). This work highlighted the high dependency of drug molten viscosity for mesopore penetration in this process. The thermal stability of the drug at the elevated temperatures required during melting is also an important consideration when choosing this loading method.

Microwave irradiation has also been employed to load drug onto silica materials. A method has recently been developed which allows samples to be heated with a feedback system to ensure the temperature can be controlled during the loading process. This protects against drug degradation (155). Waters *et al* loaded fenofibrate onto several different silica materials using this method and compared them with samples loaded by physical mixing and traditional heating methods. Their results demonstrated that a greater proportion of the loaded drug existed in an amorphous state using the microwave loaded method. Drug release from this formulations was also enhanced compared with the other formulations tested (156).

2.4.2. Solvent Loading Methods

2.4.2.1. Solvent Immersion Processes

Organic solvent drug loading methods have been extensively reported in the literature by several research groups. The most common technique employed is an immersion method involving adsorption from organic solution followed by filtration to recover the drug-loaded mesoporous silica (123, 154, 157, 158). It usually results in a low yield as adsorption is confined to a monolayer on the surface (159). Furthermore, it is necessary to reduce solvent traces to acceptable limits as outlined in the International Conference on Harmonisation (ICH) guideline Q3 (R5) (160).

Drug loading can be influenced by interactions involving drug, silica and solvent. Highly polar solvents can compete with drug molecules for adsorption sites. Charnay *et al* reported that the use of polar solvents such as DMSO (dimethyl sulfoxide), DMF

(dimethylformamide) and DMA (dimethylacetamide) resulted in a low degree of ibuprofen loading onto MCM-41 (142). In contrast, ethanol and hexane (non-polar solvents) produced relatively high drug loading concentrations. The optimal drug concentration in solvent should be determined before drug loading. If drug concentration is too high, drug molecules can adsorb onto the surface too quickly, blocking mesopores, which reduces the potential surface area available for loading drug (145).

2.4.2.2. Incipient Wetness Impregnation Process

In this process, a high degree of loading can be obtained using a concentrated drug solution (generally close to the saturation solubility of the drug). This technique exploits the large pore volume of the mesoporous silica (154). The drug's solubility in the loading solvent is important as it affects the drug loading efficiency and subsequent drug release (161, 162). Compared to the immersion method, the time consuming filtration step can be avoided as a loading solution with a volume approximately equal to the pore volume is used (163). This is generally an efficient process and the amount of drug loaded onto the carrier can be easily controlled, making it suitable for loading expensive drug molecules. However, high loading concentrations or repeated impregnations can be required to achieve high degrees of drug loading (typically in the range 5-40 % (w/w)) (163).

A frequently reported single-step incipient wetness impregnation involves preparing a concentrated solution of drug in solvent followed by its drop-wise addition to the mesoporous silica. The powder is subsequently dried using air for 24 h and then

placed under vacuum for 48 h at a temperature of 40 ^{o}C (28, 55, 76, 154, 164). Charnay *et al* reported improved drug loading using this method when compared with a traditional solvent immersion process (142). They proposed that the drug molecules diffused with the solvent into the pores by capillarity and remain trapped within the pores after solvent removal. The drug in the pores existed in an amorphous state and dissolution rates were enhanced compared to crystalline drug (142). Mellaerts *et al.* employed an incipient wetness loading method and a solvent method to load itraconazole onto SBA-15 mesoporous silica. Both methods involved drying the sample at 35 ^{o}C and then placing it under reduced pressure (1 hPa) at 40 °C for 48 h. They suggested that the rapid solvent removal encountered in the incipient wetness method may have contributed to preferential loading of the SBA-15 micropores, with the drug deposited along the pore walls. SBA-15 has a high proportion of micropores located in the walls of large ordered mesopores (165). During the incipient wetness process, drug molecules are introduced to the pores rapidly and the solvent is evaporated quickly. Using the traditional solvent method, drug loading is a slow process requiring diffusion of the molecules from an external solution onto the mesoporous silica surface. This gives the drug molecules time to rearrange and deposit in the mesopores. While drug release was improved for the incipient wetness method, the presence of itraconazole in the micropores rather than the mesopores resulted in slightly slower drug release when compared to the solvent immersion method. This preferential micropore loading was not reported for ibuprofen in the same study (154).

2.4.2.3. Loading using Supercritical Fluid Technology (SCF)

SCF drug loading techniques offer significant advantages by exploiting the solvent power variation that can be achieved by manipulation of the fluid pressure and temperature in the supercritical region. Carbon dioxide (CO_2) is the most commonly used SCF as it possesses a low critical point (7.4 MPa, 31.2 ^oC), is non-flammable, recyclable, environmentally benign and inexpensive. Many pharmaceuticals have demonstrated solubility in supercritical CO_2 (SC-CO_2) (166). A further advantage of utilising SCF for drug loading is that the final product is totally solvent-free post fluid evacuation.

Several studies have compared SCF processes directly with solvent methods (88, 167). It has been reported that SC-CO_2 produces a similar degree of drug loading to impregnation of the drug using hexane as a solvent. However, the SCF technique required a much reduced process time. This was attributed to the more homogeneous loading demonstrated using the SCF method. Fenofibrate was successfully loaded onto SBA-15 using supercritical carbon dioxide at various pressure and duration times, which did not affect the solid-state of the drug, its distribution into the mesopores or the subsequent drug release profiles (88). Ahern *et al* reported that while solvent and SC-CO_2 loaded samples displayed differences in drug distribution, they demonstrated similar release profiles and solid-state stability properties (54). There is limited published research comparing the drug release rate of silica loaded using SCF technology with the release rate from other loading methods.

2.4.3. Large scale drug loading techniques

The laboratory drug-loading methods outlined above are suitable for small batch sizes. However, there is a need to address the scale-up challenges for cost-effective commercial production. Limnell *et al* compared the traditional immersion method with rotavapor and fluid-bed loading methods (116). They reported that loading processes using this typical pharmaceutical lab equipment was straight-forward and the extent of drug loading was substantial. In addition, they proposed that these techniques overcame the requirement for excessive drug quantities to achieve high drug loading in the immersion method, which is economically beneficial. The drug does not require heating, which is advantageous as it prevents possible drug degradation. Researchers have also investigated a co-spray drying technique. They reported a high degree of drug loading and the amorphous drug/silica product displayed physical stability on testing (75, 143). Bahl *et al* utilised a co-milling method to load indomethacin onto a silica substrate using a rolling jar mill. This method has the advantage of being 'solvent free'. The co-ground amorphous indomethacin was physically stable for three to six months at 40 °C/75 % relative humidity (RH) (168).

2.5. Mesoporous Silica Characteristics Influencing Drug Loading and Release

The most significant silica properties that can influence drug loading and release are surface area, pore volume, pore size and pore arrangement. Particle properties (such as particle size and morphology) are also important. These are discussed in further

detail below. Furthermore, silica surface functionalization provides numerous opportunities to control both drug loading and release.

2.5.1. Silica Pore Architecture and Particle Properties

The pore properties of silica materials have a significant influence on the degree of drug loading, loaded drug solid-state structure and long-term drug solid-state stability. Numerous studies have investigated the impact of silica pore volume (142, 162), silica pore size (116, 136, 151, 157, 169-172) and silica pore connectivity/geometry/morphology (162, 173, 174).

Heikkila *et al* investigated the impact of pore volume on drug adsorption by loading ibuprofen onto specific mesoporous silicas (TUD-1, SBA-15 and MCM-41). They reported that total mesopore volume was significant in terms of the degree of achievable drug-loading (162). This was confirmed by Zhang *et al* who determined that total pore volume and pore size were the two limiting factors for maximum drug loading (175). Excessive loading above the limits of the total pore volume can result in a layer of crystalline drug on the silica surface which can slow drug release rate from the pores (154).

Pore size has an important role to play in drug loading, release and drug solid-state stability. The long-term stability of amorphous drug in the mesopores has been reported by a number of groups (75, 76). A drug molecule loaded into a confined space cannot recrystallize if the confinement space diameter is less than or equal to 15 times the drug molecule diameter (144, 176). The influence of pore size on drug loading and release has also been examined (116, 175, 177-179). As pore size

decreases the amount of drug loaded is reduced. The release rate also decreases as a result of increasingly tightly packed molecules in the mesopores (170). Izquierdo-Barba *et al* reported a decrease in release rate for bulkier erythromycin molecules compared to ibuprofen from pores of the same diameter. The effect becomes more evident as pore size decreases (136). Consequently, to allow for easy access during drug loading and release, pore size should be at least be three times greater than the drug molecule diameter (73). The pore diameters of ordered mesoporous silicas, such as SBA-15 and MCM-41, can be adjusted during the manufacturing process. As a result, pore size can be modified to control the drug release rate (74, 137). However, it has also been demonstrated that there is a pore size threshold limit for individual molecules, after which further increases in pore diameter do not enhance release rate (122). Furthermore, in silica samples with larger pore sizes, increased recrystallization has been reported due to the loss of nano-confinement properties (180). A comparison between *in vitro* and *in vivo* release profiles for drug loaded silica samples has provided interesting results. It was observed that a larger pore diameter resulted in faster release *in vitro* while the smaller pore diameter gave the fastest *in vivo* release profile. The authors attributed this behaviour to the slower rate of supersaturation produced by the smaller pore diameter in the intestine which enhances absorption of fenofibrate across the intestinal wall (181). This research is discussed in more detail in Section 2.7.2.

Pore channel length and morphology are also significant factors controlling drug loading and release in the silica matrix. Gao *et al* compared bimodal mesoporous silica (BMM) which possesses short channels and MCM-41 which has long ordered channels (173). They reported that BMM achieved greater drug loading and faster

release. Heikklia *et al* compared the pore morphologies of TUD-1, MCM-41 and SBA-15. They determined that TUD-1 produced the fastest drug release due to its highly accessible pore network compared to the unidirectional, uniform hexagonal mesopores of SBA-15 and MCM-41 (162). Zhu *et al* reported that hollow mesoporous spheres (HMS) resulted in higher drug loading concentrations than MCM-41 despite their similar surface area and pore volumes. This was attributed to the HMS pore channel structure which runs into a hollow core, allowing for increased drug loading (174).

Silica particle properties such as particle size and morphology have also been investigated to determine their effects on drug loading and release. Mesoporous silica particles can be manufactured to produce a monodisperse particle size (182, 183). There is limited research in the literature investigating the effectiveness of further reducing silica particle size to enhance drug loading and release for oral drug delivery. Instead, most work is focussed on controlling pore diameter. Results from the studies on the significance of particle morphology have proved inconclusive (184, 185). Work to date has not specifically looked at the effect of particle morphology in isolation so its influence cannot be accurately determined.

The large surface area of mesoporous silica is a key characteristic that makes it a potentially useful carrier for poorly water-soluble drugs (152). Many research groups have documented that increasing silica surface area improves drug loading and dissolution rate (53, 122, 151, 170, 186). However, a recent study has proposed that there is a threshold level above which increasing surface area does not result in a linear increase in drug release rate (91).

2.5.2. Surface functionalization

Surface functionalization of the silica provides numerous possibilities to control drug adsorption and release. The aim of functionalization is to increase the attraction between drug and silica. There are a number of different methods which can be employed to functionalise mesoporous silica including co-condensation (one-pot synthesis), grafting (post-synthesis modification) and imprint coating methods (183). The choice of method will influence the position of the functional groups on the silica (*i.e.* presence on the surface or internally in the pores). Studies thus far indicate that the grafting method is superior to co-condensation because the latter can damage the mesoporous framework (187). This is a rapidly developing area and many drugs have been incorporated into various functionalised silica systems (Table 2.2). One of the most widely reported is amino-functionalization pf the silica surface. Balas *et al* compared alendronate loading in non-functionalized and amino-functionalized silica. They reported a drug loading almost three times higher for the modified silica material using a solvent loading method (188). A second strategy utilised in surface functionalization is to attach hydrophobic species to the surface. The drug-surface interactions are not necessarily increased but aqueous medium does not easily penetrate the functionalized silica system and this slows drug release rate. A controlled release formulation of erythromycin was developed using SBA-15 functionalised with octyl and octadecyl groups (189). The functional groups decreased the effective pore size of the SBA-15 and decreased the wettability of the surface by aqueous solutions, thus creating a controlled release formulation. Mesoporous silica had also been modified by silylation to produce controlled release formulations using captopril and ibuprofen as model drugs (190, 191). These systems

are showing promise for controlled and targeted drug release and are an exciting prospect for the future.

Table 2.2 Examples of drugs incorporated into functionalised mesoporous silica materials

(LP-Ia3d refers to pores with Ia3d symmetry, LP refers to large pore, Al refers to aluminum-tri-sec-butoxide, APTES refers to 3-aminopropyltriethoxysilane, APMS refers to N-(2-aminoethyl)-aminopropyl dimethoxymethylsilane, APTMS refers to 3-aminopropyltrimethoxysilane, C8T refers to octyltrimethoxysilane, C18T refers to octadecyltrimethoxysilane, MPTS refers to 3-mercaptopropyl trimethoxysilane, TMCS refers to trimethylchlorosilane, TMS refers to trimethylsilyl, * indicates no information provided in article as to source material for modification)

Class of Drug	Drug	Functionalised Mesoporous Carrier	Reference
Anti-inflammatory	Ibuprofen	MCM-41- CH_3 (TMCS)	(191)
	Ibuprofen	SBA-15-NH_2 (APTMS)	(187)
	Ibuprofen	MCM-41-NH_2 (APTES)	(185)
	Ketoprofen	SBA-15-NH_2 (APTES)	(192)
	Naproxen	MCM-41-NH_2 (APTES)	(89)
Bisphosphonates	Alendronate	SBA-15-NH_2*	(188)
	Alendronate	MCM-41-NH_2*	(188)
Antibiotics	Erythromycin	SBA-15-C8T	(189)
	Erythromycin	SBA-15-C18T	(189)
	Amikacin	MCM-41-Al	(193)
	Cefuroxime	FDU-12 (MPTS and APMS)	(194)
	Cefuroxime	SBA-15 (MPTS and APMS)	(194)
	Vancomycin	FDU-12 (MPTS and APMS)	(194)
	Vancomycin	SBA-15 (MPTS and APMS)	(194)
Anti-hypertensives	Captopril	MCM-41- CH_3 (TMCS)	(190)
Anti-fungals	Griseofulvin	MCM-41-NH_2 (APTES)	(195)
	Griseofulvin	MCM-41-CH_3 (TMCS)	(195)
Steroid	Budesonide	MCM-41-NH_2 (APTES)	(92)

2.6. Physical and Chemical Stability of Drug Loaded Silica System

Various formulation approaches can be utilised to create supersaturated solutions to enhance drug bioavailability, one of which is the generation of an amorphous state of the drug in drug/mesoporous silica systems. The amorphous form is one of high energy and is thermodynamically unstable compared to the crystalline state (as described in Section 1.3.1). This leads to higher apparent solubility and dissolution rate (196). However, recrystallization can occur spontaneously in these unstable amorphous drugs and this negates any solubility advantages. Research is now ongoing to investigate how to stabilise amorphous drug/mesoporous silica formulations for drug delivery.

A key feature of mesoporous silica is that it has a large surface area which gives it a high surface free energy. Adsorption of drug molecules onto the silica surface allows the system to transfer to a lower free energy state. The adsorbed molecules exist in an amorphous but physically stable state, due to a decrease in the Gibbs free energy of the drug/silica system. Crystallisation of the drug will only occur if the thermodynamic state is disrupted (197). A further advantage of drug/mesoporous silica systems is that they can stabilise the amorphous drug by size-confinement effects. Crystal growth can occur spontaneously once a critical nucleation size is obtained. The drug molecules in the pores are constrained to such a degree that they cannot reach this point and crystal growth is inhibited (144).

The long-term physical stability of mesoporous silica formulations has been demonstrated by a number of groups. Ambrogi *et al* examined drug loaded silica samples over 60 days at 75 % relative humidity (% RH) and 40 ^{o}C. No change in drug

physical characteristics and no drug recrystallization was reported. They suggested this was due to a combination of drug nano-confinement in the pores and the interaction between drug and the silanol groups stabilising the system (158). A second study reported that drug loaded silica samples displayed no evidence of recrystallization after six months of storage at 25 ^{o}C and 52 %RH (55). Enhanced drug dissolution profiles were also maintained on storage, indicating the physical stability of the samples was preserved. The silica's average pore diameter was retained on storage but the surface area and microporosity had decreased slightly. The drug-free silica samples had absorbed water over the six-month time-frame but the drug loaded samples displayed little water uptake. This was attributed to the presence of hydrophobic drug molecules on the surface of the silica. Mellaerts *et al* investigated the stability of itraconazole loaded SBA-15 over 12 months at 4 ^{o}C and 25 ^{o}C and relative humidities of 0 %, 52 % and 97 %. They reported that storage at relative humidity of 0 % for twelve months maintained the original release behaviour of the formulation. At the higher relative humidity levels, a higher supersaturation level than that of the original formulation was achieved. The authors suggested this was due to hydroxylation of the SBA-15 surface which results in a more hydrophilic surface which facilitates drug release upon competitive adsorption of water molecules from simulated gastric fluid. The drug loaded samples displayed little variation in pore size compared to drug free samples (76).

The chemical stability of drugs loaded onto mesoporous silica materials also requires consideration. Some recent studies have described problematic chemical degradation of drug samples during storage under stressed conditions. Kinnari *et al* reported that itraconazole loaded onto mesoporous silica had degraded after

months of storage at 40 ^{o}C and 70 % RH. The differential scanning calorimetry (DSC) results presented no evidence of recrystallization. They suggested that certain functional groups in the drug molecule reacted with the silica surface resulting in chemical degradation (90). This contrasts with results from previous work which examined ibuprofen loaded silica on storage and demonstrated no evidence of chemical degradation (198). This suggests the effect may be drug specific as it depends on particular functional groups interacting with the silica surface. Limnell *et al* also observed chemical degradation of indomethacin loaded onto MCM-41 and SBA-15 during storage over 3 months at 30 ^{o}C and 56 %RH (199). One out of the ten drugs loaded onto SBA-15 by Van Speybroeck *et al* displayed chemical degradation when tested (55).

Research has also examined the complex effects of moisture on the stability of mesoporous silica formulations (159, 200-202). Qian *et al* reported that moisture could both suppress the amorphization capacity of drug molecules loaded on mesoporous silicon dioxide and reverse an already amorphous formulation. However, the presence of co-adsorbed water molecules has also been demonstrated to improve drug release (203). Exposure to moisture can result in siloxane bond fractures which have been found at normal processing conditions (159).

The presence of moisture can also affect the chemical stability of the loaded drug. Water can be involved as a reactant or a product in a drug degradation reaction, influence the polarity of amorphous matrix, serve as a medium for proton transfer and increase molecular mobility due to its plasticizing effect (200, 204, 205). As a consequence of moisture's potential effects on drug physical and chemical stability,

it is recommended that humidity during processing and storage needs to be controlled in the preparation of mesoporous silica formulations (200). Further investigation is required to fully understand the effect of moisture content on mesoporous silica formulations and the competitive role it plays in the interaction between drug and silica surface, its potential impact on drug chemical stability and the mechanism in which it can alter drug release from silica carriers.

2.7. Drug release

2.7.1. Release mechanism studies

The classic Higuchi equation has been used to describe drug release where fine drug particles are dispersed in a thin film consisting of an inert, non-soluble and non-swellable matrix former, at an initial drug loading which is much higher than drug solubility in the matrix (Equation (2.1)) (14)

$$M_t = A\sqrt{2C_{ini}DC_s t} \qquad Equation\ (2.1)$$

where M_t is the cumulative amount of drug released from the film at time t; A denotes the surface area exposed to the release medium; C_{ini} is the initial drug concentration, which is much higher than the solubility of the drug in the matrix former, C_s; D is the diffusion coefficient of the drug in the matrix former.

It has been reported that the Higuchi equation is applicable to the drug/mesoporous system (136, 170). This equation suggests the interaction of dispersion medium with the drug-silica matrix is dependent on factors such as porosity, the initial drug load, the drug's solubility in the release medium and the diffusion coefficient of the drug

molecules in the medium (206, 207). However, it has been widely demonstrated that mesoporous silica drug release can deviate from this relationship and that the drug release process comprises of a two-step profile (90, 117, 151). Xue *et al* suggested this two-step release profile is observed as drug molecules can bind both physically and chemically to the mesoporous silica. The physically entrapped drug is released quickly which provides a sharp initial burst release profile. The slower release in the second part of the process is due to drug bonded to the silica *via* hydrogen bonding with the silanol groups. Drug release rate is controlled by the equilibrium between drug bonding to the silica and drug interaction with the dissolution medium (117). It has also been proposed that drug molecules located near the surface are released quickly due to their proximity to the dissolution medium and that drug molecules located deeper in the pores are released much more slowly (55, 90, 189). Figure 2.3 illustrates the potential sites for drug distribution throughout the mesoporous silica matrix.

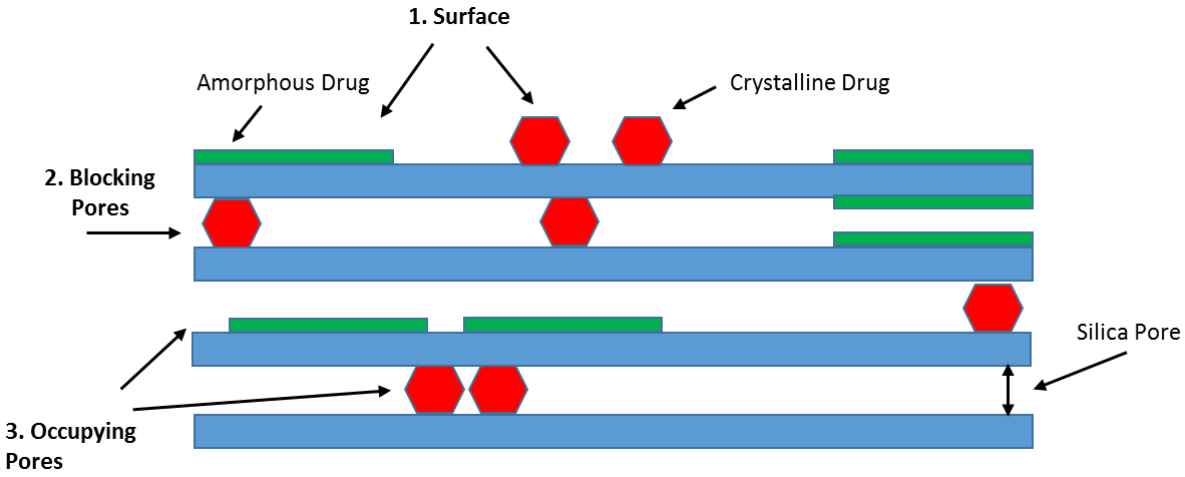


Figure 2.2 Schematic illustration of potential sites for drug distribution throughout the silica matrix

The ability of mesoporous silica to readsorb drug molecules after release is a factor to consider in the drug release profile. Mesoporous silica has been investigated as an adsorbent for chemical removal from wastewater of pharmaceutical industrial manufacturers (118). It was reported that drug molecules could adsorb both reversibly and irreversibly onto the silica surface which has potential implications for drug delivery formulation development. *Bui et al* suggested the strength of interaction between the silica and drug functional groups is implicated in this process. Furthermore, Turku *et al* reported irreversible adsorption of tetracycline onto silica. Approximately 9% of the tetracycline loaded onto the silica was irreversibly adsorbed onto the silica surface, whereas the remainder exhibited Langmuir behaviour (208).

Incomplete release of drug from mesoporous systems has been noted in several studies. Ahern *et al* reported a maximum of 70-80 % fenofibrate release from mesoporous silica formulations (Figure 2.4) (209). Incomplete release of vancomycin

and cefuroxime from various silica carriers has also been observed. The authors attributed this to strong interactions with surface functional groups and hindered diffusion of drug molecules through nano-sized windows that connect spherical mesopores (194). This property of mesoporous silica should be considered during future formulation development.

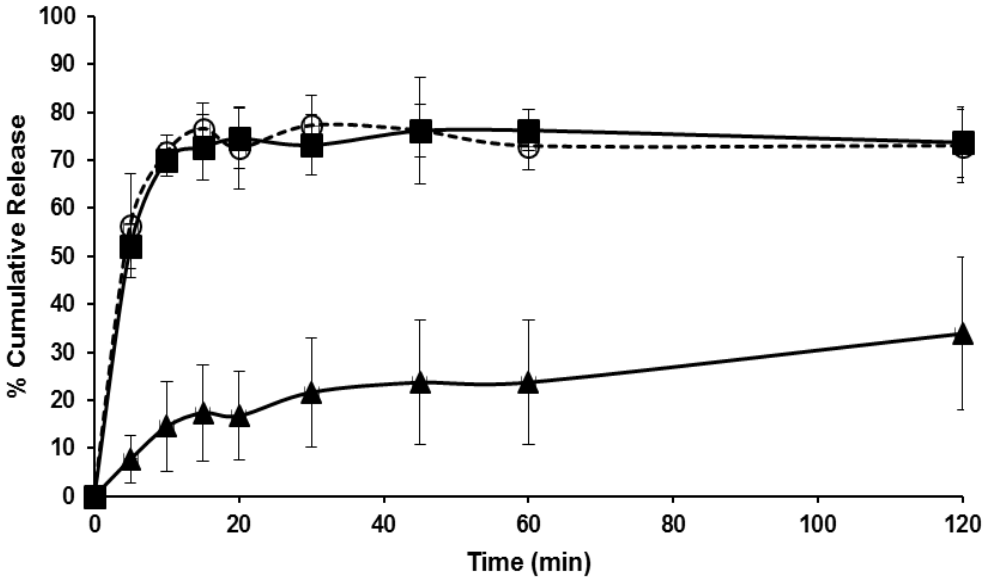


Figure 2.3 Fenofibrate release profiles from mesoporous silica formulations (○ with dashed line) solvent impregnation, (▲) physical mix method and (■) SC-CO_2 sample in 0.3 % w/v SDS in 0.1 M HCl media (mean ± SD, n = 9) (data sourced from thesis entitled 'Application of mesoporous silica for the oral delivery of poorly water soluble drugs' Ahern (209))

It has been observed that pH has a significant influence on drug interaction with the silica surface (118, 208). Adsorption of drugs onto silica can be due to both electrostatic and non-electrostatic interactions. The surface charge of silica is determined by the relative concentrations of H^+ and OH^- groups, originating from the

protonation and deprotonation reactions of the silanol group. The isoelectric point of silica is reported to be approximately pH 2. The proportion of negative charges remains low below pH 6, and increases sharply between pH 6 and 11 (210). Depending on the nature of the drug molecule (acidic or basic), it will be positively or negatively charged at specific pHs. This will influence its interaction with the silica surface and the adsorption/desorption equilibrium. To illustrate this point, Turku *et al* reported that the irreversible adsorption capacity of the silica surface is strongly dependent on the pH of the solution (208).

The influence of co-adsorbed water on adsorption, hydrophobic aggregation and migration in SBA-15 pores also warrants consideration in mesoporous silica formulation development as the drug delivery process takes place in an aqueous environment. Mellaerts *et al* examined the effect of co-adsorbed water on itraconazole drug loading and release. They observed that at a low SBA-15 hydration level, itraconazole was involved in multiple hydrogen bonding interactions with the pore walls of the SBA-15. With increasing co-adsorbed water content, water molecules aggregate between the drug molecules and the silica surface and decrease host-guest interaction. The rate of itraconazole release was enhanced with increasing co-adsorbed water content. The distribution of a hydrophobic molecule, Nile Red, in SBA-15 was also examined in the presence of high and low concentrations of co-adsorbed water. They reported a higher density of co-adsorbed water molecules resulted in a rapid influx of water molecules in the dissolution medium producing a more complete release of guest molecules (203).

2.7.2. Role of Supersaturation

The generation of an amorphous drug state in mesoporous silica systems is utilised to create a supersaturated solution which can be a means of improving oral bioavailability of poorly water-soluble drugs. Drug in supersaturated solutions exists at a concentration above their saturation solubility which represents a thermodynamically unstable state (Section 1.5). However, if the solution can be maintained in this metastable state in the gastrointestinal tract for a period of time to allow for absorption, the increased drug concentration can permit enhanced transport across the intestinal wall.

Supersaturated drug levels generated by rapid release from the mesoporous silica system can lead to drug precipitation and the conversion of drug molecules to an energetically more favourable but less soluble form that can impede absorption (59). Van Speybroeck *et al* investigated the use of a precipitation inhibitor to improve the oral absorption of itraconazole from a drug-mesoporous silica system (28). They conducted both *in vitro* and *in vivo* tests and determined that hydroxypropylmethylcellulose (HPMC) proved to be a good stabiliser of itraconazole supersaturation in intestinal media and resulted in more than a 60 % increase in absorption compared to a mesoporous silica formulation without precipitation inhibitor. Their findings highlight the importance of picking the appropriate precipitation inhibitor as hydroxypropylmethylcellulose acetate succinate (HMPCAS) was ineffective *in vivo* as it is not soluble in the stomach. A drawback of precipitation inhibitors is that they tend to be chosen on an empirical basis and structure-activity relationships have not been established (211). It is therefore useful to also consider

other methods to stabilize the rate of drug supersaturation *in vivo*. Another approach, taken by Van Speybroeck *et al,* was to decrease the drug release rate by decreasing the silica pore size. This slows down the rate of supersaturation and can prevent the drug from precipitating out of solution in the intestinal fluid. Their research involved the use of three ordered mesoporous silica materials with different pore diameters to improve the extent of fenofibrate absorption. The silica with the narrowest pore diameter produced the slowest drug release rate. As a consequence, the rate of supersaturation was decreased and fenofibrate *in vivo* absorption was improved (181).

Van Speybroeck *et al* also investigated the way in which drug supersaturation state can be harnessed to enhance certain aspects of the drug release process. It was demonstrated that by preventing early drug release in the stomach, the total absorption of the poorly water soluble drug, glibenclamide, could be enhanced *in vivo* compared to a commercially available product (164). It has also been reported that a mesoporous silica system can produce a pH independent supersaturation effect for the basic drug itraconazole. This negates the need for preceding dissolution in the stomach and allows for enhanced systemic absorption. This finding indicates there is potential for this formulation to result in more reproducible systemic exposure compared to commercially available products (71).

2.8. Conclusion

Scientific advances in the field of mesoporous silica oral drug delivery have experienced remarkable growth over the past ten years. This extensive review highlighted the advances made in research concerning drug loading methods, surface functionalisation and understanding of silica pore properties. An area which requires further research is the mechanism of drug release from mesoporous silica materials. This review highlighted several studies demonstrating incomplete release from mesoporous silica formulations. The reasons behind these incomplete release profiles are not well understood. Furthermore, it has been demonstrated in other research fields that drug molecules can passively adsorb on the silica surface. The implications of this observation for drug release from loaded silica materials requires consideration. These findings form the basis for the research hypothesis for this thesis (Section 1.7) and are investigated in detail in research chapters 4 – 6.

Chapter 3: Role of Drug Adsorption onto the Silica Surface in Drug Release from Mesoporous Silica Systems

Modified Version of Publication:

McCarthy CA, Ahern RJ, Devine KJ, Crean AM. Role of Drug Adsorption onto the Silica Surface in Drug Release from Mesoporous Silica Systems. Molecular Pharmaceutics. 2018; 15(1):141-9.

3.1 Abstract

As highlighted from the review of the literature in Chapter 2, factors contributing to incomplete drug release from mesoporous silica formulations are not well understood. This study aimed to address this gap in knowledge by exploring the role of drug adsorption onto silica substrates during the drug release process in dissolution media. Adsorption isotherms were generated to understand drug adsorption behaviour onto the silica surface. Two silica materials were selected (SBA-15 (mesoporous) and Aerosil®200 (non-porous)) to investigate the influence of porous architecture on adsorption and release processes. The ability of the dissolution medium to wet the silica surface, particularly the porous network, was investigated through the addition of a surfactant to the dissolution medium. The results demonstrated that a larger amount of drug was bound/m^2 to the non-porous surface than to the mesoporous material. Adsorption isotherms proved useful in understanding drug adsorption and release behaviour for the non-porous silica formulation. However, the quantity of drug remaining on the mesoporous silica surface after dissolution was significantly higher than the amount predicted using adsorption isotherm data. These results suggest that a fraction of loaded drug molecules were tightly bound to the silica surface or attached to sites which are inaccessible for the dissolution media. The presence of surfactant (sodium dodecyl sulphate) in the media enhanced drug release from the silica surface. This behaviour can be attributed to both the improved wetting characteristics of the media and adsorption of the surfactant to the silica surface. The findings of this study reinforce the significance of the role that silica porous architecture plays in the dissolution

process and indicates that accessible surface area is an important parameter to consider for mesoporous systems in relation to drug release.

3.2 Introduction

As described in Chapters 1 and 2, drug release from mesoporous silica formulations is not fully understood. Incomplete *in vitro* drug release from these systems has been widely reported in the literature (55, 88, 116). However, the factors contributing to these observations in dissolution experiments, performed under sink conditions, have not been elucidated. A study by Bui et al. explored the use of mesoporous silica materials as adsorbents for chemicals found in pharmaceutical wastewater (118). They determined that some drug molecules could bind irreversibly onto the silica surface. However, the impact of this irreversible drug binding on the release of drug from mesoporous silica formulations has not been considered in the literature to date.

The aim of this study was to elucidate the role of drug adsorption, onto porous and non-porous silica substrates, during drug release from these systems. Adsorption isotherms were generated to understand drug adsorption onto the silica surface. This equilibrium process describing drug bound to the silica surface and drug existing in solution emerged as a significant factor in gentamicin release from a silica carrier in a study by Xue *et al* (117). In this work, sulphamethazine (Sz) was chosen as the model drug. Sulphamethazine has the potential to form amine-hydroxyl hydrogen bonds with the silica surface (117). Two silica substrates were selected (SBA-15 (mesoporous) and Aerosil®200 (non-porous)) to investigate the influence of porous architecture on the adsorption process. The extent of passive drug adsorption was quantified and compared with drug retained during dissolution experiments to

determine whether isotherms can predict the extent of drug release from these formulations.

The ability of the dissolution medium to influence drug adsorption and release was considered through the addition of a surfactant to the dissolution medium. Sodium dodecyl sulphate (SDS), an anionic surfactant, was chosen as it is a common excipient added to dissolution media and formulations to improve the wetting characteristics and the solubilisation of drug molecules (27, 212-214). Sulphamethazine dissolution from Sz/silica systems in 0.1 M HCl media was compared with drug dissolution in media containing surfactant to determine if improved dissolution media wetting capability of the silica surface can enhance drug release from silica formulations.

3.3 Materials and Methods

3.3.1 Materials

SBA-15 was obtained from Glantreo Ltd. (Ireland). Aerosil®200 Pharma was sourced from Evonik Industries (Germany). Silica surface and pore properties were obtained from suppliers (Table 3.1). Sulphamethazine (Sz) and sodium dodecyl sulphate (SDS) (>98.5 %) were purchased from Sigma Aldrich (Ireland). Liquid carbon dioxide was supplied by Irish Oxygen Ltd (Ireland). All other chemicals and solvents were of analytical grade or HPLC grade and purchased from Sigma-Aldrich (Ireland).

Table 3.1 Properties of silica materials obtained from suppliers

Silica Material	Porosity	Particle Size (µm)	Surface Area (m^2)	Pore Volume (cm^3)	Pore Diameter (Å)
SBA-15	Mesoporous	30	678.57 ± 8.23	0.64 ± 0.02	51.85 ± 0.05
Aerosil®200	Non-porous	12	200.00 ± 25.00	N/A	N/A

3.3.2 Surface Tension Measurements

Surface tension was determined experimentally using a KRUSS processor tensiometer K12 (KRUSS GmbH, Germany) with a platinum Wilhelmy plate. The plate was washed with deionised water, followed by an ethanol wash and subsequently flamed over a Bunsen burner after each measurement. All measurements were performed at 37 ^{o}C which was maintained with the HAAKE water bath (Thermo Fisher

Scientific Inc., USA). Full independent replicates were performed in triplicate. Critical micellar concentrations (CMC) of SDS in deionised water and 0.1 M HCl were determined by analysing changes in surface tension over the surfactant concentration range investigated.

3.3.3 Solubility Measurements

Solubility studies were performed in triplicate through the addition of excess sulphamethazine (Sz) to 10 ml of buffer media (0.1 M HCl) using a standardised shake-flask method with a total shaking time of 48 h at 37 ^{o}C. Samples (2 ml volume) were removed at 24 h and 48 h time points and centrifuged at 16,500 *g* for 13 min using a Hermle z233M-2 fixed angle rotor centrifuge, (HERMLE Labortechnik GmbH, Germany). The supernatant was removed and centrifuged again under the same conditions. The resultant supernatant was analysed using HPLC following dilution with mobile phase.

3.3.4 Adsorption Studies

Sulphamethazine adsorption studies were performed in screw-capped glass vials containing 100 mg of silica (SBA-15 or Aerosil®200) in 20 ml of Sz solution at a defined concentration in buffer (0.1 M HCl, pH 1.2). Experiments were conducted under the same conditions as solubility measurements i.e. shake-flask conditions for 24 h at 37 ^{o}C. At 24 h, samples (2 ml) volume were removed and centrifuged at 16,500 *g* for 13 min using a Hermle z233M-2 fixed angle rotor centrifuge, (HERMLE Labortechnik

GmbH, Germany). The supernatant was removed and centrifuged again under the same conditions. The resultant supernatant was analysed using HPLC following dilution with mobile phase.

Adsorption studies were also conducted under the same conditions in the presence of a surfactant (sodium dodecyl sulphate (SDS)) at two defined concentrations, 10 mM SDS and 50 mM SDS. These concentrations were chosen as they reflect the range of concentrations approved for SDS by the U.S. Food and Drug Administration (FDA) Dissolution Methods (215). An isotherm was generated by plotting the concentration of drug (mM) in solution at 24 h (x-axis) versus the quantity of drug adsorbed (mmol) per gram or per m^2 of the silica carrier (y-axis). Linearized forms of the Langmuir (216) and Freundlich (217) isotherms were applied to the experimental data and the parameters determined are detailed in Table 3.2.

Table 3.2 Linearized forms of Langmuir and Freundlich isotherms

Name	Linearised Form	Plot	Parameters
Langmuir	$F/B = (1/K_L.Nt) + F/Nt$	F *versus* F/B	K_L = slope/intercept N_t = 1/slope
Freundlich	$mlogF = logB + K_F$	log F *versus* log B	K_F = intercept m = slope

where B is the concentration of drug adsorbed to the silica surface, F is the concentration of free substrate in solution at equilibrium, N_t is the total number of binding sites and K_L *and* K_F are related to the average binding affinity

3.3.5 Preparation of Sulphamethazine Loaded Silica Formulations

Sulphamethazine loaded silica formulations were prepared according to the method previously described by Ahern *et al* (88). The drug and silica material were combined at a ratio of 1 mg SZ: 3 m^2 silica (SBA-15 or Aerosil®200) in a BC 316 high-pressure reactor (High Pressure Equipment Company, USA) and stirred using a magnetic stirring. The reactor was heated to 40 °C using heating tape and maintained at this temperature for the duration of the experiment. Temperature was monitored using a temperature monitor (Horst GmbH, Germany). The reactor cell was filled with liquid CO_2 and a high pressure pump (D Series Syringe Pump 260D, Teledyne ISCO, USA) was used to pump additional CO_2 to a final processing pressure (27.58 MPa). After 24 h, the cell was depressurised rapidly by venting the CO_2. The processed material was collected from the cell and stored in a desiccator prior to analysis.

3.3.6 Drug Content Quantification

The sulphamethazine content of the silica formulations was determined by thermogravimetric analysis (TGA), using a TGA 500 instrument (TA Instruments Ltd., United Kingdom). Samples in the weight range 2–10 mg were loaded onto tared platinum pans and heated from ambient temperature to 900 °C, at a heating rate of 10 °C/min under an inert N_2 atmosphere. Samples were analysed in triplicate. The drug quantity was calculated based on the weight loss between 100 and 900 °C, corrected for the weight loss over the same temperature range for a silica reference sample (55). TGA thermograms were analysed using Universal Analysis 2000 software (TA Instruments Ltd., United Kingdom). Figure 3.1 (a) below shows the TGA

plot for unprocessed Sulphamethazine. At 900°C weight loss of the unprocessed drug is 100%. Figure 3.1 (b) shows weight loss for the unprocessed SBA-15. Weight loss from 100°C to 900°C is 3.6%.

(a) (b)

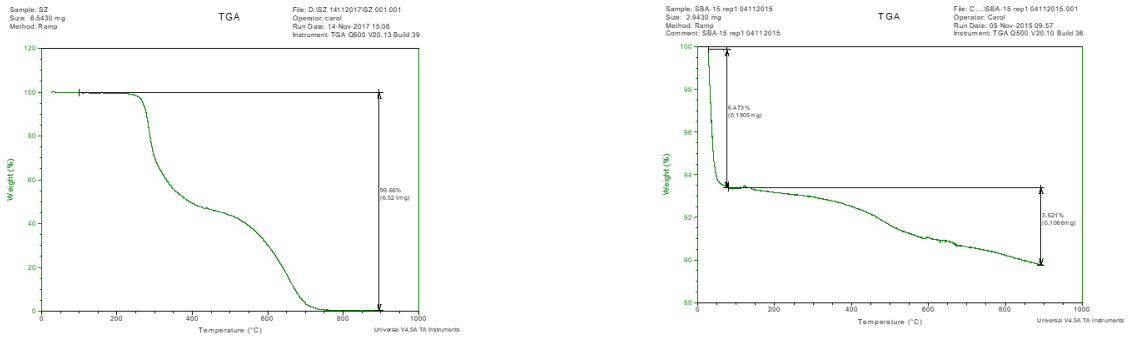


Figure 3.1 TGA profiles for degradation of (a) sulphamethazine and (b) SBA-15 over a temperature range of 100 – 900 °C.

Drug-loading efficiency was calculated using Equation 3.1:

$$Drug\ loading\ efficiency\ (\%) = \frac{Actual\ drug\ loading\ (mg)}{Theoretical\ drug\ loading\ (mg)} * 100 \qquad Equation\ (3.1)$$

The theoretical drug-loading was based on mass fraction of drug and silica used to prepare samples.

3.3.7 Dissolution Studies

Dissolution studies were performed in triplicate using USP II apparatus (Erweka® DT600 dissolution test system (ERWEKA GmBH, Germany)) in 500ml buffer (0.1 M HCl, pH 1.2) at 37 ± 5°C with a paddle rotation of 50 rpm. Sink conditions were employed for all dissolution experiments. A fixed mass of unprocessed drug (150 mg) or a mass of drug-silica formulation equivalent to 150 mg of drug was added to the

dissolution medium. Samples of 4 ml volume were withdrawn at 1, 5, 10, 15, 30, 60 and 120 min intervals with an additional sample taken at the 24 h time point. Samples were immediately replaced with an equal volume of fresh, pre-warmed medium. The withdrawn samples were centrifuged at 16,500 *g* for 13 min using a Hermle z233M-2 fixed angle rotor centrifuge, (HERMLE Labortechnik GmbH, Germany). The supernatant was removed and centrifuged again under the same conditions. The resultant supernatant was analysed using HPLC following dilution with mobile phase.

Dissolution studies were repeated as above with the addition of surfactant (SDS) to the dissolution media at two concentrations (10 mM and 50 mM).

3.3.8 HPLC Analysis of Sulphamethazine and Sodium Dodecyl Sulphate

Reversed phase high performance liquid chromatography (HPLC) was performed using an Agilent 1200 series HPLC system (Agilent Technologies, USA) equipped with both a Photo Diode Array Detector (DAD) and an Evaporative Light Scattering Detector (ELSD) in series. To quantify drug content in adsorption and dissolution studies without surfactant a reversed-phase column Kinetex C-18 column (150 mm × 4 mm) with internal pore width 2.6 µm (Phenomenex Ltd., United Kingdom) was utilised. An isocratic HPLC-DAD (diode array detector) technique adapted from a method by Ding *et al* (218) with a mobile phase consisting of acetonitrile – water – acetic acid (25:75:0.05), an injection volume of 50 µL and a flow rate of 1 $ml.min^{-1}$ at ambient temperature was employed. The detection wavelength was 265 nm. The retention time for sulphamethazine was 5.9 min.

To quantify both drug and surfactant concentrations in adsorption and dissolution studies, a HPLC-ELSD method adapted from Im *et al* (219) was utilised. The ELSD system was operated with an evaporative temperature of 80 ^{o}C, a nebulizer temperature of 70 ^{o}C and a N_2 gas flow rate of 1.0 L.min^{-1}. A reversed-phase column Prodigy ODS-3 column (150 mm × 4.6 mm) with internal pore width 5 µm (Phenomenex Ltd., United Kingdom) was utilised. Drug and surfactant were separated using a mobile phase gradient which consisted of two solutions: eluent A (water (25 mM ammonium acetate)) and B (acetonitrile). The gradient program started with 5 % eluent B for 2 min, followed a 6 min gradient up to 95 % eluent B. The column was then equilibrated with starting conditions for 2 min before the next injection. The flow rate was 1 ml.min^{-1} with an injection volume of 10 µL. Column temperature was set to 30 ^{o}C. The retention time for sulphamethazine and sodium dodecyl sulphate was 5.9 min and 7.4 min, respectively.

3.3.9 Pore Size Analysis of Mesoporous Silica Systems Before and After Dissolution

Pore size analysis by nitrogen (N_2) adsorption of the mesoporous sulphamethazine-SBA-15 formulation was carried out using a Gemini VI surface area and pore size analyser (Micromeritics, USA). Aerosil®200 is a non-porous silica material so porosity analysis was not undertaken. The samples were degassed overnight at 100 °C in a FlowPrep 060 sample degas system (Micromeritics, USA) prior to analysis. During analysis, liquid N_2 at −196 °C maintained isothermal conditions. The mesopore

volume along with mesopore width were calculated using the Barrett–Joyner–Halenda (BJH) adsorption correlation (220). Samples were analysed in duplicate.

3.3.10 Statistical Analysis

All statistical analyses were conducted using Microsoft Excel 2013 (Microsoft, USA) and GraphPad Prism (ver. 5, GraphPad Software Inc., USA). Results are expressed as mean ± standard deviation. *In vitro* dissolution and adsorption isotherm data comparing both formulations at different time points and concentrations, respectively, were tested for significance using a two-tailed, independent sample t-test, assuming Gaussian distribution and equal variance ($p < 0.05$ was considered significant).

3.4 Results

3.4.1 Sulphamethazine (Sz) Loading Efficiency

Sulphamethazine was loaded onto both silica substrates at a theoretical ratio of 1 mg SZ/ 3 m^2 silica surface area. Sulphamethazine loading onto SBA-15 was 190 mg/g silica corresponding to a drug loading efficiency of 75.86 % (calculated using Equation 3.1). SZ drug loading onto Aerosil®200 was 60 mg/g silica, equivalent to an 88.62 % loading efficiency. These results are in line with loading efficiencies previously reported using SC-CO_2 methods (88).

3.4.2 Solubility Studies

SDS increases the solubility of some drugs above its CMC (critical micellar concentration) (221). In this study, the CMC of SDS in both deionised water and 0.1 M HCl were determined. The CMC of SDS in deionised water at 37 ^oC was 7.3 mM (0.21 % w/v), while in 0.1 M HCl solution at 37 ^oC it was 0.8 mM (0.023 %). Therefore, both concentrations of surfactant investigated in this study (0.3 % w/v and 1.44 % w/v) were above the CMC in 0.1M HCl. Drug solubility (mM) in each of the adsorption/dissolution media are as follows; 0.1 M HCl as 30.00 ± 1.80, 0.1 M HCl 10 mM SDS as 30.28 ± 0.97 and 0.1 M HCl 50 mM SDS as 38.80 ± 0.40. Sz solubility in 0.1 M HCl and 0.1 M HCl with 10 mM SDS (0.3 % w/v) were not significantly different. At the higher concentration of surfactant (50 mM SDS (1.44 % w/v)), Sz solubility (38.80 ± 0.40 mM) was significantly higher than in the other two media ($p < 0.01$). However,

Sz solubility enhancement in the presence of both concentrations of SDS was considered marginal.

3.4.3 Adsorption Studies

3.4.3.1 Sulphamethazine Adsorption onto Silica in 0.1 M HCl Medium

Adsorption isotherms for sulphamethazine adsorption onto SBA-15 and Aerosil®200, at the 24 h time point, in 0.1 M HCl at 37 ^{o}C, are displayed in Figure 3.2 as both *mmol Sz/g silica* adsorbed and *mmol Sz/m^2 silica* adsorbed. Drug adsorption onto the Aerosil®200 non-porous surface levelled off. In contrast, adsorption onto the mesoporous surface increased with increasing drug concentration. There was more drug bound per *m^2* to the non-porous silica surface than the mesoporous SBA-15, indicating the drug cannot access the porous network in its entirety.

Adsorption data for the porous and non-porous silica systems were fitted to the Langmuir and the Freundlich adsorption models (Table 3.3). While both models were capable of describing the data for both silica substrates (R^2 > 0.90), the Langmuir model emerged as the best-fit for the adsorption of Sz onto non-porous Aerosil®200. In contrast, drug adsorption onto mesoporous SBA-15 was best described by the Freundlich model. The Langmuir model parameters were calculated for both silica substrates. The number of binding sites on the surface (N_t (mmol/m^2)) was determined to be greater for the non-porous Aerosil®200 than SBA-15, indicating that drug molecules cannot access the full extent of the SBA-15 porous architecture. The binding affinity (designated as K_L (mM)) of drug to the silica surface was

equivalent for both the mesoporous material and the non-porous Aerosil®200 (*adsorbed Sz mmol/m^2 silica*). Freundlich model parameters were also calculated for both substrates and are displayed in Table 3.3. The heterogeneity index (*m*) is defined over a range of 0 to 1 with values closer to 1 describing a more homogenous system. The non-porous material exhibited the most homogenous surface of the two materials. The Freundlich equation binding affinity parameter (K_F (mM)), revealed stronger binding affinities between the drug and the non-porous surface.

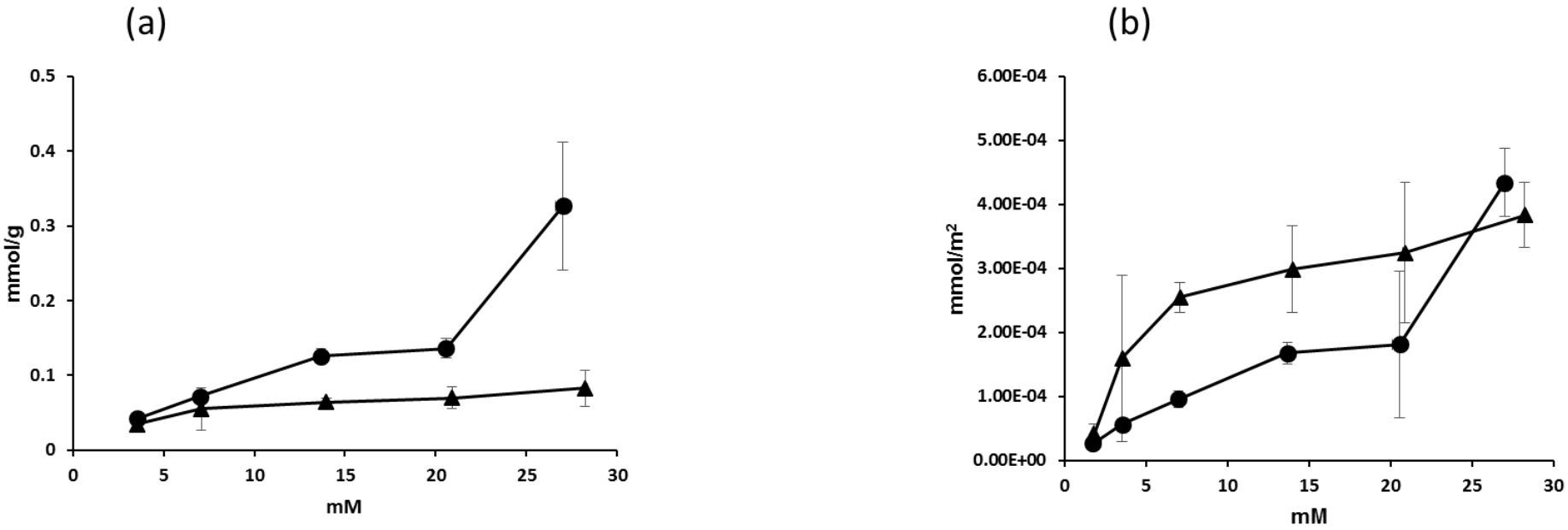


Figure 3.2 Adsorption isotherms for Sz adsorption ((a) mmol Sz /g silica and (b) mmol Sz/m^2 silica) onto SBA-15 (●) and Aerosil®200 (▲) at 24 h, 37 °C in 0.1 M HCl (n=3, X and Y error bars indicate standard deviation)

Table 3.3 Isotherm parameters obtained by fitting Sz and SDS adsorption data (mmol/m^2) onto SBA-15 and Aerosil®200 to Langmuir and Freundlich isotherms (SDS adsorption data only produced an acceptable fit with Freundlich isotherm). Measure of data fit to model is indicated by the R^2 value.

Sulphamethazine			
Langmuir Isotherm	**N_t (mmol/m^2)**	**K_L (mM)**	**R^2**
SBA-15	0.04	0.0004	0.95
Aerosil®	0.15	0.0004	0.99
Freundlich isotherm	**m**	**K_F (mM)**	**R^2**
SBA-15	0.50	5.66	0.98
Aerosil®	0.70	8.09	0.91
Sodium Dodecyl Sulphate			
Freundlich isotherm	**m**	**K_F (mM)**	**R^2**
SBA-15	0.53	10.70	0.98
Aerosil®	0.77	6.72	0.95

3.4.3.2 SDS Adsorption onto Silica in 0.1 M HCl Medium

The isotherm for SDS adsorption onto both silica substrates in 0.1 M HCl at 37 ^oC is presented in Figure 3.3. The quantity of surfactant adsorbed onto both silica materials was similar in magnitude to the quantity of drug adsorbed under the same experimental conditions (Figure 3.2 (b) *versus* Figure 3.3). For SBA-15, a correlation of $r = 0.83$ ($p < 0.04$) between surfactant and drug adsorption was determined while the correlation of adsorption on the non-porous surface was stronger at $r = 0.88$ ($p < 0.02$). The Freundlich adsorption model emerged as the best-fit model for SDS adsorption onto both substrates ($R^2 \geq 0.95$, Table 3.3). The Freundlich binding affinity

for the surfactant with the mesoporous SBA-15 was stronger than that of the drug molecule. This is most likely a result of the surfactant's ability to reduce interfacial tension leading to improved pore wetting and access to additional binding sites in the porous network.

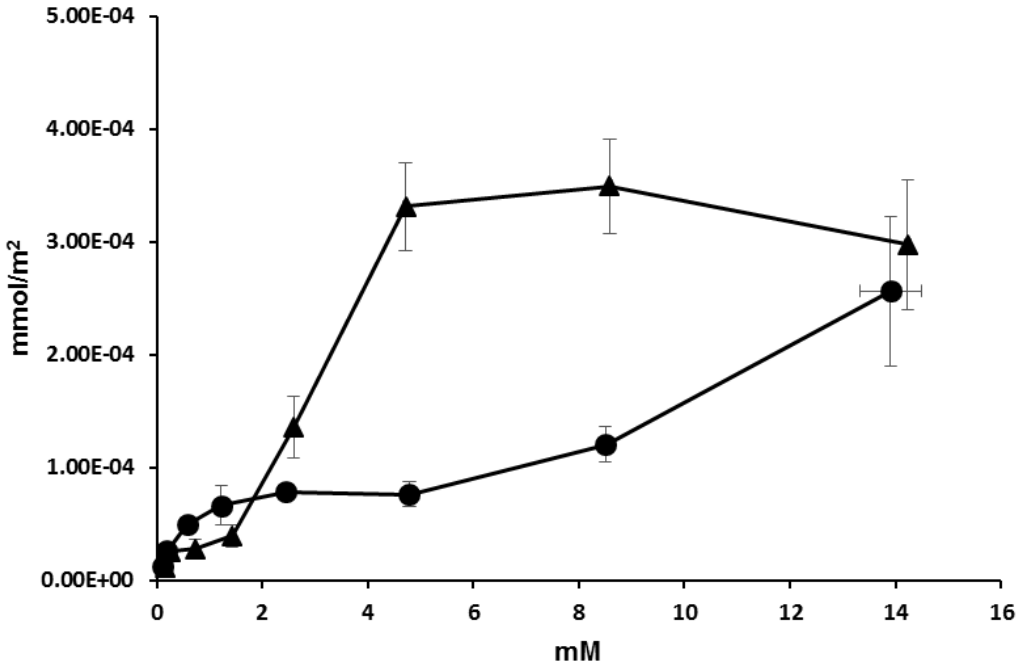


Figure 3.3 Adsorption isotherms for SDS adsorption (mmol SDS/m^2 silica) onto SBA-15 (●) and Aerosil (▲) at 24 h, 37 °C in 0.1 M HCl (n=3, X and Y error bars indicate standard deviation)

3.4.3.3 Sulphamethazine Adsorption onto Silica in 0.1 M HCl/SDS Media

Adsorption isotherms for sulphamethazine adsorption (*mmol SZ/m^2silica*) onto SBA-15 and Aerosil® at 24 h in media with 0.1 M HCl (10 mM SDS) and 0.1 M HCl (50mM SDS) at 37 ^oC are displayed in Figure 3.4. There is significantly less drug adsorbed onto both silica materials in the presence of surfactant at both SDS concentrations investigated. Similar to drug adsorption in 0.1 M HCl media without surfactant (Figure 3.2), the non-porous Aerosil® adsorbed a larger fraction of drug/m^2 than the mesoporous material. As this experiment involved a multi-component system where drug and surfactant are simultaneously adsorbing onto the silica surface, data was not fit to the Freundlich and Langmuir adsorption models.

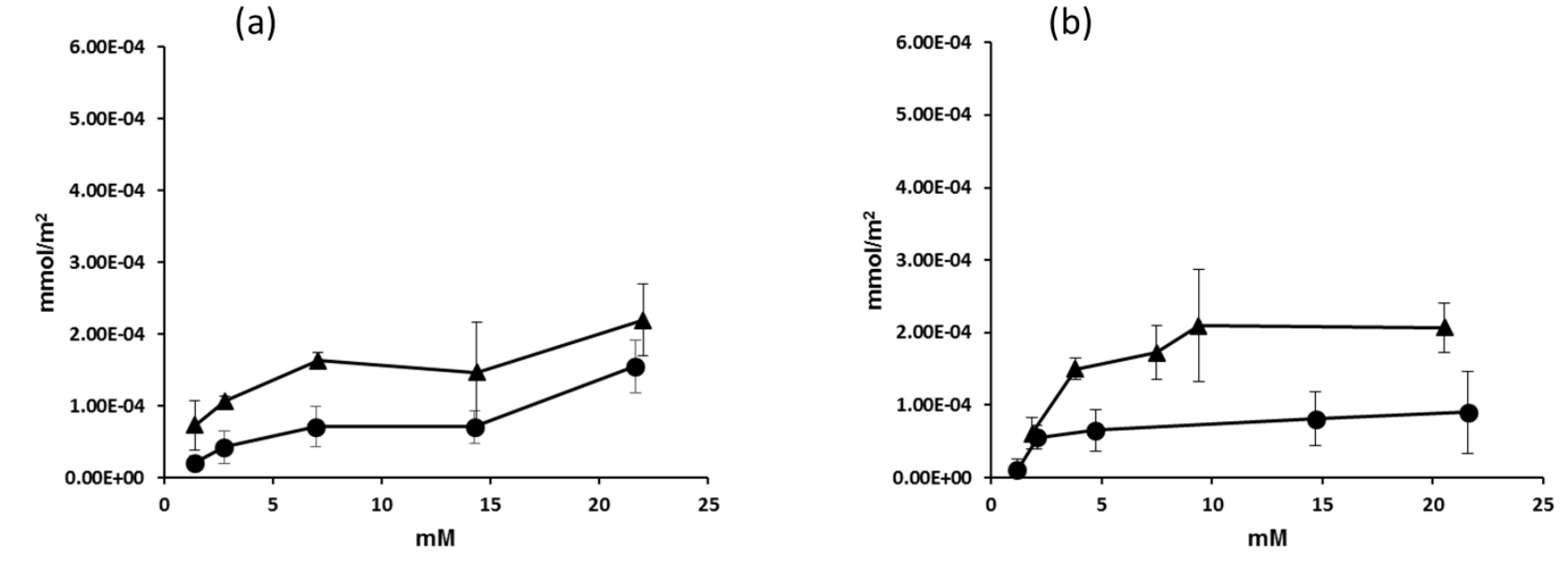


Figure 3.4 Adsorption isotherms for Sz adsorption (mmol Sz /m^2 silica) onto SBA-15 (●) and Aerosil (▲) at 24 h, 37 °C in (a) 0.1 M HCl (10 mM SDS) and (b) 0.1 M HCl (50 mM SDS) (n=3, X and Y error bars indicate standard deviation)

3.4.4 Dissolution Studies

Dissolution experiments were conducted in the same three media as used for adsorption experiments. Experiments were conducted under sink conditions and the theoretical Sz concentration following 100 % release was < 4% the Sz solubility in all cases (Table 3.4). Drug release observed followed a typical immediate release profile in all media investigated.

Table 3.4 Solubility and dissolution parameters for unprocessed Sz and Sz loaded silica formulations in the three dissolution media investigated (mean ± standard deviation is provided, n=3)

Dissolution Medium	Solubility	Dissolution	Dissolution (% Cumulative Release)				
	Solubility of Drug (mM)	% Saturated Solubility assuming 100% release	Sample	5 min	10min	15 min	24 h
0.1 M HCl	30.00 ± 1.80	3.60	*Unprocessed SZ*	25.61 ± 4.34	51.86 ± 5.02	82.41 ± 5.56	97.26 ± 1.80
			SZ loaded SBA-15	74.03 ± 7.21	76.06 ± 7.53	74.55 ± 6.10	79.58 ± 2.08
			SZ loaded Aerosil®	70.10 ± 0.35	73.47 ± 0.83	74.17 ± 0.38	77.21 ± 0.01
0.1 M HCl 10 mM SDS	30.28 ± 0.97	3.56	*Unprocessed SZ*	98.65 ± 1.04	97.77 ± 0.40	97.10 ± 0.18	97.55 ± 1.02
			SZ loaded SBA-15	90.20 ± 0.65	90.27 ± 1.06	90.32 ± 0.86	92.94 ± 1.25
			SZ loaded Aerosil®	89.13 ± 4.75	90.84 ± 4.09	89.08 ± 4.41	86.15 ± 5.23
0.1 M HCl 50 mM SDS	38.80 ± 0.40	2.70	*Unprocessed SZ*	100.93 ± 0.94	100.11 ± 0.80	99.22 ± 0.94	99.71 ± 1.06
			SZ loaded SBA-15	86.97 ± 3.15	91.95 ± 3.03	94.97 ± 6.33	98.02 ± 4.44
			SZ loaded Aerosil®	91.84 ± 5.26	92.84 ± 5.27	92.53 ± 4.74	90.40 ± 4.12

3.4.4.1 Sulphamethazine Loaded Silica Systems in 0.1 M HCl Medium

Loading Sz onto porous and non-porous silica carriers significantly enhanced the drug's dissolution rate in 0.1 M HCl buffer media compared to the unprocessed Sz (Figure 3.5 and Table 3.4). At the 5 min time point, Sz release from Aerosil®200 and SBA-15 was significantly higher than for the unprocessed drug. However, by 15 min, unprocessed Sz dissolution had significantly exceeded drug release from both silica systems. The amount of the free drug released remained higher for the unprocessed Sz than that of the drug loaded silica samples for the remainder of the experiment. At 24 h, incomplete drug release was observed for both silica systems; unprocessed Sz release was significantly greater than the extent of release from drug/silica samples (Table 3.4). Drug release from the porous and non-porous silica carriers was not significantly different at any of the dissolution time points.

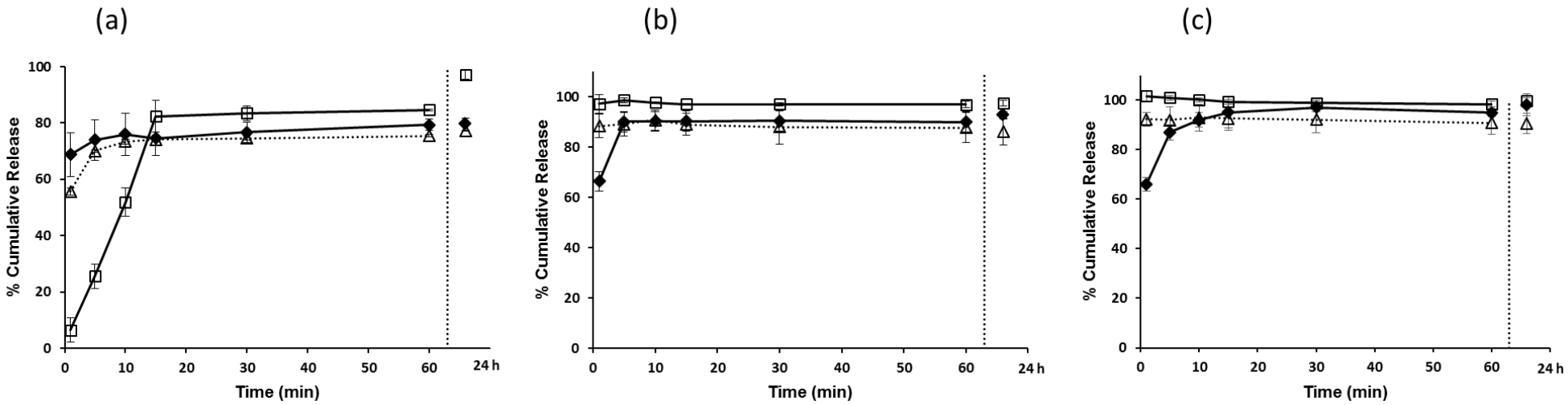


Figure 3.5 Dissolution profiles of Sz loaded SBA-15 (♦), Aerosil®200 (Δ) and unprocessed Sz (□) in (a) 0.1 M HCl, (b) 0.1 M HCl SDS 10 mM and (c) 0.1 M HCl SDS 50 mM (n=3, Y error bars indicate standard deviation)

3.4.4.2 Sulphamethazine Loaded Silica Systems in 0.1 M HCl/SDS Media

In vitro drug dissolution was investigated in the presence of surfactant (SDS) at the same concentrations investigated in the adsorption study (10 mM and 50 mM). The addition of the surfactant at low concentration (10 mM) significantly enhanced the rate and extent of drug release from both silica systems compared to dissolution in 0.1 M HCl media alone (Figure 3.5, Table 3.4). A further enhancement in the rate or extent of SZ release was not observed for the higher concentration of SDS (50 mM). Incomplete dissolution was observed for both porous and non-porous systems in the presence of 10 mM SDS (unprocessed drug dissolution reached 100% API release). Complete drug release was only observed for the drug/ SBA-15 samples in 0.1 M HCl containing 50mM SDS.

3.4.5 Porosity Analysis of Recovered SBA-15 Following Dissolution

Pore size distributions of unprocessed and recovered SBA-15 samples are displayed in Figure 3.6. Changes in silica porosity can indicate a change in the quantity and distribution of bound molecules on the silica surface. A decrease in pore diameter and pore volume is evidence of the presence of drug/surfactant molecules in the pores or blocking the pores (136). SBA-15 samples recovered after dissolution in 0.1 M HCl displayed a reduction in mesopore volume but not mesopore width. Samples exposed to media containing surfactant displayed the greatest reduction in mesopore volume and demonstrated a significant reduction in mesopore size. This suggests that SDS molecules can adsorb onto the silica surface and have the potential to deposit in the silica mesopores and block them.

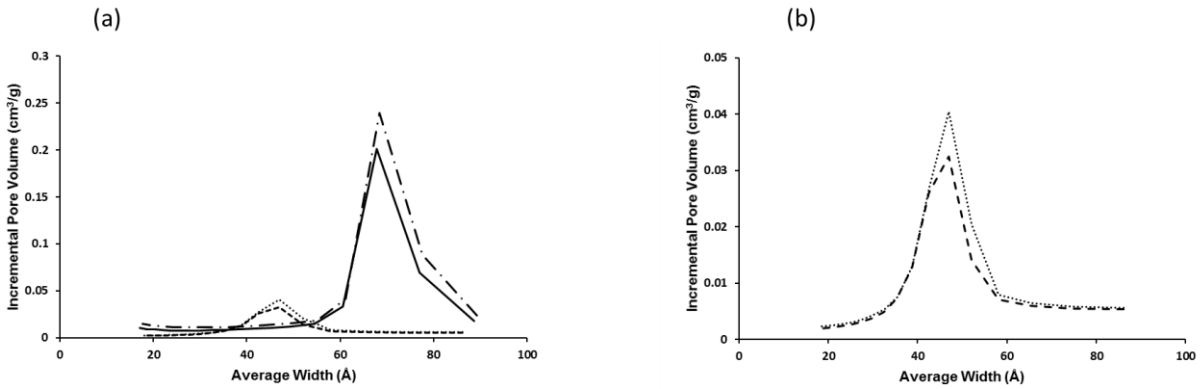


Figure 3.6 (a) Pore size distribution of unprocessed SBA-15 (dashed line with dot) and recovered SBA-15 samples after drug loading and dissolution in 0.1 M HCl (black line), 0.1 M HCl 10 mM SDS (dotted line) and 0.1 M HCl 50 mM SDS (dashed line); (b) recovered SBA samples after drug loading and dissolution in 0.1 M HCl 10 mM SDS (dotted line) and in 0.1 M HCl 50 mM SDS (dashed line)

3.4.6 Relating Dissolution Release Profiles to Adsorption Isotherms

The relationship between the quantity of Sz adsorbed on the silica surface at the end of the dissolution experiment and the estimated quantity of Sz adsorbed (calculated using the adsorption isotherm equations) was compared for the 0.1 M HCl media. Figure 3.7 (a) demonstrates that the quantity of drug that remains adsorbed to the mesoporous silica surface after dissolution is significantly higher than the predicted value. The amount retained per m^2 was considerably higher for the porous SBA-15 compared to non-porous Aerosil®200. These results indicate that retention of drug molecules on the mesoporous silica surface was not simply due to an adsorption equilibrium between adsorbed drug and drug existing in solution in the dissolution media and that the porous architecture of silica influences the retention of drug on its surface.

In contrast to drug molecule adsorption behaviour, the quantity of SDS bound at the end of the dissolution experiment was not significantly different to the predicted values from the adsorption isotherms for the porous or non-porous systems (Figure 3.7 (b)).

The presence of SDS significantly reduces the amount of drug retained on the silica surface at the end the of the dissolution experiment (Figure 3.8). This is particularly evident for the mesoporous SBA-15. It is possible that the increased wettability of the media containing the surfactant provides enhanced access to drug binding sites, resulting in less drug retention. Increasing the concentration of SDS does not result in significant further reduction in drug retention. While the presence of surfactant increases the extent of Sz dissolution, incomplete release was observed in dissolution experiments for both silica substrates (except SBA-15 loaded samples in 50 mM SDS). This indicates that some drug molecules are so tightly bound to particular silica binding sites that they are, in essence, 'irreversibly bound' under the dissolution experimental conditions.

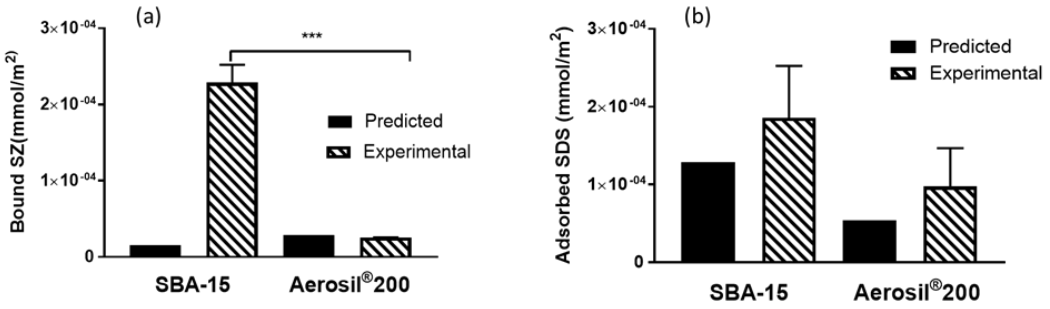


Figure 3.7 Comparison of (a) Sz and (b) SDS bound both predicted (from adsorption isotherm data) and experimentally determined after dissolution in 0.1 M HCl (n=3, error bars indicate standard deviation, * denotes p < 0.001)**

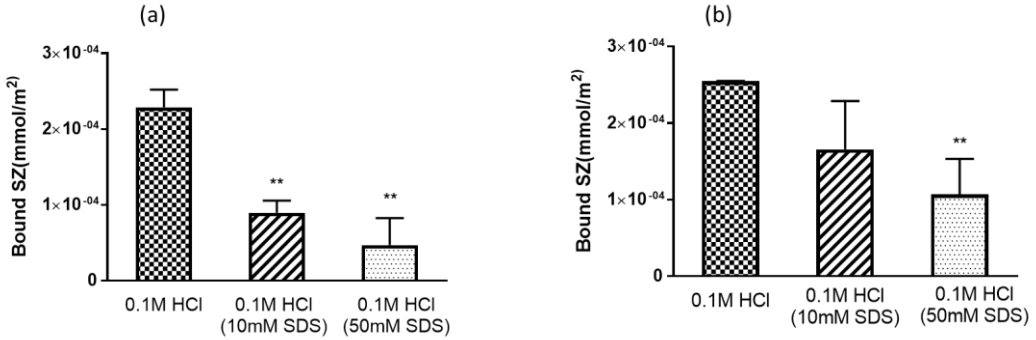


Figure 3.8 Comparison of the actual bound Sz fraction (mmol/m^2 silica) after dissolution in the three media investigated for (a) SBA-15 and (b) Aerosil®200 (n=3, error bars indicate standard deviation, ** denotes p < 0.01 of difference compared to amount bound in 0.1 M HCl

3.5 Discussion

In this study, two factors demonstrated a significant influence on drug release from silica systems. The first factor was the influence of drug and surfactant adsorption onto the silica surface. The second was the ability of the dissolution medium to wet the silica surface, particularly the porous network of the mesoporous SBA-15.

Drug adsorption onto the silica surface was noted for both silica materials across all three media investigated. The mesoporous material had a lower adsorbed drug fraction/m^2 compared to the non-porous Aerosil®. This indicates that Sz molecules cannot access the entirety of the mesoporous network. Mesoporous silica materials have a wide range of pore sizes (between 2 – 50 nm), as described in Chapter 2 (222). It is possible that adsorbed drug molecules could block smaller pores preventing access to further drug binding sites located deeper in the porous architecture. Additionally, porous binding sites may be different in terms of the number of available sites/m^2 and/or binding affinity to those located on the surface, resulting in altered drug adsorption levels compared to non-porous materials. Further evidence for this hypothesis is observed in the porosity analysis which displays a reduced pore volume for the drug loaded samples after dissolution in 0.1 M HCl, indicating bound drug molecules remaining are occupying mesopores on the surface. This finding is interesting as it suggests accessible surface area rather than specific surface area of the SBA-15 is as an important parameter in drug loading and dissolution from these porous systems.

Adsorption isotherms for single component systems were fitted to the Langmuir and Freundlich linearized equations. These two models have also been used successfully

in other studies investigating adsorption on silica substrates (118, 151, 223). The Langmuir model describes a homogeneous surface which contains only one type of binding site (224). It emerged as the best-fit for drug binding onto the non-porous Aerosil®. In contrast, Sz adsorption onto mesoporous SBA-15 produced a Freundlich model best-fit correlation. The Freundlich model is an empirical model which describes a heterogeneous surface (a system which contains a range of binding sites with different binding affinities) and indicates that multi-layer adsorption of drug onto the porous SBA-15 surface exists (225). This observation agreed with a previous literature report which demonstrated that the Freundlich isotherm proved the best-fit for the absorption of a range of pharmaceuticals onto SBA-15 (118). The number of Sz binding sites on the surface (N_t) was lower for the mesoporous material. This is further evidence that the accessible surface area of the porous silica is an important parameter to consider for these formulations. The binding affinity (designated as K_L for the Langmuir isotherm and K_F for the Freundlich model) of drug to the surface is stronger for the non-porous Aerosil®. This is most likely a result of SBA-15's porous architecture as drug interactions with the surface could vary depending on the dimensions of the pores and silica surface chemistry.

The quantity of surfactant adsorbed onto both silica substrates was significantly similar in magnitude to the quantity of drug adsorbed under the same experimental conditions and concentration range (from adsorption isotherms, Figure 3.2 (b) and Figure 3.3). This was determined by comparing drug and surfactant adsorption onto both silica surfaces. Both molecules have a similar molecular mass (278.33 g/mol for SZ and 288.372 g/mol for SDS). SDS is an anionic surfactant and SZ has an aromatic amine functional group with a pK_a of 2.06 ± 0.30. The isoelectric point of the silica

surface has been measured as pH 2 (226). In 0.1 M HCl, the results indicate that the more positively charged silica has a similar potential to attract both surfactant and drug molecules. Drug interaction with the silica surface is most likely a result of hydrogen bonding between the aromatic amine functional group and the silanol hydroxyl groups. Amine-silanol hydrogen bonding between drug molecules and the silica surface has been reported previously in a study by Xue *et al* (117). The interaction of the surfactant with the silica surface is not well understood. In this case, it is likely that the negatively charged head group interacts with the silica surface (which is slightly positively charged under these experimental conditions). It is possible that the SDS molecules adsorb in a multilayer hemi-micelle formation. This phenomenon has been described for cationic surfactant adsorption at the silica gel – water interface (227). The nature of this surfactant-silica interaction requires further investigation.

The results of this study indicate that the retention of drug molecules on the mesoporous silica surface is not simply due to an equilibrium adsorption related to the concentration of drug in solution in the dissolution media. A certain fraction of the loaded drug molecules are bound very tightly or to sites which are inaccessible for the dissolution media. These findings reinforce the influence of the porous network in drug dissolution from these systems. While the quantity of loaded drug retained at the end of dissolution was greater than the predicted quantity, the amount of surfactant adsorbed was not significantly different when predicted and experimental values were compared. The surfactant was not loaded onto the silica material in the dissolution experiment. This observation indicates that the drug loading process utilised in this study (SC-CO_2 loading) is another factor to consider in

determining drug adsorption and release behaviour. It has been reported in the literature that water molecules can adsorb onto silica by interacting with surface functional groups (228). It is possible that during drug loading under SC-CO_2 conditions, water that was bound to the silica surface was removed thus activating potential binding sites which would otherwise be unavailable in the mesoporous material. This could increase the bound drug fraction remaining at the end of dissolution as drug molecules are potentially more difficult to remove from these binding sites.

While both concentrations of SDS investigated were determined to be above the surfactant CMC in 0.1 M HCl (0.8 mM), drug solubility was only marginally enhanced in the dissolution media containing 50mM SDS. This is most likely due to the extent of incorporation of SZ (an acidic drug) into surfactant micelles which is dependent on the pK_a (acid dissociation constant) of the drug and the ionic nature of the surfactant (40). As the pK_a of the aromatic amine (2.06 ± 0.30) is only marginally above the pH, it is possible the drug is not fully protonated, reducing drug partitioning into anionic SDS micelles.

However, despite the marginal improvement in drug solubility, the addition of surfactant at both concentrations (10 mM and 50 mM) significantly enhanced the rate and extent of drug release from both porous and non-porous systems compared to dissolution in 0.1 M HCl alone. In this case, the improved wetting characteristics of the media in the presence of the surfactant is the most likely explanation for the improved dissolution profile. Surfactants decrease the solid/liquid surface tension (229) which could allow the dissolution media to access additional drug binding sites

thus enhancing drug release. Superior release was observed for the non-porous Aerosil® at 1 min compared to SBA-15. This could be attributed to the time taken for the media to wet the pores. At 5 min, there is no significant difference in the extent of release between the two silica systems. This remains the case for the remainder of the experiment (24 h).

3.6 Conclusions

This study demonstrates that drug adsorption plays a role in the release of drug molecules from drug/silica systems. Adsorption isotherms proved useful for understanding drug release for non-porous silica formulations. However, adsorption behaviour does not explain the high quantity of drug retained on mesoporous formulations. The addition of sodium dodecyl sulphate to the dissolution media significantly increased sulphamethazine dissolution from both porous and non-porous silica systems. The study findings highlight the importance of considering drug and dissolution media interaction with the silica substrate and accessibility of dissolution media to the silica porous architecture when optimising drug release from drug/silica systems.

Chapter 4: Drug Release from Mesoporous Silica Systems: The Influence of Dissolution Media Composition

Manuscript in preparation for publication

4.1 Abstract

Increasingly, *in vitro* dissolution studies of pharmaceutical systems utilize biorelevant media containing various pH modifiers, salts, lipids and proteins which have the potential to interact with the silica material. The role of interfacial interactions between dissolution media components and the silica surface with respect to their ability to influence drug release warrants investigation.

This study builds on work from Chapter 3 and investigates factors impacting drug adsorption, release and retention behaviour for a drug-loaded silica system in two biorelevant media; simulated gastric fluid (SGF) and fasted state simulated intestinal media (FaSSIF-V2). The aim of this chapter was to examine the influence of dissolution media composition on both drug release and drug retention on the silica surface. The results demonstrate that constituents of dissolution media can impact *in vitro* drug dissolution profiles from silica systems when studied under sink conditions. Reduced surface tension of dissolution medium and its subsequent ability to wet the silica surface emerged as the significant factor influencing the extent of drug release. This is an important finding as it demonstrates the importance of using biorelevant media over traditional buffer media when studying drug loaded mesoporous silica systems under sink conditions as well as non-sink conditions. It was also established that drug retention on the silica surface can be attributed to loaded drug located in pores which are inaccessible to dissolution media. Drug and dissolution media passive adsorption contributed to the observed adsorption isotherm data but was not a significant factor affecting drug release under sink conditions.

4.2 Introduction

This chapter builds on work from Chapter 3 which was the first study of its kind to explore the role of drug adsorption onto the silica surface during the dissolution process. It was observed that quantifiable levels of both drug and surfactant adsorbed passively onto the silica surface. Adsorption isotherms generated in parallel to the dissolution experiments proved useful in enhancing knowledge concerning drug release and retention behaviour on silica materials. Three factors emerged as having a significant influence on drug adsorption, release and retention on the silica surface; the porous architecture of the material, competitive adsorption and the surface tension of the dissolution medium. While this study was undertaken in a simple dissolution medium (0.1 M HCl), it is now increasingly recommended that *in vitro* dissolution studies utilize biorelevant media for dissolution testing of novel oral dosage forms (230-232). The use of biorelevant media has been promoted as it is designed to resemble aspects of the fluid composition of the gastrointestinal (GI) tract (233). These media contain various pH modifiers, salts, lipids and proteins which are themselves potential silica surface adsorbates (119). However, their interaction with the silica surface has not been investigated to date. It was our hypothesis, in this study, that interfacial interactions between dissolution media components and the silica material could impact drug release from these materials. It is the first study to investigate this aspect of the relationship between biorelevant dissolution media and mesoporous silica formulations.

In this work, dissolution experiments were performed on a silica formulation in both simulated gastric fluid (SGF), intestinal fluid (FaSSIF-V2) and the individual

components of these media. The aim of these experiments was to examine the influence of dissolution media composition on both drug release and drug retention on the silica surface. In parallel, adsorption isotherms were generated in equivalent media to examine passive drug and specific media component adsorption onto the silica surface. The two sets of experiments were then related to each other to provide insight into the relationships between drug adsorption, release and retention behaviour and to identify potential interactions between the silica surface and biorelevant media components. Surface tension measurements were conducted on all dissolution media utilized in the study to ascertain the influence of dissolution media wettability of the silica surface on drug release from mesoporous silica systems.

The model drug utilized was sulphamethazine (Sz) which has the potential to adsorb onto the silica surface as demonstrated in Chapter 3. Its aqueous solubility (0.47 ± 0.01 mg/ml in NaOH (pH 6.5) and 7.63 ± 0.33 mg/ml in 0.1 M HCl (pH 1.2)) was sufficient to enable dissolution behaviour to be assessed under sink conditions, defined as under 33 % saturated solubility (as described in Section 1.4.1) (81, 82). This study was designed to focus specifically on the interactions between silica surface and dissolution medium that can potentially affect drug release. Conducting the experiments under sink conditions minimised the potential effects of drug concentration gradients and removed the potential confounding issue of drug recrystallization and precipitation, thus enabling effects due to drug adsorption and dissolution media surface tension on the extent of drug release to be explored.

4.3 Materials and Methods

4.3.1 Materials

SBA-15 was obtained from Glantreo Ltd. (Ireland). Silica surface and pore properties were obtained from suppliers (particle size 30 µm, surface area 678.57 ± 8.23 m^2/g, pore volume 0.64 ± 0.02 cm^3 and pore diameter 51.85 ± 0.05 Å). Sulphamethazine (Sz) was purchased from Sigma Aldrich (Ireland). Liquid carbon dioxide was supplied by Irish Oxygen Ltd (Ireland). All other chemicals and solvents were of analytical grade or HPLC grade and purchased from Sigma-Aldrich (Ireland).

4.3.2 Solubility Measurements

Solubility studies were performed in triplicate by the addition of excess sulphamethazine (Sz) to 10 ml of SGF and FaSSIF-V2 (Table 4.1) using a standardised shake-flask method with a total shaking time of 24 h at 37 ^oC. Simulated gastric fluid (SGF) was prepared as outlined in the USP NF 26 (234). FaSSIF-V2 was prepared as outlined by Jantratid *et al* (233). Solubility studies were also conducted in solutions of the individual components of biorelevant media. The pH of SGF and its individual components was pH 1.2 while the pH of FaSSIF-V2 and its components was pH 6.5 (except in the case of maleic acid). Solutions were adjusted to the required pH using dilute HCl or NaOH, where appropriate. Samples (2 ml volume) were removed at the 24 h time point and centrifuged at 16,500 *g* for 13 min using a Hermle z233M-2 fixed angle rotor centrifuge (HERMLE Labortechnik GmbH, Germany). The supernatant

was removed and centrifuged again under the same conditions. The resultant supernatant was analysed using HPLC following dilution with mobile phase.

Table 4.1 Composition of Simulated Gastric Fluid (SGF) and Fasted State Simulated Intestinal Fluid Version 2 (FaSSIF-V2)

COMPONENT	SGF	COMPONENT	FASSIF-V2
Pepsin (g L^{-1})	3.2	***Sodium Taurocholate (mM)***	3.0
Sodium Chloride (mM)	34.2	***Lecithin (mM)***	0.2
HCl (mM)	226.6	***NaOH (mM)***	34.8
		Sodium Chloride (mM)	68.6
		Maleic Acid (mM)	19.1
pH	1.2	***pH***	6.5

4.3.3 Surface Tension Measurements

The surface tension of SGF, FaSSIF-V2 and solutions of their components listed in Table 4.1 were measured using a method adapted from Enright *et al* using a Attension Theta Optical Tensiometer (Attension Biolin Scientific, Finland), calibrated by prior measurements with deionized water (72.8 mN/m) (235). All measurements were based on a 10 µL droplet size and were performed at ambient temperature. Surface tension data are presented as mean ± standard deviation (n = 3).

4.3.4 Adsorption Studies

Adsorption studies were performed in screw-capped glass vials containing 100 mg of silica in 10 ml of sulphamethazine solution over a defined concentration range (from low concentration increasing gradually to concentrations nearing equilibrium solubility) in the particular medium. Adsorption studies were also conducted for pepsin in the presence of 100 mg SBA-15 in dilute HCl (pH 1.2). Experiments were conducted under the same conditions as solubility measurements i.e. shake-flask conditions for 24 h at 37 ^{o}C. At 24 h, samples (2 ml) were removed and centrifuged at 16,500 *g* for 13 min using a Hermle z233M-2 fixed angle rotor centrifuge, (HERMLE Labortechnik GmbH, Germany). The supernatant was removed and centrifuged again under the same conditions. The resultant supernatant was analysed using HPLC or UV spectroscopy following appropriate dilution. UV spectroscopy was used for pepsin quantification only (Section 4.4.4.1)

4.3.5 Preparation of Sulphamethazine Loaded Silica Formulations

Sulphamethazine loaded silica formulations were prepared according to the method previously described by Ahern *et al* (88). The drug and silica material was combined at a ratio of 1 mg Sz: 3 m^2 silica in a BC 316 high-pressure reactor (High Pressure Equipment Company, USA) and stirred using magnetic stirring. The reactor was heated to 40 °C using heating tape and maintained at this temperature for the duration of the experiment. Temperature was monitored using a temperature monitor (Horst GmbH, Germany). The reactor cell was filled with liquid CO_2 and a high pressure pump (D Series Syringe Pump 260D, Teledyne ISCO, USA) was used to

pump additional CO_2 to a final processing pressure (27.58 MPa). After 24 h, the cell was depressurised rapidly by venting the CO_2. The processed material was collected from the cell and stored in a desiccator prior to analysis.

4.3.6 Drug Content Quantification

The sulphamethazine content of the silica formulations was determined by thermogravimetric analysis (TGA), using a TGA 500 instrument (TA Instruments Ltd., United Kingdom). Samples in the weight range 2–10 mg were loaded onto tared platinum pans and heated from ambient temperature to 900 °C, at a heating rate of 10 °C/min under an inert N_2 atmosphere. Samples were analysed in triplicate. The drug quantity was calculated based on the weight loss between 100 and 900 °C, corrected for the weight loss over the same temperature range for a silica reference sample (55). TGA thermograms were analysed using Universal Analysis 2000 software (TA Instruments Ltd., United Kingdom). Drug-loading efficiency was calculated using Equation 3.1.

4.3.7 Dissolution Studies

Dissolution studies were performed in triplicate using USP II apparatus (Erweka® DT600 dissolution test system (ERWEKA GmBH, Germany)) in 500ml dissolution medium at 37 ± 5 ^{o}C at a paddle rotation of 50 rpm. Drug dissolution was investigated in SGF, FaSSIF-V2 and the individual components of both media. Sink conditions (10% saturated solubility) were employed for all dissolution experiments. Samples of 4 ml volume were withdrawn at 1, 5, 10, 15 and 30 min intervals with an additional sample

taken at the 24 h time point. Samples were immediately replaced with an equal volume of fresh, pre-warmed medium. The withdrawn samples were centrifuged at 16,500 *g* for 13 min using a Hermle z233M-2 fixed angle rotor centrifuge, (HERMLE Labortechnik GmbH, Germany). The supernatant was removed and centrifuged again under the same conditions. The resultant supernatant was analysed using HPLC following dilution with mobile phase.

4.3.8 HPLC Analysis of Sulphamethazine

Reversed phase high performance liquid chromatography (HPLC) was performed using an Agilent 1200 series HPLC system (Agilent Technologies, USA) equipped with a Photo Diode Array Detector (DAD). To quantify drug content in adsorption and dissolution studies a reversed-phase column Kinetex C-18 column (150 mm × 4 mm) with internal pore width 2.6 µm (Phenomenex Ltd., United Kingdom) was utilised. An isocratic HPLC-DAD (diode array detector) technique utilised in Chapter 3 and adapted from a method by Ding *et al* (218) with a mobile phase consisting of acetonitrile – water – acetic acid (25:75:0.05), an injection volume of 50 µL and a flow rate of 0.75 $ml.min^{-1}$ at ambient temperature was employed. The detection wavelength was 265 nm. The retention time for sulphamethazine was 5.9 min.

4.3.9 UV-Vis Spectroscopy Analysis of Pepsin Adsorption

Pepsin adsorption onto silica was analysed by quantifying the remaining pepsin in solution at 24 h time point of the adsorption study and subtracting this value from

the pepsin starting concentration. Experiments were conducted over a defined range of pepsin concentrations. UV-Vis spectroscopy (Unicam 500 spectrometer) enabled with Vision 32 software was utilised to quantify the amount of pepsin in solution at 24 h. The λ_{max} for pepsin in dilute HCl (pH 1.2) was determined as 209 nm. Samples were diluted appropriately prior to analysis.

4.3.10 Statistical Analysis

All statistical analyses were conducted using Microsoft Excel 2013 (Microsoft, USA) and GraphPad Prism (ver. 5, GraphPad Software Inc., USA). Results are expressed as mean ± standard deviation. *In vitro* dissolution and adsorption isotherm data comparing the formulations and different time points was tested for significance using a two-tailed, independent sample *t*-test, assuming Gaussian distribution and equal variance or a one-way-analysis of variance (ANOVA) with Tukey's multiple comparison test where appropriate ($p \leq 0.05$ was considered significant).

4.4 Results

4.4.1 Solubility Studies

Sulphamethazine solubility in SGF, FaSSIF-V2 and solutions of their individual components are displayed in Figure 4.1. Comparing components of SGF, solubility is highest in solutions containing HCl alone and decreases in the presence of NaCl and pepsin (Figure 4.1 (a)). Drug solubility is significantly higher in SGF compared to FaSSIF-V2 (Figure 4.1 (a) and 4.1 (b)). Sulphamethazine (Sz) has two pK_a values due to dissociation of its primary amine (pK_{a1} = 2.1) and secondary amine groups (pK_{a2} = 7.5) (236). At pH values below the pK_{a1}, the Sz molecule exists in its cationic form which is more soluble than the neutral form which exists at pH 6.5 (pH of FaSSIF-V2) (237). In the presence of HCl, Sz exists in a salt form as the amine becomes protonated to form an ammonium ion with a Cl^- counter ion. This results in enhanced solubility compared to solubility in solutions of maleic acid which have a pH 2.9 where solubility enhancement relies solely on the influence of pH (Figure 4.1 (b)).

There is a statistically significant enhancement of Sz solubility at pH 6.5 both in the presence of sodium taurocholate (TCA) (a bile salt and naturally occurring surfactant) and FaSSIF-V2, compared to its solubility in the solution containing NaOH alone. However, this improvement in solubility was marginal. As Sz is an acidic drug with a low pK_a, it is predominately ionised at pH 6.5. Sodium taurocholate exists in an anionic state at pH 6.5 and this results in repulsion between the anionic charge of the drug and surfactant, hindering drug partitioning into bile salt micelles (40, 238).

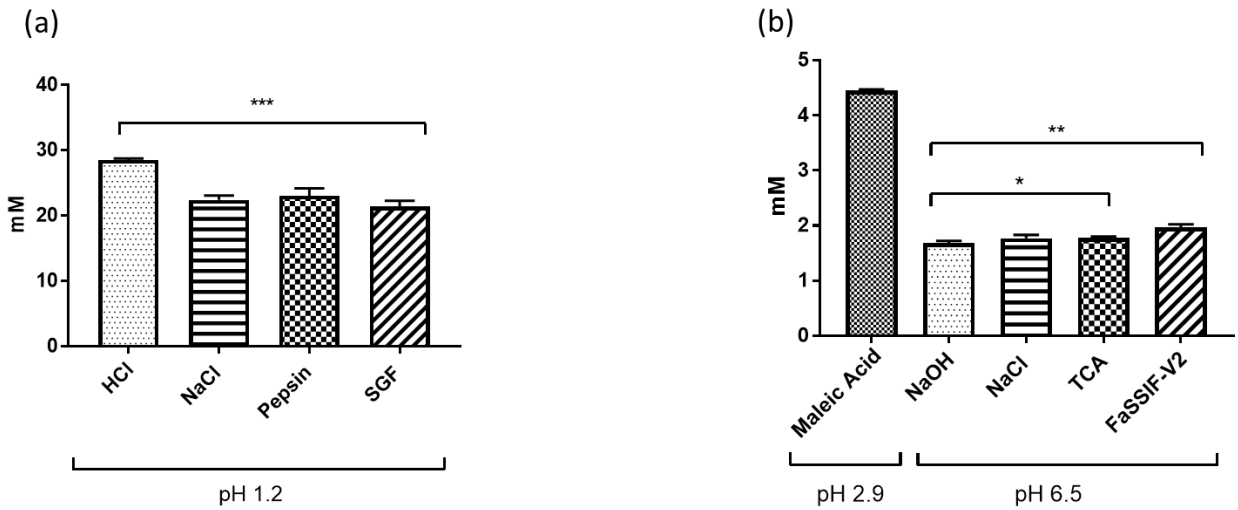


Figure 4.1 Solubility of sulphamethazine in (a) SGF and solutions of its individual components and (b) FaSSIF-V2 and solutions of its individual components (TCA = sodium taurocholate) at 37 °C. Concentrations of individual components utilised are based on composition of SGF and FaSSIF-V2 from Table 4.1. The pH of SGF and its individual components was pH 1.2 while the pH of FaSSIF-V2 and its components was pH 6.5 (except in the case of maleic acid). The pH was adjusted where necessary using dilute HCl and NaOH (n = 3, mean ± SD).

4.4.2 Surface Tension Measurements

Surface tension measurements for SGF, FaSSIF-V2 and solutions of their individual components are displayed in Table 4.2. NaOH, HCl, maleic acid and NaCl components of SGF or FaSSIF-V2 did not contribute to the significant reduction in surface tension determined for SGF or FaSSIF-V2 compared to that of deionised water (72.8 mN/m). The presence of pepsin in SGF significantly reduces surface tension ($p < 0.001$). This effect has also been reported by Vertzoni *et al* (239). The bile salt, sodium taurocholate, contributed to the surface tension reduction observed in FaSSIF-V2. The measured surface tension (48 mN/m) agrees with literature reports for this parameter in FaSSIF-V2 (93).

Table 4.2 Surface tension measurements for SGF, FaSSIF-V2 and individual components of both biorelevant media. Concentrations of individual components utilised are based on composition of SGF and FaSSIF-V2 from Table 4.1. The pH of SGF and its individual components was pH 1.2 while the pH of FaSSIF-V2 and its components was pH 6.5 (except in the case of maleic acid). The pH was adjusted where necessary using dilute HCl and NaOH (mean ± SD, n = 3).

Components of SGF	Surface tension (mN/m)	Components of FASSIF-V2	Surface tension (mN/m)
SGF	59.48 ± 0.48	***FaSSIF-V2***	48.27 ± 0.23
HCl	72.16 ± 0.62	***NaOH***	73.31 ± 0.63
NaCl	72.21 ± 1.42	***NaCl***	71.42 ± 2.34
Pepsin	57.48 ± 0.82	***Maleic Acid***	71.09 ± 2.11
		Sodium Taurocholate	43.76 ± 0.82

4.4.3 Sulphamethazine (Sz) Loading Efficiency

Sulphamethazine loading onto SBA-15 was 203.40 mg/g silica corresponding to a drug loading efficiency of 89.20% (calculated using Equation 3.1). These results are in line with loading efficiencies previously reported using SC-CO_2 methods (88).

4.4.4 Adsorption Isotherm

To ascertain to what extent incomplete release of drug from the drug loaded silica system could be explained by passive drug adsorption onto the silica surface, drug adsorption isotherms in each of the dissolution media utilized in the dissolution experiments were generated.

4.4.4.1 Simulated Gastric Fluid (SGF)

Adsorption isotherms for sulphamethazine adsorption onto silica in the presence of specific components of SGF are displayed in Figure 4.2. Drug adsorption onto SBA-15 in the dilute HCl media was significantly higher than adsorption onto the silica surface in the presence of NaCl, pepsin or SGF at free drug concentrations above 1 mM ($p < 0.001$). There was no significant difference in drug adsorption onto the silica surface in SGF media and media containing pepsin or NaCl (Figure 4.2). In these three media, adsorption does not greatly increase with increasing drug concentrations above 3 mM (low drug concentrations). Drug adsorption does increase with increasing free drug concentration in dilute HCl (pH 1.2).

In dilute HCl (pH 1.2), the silica surface has a slight positive charge as the pH is below the isoelectric point of silica (pH 2) (226). The drug molecule is also positively charged in this acidic media (below pK_{a1}). However, this charge is balanced by a Cl^- counter ion. The drug molecule can form hydrogen bonds with the silica surface through interactions between the aromatic amine group and the silica hydroxyl groups as discussed in Chapter 3. Amine-silanol bonding has been reported previously by Xue *et al* (117). Hydrogen bonding between molecules and the silica surface can overcome electrostatic repulsion as demonstrated by Shi *et al* if the repulsion can be effectively screened by counter ions at the surface, in this case Cl^- and H^+ ions (240).

The significant drop in adsorption when NaCl was added to the medium is attributed to the interaction of salt ions with the silica surface, which has previously been reported at low pH (241). This interaction could shield drug binding sites resulting in the observed significant decrease in drug adsorption. Figure 4.3 demonstrates that

pepsin was adsorbed to a greater extent than sulphamethazine on the silica material. The reduction in drug adsorption observed when pepsin is present indicates that pepsin competes with the drug for binding sites/occupies potential drug binding sites.

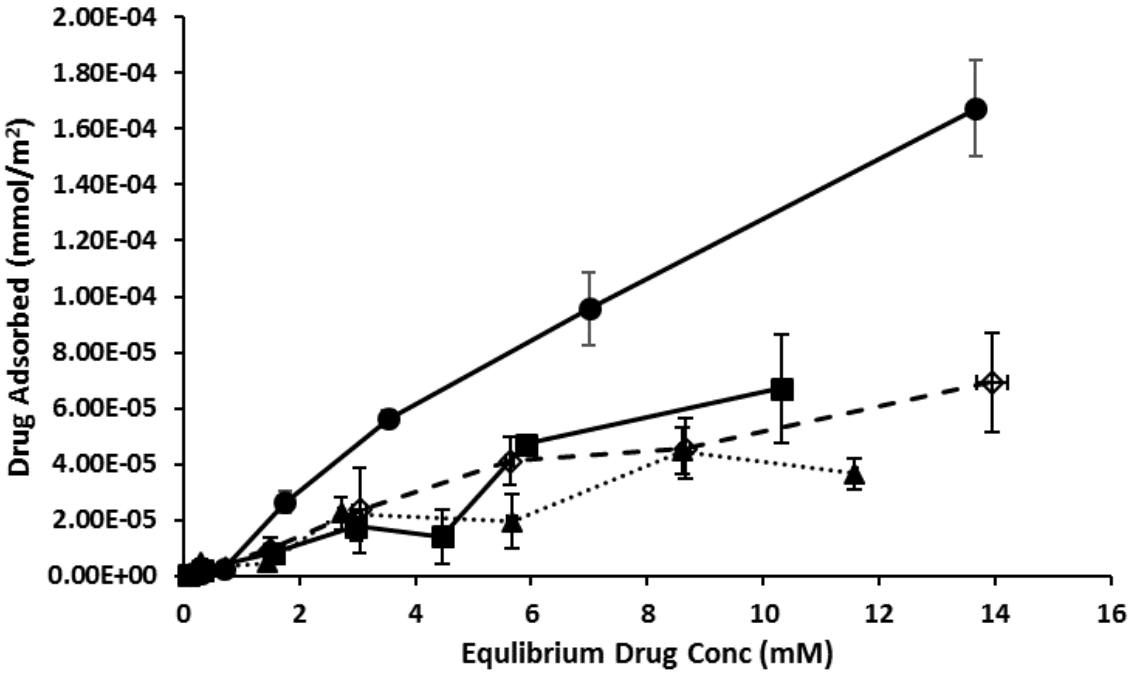


Figure 4.2 Adsorption isotherms for Sz adsorption (mmol Sz /m² silica) onto SBA-15 in dilute HCl (●), NaCl (▲), pepsin (◇) and SGF (■) at 37 °C. All concentrations of components of SGF are as per Table 4.1 and pH was adjusted to pH 1.2 (n=3, X and Y error bars indicate standard deviation).

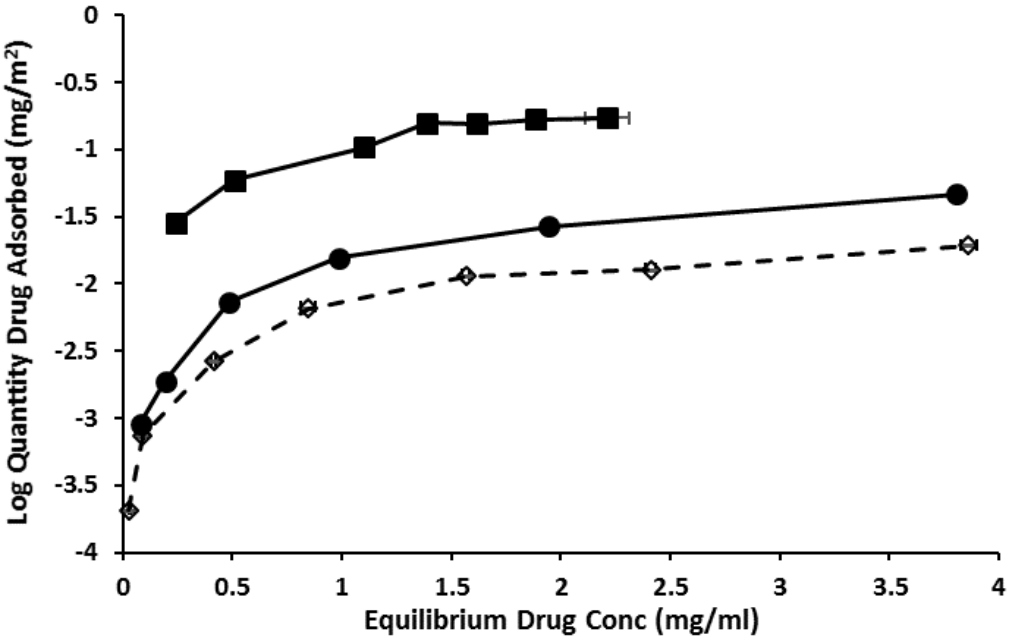


Figure 4.3 Adsorption isotherms for Sz adsorption (expressed as Log Quantity Adsorbed (mg Sz /m² silica)) onto SBA-15 in dilute HCl (●) and pepsin (◇) at 37°C. The adsorption isotherm for pepsin adsorption (mg pepsin/m² silica) onto SBA-15 in dilute HCl (■) (in the absence if Sz) at 37 °C is also displayed. All concentrations of components of SGF are as per Table 4.1 and pH was adjusted to pH 1.2 (n=3, X error bars indicate standard deviation).

4.4.4.2 FaSSIF-V2

Adsorption isotherms for sulphamethazine adsorption onto silica in solutions of individual components of FaSSIF-V2 are displayed in Figure 4.4. Drug adsorption was significantly higher in dilute NaOH (pH 6.5) than dilute HCl (pH 1.2) at the same free drug concentrations. However, the solubility of Sz in dilute acid was higher than that in dilute NaOH (Figure 4.1) and adsorption increased significantly at these higher drug concentrations (Figure 4.2). Sulphamethazine adsorption was decreased in the presence of salt (a trend which was also observed in SGF (Section 4.4.4.1). However, the decrease is not as pronounced as that for the acidic medium. This is due to a

decrease in interaction between salt ions and the silica surface at pH above the silica isoelectric point which results in a reduction of the shielding effect that hinders drug adsorption (226, 242).

The presence of sodium taurocholate decreased drug adsorption onto the silica surface (Figure 4.4) at concentrations from 0.5 mM but not to the same extent as pepsin (Figure 4.2). Sulphamethazine adsorption was further decreased in the presence of FaSSIF-V2 which indicates that lecithin adsorption onto the silica surface can further decrease drug adsorption levels. It was not possible to study the effect of lecithin in isolation as its solubility is dependent on the presence of bile salt micelles (243).

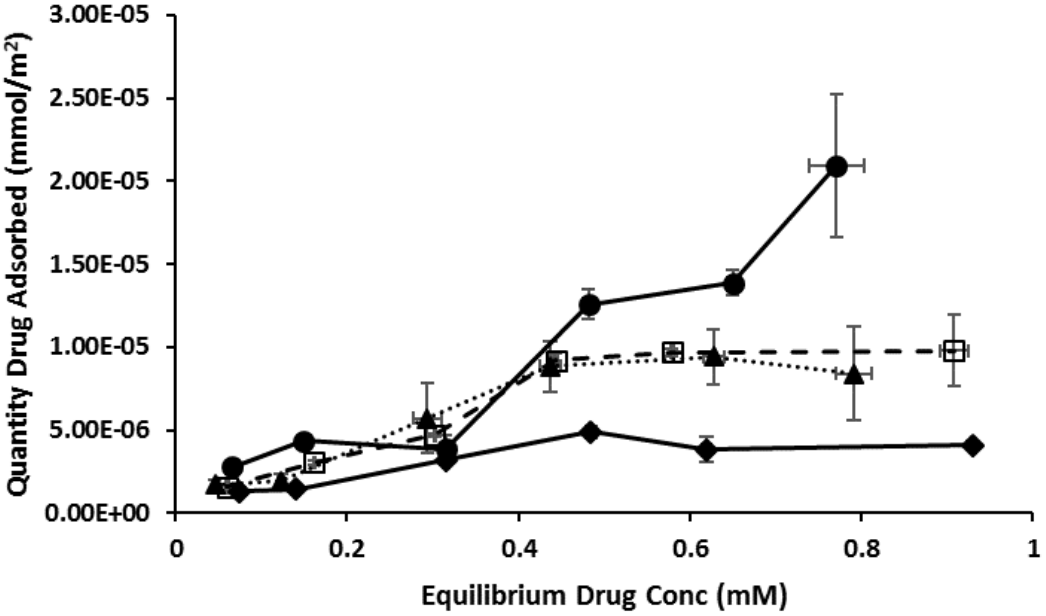


Figure 4.4 Adsorption isotherms for Sz adsorption (mmol Sz /m² silica) onto SBA-15 in dilute NaOH (●), NaCl (▲), TCA (□) and FaSSIF-V2 (♦) at 37°C. All concentrations of components of FaSSIF-V2 are as per Table 4.1 and pH was adjusted to pH 6.5 (n=3, X and Y error bars indicate standard deviation).

4.4.5 Dissolution Studies

Dissolution experiments were conducted in dissolution media identical to those used in the adsorption studies. Drug release was measured over 30 min with a final 24 h time point to study the effect of silica adsorption (determined in the adsorption experiments) on drug release.

4.4.5.1 Simulated Gastric Fluid

Loading sulphamethazine onto SBA-15 significantly enhanced the initial rate of drug release in the presence of dilute HCl and NaCl (pH 1.2) (Figure 4.5). In media containing pepsin, the dissolution enhancement at 5 min was not observed. This was attributed to the decreased surface tension of these media resulting in improved wettability of the unprocessed drug. After 30 min, there was no significant difference between unprocessed drug release and Sz release from the silica systems in the dissolution media examined. However, at 24 h, drug release from the unprocessed samples was significantly higher than that from the silica formulation in all four media ($p < 0.05$) (Table 4.3). When behaviour across the dissolution and adsorption isotherm experiments are considered, it can be observed that while NaCl and pepsin had similar effects on drug adsorption behaviour, the extent of release during dissolution studies from pepsin was higher. This indicates that reduced surface tension is plays a more significant role influencing drug release from silica systems in SGF than passive adsorption. Complete drug dissolution was not observed from any of the silica samples. This incomplete release was most significant in dilute HCl and decreased when other components of the SGF are added to the acidic medium (Table

4.3). These results suggest that the composition of the dissolution media is instrumental in governing the extent of potential drug release under sink conditions.

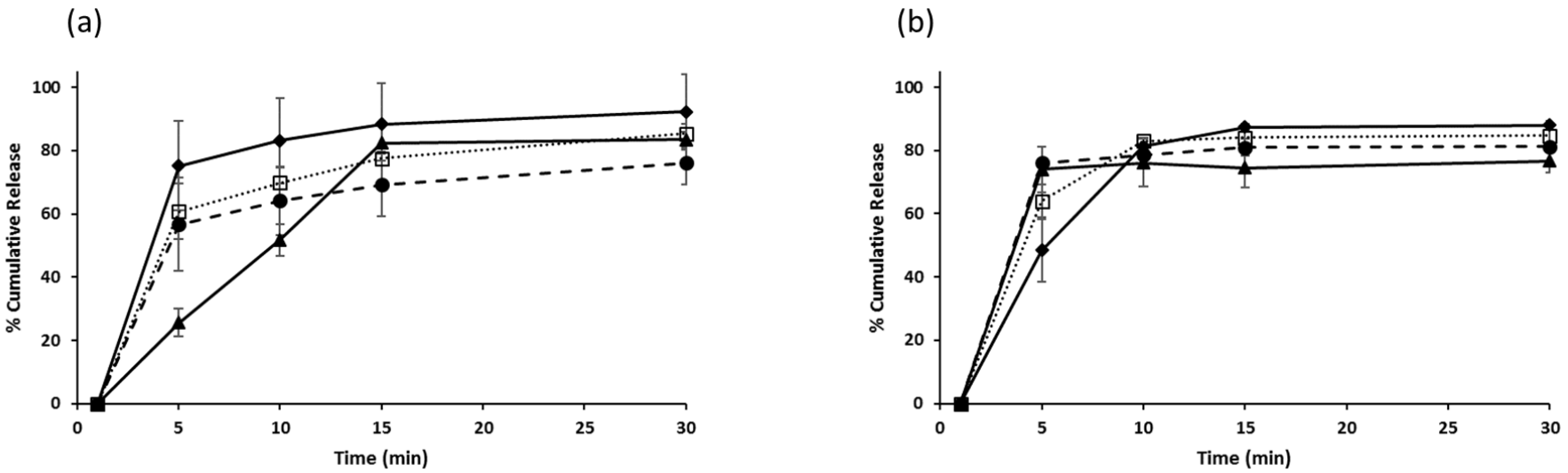


Figure 4.5 Dissolution profiles of (a) unprocessed Sz and (b) Sz loaded SBA-15 in specific dissolution media ((♦) represents SGF, (●) pepsin, (□) NaCl and (▲) 0.1 M HCl). All concentrations of components of SGF are as per Table 4.1 and pH was adjusted to pH 1.2 (n=3, Y error bars indicate standard deviation)

Table 4.3 Cumulative drug dissolution (%) for unprocessed drug and drug-loaded silica formulation at 24 h in SGF, FASSIF and their respective components. All concentrations of components of SGF and FASSIF are as per Table 4.1 and pH was adjusted to pH 1.2 and pH 6.5 respectively (n=3)

Dissolution Media	Sz loaded SBA-15 release at 30 min (%)	Sz loaded SBA-15 release at 24h (%)	Unprocessed Sz release at 24h (%)
HCl	76.7 ± 3.7	79.6 ± 2.1	97.2 ± 1.8
NaCl	81.2 ± 1.3	86.5 ± 3.2	102.5 ± 0.3
Pepsin	84.8 ± 3.2	94.7 ± 4.2	102.2 ± 1.6
SGF	88.1 ± 1.4	96.1 ± 0.6	103.8 ± 1.3
NaOH	78.9 ± 12.3	77.1 ± 4.6	93.2 ± 0.2
NaCl	81.2 ± 6.7	87.1 ± 4.4	96.1 ± 6.8
Sodium Taurocholate	78.0 ± 2.3	95.7 ± 1.7	98.7 ± 3.2
FaSSIF-V2	80.3 ± 5.3	94.5 ± 4.2	95.4 ± 4.0

4.4.5.2 FaSSIF-V2

Drug dissolution enhancement from the SBA-15 system was observed in the presence of TCA and FaSSIF-V2 ($p < 0.05$ at 24 h) but not in the other individual components of FaSSIF-V2 media (Table 4.3). This was most likely a result of more favourable wettability of the formulation in the presence of the bile salt, further indicating that reduced surface tension is the most important dissolution media characteristic influencing drug release in this study. Greater variability in dissolution profiles was observed in media without the bile salt which was attributed to their inferior wetting characteristics (Figure 4.6). After 24 h, incomplete release was observed from the silica formulation in all dissolution media investigated (Table 4.3).

The same trend noted in Section 4.4.5.1 SGF (i.e. unprocessed drug release significantly higher than drug release from the silica systems) was also observed in dilute NaOH and NaCl (pH 6.5) dissolution media. However, the extent of drug release in the presence of sodium taurocholate (TCA) alone and in FaSSIF-V2 was not significantly different from unprocessed drug release at 24 h. When adsorption and dissolution experiments were compared, it was noted that while NaCl and TCA had a similar effect on drug adsorption behaviour during adsorption studies, TCA provided a more significant enhancement of drug dissolution. This is a result of its ability to reduce surface tension of the media which proved superior in augmenting drug release compared to the drug binding site 'shielding effect' of NaCl.

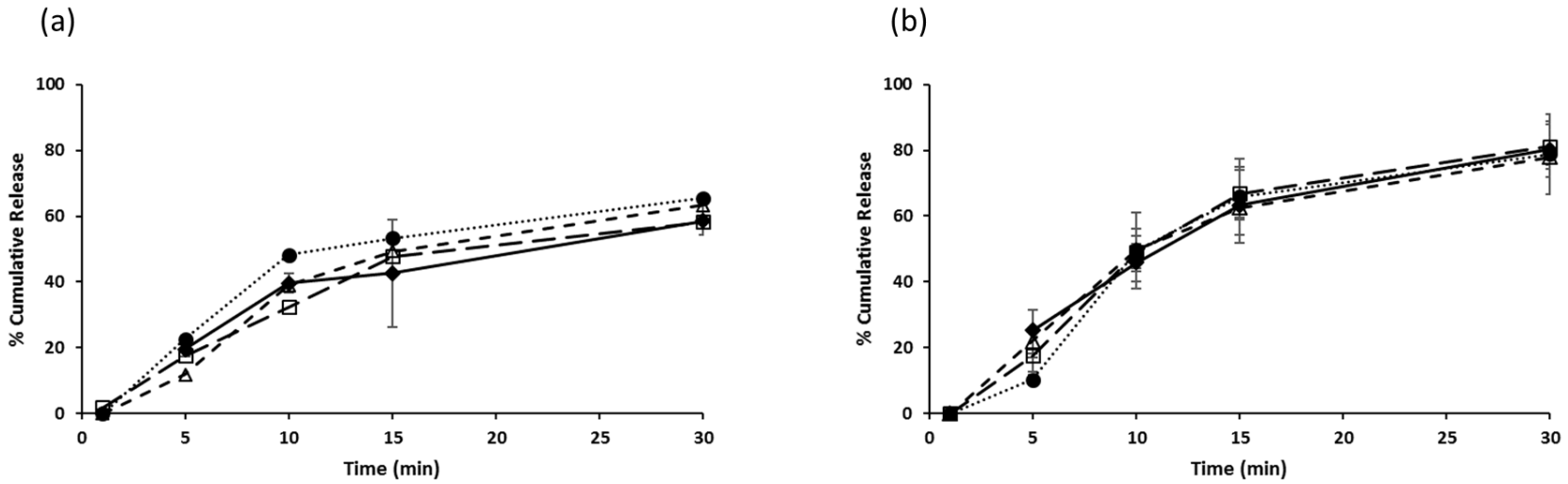


Figure 4.6 Dissolution profiles of (a) unprocessed Sz and (b) Sz loaded SBA-15 in specific dissolution media ((♦) represents FaSSIF, (Δ) TCA, (□) NaCl and (●) dilute NaOH). All concentrations of components of FaSSIF are as per Table 4.1 and pH was adjusted to pH 6.5 (n=3, Y error bars indicate standard deviation)

4.4.6 Relating Dissolution Release Profiles to Adsorption Isotherms

The quantity of drug retained after dissolution experiments was significantly higher than the quantity adsorbed during the isotherm studies for all dissolution media investigated (assuming drug not released at the end of the dissolution study (24 h time point) represents drug bound to SBA-15) (Figure 4.7). This behaviour demonstrates that incomplete release of drug from these systems cannot be explained solely by drug adsorption behaviour in solution. It indicates that a considerable quantity of loaded drug remains on the silica surface, possibly located in pores which are inaccessible to the dissolution media. The extent of this inaccessible pore network is governed by the ability of the dissolution media to wet the surface. There is a significant reduction in % drug retained after dissolution in media containing components which reduce surface tension compared to simple traditional media (Figure 4.7). However, in all cases a substantial incomplete release is observed following dissolution.

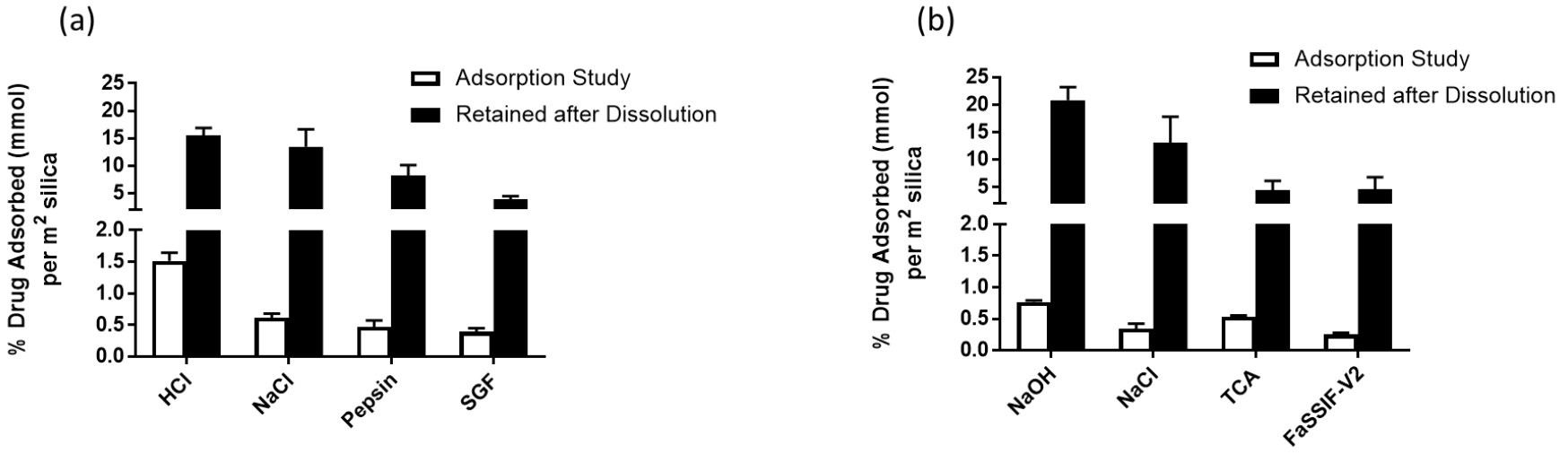


Figure 4.7 Comparison of % drug adsorbed (mmol/m^2 silica) during adsorption and dissolution studies in components of (a) SGF and (b) FaSSIF-V2 media (n=3, error bars indicate standard deviation)

4.5 Discussion

The results of this study demonstrate that constituents of dissolution media can have a significant influence on *in vitro* drug release from silica systems when studied under sink conditions. Two features of the dissolution media composition, in particular, were investigated; dissolution media surface tension and adsorption of media components onto the silica material.

The surface tension of the dissolution medium and its subsequent ability to wet the silica surface emerged as the significant factor influencing the extent of drug release. This is highlighted in Figure 4.7 where it can be observed that drug retention on the surface was lowest in media containing surface active agents such as pepsin or TCA. Both of these components decreased the surface tension of the dissolution medium (93, 239). This finding agreed with the results in Chapter 3 where drug retention was reduced in the presence of a non-biological surfactant (sodium dodecyl sulphate). The Nernst-Brunner equation provides justification for these observations as it explains how contact area between media and solid surface influences dissolution (244). In this study, it was observed that a reduction in surface tension enhanced the wettability of the silica mesoporous network and thereby increased the effective surface area for dissolution (14). This finding demonstrates the importance of using biorelevant media over traditional buffers (i.e. dilute HCl and phosphate buffer) when studying drug release from mesoporous silica systems under sink conditions. Biorelevant media is commonly employed to study drug release in non-sink conditions due to its impact on drug solubility and supersaturation levels (78, 94, 245). Together with results described in Chapter 3, this data provides evidence that

media surface tension can significantly influence drug release from mesoporous silica formulations under sink conditions.

The higher levels of retention noted after dissolution experiments compared to adsorption studies suggest that drug retained on the surface after dissolution could be located in pores inaccessible to the dissolution media. Mesoporous silica materials have a wide range of pore size (2 -50 nm) (222). During the drug loading process, it is feasible that a quantity of drug was loaded deep in the porous network which was accessible to the loading solvent (supercritical CO_2) but not accessible to the dissolution medium during release studies (54). The hypothesis of a relationship between loading methodology and release is not resolved in this current study and warrants further investigation.

The impact of media composition on drug adsorption onto the silica material was a secondary factor impacting drug release. Dissolution media pH influenced drug adsorption by altering silica surface charge, drug ionisation state and drug solubility. At low pH the silica surface is positively charged and at pH 6.5 the silica surface is negatively charged allowing for electrostatic attraction or repulsion interactions with solute molecules. Sulphamethazine has the ability to form hydrogen bonds with the silica surface through interactions between the aromatic amine group and the silica hydroxyl groups. Amine-silanol bonding has been reported previously by Xue *et al* (117). At the same free drug concentrations, adsorption onto the silica surface is higher in the presence of dilute NaOH as the drug is unionised at this pH. However, in acidic pH, hydrogen bonding between molecules and the silica surface can overcome electrostatic repulsion as demonstrated by Shi *et al* if the repulsion can be

effectively screened by counter ions at the surface, in this case Cl^- and H^+ ions (240). As free drug concentration increased in HCl (Figure 4.1), drug adsorption increased significantly indicating the importance of drug solubility in the dissolution medium as a factor influencing passive drug adsorption.

Competitive adsorption of drug and dissolution media components on the silica surface was observed in this study. Both pepsin and TCA demonstrate a competitive adsorption behaviour with the drug in isotherm experiments. Drug adsorption observed in isotherm experiments was significantly reduced in the presence of pepsin (Figure 4.3). This was attributed to competitive binding of pepsin with the silica surface. In dilute HCl, pepsin is uncharged and competes with the drug for binding sites on the silica surface (it has been reported that protein adsorption onto the solid surface is maximised at the isoelectric point (246-248)). While sulphamethazine adsorption was significantly reduced, quantifiable adsorption was observed. It is possible that certain drug binding sites remain available to the drug on the silica surface despite the influence of factors which significantly affect drug adsorption levels. Sodium taurocholate (TCA) also decreased drug adsorption onto the silica surface (Figure 4.4). Adsorption of bile salts onto silica surfaces have been reported in the literature (119). Sulphamethazine adsorption was further decreased in FaSSIF-V2 which indicates that a combined competitive effect incorporating NaCl, bile salt and lecithin can further decrease drug adsorption levels.

4.6 Conclusion

This study is the first to consider interfacial interactions between dissolution medium and the silica surface with respect to their effect on drug release. The results highlight that dissolution media surface tension was the most significant factor affecting drug release from drug loaded mesoporous silica systems. The ability of media components to alter passive drug adsorption and to competitively adsorb on the silica surface was a secondary factor. These results highlight the importance of employing biorelevant media when studying drug dissolution from mesoporous silica formulations under sink conditions.

Chapter 5: Mechanism of Drug/Silica Interaction and its Influence on Drug Adsorption and Release Under Supersaturating Conditions

Manuscript in preparation for publication

Acknowledgements: I wish to thank Prof. Lynne Taylor for providing me the opportunity to join her lab as a Visiting Scholar to undertake the experiments described in this chapter. I would also like to thank the members of the Taylor lab who facilitated training on the equipment necessary to undertake these experiments, in particular, Dr. Niraj Trasi, Ms. Chailu Que and Dr. Van Tu Duong.

5.1. Abstract

The specific nature of drug-silica interactions is not well understood. It has been suggested that drug can bind to the silica surface via hydrogen bonding and non-specific hydrophobic interactions. In this chapter, the mechanism of these interactions was investigated using spectroscopic techniques and competitive adsorption experiments. It was determined that drug interacts with mesoporous silica via hydrogen bonding and not through non-specific hydrophobic interactions. It was also determined that hydrogen bonding capability can potentially influence drug adsorption onto mesoporous silica. The role of drug adsorption onto the silica surface was investigated under supersaturating conditions through the generation of adsorption isotherms up to and exceeding amorphous solubility levels. It was observed that the equilibrium between drug adsorbed on the silica surface and free drug in solution was related to drug activity in solution. This activity is a function of the chemical potential of the drug in the system with silica and dissolution medium. The results suggest that solute activity in solution can potentially influence drug release from mesoporous silica materials. An equilibrium was also confirmed between adsorbed drug and free drug in solution during drug dissolution from silica formulations under supersaturating conditions (at amorphous solubility). It was demonstrated that this equilibrium was not dependant on the quantity of silica present, rather the equilibrium relationship between drug adsorbed and drug in the dissolution medium. This provides further evidence that knowledge of drug activity in solution can aid in our understanding of drug release from mesoporous silica formulations.

5.2. Introduction

As previously described in Chapter 2, drug molecules have been loaded onto mesoporous silica substrates to enhance aqueous solubility and control drug release (72, 120, 249, 250). However, the specific nature of the interaction between the silica surface and the adsorbed drug molecules has not been confirmed. The literature differs with some authors suggesting drug-silica interactions are solely due to hydrogen bonding while others report they are a mixture of hydrogen bonding and non-specific hydrophobic interactions (73, 251-254). However, there is no detailed study published in the literature to confirm the mechanism of interaction. This work aims to fill this gap in knowledge by exploring the adsorption of two similar compounds with different hydrogen bonding capabilities onto the mesoporous silica surface. Indomethacin has one hydrogen bond donor and four hydrogen bond acceptors while indomethacin methyl ester has no hydrogen bond donor and four hydrogen bond acceptors. It was hypothesized that the lack of a hydrogen bond donor would impact adsorption of the methyl ester compared to that of indomethacin. Drug-silica interactions were examined using specific spectroscopic techniques (FT-IR and fluorescence spectroscopy) alongside competitive adsorption studies using indicators of hydrogen bonding (urea (255)) and hydrophobic interactions (NaCl (256)).

Chapter 3 and 4 of this thesis investigated the role of drug adsorption onto the silica surface during dissolution in sink conditions. However, mesoporous silica systems are noted for their ability to achieve supersaturated levels of drug release (257-260). To address this, drug adsorption onto SBA-15 was examined under supersaturating

conditions in this chapter up to and exceeding amorphous solubility levels. Amorphous solubility is defined as the maximum increase in solution concentration that can be obtained relative to the crystalline form (261). At concentrations above the amorphous solubility a metastable equilibrium can exist for slow crystallizers as the system splits into two liquid phases to lower free energy - one phase is water rich and the other is drug rich. This is defined as liquid-liquid phase separation (LLPS) (262). The drug-rich species formed following LLPS typically have a size of 100–500 nm when characterized immediately after formation using techniques such as dynamic light scattering (263, 264). Growth of the drug-rich droplets/particles can subsequently occur or can be inhibited if additives such as polymers are present (265, 266). Thus, some compounds can clearly persist as a two-phase solution which remains supersaturated at a constant level (at the co-existence concentration) until crystallization occurs. LLPS is most commonly observed in systems where there is very high supersaturation, rapid generation of supersaturation, when crystallization inhibitors or high levels of impurities are present and where there is inadequate mixing causing high local supersaturations (267). The amorphous phase generated can be considered a precursor to crystallization as the system remains supersaturated after LLPS has occurred and is expected to subsequently crystallize. Conducting drug release studies under conditions which promote LLPS has been widely employed for amorphous solid dispersions (268-271). However, to date, only one study has examined drug release from mesoporous systems under such experimental conditions (272). This work aims to expand knowledge in this area by investigating drug dissolution and adsorption onto mesoporous silica materials up to and exceeding amorphous solubility levels.

It has recently been confirmed in a paper by Dening *et al* that an equilibrium exists between drug adsorbed on the silica surface and free drug in solution (272). This study aims to build on this work by further investigating the basis of this equilibrium using Langmuir and Freundlich adsorption isotherms, which have been successfully used to describe drug adsorption onto the silica surface in Chapter 3 and in the literature (118, 151, 273). The influence of the drug's activity in solution which is related to the chemical potential (μ) of the adsorbed drug and the free drug in solution during the equilibrium process was considered. The chemical potential of a component is defined as the contribution that component makes to the overall free energy of the system (12). The Langmuir constant (K_L) explains this change in the free energy of adsorption and can provide information on the chemical potential of the drug adsorbed to the silica surface (274-278). To examine chemical potential where more than one component is present, the concept of activity is utilized which provides a method to quantify the way in which the chemical potential of a pure substance changes when it becomes a component in a system (12). In this study, adsorption isotherms were generated up to and exceeding both drug's amorphous solubility. To compare the drug adsorption between the two model drugs, equilibrium concentrations were converted to drug activity levels with amorphous solubility designated an activity of 1.

5.3. Materials and Methods

5.3.1. Materials

Indomethacin (IND) (γ form) was purchased from Letco Medical (Decatur, AL). Indomethacin methyl ester (INDME) was synthesised using a method by Trask *et al* (279). SBA-15 material with pore diameter 7.1 nm, pore volume 0.80 cm^3/g and SSA 586 m^2/g was supplied by Glantreo Ltd. (Cork, Ireland). Hydroxypropyl methylcellulose (HPMC) (Pharmacoat® 606) was purchased from Shin-Etsu Chemical Co. Ltd. (Tokyo, Japan). Pyrene and urea were obtained from Sigma-Aldrich (St. Louis, MO, USA). Buffer salts and analytical grade solvents were supplied by Fisher Chemical (Fair Lawn, NJ, USA). The aqueous media used in all experiments was McIllvaine buffer (pH 2.2) (280). HPMC at a concentration of 100 µg/ml was used, when required, to inhibit drug crystallization during experiments.

5.3.2. Crystalline and Amorphous Solubility Measurements

The crystalline solubilities of indomethacin (γ form) and indomethacin methyl ester in McIllvaine buffer (pH 2.2) were determined by equilibrating an excess of crystalline IND and INDME in 20 mL of medium using an agitating water bath (Dubnoff metallic shaking incubator, PGC Scientific, Palm Desert, CA, USA) set at 37 °C for 48 h. The undissolved crystalline material was separated from solution by centrifugation at 21,100 × *g* for 30 min (37 °C), using a Sorvall™ Legend™ Micro 21R Microcentrifuge (ThermoFisher Scientific, Waltham, MA, USA). The supernatant was diluted with acetonitrile and analyzed via high performance liquid chromatography (HPLC) using the method described below.

The amorphous solubility of both compounds was determined by both UV spectroscopy and ultracentrifugation. The LLPS (liquid – liquid phase separation) onset concentration (i.e. amorphous solubility) can be detected by UV spectroscopy as an increase in UV signal at a wavelength where the drug does not show absorption, manifested as a change in baseline. The extinction was monitored at 450 nm at 15 s intervals using a UV-vis spectrometer (SI Photonics Inc, Tuscon, AZ,USA) coupled with an in situ fiber optic probe (1 cm pathlength). Drug absorbance at 319 nm (IND) and 254 nm (INDME) was also measured to determine whether an increase in extinction at 450 nm was due to the formation of crystals (where a sharp decrease in absorbance would be anticipated) or a new liquid droplet phase (absorbance remains high). The concentration of both compounds was controlled by pumping a stock methanol solution of IND or INDME (5 mg/ml) at a rate of 50 µL/min for 16 min into 50 ml McIllvaine buffer pH 2.2 with pre-dissolved HPMC (100 µg/ml). The buffer solutions were stirred at 300 rpm and maintained at 37 ^{o}C in a jacketed beaker.

The amorphous solubility of both compounds was also determined using ultracentrifugation. A methanolic solution of drug concentration 10 mg/mL was prepared and 250 µL was added to 50 mL of McIllvaine buffer (pH 2.2) containing HPMC 100 µg/ml at 37 °C under stirring at 300 rpm. The opaque solutions were immediately centrifuged at 35,000 rpm for 60 min in a Beckman L7-56 ultracentrifuge (Beckman Instruments, Palo Alto, USA) equipped with an NVT90 rotor. The supernatant was diluted with acetonitrile and analyzed via HPLC as described below.

5.3.3. Fourier Transform Infrared Spectroscopy (FTIR)

Attenuated total reflectance fourier transform infrared (ATR-FTIR) spectroscopy was utilized to investigate interactions between drug and silica. Spectra were obtained using a Bruker Vertex 70 spectrometer. Measurements were carried out over the scan range 600 to 4000 cm^{-1}, accumulating 64 scans with a resolution of 4 cm^{-1}.

5.3.4. Fluorescence Spectroscopy

A fluorescence probe technique was used to provide information on the mechanisms by which SBA-15 interacts with hydrophobic molecules in solution, as well as to confirm the presence of drug multilayers within the SBA-15 mesopores following adsorption. Pyrene, which exhibits different fluorescence characteristics depending on the polarity of its environment, was used as a fluorescent probe. Fluorescence spectra were obtained using a Shimadzu spectrofluorophotometer RF-5301PC (Shimadzu Scientific Instruments Inc., Columbia, MD, USA). Pyrene stock solution (1 mg/mL in ethanol) was added to each sample to generate a pyrene concentration of 0.25 µg/mL. Emission spectra of pyrene were obtained by exciting samples at 332 nm, using an excitation slit width of 1.5 nm and 1.5 nm emission slit width. The change in the ratio of intensities between the first (I_1 at 371-373 nm) and third (I_3 at 382-384 nm) peaks of the pyrene emission spectra was monitored; this ratio of I_1/I_3 intensities is very sensitive to changes in the polarity of the surrounding environment.

5.3.5. Adsorption Experiments

Adsorption experiments were conducted using 50 mg SBA-15 which was added to 40 ml McIllvaine buffer pH 2.2 (containing HPMC 100 µg/ml) and equilibrated at 37 °C under stirring at 300 rpm. IND stock solution (10 mg/mL in methanol) was added at specific concentrations over a defined range (1 – 60 µg/mL) and samples were equilibrated for 8 h. Samples were centrifuged at 21,100 *g* for 10 min (37 °C), and the supernatant was diluted with acetonitrile and analyzed via HPLC. The procedure was repeated for the INDME over the concentration range 1 – 14 µg/ml. The quantity of drug adsorbed onto the silica surface at equilibrium, Q_a, was calculated using the following equation (Equation 5.1):

$$Q_a = \frac{(C_i - C_e)V}{m} \qquad (Equation\ 5.1)$$

where, C_i is the initial drug concentration, C_e is the equilibrium drug concentration in the supernatant following adsorption, V is the total volume of solution, and m is the mass of SBA-15 added to the solution.

Desorption of both IND and INDME from SBA-15 was investigated to study the strength of interaction between drug and the silica surface. Following adsorption (as described above), 1 mL sample aliquots were removed and diluted with fresh buffer to attain IND and INDME concentrations of equal activity. These concentrations were calculated by first assigning amorphous solubility for both drugs an activity of 1. Concentrations of equal activity were then calculated using the Equation 5.2

$$Activity\ \left(\frac{C_e}{Amorphous\ Solubility}\right) x\ Concentration\ \left(\frac{ug}{ml}\right) \qquad (Equation\ 5.2)$$

A 20% activity level was determined as 8 µg/ml for IND and 2 µg/ml for INDME. Samples were equilibrated at 37 °C under stirring at 300 rpm for 24 h, and then centrifuged at 21,100 *g* for 10 min (37 °C). Drug concentration in the supernatant was analyzed via HPLC.

To investigate the mechanism of interaction between IND and INDME molecules with the silica surface, adsorption experiments were conducted at different ionic strengths (*i.e.* water, 0.1 M NaCl and 0.5 M NaCl) and in the absence and presence of urea (5 M urea in McIllvaine buffer pH 2.2). Competitive adsorption experiments were also performed where both drugs were present in solution with SBA -15. These experiments were all undertaken at equal activity levels of IND and INDME, as specified above.

5.3.6. Estimation of IND and INDME Molecular Dimensions

The molecular dimensions of both IND and INDME were measured using Mercury CSD 3.10.1 software (Cambridge Crystallographic Data Centre, Cambridge, United Kingdom). The single crystal structure with a reference code of INDMET was utilised for indomethacin and ETIJOG for the methyl ester. The “measure distance” tool was used to determine the distance between the atoms furthest apart in approximately orthogonal directions. Surface area for adsorption was then estimated from the product of the two longest dimensions.

5.3.7. Preparation of Drug Loaded SBA-15 Systems

IND and INDME were loaded onto SBA-15 using a solvent incipient wetness impregnation method. Theoretical monolayer coverage within the SBA-15 particles (calculated based on an equation by Dening *et al* (272)) was the basis for determining the drug loading quantities utilized in the study (Equation 5.3)

$$X_m = \frac{SSA\ adsorbent\ \times\ 10^{20}\ \times\ MWadsorbate}{S_c\ \times\ N_A} \qquad (Equation\ 5.3)$$

where, X_m is the quantity of adsorbate required for monolayer coverage of the adsorbent (g/g), *MW* is the molecular weight of the adsorbate molecule (g/mol), S_c is the contact surface area for each adsorbate molecule (Å^2), and N_A is Avogadro's number. The molecular dimensions of both compounds (Figure 5.1) were calculated using Mercury software as described above. The SSA of SBA-15 was 586 m^2/g (provided by supplier).

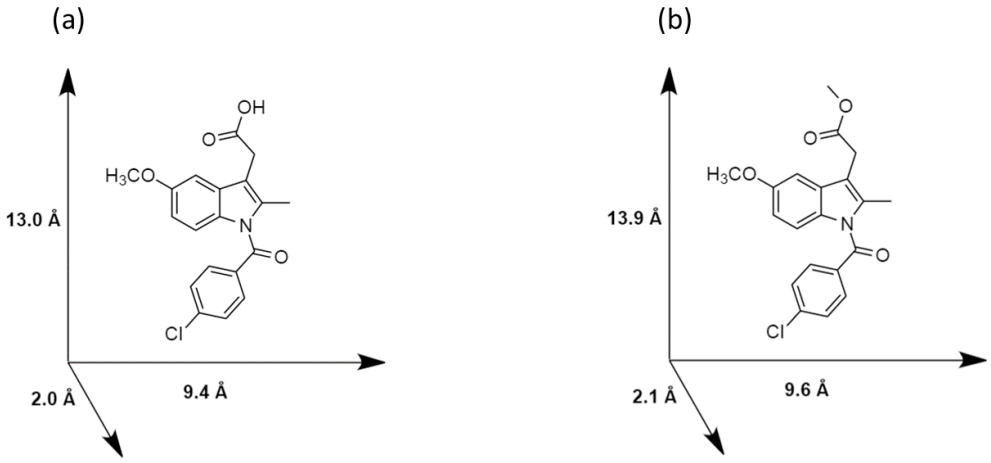


Figure 5.1 Molecular structure and estimated molecular dimensions for (a) IND and (b) INDME

The solvent was subsequently removed from the sample by drying in an oven at 40 °C for 24 h, followed by 48 h under reduced pressure at ambient temperature. The drug content was analyzed using a solvent extraction technique, whereby a known quantity of sample was dissolved in methanol with the aid of ultrasonication (Cole Parmer Ultrasonic Cleaner Model 8892, Vernon Hills, IL, USA) for 30 min. Samples were then centrifuged at 21,100 *g* for 10 min, and the supernatant was diluted with acetonitrile prior to HPLC analysis.

5.3.8. X-Ray Powder Diffraction (XRPD) Analysis

Drug crystallinity of the loaded SBA systems was analyzed by measuring the X-ray powder diffraction pattern using a Rigaku Smartlab™ diffractometer (Rigaku, Tokyo, Japan). Samples were scanned over the range 5 to 40° 2θ at a scanning rate of 10°/min and step size of 0.02°. The voltage and current were set at 40 kV and 44 mA, respectively.

5.3.9. *In vitro* dissolution experiments

Dissolution experiments were performed in McIllvaine buffer pH 2.2 containing HPMC 100 µg/ml. The buffered solution (75 mL) was equilibrated in a jacketed-vessel maintained at 37 °C under stirring at 300 rpm. A known quantity of sample was added to the dissolution medium to generate a supersaturated solution of IND or INDME and 0.7 mL sample aliquots were withdrawn at fixed time points up to 120 min.

Samples were centrifuged at 21,100 *g* for 10 min (37 °C), and the supernatant was diluted with acetonitrile and analyzed via HPLC.

5.3.10. High Performance Liquid Chromatography (HPLC)

HPLC analysis was performed using an Agilent HPLC 1260 Infinity System (Agilent Technologies, Santa Clara, CA, USA) equipped with an Agilent Poroshell 120 EC – C_{18} analytical column (2.7 µm, 4.6 mm ID × 100 mm). The mobile phase consisted of acetonitrile and water at a ratio of 60:40 (v/v) with a flow rate of 1 mL/min. Analyses were conducted at room temperature and ultraviolet (UV) detection was at 254 nm. The injection volume was 20 µL. Retention time for IND and INDME was 3.2 min and 7.1 min, respectively.

5.3.11. Statistical Analysis

The experimental data were analyzed statistically using a Student's *t*-test (unpaired) in GraphPad Prism Version 7.01 (CA, USA). Data were considered statistically significant when $p < 0.05$.

5.4. Results

5.4.1. Crystalline and Amorphous Solubility

The crystalline solubility for IND was determined as 2.29 ± 0.13 µg/ml (Table 5.1). Equilibrium solubility for INDME was lower at 0.42 ± 0.05 µg/ml. The experimental amorphous solubility/liquid-liquid phase separation (LLPS) concentration determined using the UV spectroscopy method was 39.86 ± 2.05 µg/ml for indomethacin and 9.44 ± 2.92 µg/ml for the methyl ester. This represents a 17.4 fold increase in solubility for indomethacin compared to the equilibrium solubility and a 22.5 fold increase for the methyl ester. These amorphous solubility values are in agreement with the results obtained using the ultracentrifugation method. Using this approach, amorphous solubility for indomethacin was measured as 35.13 ± 2.31 µg/ml and 8.96 ± 0.56 µg/ml for the methyl ester (Table 5.1). Amorphous solubility determined via ultracentrifugation was deemed to be the more precise measurement compared to the UV spectroscopy method where LLPS is detected as drug is continuously added to the system. The limitation of the UV spectroscopy method is the point of detection may overshoot the amorphous solubility (262).

Table 5.1 Equilibrium and amorphous solubility values for IND and INDME (n = 3, values represent mean ± standard deviation)

	Indomethacin Conc (µg/ml)	Indomethacin Methyl Ester Conc (µg/ml)
Equilibrium Solubility	2.29 ± 0.13	0.42 ± 0.05
Amorphous Solubility ***(UV method)***	39.86 ± 2.05	9.44 ± 2.92
Amorphous Solubility ***(Ultracentrifugation method)***	35.13 ± 2.31	8.96 ± 0.56

5.4.2. Mechanism of Interaction

5.4.2.1. FTIR Spectroscopy

FTIR spectroscopy was utilised to characterize specific interactions between drug and the silica surface. Figure 5.2 displays IR spectra for the amorphous forms of IND and INDME, IND and INDME loaded SBA-15 and blank SBA-15 in the region 1600 to 1800 cm^{-1}. It is evident from the spectra that SBA-15 does not absorb in this region. Amorphous indomethacin displays a peak at 1682 cm^{-1} that represents the benzoyl C=O. This shifts to 1669 cm^{-1} when the drug is loaded onto the silica surface indicating hydrogen bonding with the silanol groups on the silica. These silanol groups (Si – OH) can act as proton donors or proton acceptors to form hydrogen bonds with adsorbate molecules (281-283). A peak at 1710 cm^{-1} is also observed in the amorphous IND spectrum. This represents the asymmetric acid C=O present in the dimer species formation which has been reported for indomethacin (61). A shoulder peak is also visible here at 1732 cm^{-1} which corresponds to the non-hydrogen bonded acid C=O.

Loading the drug onto SBA-15 results in a shift of the peak at 1710 cm^{-1} to 1688 cm^{-1} while the shoulder peak disappears. This provides further evidence of hydrogen bond formation between amorphous IND and the silica surface as the -COOH group donates a proton to hydrogen bond with silanol -OH acceptor groups.

Amorphous indomethacin methyl ester also possesses a benzoyl C=O group which is visible on the IR spectra at 1674 cm^{-1} (Figure 5.2). This shifts to 1663 cm^{-1} when the methyl ester is loaded onto the silica surface indicating that it can also form hydrogen bonds with silica silanol donor groups, similar to indomethacin. The ester group present at 1735 cm^{-1} shifts to 1725 cm^{-1} when loaded onto SBA-15. This indicates that the proton acceptor on the ester functional group can interact with silica silanol groups.

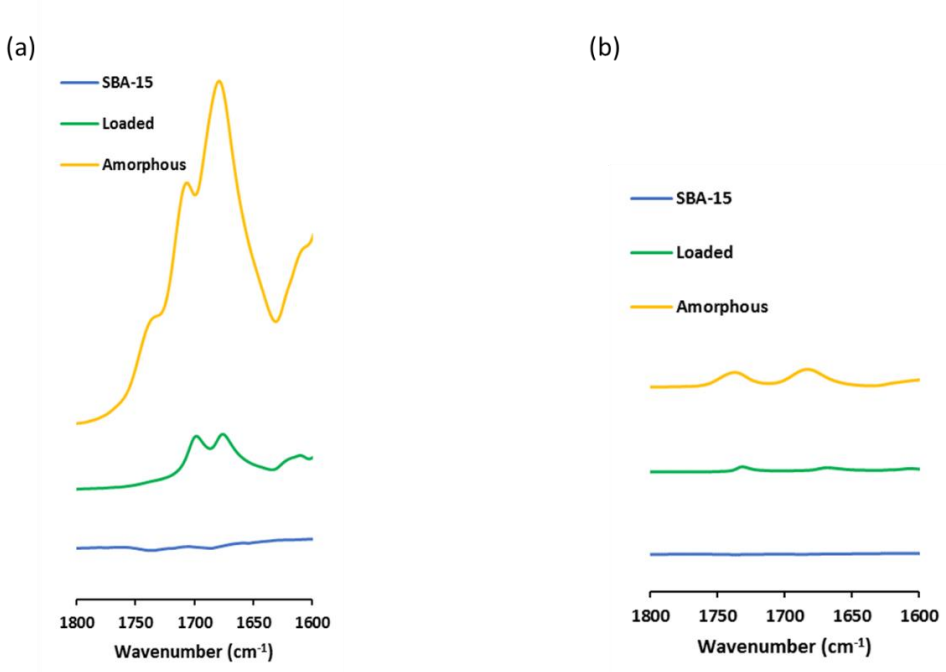


Figure 5.2 IR spectra of blank SBA-15, IND and INDME ((a) and (b) respectively) amorphous forms and drug loaded SBA-15 systems in the region of 1600 to 1800 cm^{-1}

5.4.2.2. Fluorescence Spectroscopy

Fluorescence spectroscopy was utilised to further examine the nature of interactions between drug and the silica surface (284, 285). Pyrene was selected as the fluorescent dye as it displays different fluorescence characteristics, depending on the polarity of its environment (286). Pyrene can interact with other molecules only via hydrophobic interactions resulting in the ratio of its first and third vibronic peaks (I_1/I_3) decreasing as the pyrene partitions into a more hydrophobic environment (287). The results presented in Table 5.2 demonstrate that pyrene is unable to interact with the silica surface as the I_1/I_3 ratio does not decrease compared to that in McIllvaine buffer pH 2.2 alone. This result is further evidence that the interactions between both IND and INDME and the silica surface are due to hydrogen bond formation. Pyrene itself cannot form hydrogen bonds with other molecules.

Table 5.2 Ratio of the intensity of the first and third peaks (I_1/I_3) for pyrene in the presence of various additives in McIllvaine buffer pH 2.2 containing HPMC 100 µg/ml at 37 °C (* indicates concentration is above LLPS level)

Sample	I_1/I_3 Peak Ratio
McIllvaine Buffer pH 2.2	1.96
SBA 50 µg/ml	2.00
Indomethacin	
*Indomethacin 50 µg/ml	1.54
Indomethacin 30 µg/ml and SBA-15 50 µg/ml	1.72
Indomethacin Methyl Ester	
*Indomethacin Methyl Ester 12 µg/ml	1.70
Indomethacin Methyl Ester 8 µg/ml and SBA-15 50 µg/ml	1.88

Fluorescence studies with pyrene also provide evidence of drug multilayer formation on the silica surface. Above the LLPS concentration of a drug, the colloidal dispersions formed produce a hydrophobic environment with which pyrene can interact, resulting in a reduction of I_1/I_3 ratio compared to buffer alone (265). This behaviour is observed for both drugs when dosed above their respective amorphous solubilities (Table 5.2). Furthermore, if drug multilayers are present on SBA-15, the pyrene should also partition into the hydrophobic environment they would create. To confirm this, drug and silica material were added to buffer at initial concentrations that would not exceed LLPS based on isotherm data (Figure 5.3). The I_1/I_3 ratio decreased for both drugs indicating the probe had partitioned to drug-rich layers on the SBA-15 surface.

5.4.3. Adsorption Studies

5.4.3.1. Adsorption Isotherms

The adsorption isotherms for IND and INDME on SBA-15 from McIllvaine buffer pH 2.2 at 37 ^{o}C are displayed in Figure 5.3. Significant adsorption was observed for both drugs on the silica surface. This adsorption begins to exceed theoretical monolayer coverage at the highest C_i (initial drug concentration) investigated for both drugs (60 µg/ml for IND and 14 µg/ml for INDME). To gain a better understanding of the adsorption phenomenon observed, the data was fit to Langmuir and Freundlich isotherm models (previously utilised in Chapter 3).

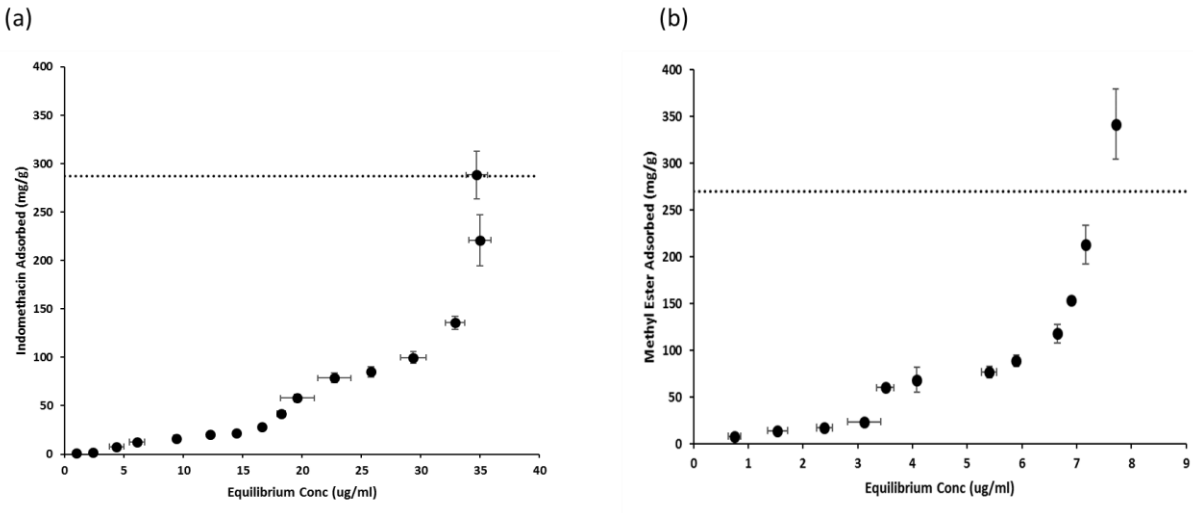


Figure 5.3 Adsorption isotherm of (a) IND and (b) INDME on SBA-15 from McIllvaine buffer pH 2.2 containing HPMC 100 µg/ml at 37 °C. The dashed lines indicate theoretical monolayer coverage of IND and INDME

The linear equations for these models are described in Chapter Three (Table 3.2). The isotherms for both drugs produced a reasonable fit for both the Langmuir and

Freundlich models. This suggests that both monolayer and multilayer adsorption contribute to drug adsorption onto the silica surface. The Freundlich isotherm (which describes multi-layer adsorption) resulted in a more favorable fit for the indomethacin data possibly due to indomethacin self-interactions through its dimer formation capability (61).

Table 5.3 Binding affinity parameters (K_L and K_F) and R^2 values obtained by fitting drug adsorption onto SBA-15 to Langmuir and Freundlich isotherm linear equations.

Langmuir Isotherm	K_L	R^2
Indomethacin	0.07	0.82
Indomethacin Methyl Ester	0.40	0.85
Freundlich Isotherm	**K_F**	**R^2**
Indomethacin	1.09	0.96
Indomethacin Methyl Ester	1.76	0.89

The binding affinity parameters were calculated for both isotherms (K_L for Langmuir and K_F for Freundlich, Table 5.3). In both cases, INDME displayed a stronger binding affinity to the silica surface than IND.

The quantity of drug adsorbed onto the silica surface for both compounds is very similar across the concentration ranges investigated (Figure 5.3). The initial concentrations (C_i) utilized represent a range from 1 µg/ml up to amorphous solubility levels (37.5 µg/ml for indomethacin and 9.2 µg/ml for indomethacin methyl ester) and beyond. The highest initial drug concentrations (C_i) employed were 60

µg/ml and 14 µg/ml for indomethacin and indomethacin methyl ester, respectively. To compare adsorption of the two compounds directly, equilibrium concentrations obtained were converted to their corresponding activity levels in solution using Equation (5.4):

$$\frac{C_e}{Amorphous\ Solubility} \qquad (Equation\ 5.4)$$

where C_e is equilibrium concentration of the drug in solution (mM) and amorphous solubility is 0.11 mM and 0.02 mM for IND and INDME, respectively. The results presented in Figure 5.4 demonstrate that adsorption of the two compounds over their corresponding activity ranges follow the same trend.

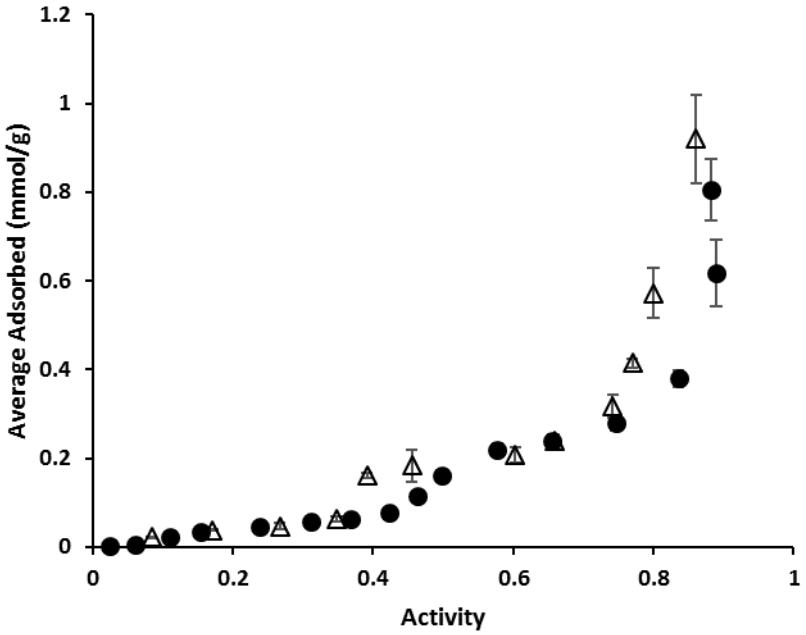


Figure 5.4 Adsorption isotherm of IND (●) and INDME (Δ) in McIllvaine buffer pH 2.2 containing HPMC 100 µg/ml at 37 °C based on solute activity in solution. Each value represents mean ± standard deviation.

5.4.3.2. Desorption Studies

Following adsorption studies at the same activity levels, desorption experiments were conducted to better understand the strength of interaction between the drugs and the silica surface. Adsorption samples were diluted to sink conditions (20% of saturated solubility for this study) and the free drug concentration in solution was sampled after equilibration for 24 h. The level of desorption from indomethacin loaded SBA-15 was 73 % whereas this dropped to 57 % for the methyl ester (Figure 5.5), indicating it has a stronger attraction to the silica surface which was predicted using the Langmuir and Freudlich isotherm models (Section 5.4.3.1). This increased affinity for the silica carrier may explain the slower release rate during dissolution studies (Section 5.4.5). Importantly, this result indicates that the adsorption of both indomethacin and indomethacin methyl ester by SBA-15 is not completely reversible.

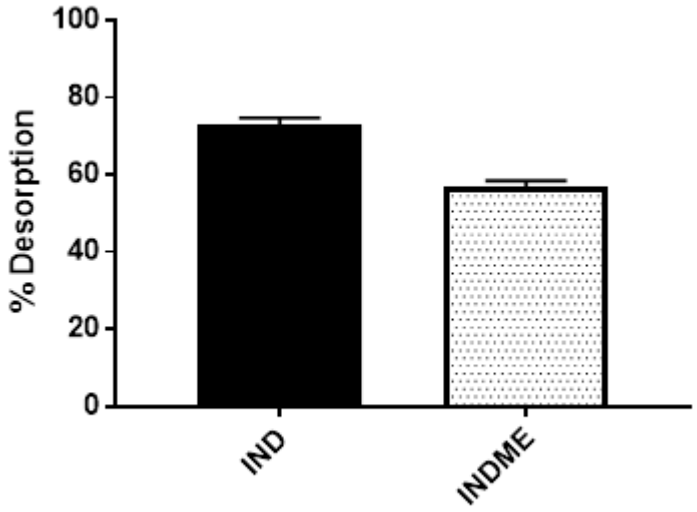


Figure 5.5 Desorption of IND and INDME after adsorption onto SBA-15 in McIlvaine buffer pH 2.2 containing HPMC 100 µg/ml at 37 °C (mean ± standard deviation, n=3)

5.4.3.3. *Competitive Adsorption*

Competitive adsorption studies were conducted to compare the strength of interaction of both drugs with the silica surface. In the first experiment, both drugs were present in solution at the same activity levels (20% of total activity (amorphous solubility) i.e. 8 µg/ml for IND and 2 µg/ml for INDME) (Section 5.3.5). The quantity of drug adsorbed onto the silica surface was compared to their individual isotherm adsorption at the same initial drug concentration (Figure 5.3). The results displayed in Figure 5.6 demonstrate that indomethacin adsorption is significantly decreased by the presence of the methyl ester whereas adsorption of INDME is not statistically different in the presence of the indomethacin.

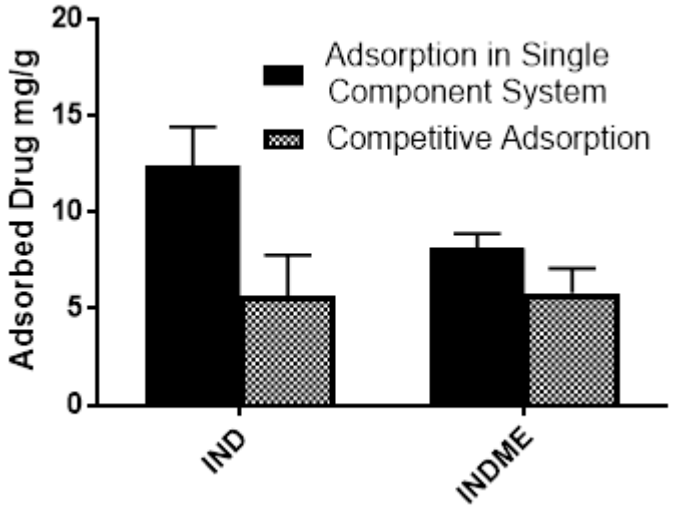


Figure 5.6 Adsorption of IND and INDME onto SBA-15 during individual isotherm experiments and competitively (with the alternate drug in solution) (mean ± standard deviation, n=3)

5.4.3.4. *Influence of Urea on Adsorption*

Adsorption studies in the presence and absence of urea were undertaken to further investigate the nature of the interaction between drug and silica surface. Urea is a strong hydrogen bonder and a reduction in drug adsorption would be expected if hydrogen bonding played a significant role in drug/silica interactions (255). The results demonstrate a significant decrease in adsorption of both drugs. Indomethacin adsorption decreased from 12.4 ± 1.9 mg/g to 6.1 ± 1.7 mg/g while indomethacin methyl ester adsorption was reduced from 14.2 ± 0.3 mg/g to 5.8 ± 1.0 mg/g (Figure 5.7). This data provides further evidence that drug interaction with the surface is indeed the result of hydrogen bonding.

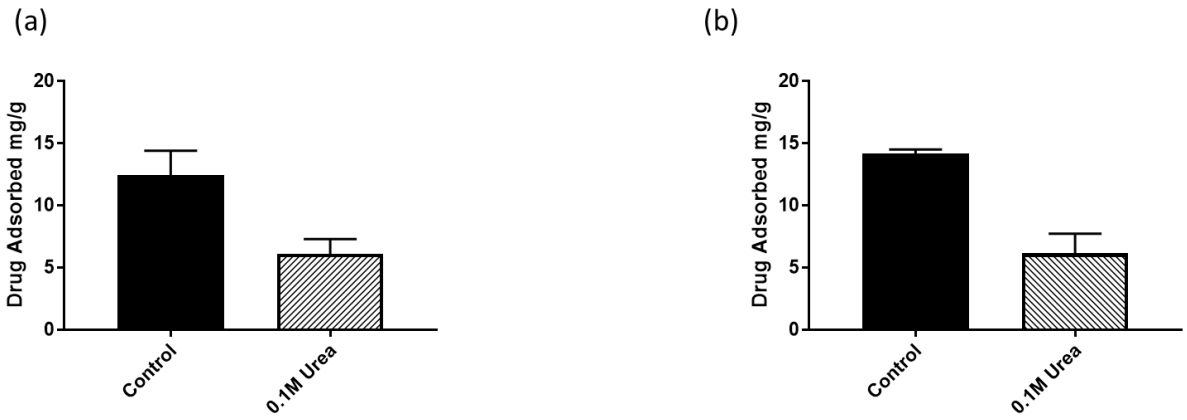


Figure 5.7 Adsorption data for (a) IND and (b) INDME (at the same activity level) in McIllvaine buffer pH 2.2 containing HPMC 100 µg/ml at 37 °C in the absence and presence of 0.1 M urea (mean ± standard deviation, n=3)

5.4.3.5. *Influence of Ionic Strength*

The effect of increasing ionic strength on drug adsorption onto the silica surface was investigated to determine the influence of non-specific hydrophobic interactions on the process. If such interactions exist between drug and silica, increased NaCl concentration should increase drug adsorption, due to the 'salting out' effect (255, 256). In this experiment, the adsorption of both drugs was examined at two concentrations representing equal activity levels (2 and 8 µg/ml) in media of increasing ionic strength (distilled water, 0.1 M NaCl and 0.5 M NaCl) (Figure 5.8). There is no significant change in drug adsorption across all three media indicating that hydrophobic interactions do not play a role in drug adsorption onto the silica surface.

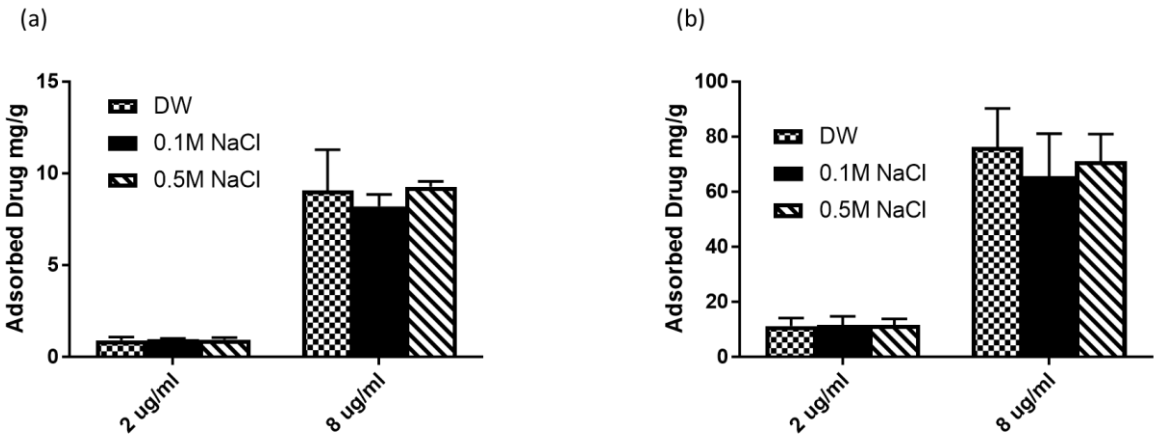


Figure 5.8 Adsorption data for (a) IND and (b) INDME at two initial drug concentrations (2 µg/ml and 8 µg/mL) in three media of varying ionic strength: distilled water, 0.1 M NaCl and 0.5 M NaCl containing HPMC 100 µg/ml at 37 °C (mean ± standard deviation, n=3)

5.4.4. Preparation of Drug Loaded SBA-15 Systems

Based on the estimated molecular dimensions of indomethacin and indomethacin methyl ester (Figure 5.1) and the SSA of SBA-15 (586 m^2/g), the quantity of both compounds required to achieve theoretical monolayer coverage on the silica surface was calculated using Equation 5.1. For indomethacin theoretical monolayer coverage was determined as 0.287 g/g (i.e. 28.7 % w/w) and for indomethacin methyl ester 0.269 g/g (i.e. 26.9 %w/w). IND was loaded onto SBA-15 at levels corresponding to specific theoretical surface coverages in the range 25 – 150 % as displayed in Table 5.4. The same procedure was repeated for INDME. The % drug loading efficiency for both drugs at the specified loading levels utilised was calculated (Figure 5.9). The results demonstrate a significantly higher loading efficiency for IND at 25% and 50% monolayer coverages. The loaded powders were analysed by p-XRD to assess drug solid-state (Figure 5.10). Both drugs were X-ray amorphous on the silica surface at 25 % and 50 % monolayer coverage. However, at levels of 75 % coverage and above, crystalline peaks were observed. At this point both drugs may have exceeded the total pore volume limits of the SBA-15 (288). Strong INDME crystalline peaks are visible from 100 % monolayer coverage. This is most likely due to instability as a result of the methyl ester's low T_g (glass transition temperature), measured as -20 ^oC**.** Indomethacin has a higher T_g of 50 ^oC and is therefore more physically stable in the amorphous state under ambient preparation conditions (289).

Table 5.4 SBA-15 formulations with loaded IND and INDME at specific theoretical monolayer coverage levels (for actual drug load, each value represents mean ± standard deviation, n=3)

% THEORETICAL MONOLAYER COVERAGE	INDOMETHACIN		INDOMETHACIN METHYL ESTER	
	Theoretical Drug Load (% w/w)	Actual Drug Load (% w/w)	Theoretical Drug Load (% w/w)	Actual Drug Load (% w/w)
25	7.17	5.6 ± 0.74	6.74	3.84 ± 0.39
50	14.33	10.46 ± 0.62	13.48	7.65 ± 0.33
75	21.50	15.55 ± 3.27	20.22	14.00 ± 2.31
100	28.66	20.82 ± 3.42	27.97	15.60 ± 0.49
125	35.83	22.01 ± 2.49	33.71	20.13 ± 1.90
150	43.00	39.02 ± 6.63	40.45	29.26 ± 0.69

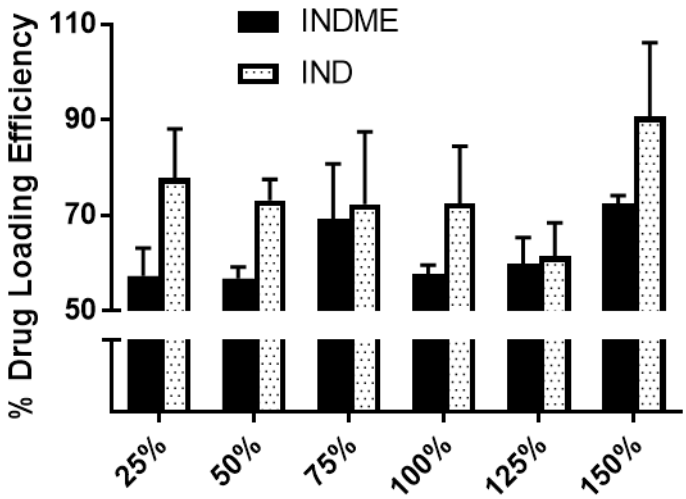


Figure 5.9 Comparison of % drug loading efficiency for IND and INDME (n=3, mean ± standard deviation)

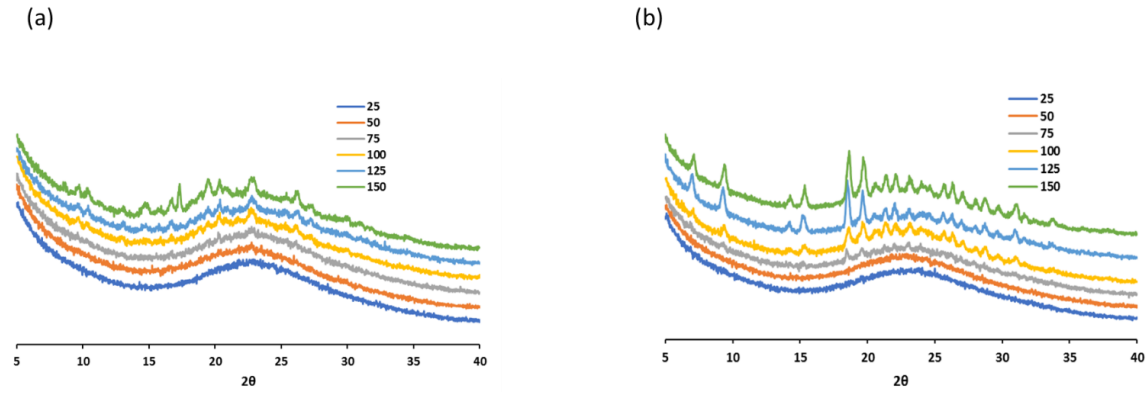


Figure 5.10 p-XRD diffractograms of (a) IND loaded SBA-15 and (b) INDME loaded SBA-15 at specified loading levels in the range 25 – 150% monolayer coverage

5.4.5. *In Vitro* Release under Supersaturating Conditions

Dissolution studies were performed on 50 % monolayer coverage drug-loaded formulations to ensure drug in both systems was X-ray amorphous in nature (Figure 5.10). The SBA-15 formulation was dosed at the amorphous solubility of IND or INDME, where appropriate, theoretically resulting in a 100 % drug release of 37.5 µg/ml and 9.2 µg/ml respectively. These dissolution studies were thus conducted at a supersaturation ratio (*S*) of 17.5 for IND and 19.1 for INDME. A rapid burst release of drug was observed with a supersaturated solution of both drugs generated at the initial time point, 5 min (Figure 5.11). Drug release from the IND loaded system peaked at 5 min whereas drug dissolution from the INDME formulation continued to increase until 30 min, after which release plateaued for the remainder of the experiment. The gradual initial release from the methyl ester loaded SBA-15 could be attributed to its stronger affinity for the silica surface which was predicted by the isotherm models (Section 5.4.3.1) and confirmed by desorption and competitive adsorption experiments (Section 5.4.3.2 and Section 5.4.3.3).

The maximal concentration of drug in solution (C_{max}) was recorded as 16.6 µg/ml for indomethacin and 2.9 µg/ml for indomethacin methyl ester. This translates to a significantly higher % release from the indomethacin system (44% release) compared to that from the methyl ester formulation (32% release). However, the release from both drugs is comparable in terms of supersaturation achieved as the ratio of C_{max} to equilibrium solubility for both drugs is similar (7.2 for IND and 8.2 for INDME).

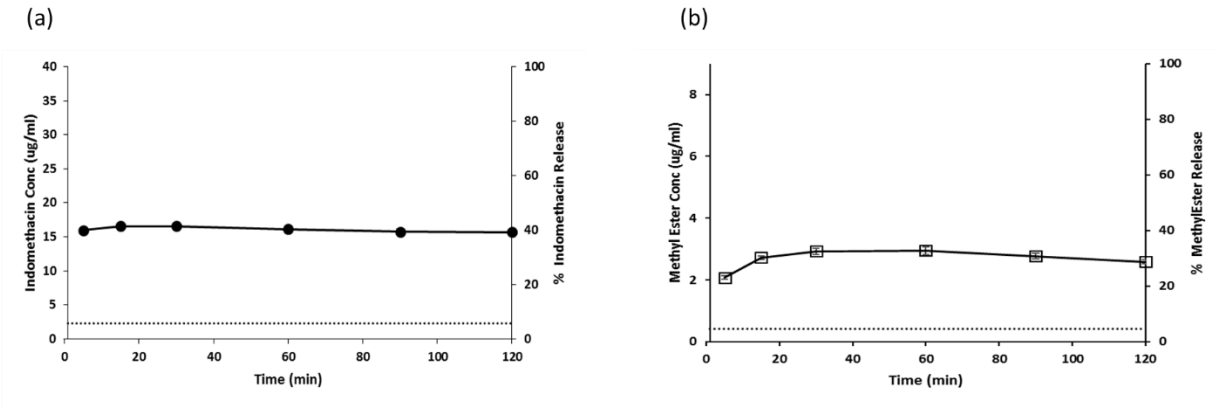


Figure 5.11 Dissolution of (a) IND and (b) INDME loaded SBA-15 systems in McIllvaine buffer (pH 2.2) containing HPMC 100 µg/ml at 37 °C dosed at amorphous solubility levels (37.5 µg/ml for IND and 9.2 µg/ml for INDME). The dashed line represents equilibrium solubility levels for both drugs (2.3 µg/ml for IND and 0.42 µg/ml for INDME). Values represent mean ± standard deviation, n=3 (error bars too small to be visible).

While drug release for both IND and INDME was significantly enhanced compared to equilibrium solubility levels, drug release was incomplete. To exclude the possibility of drug crystallisation as a cause of this incomplete release, the media was filtered following dissolution, the precipitate collected and dried under vacuum overnight. The precipitate was analysed by pXRD and the results are presented in Figure 5.12. No crystalline peaks were detected in the recovered material indicating drug retained on the surface remained in an amorphous state and no precipitation of crystalline drug was detected. The retained drug in the precipitate was dissolved in methanol using ultrasonication for analysis by HPLC to quantify drug content. The results are in agreement with drug release measured during the dissolution study. Retained indomethacin was calculated as 58.8 ± 6.6 % and indomethacin methyl ester as 61.8 ± 6.8 % (n=3, mean ± standard deviation) which accounts for 103% of the indomethacin dosed and 94% of the indomethacin methyl ester.

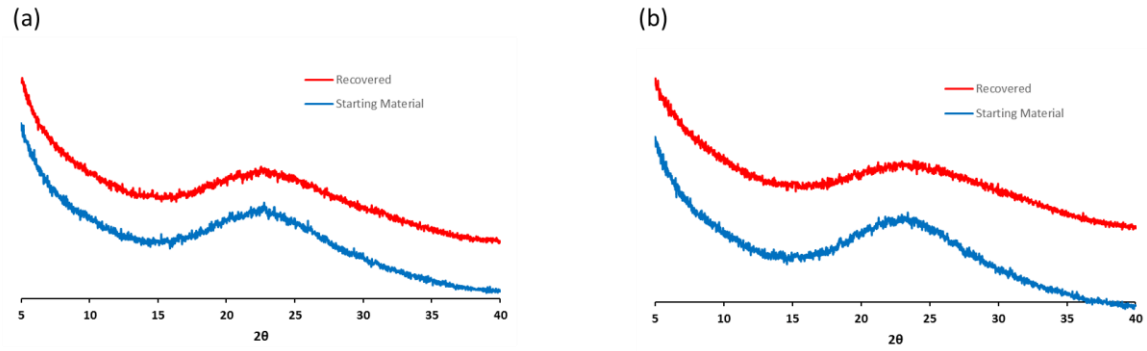


Figure 5.12 p-XRD diffractorgrams of (a) IND and (b) INDME formulations before and after dissolution

A second dissolution study was conducted with the precipitate collected to further investigate the presence for an equilibrium between drug retention and release from SBA-15 systems (Figure 5.13). The release profiles were not statistically significantly different to those of the original dissolution study. In this case, a C_{max} of 41.6 % indomethacin and 34.4 % indomethacin methyl ester were obtained. This result provides further evidence of the dynamic equilibrium existing between drug adsorbed on the silica surface and free drug in solution. Interestingly, even though the quantity of silica in the dissolution medium was double that of the original experiment, the extent of release was unchanged (Table 5.5).

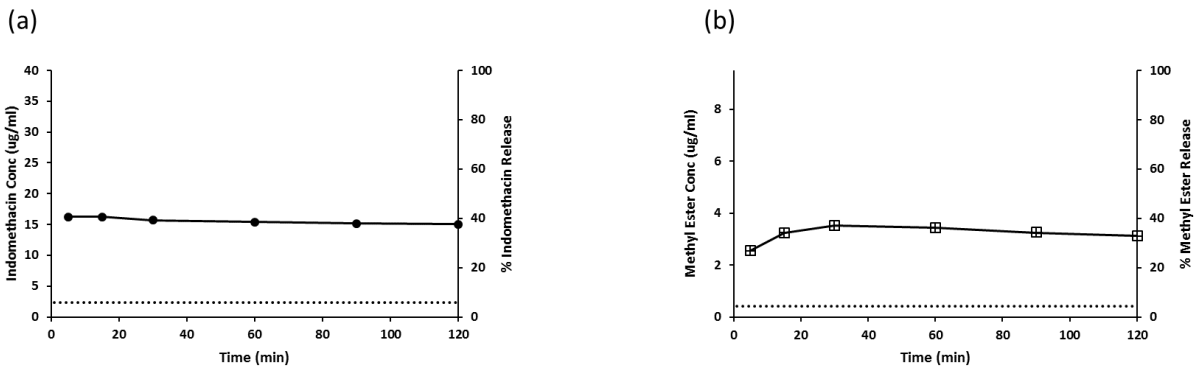


Figure 5.13 Dissolution of recovered precipitate of (a) IND and (b) INDME loaded SBA-15 systems in McIllvaine buffer (pH 2.2) containing HPMC 100 µg/ml at 37 °C dosed at amorphous solubility levels (37.5 µg/ml for IND and 9.2 µg/ml for INDME). The dashed line represents equilibrium solubility levels for both drugs (2.3 µg/ml for IND and 0.42 µg/ml for INDME) (n=1).

Interestingly, it was also observed that drug retention following dissolution from solvent loaded SBA-15 formulations was higher than that predicted on the isotherm at 2.1 mmol/g for IND and 3.4 mmol/g for INDME compared to 0.38 mmol/g for IND and 0.41 mmol/g for INDME during adsorption studies. These formulations were loaded using methanol as the solvent which has a much lower surface tension than McIllvaine buffer pH 2.2 (21 nM/m^2 (290) versus 72 nM/m^2 for McIllvaine buffer). It could therefore access areas in the porous network inaccessible to the dissolution medium, resulting in greater retention on the surface than predicted by the adsorption isotherm. A similar finding has been reported in this thesis in Chapters 4 and 4 for SC-CO_2 loaded mesoporous silica formulations.

Table 5.5 Amount of drug and silica present (mg) with supersaturation ratios (*S*) attained for original dissolution and dissolution of precipitate

	ORIGINAL DISSOLUTION			DISSOLUTION OF PRECIPITATE		
Drug	**Amount of drug (mg)**	**Amount of silica (mg)**	**(*S*)**	**Amount of silica (mg)**	**Amount of silica (mg)**	**(*S*)**
Indomethacin	2.93	21.71	7.2	2.93	38.19	6.6
Indomethacin Methyl Ester	0.69	3.72	8.2	0.69	5.61	7.4

5.5. Discussion

In this study, two similar drug molecules with different hydrogen bonding capabilities were examined to elucidate the mechanism of drug/silica interactions and the influence of hydrogen bond donor and acceptor groups in drug/silica interactions. Indomethacin contains 1 hydrogen bond donor and 4 hydrogen bond acceptors. Indomethacin methyl ester also possesses 4 hydrogen bond acceptors but no hydrogen bond donor (Figure 5.1).

When discussing drug/silica interactions, it is important to first consider the surface chemistry of the mesoporous silica material. Two functional groups are predominant on the heterogeneous silica surface - siloxane bridges and silanol groups (228). Siloxane sites are hydrophobic in nature, whereas hydrophilic silanol groups are considered the key functional group participating in adsorptive interactions. Siloxane (O – Si – O) bridges are strengthened by d_{π}-p_{π} interaction. Both lone pairs of electrons on the oxygen atom are involved in π-interactions meaning the siloxane sites on the silica surface cannot form hydrogen bonds with adsorbates (291). Silanol groups are capable of hydrogen bonding and can be further described as isolated (a single Si-OH group), geminal ($Si(OH)^2$ groups) or vicinal (isolated or geminal silanols hydrogen bonded with each other) (292). It has been documented that not all silanol groups possess equal reactivity, which can determine the strength of potential interactions formed with the silica surface. Reactivity depends on functional group acidity (influenced by pK_a and pH of the dissolution medium). Hydrogen-bonded geminal groups are more acidic in nature than isolated silanols, indicating they have the capability to form stronger hydrogen bonds (291). Importantly, silanol groups can act

as hydrogen bond donors or acceptors (293). It has been reported that drug molecules interact with the silica surface via three main mechanisms; hydrogen bonding and ion-exchange with hydrophilic groups (294). In this study, it was hypothesized that both hydrophobic drug molecules would interact with the silica material through a combination of hydrogen bonding and non-specific hydrophobic interactions. It was also postulated that there would be a disparity in interaction between IND and INDME with the silica surface, as a result of their different hydrogen bonding capabilities.

The data strongly demonstrates that drug/silica interactions for both compounds investigated are a result of hydrogen bonding *via* silanol groups. Evidence for specific intermolecular interactions indicating the presence of hydrogen bond formation is provided in FTIR data displayed in Figure 5.2. The ability of urea, as a strong hydrogen bonding molecule, to reduce the extent of interaction between both drugs and SBA-15 provided further evidence that hydrogen bonding drives drug adsorption (Figure 5.7). This finding supports reports in several published works proposing a range of molecules interact with mesoporous silica through hydrogen bonding (76, 295-297). Interestingly, there was no evidence that either drug interacts with the silica surface via non-specific hydrophobic interactions. As both molecules have a logP of less than 5 (LogP IND = 4.27 and LogP INDME = 4.6 (298)), it was hypothesized that they could interact with siloxane bridges through a hydrophobic interaction mechanism. However, manipulation of medium ionic strength conclusively revealed that neither drug interacts with SBA-15 in a hydrophobic manner. When solvent ionic strength is increased by the addition of salts, hydrophobic drug molecules are expected to associate more strongly with hydrophobic siloxane bridges on the silica surface,

thereby promoting adsorption (255, 256). As shown in Figure 5.8, the level of drug adsorption was not affected by ionic strength, indicating the absence of hydrophobic drug/silica interactions. The results of fluorescence studies further supported this finding, whereby hydrophobic pyrene did not interact with SBA-15 particles in buffer media (Table 5.2).

To ascertain whether hydrogen bonding capability influenced drug adsorption, drug/silica interactions during the solvent loading process were first explored. As can be observed from Figure 5.9 and Table 5.4, at lower monolayer coverage (25 % and 50 %), drug loading of indomethacin was significantly higher indicating the presence of the hydrogen bond donor was advantageous for drug adsorption. However, at monolayer coverage levels of 75 % and above, no difference was displayed in loading efficiency for both molecules. This may be attributed to both drugs exceeding the total pore limit of the silica material as crystalline peaks were observed in XRD data for both IND and INDME. SBA-15 has a wide range of pore sizes (between 2 – 50 nm) with a significant micropore volume, which potentially became blocked by adsorbed drug, reducing achievable monolayer coverage below the theoretical calculated values as described in Section 2.5.1 (288). Based on these results, there is a suggestion that the presence of the hydrogen bond donor enhanced drug/silica interactions. However, the choice of loading solvent should also be considered and has a demonstrated influence on drug loading. It has been reported that the use of SC-CO_2 can result in drug loading deeper in the porous network which could have implications for the results described in this study (273, 299). Future work examining loading of these two drugs using various techniques will be required to further investigate these preliminary findings.

During competitive adsorption experiments, indomethacin methyl ester displayed the strongest affinity for the silica surface (Figure 5.6). This is an interesting finding as it is contrary to observations made during solvent loading. It can be attributed to the relationship between drug, silica and dissolution medium. Both drugs were soluble to a similar extent in methanol, the loading solvent, whereas in McIllvaine buffer (pH 2.2), indomethacin equilibrium solubility was 5.5 times higher and amorphous solubility was 4 times higher than that for the indomethacin methyl ester (Table 5.1). Both drugs are also ionised in the acidic dissolution medium (the pH is below the pK_a of both indomethacin and the methyl ester), indicating there was no difference between the two compounds with respect to electrostatic interactions with the neutral silica surface (226, 300, 301). These results highlight that interactions between drug, silica and the dissolution medium can influence drug adsorption and release from the silica surface.

To understand the nature of drug adsorption onto the silica surface, under conditions up to and exceeding amorphous solubility levels, adsorption isotherms were generated. The adsorption isotherms developed are displayed in Figure 5.3 and were fitted to various isotherm equations including the Langmuir model which describes monolayer adsorption onto a homogeneous surface which contains only one type of binding site. Under the constraints of this model no lateral interactions can exist between adsorbed molecules (224, 302). The Freundlich model which depicts non-ideal adsorption onto heterogeneous surfaces, including multi-layer adsorption, was also applied to the data. This empirical model accounts for an adsorptive surface possessing a range of binding sites, having different binding affinities for the adsorbate. The SBA-15 surface can be considered heterogeneous, due to the

presence of silanol functional groups possessing different binding affinities for adsorbate molecules (225). These isotherm models have already been applied successfully in published studies and in Chapter 3 of this thesis (118, 151, 223). As can be evidenced in Table 5.3, the data fit reasonably well to Langmuir and Freundlich equations which indicates both monolayer and multilayer drug adsorption contribute to overall drug adsorption on the surface. Interestingly, multilayer adsorption was demonstrated below theoretical monolayer coverage (Figure 5.3). This was demonstrated in the fluorescence spectroscopy data where the fluorescent dye, pyrene, interacted with drug multilayers on the silica surface at concentrations below liquid-liquid phase separation levels (Table 5.2). This explains the good fit to the Freundlich model and indicates drug molecules do not adsorb initially as a full monolayer before multilayer adsorption occurs. The Freundlich model proved to be a better fit for indomethacin adsorption onto SBA-15. This can be attributed to indomethacin's superior ability to self-interact through dimerization, thus forming multilayers more easily on the silica surface (61).

Isotherm parameters related to binding affinity were also calculated. For IND and INDME, the binding affinities derived from both isotherm models were stronger for the methyl ester than indomethacin (Table 5.3). The Langmuir constant, K_L, can be related to the chemical potential of the drug which is defined as the contribution it makes to the overall free energy of the system (12). As the binding affinity of the methyl ester to the silica surface is stronger than that of the indomethacin (as determined by its larger K_L value), it would be energetically favourable to have methyl ester bound on the surface than existing as free drug in solution. Further evidence of this is demonstrated in the competitive adsorption experiments where methyl ester

has the ability to displace indomethacin from the silica surface but the reverse is not observed (Figure 5.6).

To compare adsorption of both drugs directly, equilibrium concentrations were converted to their corresponding activity levels in solution using Equation 5.4 and plotted against quantity of drug adsorbed (mmol) per gram SBA-15. Activity is related to chemical potential as described in Equation 5.5,

$$\mu = \mu_i^o + RT \ln a_i \qquad (Equation\ 5.5)$$

where μ is the chemical potential of the component, μ_i^o is the chemical potential of component *i* in the standard state, that is, at 1 bar pressure. The quantity a_i is known as the activity of component *i* of the system.

The activity allows us to quantify how the chemical potential of a pure substance changes when it becomes a component in a mixture as is the case when drug is adsorbing on the surface of the silica material. The concept of activity rather than chemical potential is required because it has been found that the amount of a substance in a system which is active (that is which is causing an effect of some sort) is not always identical to the concentration (12). In this study, amorphous solubility was designated an activity of 1. Data from both IND and INDME overlay closely on this graph indicating that activity of free drug in solution determines passive drug adsorption on the silica surface. A similar finding was observed by Hansen *et al* in a study that examined aliphatic alcohol and acid adsorption onto carbon material (303). They observed marked progression of amounts adsorbed at a given concentration on ascending a homologous series becomes almost non-existent if amounts adsorbed are compared at given absolute activity of the organic solute and

concluded that relative adsorption of members in a homologous series is determined primarily by solute activity on non-porous carbon. A second study investigated diazepam adsorption onto a different carbon system and reported similar findings (304). They observed a relationship between drug adsorption affinity for the adsorbent surface and drug solubility in solution. Both studies utilized activity *versus* adsorption plots to represent their data similar to the approach adopted in this study (Figure 5.4). However, this is the first study which examines the influence of solute activity at supersaturating conditions. The findings could have implications for mesoporous silica formulations as they suggest that drug adsorption onto the silica surface can be predicted to some extent by solute activity in solution. This hypothesis would need to be tested further using a range of drugs with various physicochemical properties and using solvents utilized in drug loading processes.

To investigate the implications of the observations made during adsorption studies on drug release from loaded silica formulations, dissolution studies were conducted for both formulations. The two model compounds displayed significant incomplete release (44 % release of IND and 32 % release of INDME) (Figure 5.11). Further dissolution experiments of the precipitate revealed similar dissolution profiles to the original study, indicating the presence of a dynamic equilibrium process during drug release from these formulations. This equilibrium can be expressed in Equation 5.6,

$$Adsorbed\ drug + solvent\ in\ solution \rightleftharpoons Adsorbed\ solvent + drug\ in\ solution \quad (Eq. 5.6)$$

and has recently been described for these systems by Dening *et al* (272). Further evidence for the presence of this dynamic equilibrium is presented in this work as theoretical supersaturation ratio for both drugs is compared with supersaturation

achieved during the dissolution study. Theoretical supersaturation ratio for IND was 17.5 while INDME was calculated as 19.1. However, the supersaturation achieved was approximately only half that at 7.2 for IND and 8.2 for INDME. This compares favourably with data from the study by Dening *et al* for ritonavir where theoretical supersaturation was 7.8 while a supersaturation of only 3.9 was realised. The supersaturation levels reached for these three drug molecules was approximately 50 % of theoretical limits at amorphous solubility. This finding poses challenges for drug delivery from these mesoporous silica systems when compared with other solubility enhancing formulations, such as polymer based amorphous solid dispersions, as they are not capable of comparable supersaturation (287). It has been demonstrated in Chapter 3 and 4 of this thesis that the presence of incomplete release is not confined to supersaturation conditions. Several studies have also published incomplete release profiles under sink conditions (116, 249, 299). In this study, samples containing both drugs adsorbed on the silica surface were diluted to 'sink conditions' (20 % saturated solubility (81)). However, a significant quantity of drug remained adsorbed to the silica material after 24 h (27 % for IND and 43 % for INDME, Figure 5.5).

It is interesting to note that drug release from the original dissolution study and the precipitate are identical even though the quantity of silica utilized in both studies varied (approximately double the amount of silica was required for the precipitate experiment for both drugs). This indicates that that quantity of silica present is not the determining factor for drug release, rather the equilibrium exists between drug in solution and drug on the silica surface. This is related to the activity of drug in

solution providing further evidence for the hypothesis that drug adsorption onto the silica surface is influenced to some extent by solute activity in solution.

5.6. Conclusion

This study is the first to demonstrate experimentally that drug/silica interactions occur via hydrogen bonding. Non-specific hydrophobic interactions did not contribute to the mechanism of interaction. The data suggests that hydrogen bond donor capability may influence drug adsorption during the loading process. However, other factors play a role in drug adsorption and retention during dissolution which depends on the relationship between drug, silica and dissolution medium. Adsorption isotherms proved useful in understanding the equilibrium between drug adsorbed on the surface and free drug in solution. Adsorption of the two model drugs was comparable when examined as a function of drug activity in the system. The data suggests that solute activity in solution could help predict drug adsorption on mesoporous silica materials. Dissolution studies also confirm the presence of an equilibrium between drug adsorbed on the silica surface and drug in solution during drug release. It was observed that this equilibrium is not a consequence of the quantity of silica present but rather the relationship between drug on the silica material *versus* drug in the dissolution medium. This provides further evidence that knowledge of drug activity in solution can aid in our understanding of drug release from mesoporous silica formulations.

Chapter 6: *In Vitro* Dissolution Models for the Prediction of *In Vivo* Performance of an Oral Mesoporous Silica Formulation

Modified Version of Publication:

McCarthy CA, Faisal W, O'Shea JP, Murphy C, Ahern RJ, Ryan KB, Griffin BT, Crean AM. *In vitro* dissolution models for the prediction of *in vivo* performance of an oral mesoporous silica formulation. Journal of Controlled Release. 2017;250:86-95.

Acknowledgements: I would like to thank Dr. Joseph O'Shea and Dr. Brendan Griffin (School of Pharmacy, University College Cork) for performing the *in silico* modelling and for help with interpretation of the results.

6.1 Abstract

Drug release from mesoporous silica systems has been widely investigated *in vitro* using USP Type II (paddle) dissolution apparatus. However, it is not clear if the observed enhanced *in vitro* dissolution can forecast drug bioavailability *in vivo*. In this study, the ability of different *in vitro* dissolution models to predict *in vivo* oral bioavailability in a pig model was examined. The fenofibrate loaded mesoporous silica formulation was compared directly to a commercial reference product, Lipantil Supra®. Three *in vitro* dissolution methods were considered; USP Type II (paddle) apparatus, USP Type IV (flow-through cell) apparatus and a USP IV Transfer model (incorporating an SGF to FaSSIF-V2 media transfer). *In silico* modelling, using a physiologically based pharmacokinetic modelling and simulation software package (Gastroplus™), to generate *in vitro/in vivo* relationships was also investigated. The study demonstrates that the *in vitro* dissolution performance of a mesoporous silica formulation varies depending on the dissolution apparatus utilised and experimental design. The findings demonstrate that the USP IV transfer model was the best predictor of *in vivo* bioavailability. The USP Type II (paddle) apparatus was not effective at forecasting *in vivo* behaviour. This observation is likely due to hydrodynamic differences between the two apparatus and the ability of the transfer model to better simulate gastrointestinal transit. The transfer model is advantageous in forecasting *in vivo* behaviour for formulations which promote drug supersaturation and as a result are prone to precipitation to a more energetically favourable, less soluble form. The USP IV transfer model could prove useful in future mesoporous silica formulation development. *In silico* modelling has the potential to

assist in this process. However, further investigation is required to overcome the limitations of the model for solubility enhancing formulations.

6.2 Introduction

While the previous research chapters in this thesis have focused on *in vitro* dissolution at a molecular level, the final chapter investigates the apparatus utilized in these dissolution studies and examines which experimental set-up best predicts *in vivo* performance.

The majority of *in vitro* dissolution experiments conducted involving mesoporous silica formulations have utilised traditional methods: USP Type II apparatus and sink conditions with simple buffer solutions as the dissolution medium (88-92). There are limitations associated with this traditional approach to dissolution which are of particular relevance to poorly water-soluble drug candidates (80). Augustijns *et al* recommended that non-sink *in vitro* dissolution conditions are required for silica-based formulations to provide meaningful data that can be correlated with *in vivo* studies (85). Furthermore, as described in Chapter 4, simple buffer solutions utilised in most *in vitro* experiments do not represent all aspects of the fluid composition of the gastrointestinal (GI) tract and it is now recommended to use biorelevant media that better simulate physiological fluids (233). The Type IV dissolution apparatus offers the ability to change the dissolution medium during an experiment, which results in conditions that more closely reflect the pH gradient associated with transit through the GI tract (305). It has been reported that the Type IV dissolution apparatus is a better simulator of *in vivo* hydrodynamics than the paddle apparatus (101). However, the number of studies which utilise this model are limited and published data with regards to the superiority of the Type IV flow-through cell over the Type II apparatus is not in agreement (103, 104).

In this study, the ability of *in vitro* dissolution methods to predict *in vivo* performance of an oral mesoporous silica drug delivery system was compared. Type II and Type IV dissolution apparatus were employed to investigate the release of a poorly water-soluble drug, fenofibrate, from this formulation. This study is the first to use the Type IV apparatus to assess dissolution of a BCS Class II drug loaded mesoporous silica system. Fenofibrate was chosen as the model compound in this study. Fenofibrate is a neutral, lipophilic drug (log P = 5.2), which is practically insoluble in water (20). The *in vivo* performance of the mesoporous silica formulation was assessed following oral administration in a fasted pig model and compared to the commercial fenofibrate formulation, Lipantil Supra® (which utilises NanoCrystal® technology) (306).

In vitro/in vivo correlations (IVIVC) and *in vitro/in vivo* relationships (IVIVR) are being increasingly used as part of the formulation 'toolbox' to build on knowledge from *in vitro* data and forecast formulation effects. The best candidates for *in vitro/in vivo* correlations are drugs where dissolution is the rate-limiting step to drug absorption and biorelevant dissolution models are utilised in the experimental design (307). In this study, data from the *in vitro* and *in vivo* experiments was analysed using a physiologically-based pharmacokinetic modelling and simulation software package (Gastroplus™) to generate IVIVR. The potential benefits and limitations of this *in silico* modelling approach are discussed.

6.3 Material and Methods

6.3.1. Materials

Fenofibrate was purchased from Kemprotec Ltd. (United Kingdom). SBA-15 was obtained from Glantreo Ltd. (Ireland). Liquid carbon dioxide was supplied by Irish Oxygen Ltd. (Ireland). Fenofibric acid, sodium taurocholate (>95%) and pepsin (from porcine gastric mucosa, 800-2500 units/mg protein) were obtained from Sigma Aldrich (Ireland). Lecithin (Lipoid E PC S, >98 % pure) was kindly donated by Lipoid GmbH, Germany. All other chemicals and solvents were of analytical grade or HPLC grade and purchased from Sigma-Aldrich (Ireland). Lipantil® Supra 145 mg film-coated tablets were sourced through a local community pharmacy.

6.3.2. Preparation of Fenofibrate Loaded Silica Formulation

Fenofibrate loaded SBA-15 was prepared according to the method previously described by Ahern *et al* (88). The drug and mesoporous silica (2 g) at a drug:silica mass ratio of 2:3 were combined in a BC 316 high-pressure reactor (High Pressure Equipment Company, USA) and stirred using a magnetic stirring. The reactor was heated to 40 °C using heating tape and maintained at this temperature for the duration of the experiment. Temperature was monitored using a temperature monitor (Horst GmbH, Germany). The reactor cell was filled with liquid CO_2 and a high pressure pump (D Series Syringe Pump 260D, Teledyne ISCO, USA) was used to pump additional CO_2 to a final processing pressure (27.58 MPa). After 12 h, the cell

was depressurised rapidly by venting the CO_2. The processed material was collected from the cell and stored in a desiccator prior to analysis.

6.3.3. Drug Content Quantification

The fenofibrate content of the silica formulation was determined by thermogravimetric analysis (TGA), using a TGA 500 instrument (TA Instruments Ltd., United Kingdom). Samples in the weight range 2–10 mg were loaded onto tared platinum pans and heated from ambient temperature to 900 °C, at a heating rate of 10 °C/min under an inert N_2 atmosphere. Samples were analysed in triplicate. The drug quantity was calculated based on the weight loss between 100 and 900 °C, corrected for the weight loss over the same temperature range for a silica (SBA-15) reference sample (55). TGA thermograms were analysed using Universal Analysis 2000 software (TA Instruments Ltd., United Kingdom). Drug-loading efficiency was calculated using Equation 3.2.

6.3.4. Solubility Measurements

Solubility studies were carried out by the addition of excess fenofibrate to biorelevant media using a standardised shake-flask method with a shake time of 24 h at 37 °C (308). Simulated gastric fluid (SGF) was prepared as outlined in the USP NF 26 (234). FaSSIF-V2 was prepared as outlined in the literature (233). Samples (2 ml volume) were removed at 24 h and centrifuged at 16,500 *g* for 13 min using a Hermle z233M-2 fixed angle rotor centrifuge, (HERMLE Labortechnik GmbH, Germany). The

supernatant was removed and centrifuged again under the same conditions. The resultant supernatant was analysed using HPLC following dilution with acetonitrile.

6.3.5. *In Vitro* Dissolution Experiments

USP Type II (Paddle) Apparatus: Dissolution studies were carried out in triplicate with an Erweka® DT600 dissolution test system (Erweka GmbH, Germany). Tests were performed in 500 ml of SGF or FaSSIF-V2 at 37 ± 0.5 ^{o}C at a paddle rotation of 50 rpm. Drug loaded silica samples equivalent to 50 mg fenofibrate were placed in the dissolution medium. The dose of 50 mg fenofibrate in the release media corresponded to a theoretical concentration of 100 µg/ml following complete dissolution which represents a supersaturated state in SGF and FaSSIF-V2 (see fenofibrate solubility values in section 6.4.2). Samples of 4 ml volume were withdrawn at 1, 5, 10, 15, 30, 60 and 120 min intervals (with additional samples taken from the FaSSIF-V2 media at 180 and 240 min). Samples were immediately replaced with an equal volume of fresh, pre-warmed medium. The withdrawn samples were filtered through a 0.20 µm PES membrane filter (Filtropur S0.2, Sarstedt AG & Co., Germany). Samples were diluted with acetonitrile prior to analysis by HPLC.

USP Type IV (Flow-Through Cell) Apparatus: Dissolution studies were carried out in triplicate with an Erweka® flow-through apparatus (DFZ 720 with HKP 720 piston pump) equipped with 22.6 mm diameter cells. The temperature of the water bath was maintained at 37 ^{o}C. The dissolution medium of either 100 ml SGF or FaSSIF-V2, recirculated in closed loop model at a flow rate of 4 ml/min. A glass ball (5 mm) and 1 g of glass beads (1 mm) were placed in the bottom of the cone to ensure laminar

flow of the jet of fluid entering the cell. Formulation samples equivalent to 10 mg fenofibrate were placed on top of the glass beads. Undissolved fenofibrate particles were retained in the sample holder using a glass fibre filter located in the top of the cone. The dose of fenofibrate in the release media thus corresponded to a theoretical concentration of 100 µg/ml which represents a supersaturated state in SGF and FaSSIF-V2 (see fenofibrate solubility values in section 6.4.2). Samples of 1 ml volume were withdrawn at 1, 5, 10, 15, 30, 60 and 120 min intervals (with additional samples taken from the FaSSIF-V2 media at 180 and 240 min). Samples were immediately replaced with an equal volume of fresh, pre-warmed medium. The withdrawn samples were filtered through a 0.20 µm PES membrane filter (Filtropur S0.2, Sarstedt AG & Co., Germany). Samples were diluted with acetonitrile and analysed by HPLC. In addition to conducting individual dissolution experiments using the Type IV apparatus employing either SGF or FaSSIF-V2, a dissolution experiment involving a SGF to FaSSIF-V2 transfer method was conducted. Samples were removed as described above for the initial SGF stage of the experiment up to the 120 min time point. The SGF dissolution medium supply beaker was then removed and replaced with a beaker containing 100 ml of FaSSIF-V2 medium. Subsequent sampling time points were taken at 1, 5, 10, 15, 30, 60 and 120, 180 and 240 min) following transfer from SGF to FaSSIF-V2 medium.

6.3.6. *In Vivo* Oral Bioavailability Study

The study was carried out under licences issued by the department of Health, Ireland as directed by the Cruelty to Animals Act Ireland and EU Statutory Instructions. Local

university ethical committee approval was also obtained. The data from this intravenous study has been previously used for the calculation of fenofibrate clearance in pigs to allow absolute bioavailability to be determined in separate studies (309, 310). Female landrace pigs (17–19 kg) housed at the University College Cork's Biological Services Unit were used for these experiments. Animals were fasted for 16 h before experimentation. On day 1, an indwelling intravenous catheter was inserted in the jugular vein, under general anaesthesia, as previously described (311). Following recovery, pigs were returned to their pens and allowed access to food and water.

On day 2 (following an overnight fast), the oral formulations containing a dose of 67 mg fenofibrate were administered in gelatin capsules with the aid of a dosing gun. After dosing the pigs received 50 ml of water via an oral syringe. Blood samples (5 ml) were withdrawn from the jugular line at time zero (pre-dosing) and at 0.5, 1, 1.5, 2, 3, 4, 6, 8, 12 and 24 h intervals post dosing. Water was available *ad libitum* throughout the study period and the animals were fed 8 h post-dose. For the intravenous treatment (i.v.), animals were administered 25 mg fenofibrate by slow infusion, over 2 min, via 3 ml of a solution containing 8.33 mg/ml fenofibrate in 80 %w/w ethanol and 20 %w/v physiological saline into an ear vein. Blood sampling was performed as outlined above. All blood samples were collected in heparinised tubes (Sarstedt, Germany) and centrifuged immediately after withdrawal at 3220 *g* for 5 minutes at 4 °C. Plasma samples were stored at −80 °C prior to HPLC assay.

6.3.7. Quantitative Analysis of Fenofibrate

HPLC analysis of the *in vitro* dissolution samples was performed using an Agilent 1200 series HPLC system with an UV/Vis detector (Agilent Technologies, USA). A reversed-phase column (Kinetex C-18, 150 × 4 mm x 2.6 µm, Phenomenex Ltd. UK), mobile phase of acetronitrile and water (80:20) at a flow rate of 1 ml/min and injection volume of 20 µl were employed. The wavelength for fenofibrate detection was set at 286 nm and retention time was 4.5 min.

In vivo plasma samples were quantified for fenofibric acid (the major active metabolite of fenofibrate). Based on a method by Griffin *et al* (310), a volume of 0.5 ml plasma was spiked with 50 µl of internal standard (sulindac) and vortexed. Proteins were precipitated through the addition of 0.5 ml of 25 %w/v NaCl solution and 1 ml of 1 %w/v H_3PO_4 in methanol with thorough mixing. Samples were centrifuged at 11,500 *g* for 9 min using a Hermle z233M-2 fixed angle rotor centrifuge (HERMLE Labortechnik GmbH, Germany). The supernatant (20 µl) was injected onto a Synergi C18 reversed phase column (250 x 4.6 x 2.6 µm, Phenomenex Ltd. UK) using the Agilent system described above. The mobile phase consisted of acetronitrile and water (80:20) adjusted to pH 2.5. The flow rate was set at 1 ml/min resulting in elution of fenofibric acid and fenofibrate at 6.5 and 10.5 min, respectively. The concentration of drug was determined at 286 nm.

6.3.8. *In Vitro* and *In Vivo* Data Analysis

The extent of fenofibrate release was calculated as area under the dissolution curve (AUC) using Prism (ver. 5, GraphPad Software Inc., USA.). Peak fenofibrate concentrations (C_{max}) and the time for their occurrence (T_{max}) were noted directly from the individual dissolution profiles. Intravenous pharmacokinetic parameters were fitted to a two-compartment model using the PKPlus™ module in Gastroplus™ (ver. 8.6, Simulations Plus Inc., USA). AUC for fenofibric acid after oral administration of both formulations was calculated for 24 h post-dosing using Prism. The peak plasma concentrations (C_{max}) and the time for their occurrence (T_{max}) were noted directly from the individual plasma concentration vs. time profiles. Absolute bioavailability (F_{abs}) was calculated according to Equation 6.1:

$$F_{abs} = \left(\frac{\text{AUC oral}}{\text{AUC i. v.}}\right) x \left(\frac{\text{Dose i. v.}}{\text{Dose oral}}\right) \qquad Equation\ (6.1)$$

Relative bioavailability was calculated as the ratio of $AUC_{0\rightarrow24}$ obtained after oral administration of the silica and Lipantil Supra® formulations. The relative extent of fenofibrate release from both formulations in the three different dissolution models was calculated as the ratio of AUC values. Results are reported as mean ± standard deviation.

In vitro dissolution data comparing the two formulations was tested for significance ($p < 0.05$) using a two-tailed, independent sample *t*-test, assuming Gaussian distribution and equal variance. Statistical analysis of the C_{max} and AUC values from the dissolution profile for both formulations were performed using a one-way analysis of variance (ANOVA) and post hoc Tukey's multiple comparisons test. *P*-

values of <0.05 were considered significant. Paired *t*-tests were used to determine the statistical significance ($p < 0.05$) of calculated *in vivo* bioavailability and pharmacokinetic results, as each animal acted as its own control in this crossover study. All statistical analyses were performed using GraphPad Prism (Version 5, USA).

6.3.9. *In Silico* Predictive Modelling

In silico modelling was conducted using GastroPlus™ (ver. 9.0, Simulations Plus, USA.). The ADMET Predictor™ module was used to estimate fenofibrate physiochemical characteristics. Predictive mathematical models were generated using the IVIVCPlus™ component of the software. In this study, the Loo-Riegelman two-compartment method was implemented to deconvolute the *in vivo* oral plasma concentration profiles using intravenous data as previously published (309, 310). An IVIVR was generated by correlating the fraction of drug absorbed *in vivo* with the fraction of drug dissolved *in vitro* (for the initial period of fenofibrate dissolution i.e. time points up to T_{max}). The data was then convoluted to generate a predicted plasma concentration-time profile, which was compared with the observed *in vivo* data. The software displayed C_{max} and AUC for the observed and predicted profiles. It also generated the prediction error between the two profiles which can be used to evaluate the predictability of the correlation as described by the FDA (Food and Drug Administration) (312). The FDA require an average absolute percentage error (%PE) of 10 % or less for AUC and C_{max} for internal predictability. The % PE for each formulation should not exceed 15 %.

6.4 Results

6.4.1. Drug Content Quantification

Fenofibrate loading onto SBA-15 was 251.3 mg drug/g silica (25.13 % ± 0.68). The low variability observed in the drug loading for this SC-CO_2 process is indicative of a homogeneous drug distribution on the silica surface (54). The drug loading efficiency, calculated using Equation 3.2, was 62.83%. The loading technique converted the fenofibrate to a non-crystalline solid phase as previously reported by Ahern *et al* (88).

6.4.2. Fenofibrate Solubility

Fenofibrate solubility in SGF was determined as 0.17 ± 0.05 µg/ml. Fenofibrate solubility in FaSSIF-V2 (3.64 ± 0.62 µg/ml) was significantly enhanced, which indicates that fenofibrate is solubilised in the micelles of simulated intestinal fluid (308).

6.4.3. *In Vitro* Dissolution

6.4.3.1. USP Type II (Paddle) Apparatus

Dissolution experiments using the USP Type II (paddle) method were conducted under supersaturated conditions (580 times drug saturated solubility in SGF and 27 times the saturated solubility in FaSSIF-V2). There was no detectable release of fenofibrate from the silica formulation in SGF. This could be explained by the mechanism of drug release previously published for mesoporous silica systems *in vitro* (207, 313). These reported dissolution profiles involve an initial burst release

(where the majority of loaded drug is released) followed by a sustained secondary release (117). As a result of the drug's low solubility in conditions of low pH and the absence of additional excipients to enhance solubility or stabilise dissolution, the release of fenofibrate was not quantifiable (the limit of quantification was 200 ng/ml). Fenofibrate dissolution from the Lipantil Supra® formulation resulted in a sustained supersaturation (Figure 6.1). Drug release increased over the first 15 mins (C_{max} 2.79 ± 0.70 µg/ml), before reaching a plateau for the remainder of the experiment. The supersaturation ratio during this plateau phase (defined as C/C_s, where C_s is the saturated solubility) was 15.49. This marked solubility increase is most likely due to the composition of the Lipantil Supra® formulation which contains surfactants, sodium dodecyl sulfate (SDS) and sodium docusate. SDS can significantly increase the solubility and dissolution rate of fenofibrate through a combination of wetting, micellar solubilisation and deflocculation (314, 315).

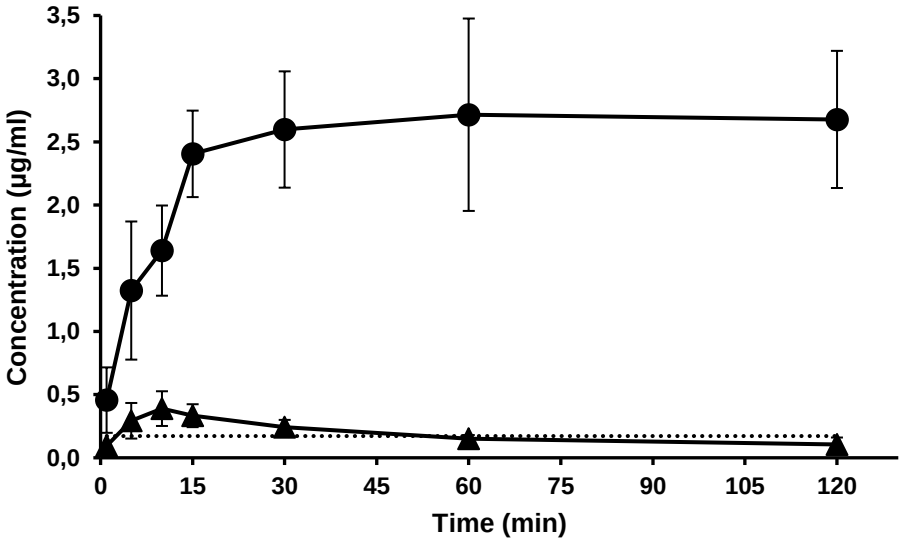


Figure 6.1 Fenofibrate release profiles for Lipantil Supra® in SGF at 37 °C; (▲) indicates Type IV apparatus, (●) indicates Type II (paddle) apparatus. Dotted line indicates equilibrium solubility of fenofibrate in SGF. (n=3, Y error bars indicate standard deviation)

Compared to SGF, fenofibrate release from both formulations was significantly higher in FaSSIF-V2 due to the greater amount of physiologically relevant surfactants in the medium. FaSSIF-V2 allows for increased micellar solubilisation of the drug (Figure 6.2). However, the extent of release from the commercial product was significantly higher than release from the silica formulation ($p < 0.001$). Fenofibrate release from the silica formulation in FaSSIF-V2 media exhibited the classic 'burst release' profile characteristic of silica formulations (207, 313). Drug dissolution maintained supersaturation levels for the first 30 min of the experiment (C_{max} = 5.76 ± 0.28 µg/ml, supersaturation ratio of 1.58). However, at 60 min, release had dropped below fenofibrate thermodynamic solubility levels. Fenofibrate release from the Lipantil Supra® formulation demonstrated high levels of supersaturation

(C_{max} = 53.68 ± 2.73 µg/ml, peaking at a supersaturation ratio of 14.74). Drug dissolution decreased after 30 min for the remainder of the experiment but never dropped below supersaturation levels over the 4 h experiment.

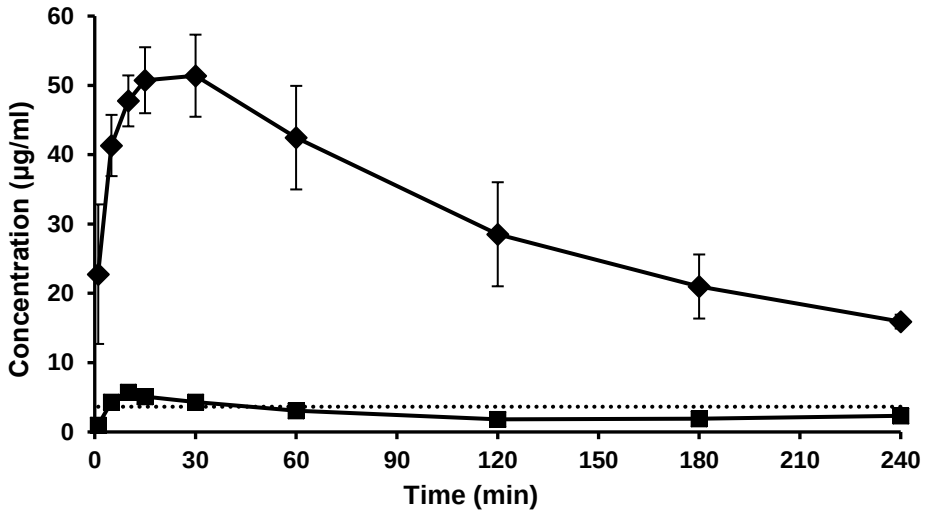


Figure 6.2 Fenofibrate release profiles from mesoporous silica formulation (■) and Lipantil Supra® (◆) in FaSSIF-V2 media at 37 °C for Type II (paddle) apparatus. Dotted line indicates fenofibrate solubility in FaSSIF-V2 media. (n=3, Y error bars indicate standard deviation)

A summary of the *in vitro* release parameters are detailed in Table 6.1. The high levels of release observed in this dissolution experiment with FaSSIF-V2 alone might not be indicative of *in vivo* performance. *In vivo*, the formulation will experience the low pH of the stomach initially (where the drug has extremely low solubility), which may result in significant precipitation. Precipitation to a lower energetically favourable, less water-soluble form can have a dramatic effect on drug release following transit to the small intestine environment mimicked by FaSSIF-V2. *In vitro* experiments simulating this transition were therefore conducted and are described in the section 6.4.3.3.

Table 6.1 Summary of *in vitro* dissolution parameters. Mean values +/- standard deviation are provided (n=3)

Type II (Paddle) Apparatus			
Formulation	$C_{max\ FASSIF}$ (µg/ml)	$AUC_{240min\ FASSIF}$ (µg/ml.min)	T_{max} (min)
Mesoporous Silica	5.76 ± 0.28	631 ± 9	10 ± 0
Lipantil Supra®	53.68 ± 2.73	7493 ± 1177	20 ± 8.7
Type IV (Flow Through Cell) Apparatus			
Formulation	$C_{max\ FASSIF}$ (µg/ml)	$AUC_{240min\ FASSIF}$ (µg/ml.min)	T_{max} (min)
Mesoporous Silica	2.96 ± 0.79	398 ± 81	20 ± 8.7
Lipantil Supra®	4.45 ± 0.29	924 ± 36	15 ± 0
Transfer Model			
Formulation	$C_{max\ FASSIF}$ (µg/ml)	$AUC_{240min\ FASSIF}$ (µg/ml.min)	T_{max} (min)
Mesoporous Silica	1.49 ± 0.07	322 ± 18	160 ± 69.3
Lipantil Supra®	2.04 ± 0.06	364 ± 30	240 ± 0

6.4.3.2. USP Type IV (Flow-Through Cell) Apparatus

Non-sink conditions in the Type IV model were equivalent to those employed for USP II apparatus (580 times drug equilibrium solubility in SGF and 27 times the saturated solubility in FaSSIF-V2). Similar to results observed for the Type II model, fenofibrate release from the mesoporous silica formulation in SGF was not quantifiable. Fenofibrate release from Lipantil Supra® in SGF reached supersaturation levels for the first 30 min of the experiment (C_{max} = 0.41 ± 0.09 µg/ml) but at 60 min release had fallen to the drug's equilibrium solubility (Figure 6.1). As illustrated in Figure 6.1, the C_{max} level and the extent of fenofibrate release was significantly higher using the Type II apparatus compared to the Type IV flow through cell ($p < 0.005$). This indicates that hydrodynamic differences between the two model apparatus have a significant impact on the dissolution process and the final dissolution profile. This is discussed in more detail in Section 6.5.

Similar to the Type II apparatus, both formulations exhibit enhanced drug release in the FaSSIF-V2 media using the Type IV apparatus. The extent of release from Lipantil Supra® was significantly higher than that of the silica formulation ($p < 0.001$, Figure 6.3). However, release from the SBA-15 system did not reach supersaturation levels in the Type II apparatus. Fenofibrate release from the Lipantil Supra® formulation peaked at 15 min (C_{max} = 4.45 ± 0.29µg/ml, supersaturation ratio of 1.22), then dropped to remain at the thermodynamic solubility level for the duration of the four hour experiment. A summary of *in vitro* release parameters is provided in Table 6.1.

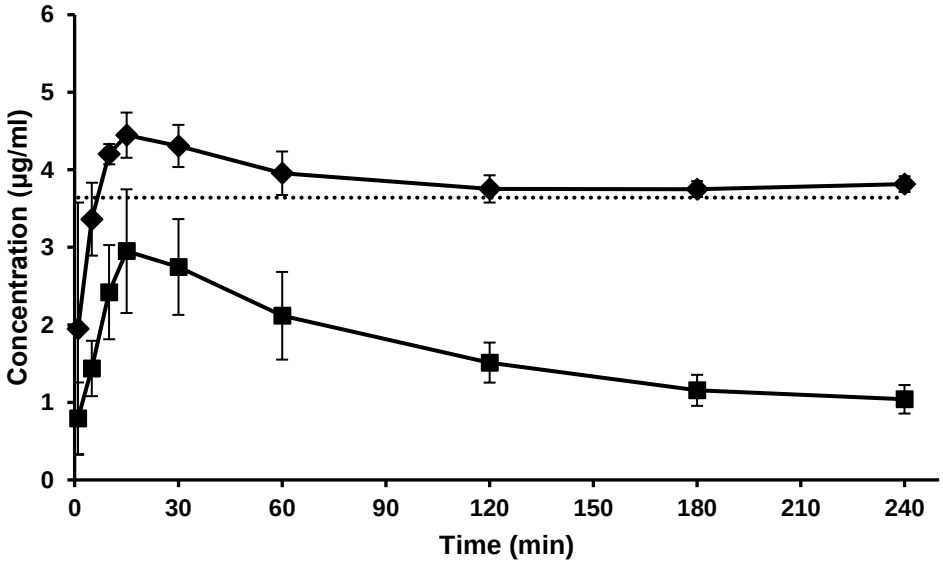


Figure 6.3 Fenofibrate release profiles from mesoporous silica formulation (■) and Lipantil Supra® (◆) in FaSSIF-V2 media at 37 °C for Type IV (flow through cell) apparatus. Dotted line indicates fenofibrate solubility in FaSSIF-V2 media. (n=3, Y error bars indicate standard deviation)

6.4.3.3. Transfer Model in USP Type IV (Flow-Through Cell) Apparatus

In the Type IV transfer model, samples were first exposed to SGF for 120 min followed by FaSSIF-V2 media for 240 min, to simulate GI transit in the dissolution model. As described in section 6.4.3.2, the Lipantil Supra® formulation reached supersaturation levels in the SGF, whereas release from the mesoporous silica system was unquantifiable (Figure 6.4). The shape of the dissolution profile for the silica formulation in the transfer model (FaSSIF-V2 stage) is different from that of the Type II or Type IV FaSSIF-V2 profiles (Figure 6.4). The classic 'burst' release in FaSSIF-V2 media was not evident using the transfer model and neither formulation reached supersaturation levels in the FaSSIF-V2 media (C_{max} = 2.04 ± 0.06 µg/ml for Lipantil Supra® and C_{max}= 1.49 ± 0.07 µg/ml for the silica formulation). It is probable that the

reduction in the extent of dissolution in FaSSIF-V2 is due to fenofibrate precipitation upon exposure to SGF media for both formulations. While C_{max} for Lipantil Supra® was significantly higher than for the silica system ($p < 0.001$), there was no significant difference in the overall extent of fenofibrate release over the duration of the experiment ($p > 0.1$). This is in contrast to release profiles for both formulations in FaSSIF-V2 media alone in USP Type II and USP Type IV apparatus (Table 6.1).

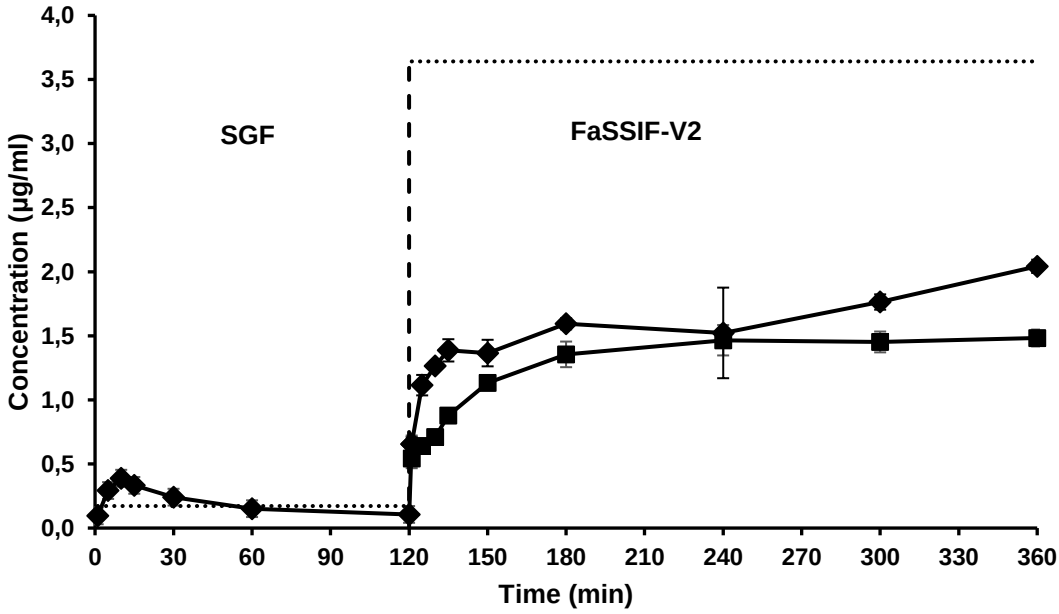


Figure 6.4 Fenofibrate release profiles from mesoporous silica formulation (■) and Lipantil Supra® (◆) in USP IV Transfer Model at 37 °C (incorporating SGF to FaSSIF-V2 transfer). Dotted line indicates fenofibrate solubility in SGF and FaSSIF-V2 media. (n=3, Y error bars indicate standard deviation)

6.4.4. *In Vivo* Oral Bioavailability

The plasma concentration profiles obtained following oral administration of 67 mg of fenofibrate (in the form of either Lipantil Supra® or the silica formulation) to fasted pigs are displayed in Figure 6.5. A maximum plasma concentration of 3.96 ± 1.29 µg/ml was observed for Lipantil Supra® at 5.0 ± 2.4 h. The absorption of fenofibrate from the silica formulation was slower with a C_{max} of 2.34 ± 1.23 µg/ml at T_{max} 9.5 ± 3.0 h. A summary of the *in vivo* parameters for both formulations is provided in Table 6.2. The classical 'burst' release of the silica formulation, observed during both dissolution experiments conducted in FaSSIF-V2 alone was not evident in the *in vivo* pig model. No corresponding sharp onset of fenofibrate absorption was observed for the silica formulation. A slower rate of drug absorption was noted which indicates a slower release profile as noted in the transfer model FaSSIF-V2 phase. This data suggests the transfer model better simulates how the formulation will perform *in vivo*.

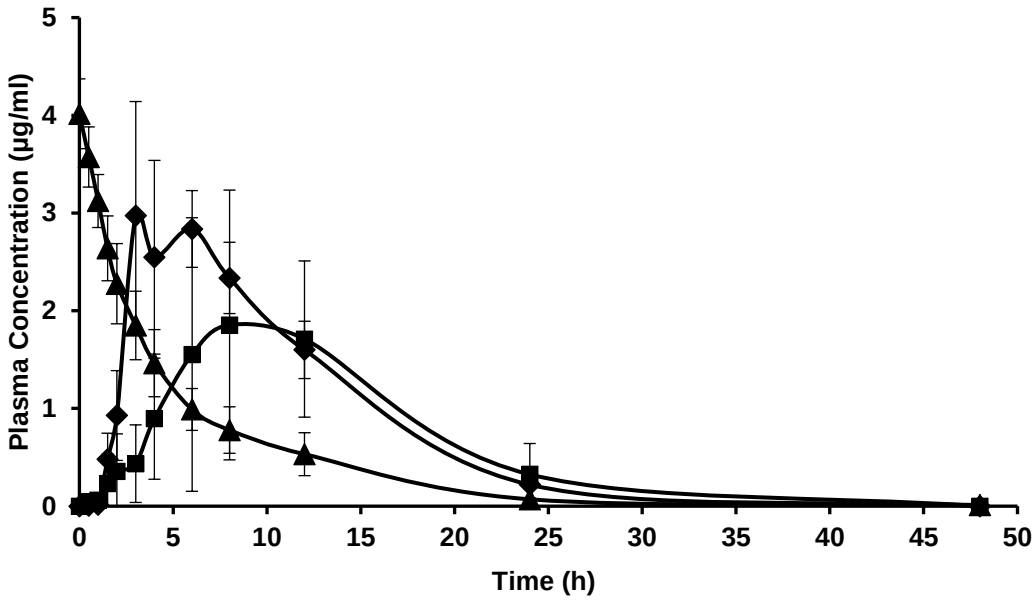


Figure 6.5 Plasma concentration of fenofibric acid vs. time profiles after oral administration of 67 mg fenofibrate to fasted pigs, (■) indicates mesoporous silica formulation, (◆) indicates Lipantil Supra®, (▲) indicates intravenous preparation (n=4, Y error bars indicate standard deviation

Table 6.2 Summary of *in vivo* pig model parameters. Mean values +/- standard deviation are provided (n=4). (*) denotes values which are significantly different (p <0.05)

Formulation	C_{max} (µg/ml)*	$AUC_{0\rightarrow 24h}$	T_{max}	$F_{abs0\rightarrow 24h}$
Mesoporous Silica	2.34 ± 1.23	26502 ± 11377	9.5 ± 3	54.55 ± 23.42
Lipantil Supra®	3.96 ± 1.29	34536 ± 12527	5 ± 2.4	71.08 ± 25.78

Absolute bioavailability was determined for both formulations relative to an intravenous control. An absolute bioavailability of 54.55 ± 23.42 % was observed for the silica formulation which was not significantly different to that of the commercial product, 71.08 ± 25.78 % ($p > 0.1$). This confirms the potential of the silica system to enhance the bioavailability of fenofibrate. However, the silica formulation displayed a slower onset of release when compared with the Lipantil Supra® (T_{max} of 5.0 ± 2.4 h and 9.5 ± 3.0 h, respectively). The relative bioavailability *in vivo* of the silica formulation *versus* Lipantil Supra® was 73.33 ± 17.07 %.

To enable comparison of the *in vitro* dissolution and the *in vivo* bioavailability results, the relative extent of drug release (as a ratio of the silica formulation to Lipantil Supra® AUC) for the Type II, Type IV and USP IV transfer methods were plotted adjacent to the relative bioavailability of both formulations *in vivo* (Figure 6.6). This figure highlights the differences between the extent of release from both formulations using the Type II (a) and Type IV (b) apparatus and similarity using the Type IV Transfer Model (c) and oral bioavailability in the *in vivo* pig model (d). To facilitate further quantitative comparison, the ratio of extent of release of the silica vs. commercial formulation were calculated (Figure 6.7). The ratios of extent of release determined for the Type II and Type IV dissolution data were 8.55±1.28 % and 43.32±10.50 %, respectively. In contrast, the ratio of extent of fenofibrate release from the Type IV transfer method data was 89.16±12.49 %. This ratio did not significantly differ from the relative *in vivo* oral bioavailability of these formulations ($p > 0.05$, Figure 6.7). This indicates that the USP IV transfer method was a superior predictor of *in vivo* performance compared to USP Type II and Type IV using FaSSIF-V2 alone.

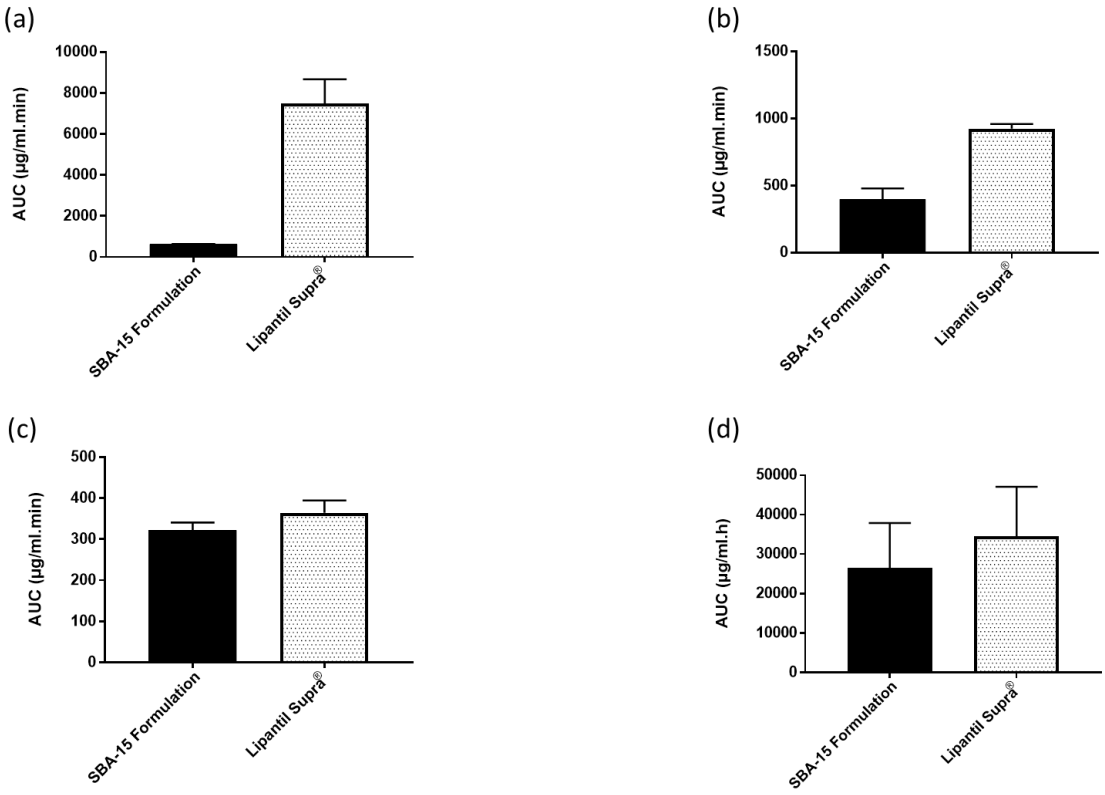


Figure 6.6 Extent of release (AUC) and oral bioavailability of fenofibrate from mesoporous silica and Lipantil Supra® formulations. A = extent of release using Type II apparatus, B = extent of release using FaSSIF-V2 media in a Type IV apparatus, C = extent of release using Type IV Transfer model, D = oral bioavailability determined using an *in vivo* pig model. (Graphs show AUC over 240 min for Type II and Type IV, 360 min for Transfer and 24 h for *in vivo* pig model). (n=3 for *in vitro* dissolution models, n=4 for *in vivo* pig bioavailability model, Y error bars indicate standard deviation)

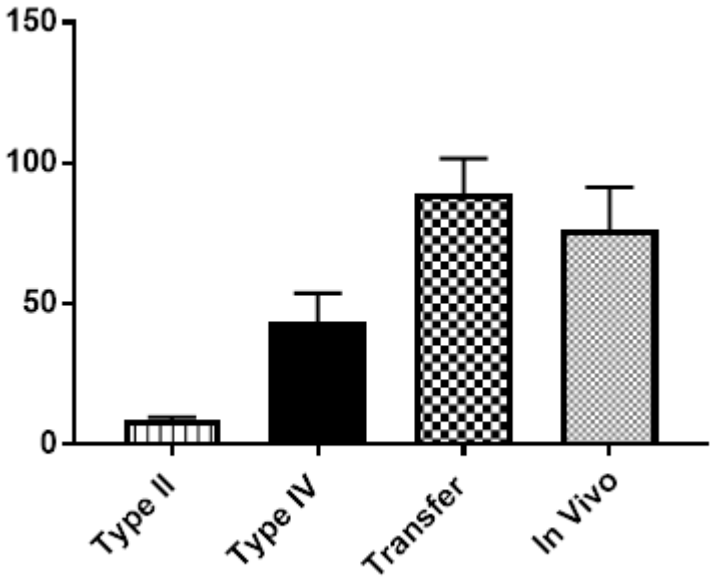


Figure 6.7 Ratio of extent of release of fenofibrate from the silica formulation vs. the commercial product, Lipantil Supra®, for the *in vitro* dissolution experiments and the *in vivo* pig study. Graphs display ratio of AUC release of silica formulation: Lipantil Supra® over 240 min for Type II and Type IV, 360 min for Transfer and 24 h for *in vivo* pig model). (n=3 for *in vitro* dissolution models, n=4 for *in vivo* pig bioavailability model, Y error bars indicate standard deviation)

6.4.5. *In Silico* IVIVR Modelling

The IVIVRs for the two formulations were generated using Gastroplus™ software. Previously published intravenous data was used to deconvolute the *in vivo* oral plasma concentration profiles using the Loo-Riegelman model (309, 310). This two compartment model was chosen over a single compartment model as it has been reported that it is not possible to perform a rigorous pharmacokinetic analysis of an absorption process from oral data, unless the parameters of the model have first been derived from a separate intravenous experiment (316-318).

No quantitative IVIVR could be established with the dissolution profiles from the Type II apparatus. IVIVRs could be generated for the Type IV (FaSSIF-V2) and the Type IV transfer Model (Figure 6.8 and Figure 6.9 respectively). Deconvolution of the Type IV data produced a linear best-fit correlation between the fraction of *in vitro* release and the fraction of absolute bioavailability (R^2 = 0.883 for the silica formulation and R^2 = 0.802 for the Lipantil Supra®).

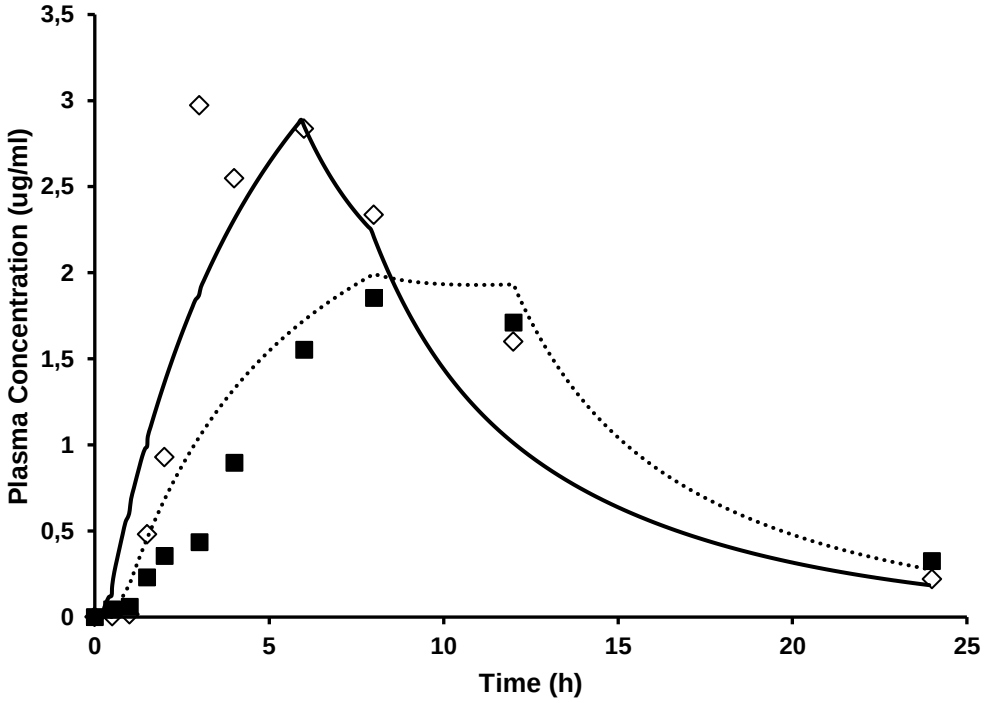


Figure 6.8 Plasma concentration profiles for observed data (designated by the markers – (■) indicates mesoporous silica formulation, (◇) indicates Lipantil Supra®) and predicted plasma concentration-time profiles based on Type IV apparatus (designated by the solid lines - SBA-15 formulation (dotted line) and Lipantil Supra® (black))

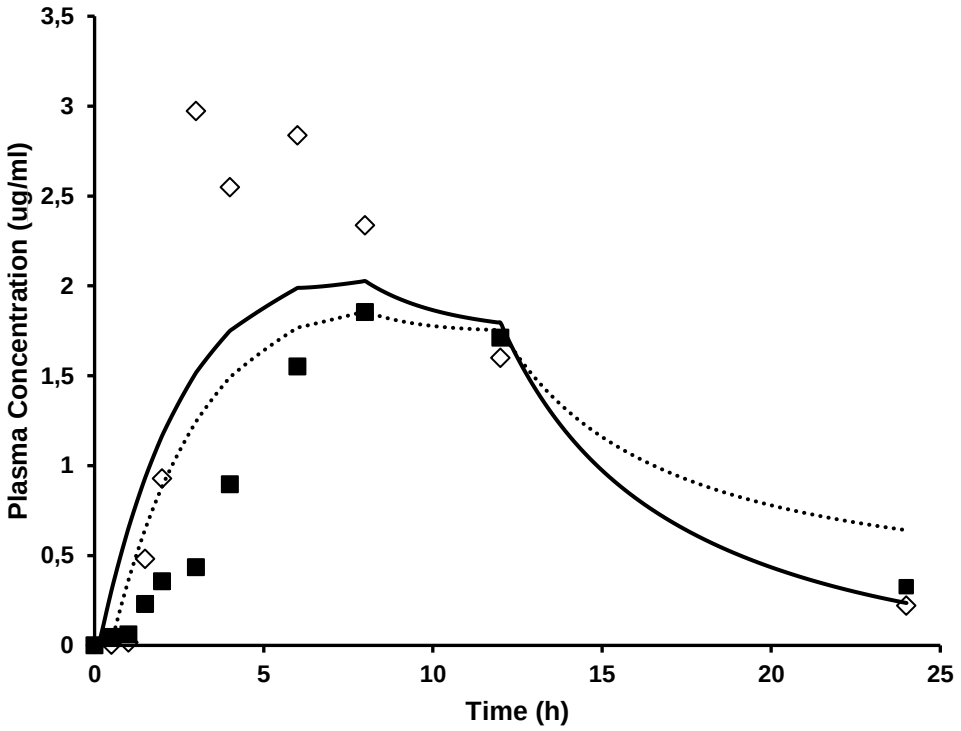


Figure 6.9 Plasma concentration profiles for observed data (designated by the markers – (■) indicates mesoporous silica formulation, ◇) indicates Lipantil Supra®) and predicted plasma concentration-time profiles based on USP IV Transfer model (designated by the solid lines - SBA-15 formulation (dotted line) and Lipantil Supra® (black))

The mean absolute prediction error (MAE) was 5.18 % for C_{max} and 12.14 % for AUC (this falls outside the FDA limit of 10 % error). The full list of validation statistics is displayed in Table 6.3. Optimisation of the deconvoluted Transfer model data produced a second-order polynomial best-fit correlation (R^2 = 0.771 for the SBA-15 formulation and R^2 = 0.569 for the Lipantil Supra®). The MAE was 16.02 % for C_{max} and 15.55 % for AUC, indicating the correlation is not as powerful as the Type IV model using FaSSIF-V2 media alone. The IVIVRs generated using Gastroplus™ software identify the Type IV apparatus as more effective at forecasting *in vivo*

performance than the traditional paddle apparatus. However, it also suggests that the Type IV dissolution, using FaSSIF-V2 alone, is the best prediction model. These findings are in contrast to data generated based on the extent of release discussed in section 6.4.3, which identified the Type IV Transfer model as the superior *in vitro* dissolution model.

Table 6.3 Summary of *in vitro/in vivo* relationship parameters. Observed and predicted C_{max} and AUC values and the correlation (R^2) between the observed and predicted plasma profiles generated by the Gastroplus™ IVIVCPlus® software are displayed.

Formulation	C_{max} (µg/ml)			AUC (µg/ml.h)			Reconstructed Plasma Concentration-Time Profile from Convolution Tab (R^2)
	Observed	**Predicted**	**% Prediction Error**	**Observed**	**Predicted**	**% Prediction Error**	
Type IV Apparatus							
Mesoporous Silica Formulation	1.85	1.99	-7.50	24.31	26.45	-8.80	0.88
Lipantil Supra®	2.97	2.89	2.86	31.87	26.94	15.47	0.80
USP IV Transfer Model							
Mesoporous Silica Formulation	1.85	1.86	-0.22	24.31	28.97	-19.17	0.77
Lipantil Supra®	2.97	2.03	31.82	31.87	28.07	11.92	0.57

6.5. Discussion

To date, mesoporous silica drug formulations have been widely investigated *in vitro* using USP Type II dissolution methods. There have been limited studies to determine whether the enhanced dissolution observed during these *in vitro* dissolutions tests is capable of forecasting their oral *in vivo* bioavailability. This study demonstrates that the *in vitro* dissolution performance of a mesoporous silica fenofibrate formulation varies depending on dissolution apparatus and experiment design. The findings provide evidence that a USP IV dissolution method incorporating a SGF to FaSSIF-V2 media transfer is the best predictor of *in vivo* oral bioavailability in a pig model.

The study highlighted that the C_{max} and $AUC_{0\rightarrow240min}$ of both the commercial, Lipantil Supra®, and silica formulations in FaSSIF-V2 was significantly higher in the Type II compared to the Type IV apparatus. This observation is most likely due to hydrodynamic differences between the two dissolution models. The hydrodynamic properties of the Type II apparatus have been studied in detail and significant limitations have been recognised (80, 319-321). The USP IV has the potential to operate at lower agitation rates than the paddle apparatus, resulting in lower fluid velocities considered to be more biorelevant (101, 102). *In vivo* studies have demonstrated that oral dosage forms can be exposed to small volumes of fluid in the gastro-intestinal tract, which can also be modelled using the Type IV apparatus (96). This is the first study to utilize the Type IV flow-through apparatus to investigate release from drug loaded mesoporous silica systems. It is also the first to compare the Type IV and the Type II apparatus directly to study the dissolution behaviour of this formulation approach. The similarity between the relative bioavailability of the

silica formulation versus Lipantil Supra®, and the relative AUC (extent of release) of the formulations determined using the USP IV transfer method, suggests that the USP IV is a more biorelevant *in vitro* test for these formulations. These results indicate that a supersaturation/precipitation process plays a significant role in the dissolution process of these systems and is best simulated using a transfer model.

The advantages of using a transfer model to investigate formulation approaches which promote drug supersaturation, and are therefore prone to precipitation, have been reported by other groups (78, 322, 323). Both formulations in this study utilise a supersaturation formulation strategy to enhance the oral bioavailability of fenofibrate (79). The transfer model is a two-compartment dissolution method to simulate GI transit from the stomach to the intestine. Fenofibrate release from the mesoporous formulation in SGF was below the HPLC assay detection limit. In contrast, fenofibrate release at supersaturation levels from Lipantil Supra® was evident in the gastric component of the transfer model. The exposure of the formulations to the acidic component in the transfer model affected their subsequent release profile in FaSSIF-V2 media. This is evident in the significant decrease in C_{max} for both formulations in the Type IV transfer model compared to the Type IV FaSSIF-V2 only model. As described in Chapter 1, the exposure of high energy amorphous drug forms to an aqueous environment where it has very limited solubility is reported to promote recrystallization of the drug to a lower energy less soluble form (78). Partial recrystallization and precipitation of drug in the silica formulation would explain the reduction in C_{max} and $AUC_{0\rightarrow240min}$ upon exposure to FaSSIF-V2 media.

The importance of controlling supersaturation in mesoporous silica formulations has been investigated by Van Speybroeck *et al* (28, 181). Although supersaturation has been explored intensively *in vitro*, there is little evidence to support what occurs in the *in vivo* environment. A recent study investigated the impact of gastrointestinal dissolution, supersaturation and precipitation of posoconazole in humans (324). After administration of the formulations, gastric and duodenal fluids were aspirated and blood samples were collected in parallel. Supersaturation followed by significant intestinal precipitation was reported. This is in contrast to a study which reported limited duodenal precipitation for ketoconazole and dipyridamole in a human study (325). In this study, previously reported *in vitro* dissolution dipyridamole data over-estimated the subsequent *in vivo* observations (322). This indicates that drug supersaturation/precipitation is a complex process which can depend on the physiochemical properties of the drug, the formulation and physiological variables (78).

The relationship between dosage form and physiological variables, such as the fed and fasted state warrant discussion. In this study, *in vitro* dissolution studies were performed in FASSIF-V2 media designed to mimic the fastest state and pigs were dosed following an overnight fast, with food administered 8 hours post dose. The oral bioavailability of poorly water-soluble drugs, such as fenofibrate, is limited by their poor solubility within gastrointestinal fluid (326) and oral bioavailability can be variable depending on the food effect (327). Formulation strategies can enhance bioavailability by reducing or eliminating the food effect (308, 309, 328). For example, the commercial micronized fenofibrate formulation, Lipantil Micro®, displays food dependent bioavailability while the Lipantil® Supra formulation,

encompassing NanoCrystal® technology, enables food independent administration and dose reduction (329). These findings emphasise the need for studies of this nature which use *in vivo* reference data to optimize *in vitro* dissolution models and inform the development of bio-enabling formulation strategies.

The IVIVRs generated using the Gastroplus™ software support the relationships observed between the relative bioavailability of the formulations and their relative AUC (extent of release) determined from raw dissolution profiles. IVIVRs were determined for the Type IV FaSSIF-V2 model and the Type IV transfer model. No quantitative IVIVR could be determined for the Type II (paddle) apparatus. Correlations suggest that the Type IV apparatus with FaSSIF-V2 alone was better at forecasting *in vivo* performance than the transfer model. This finding can be explained by outlining the mechanism in which the model is generated and hence model assumption. The initial part of the dissolution profile (time points up to C_{max}) was used to generate the IVIVR. The assumption of the model was that the second part of the dissolution profile, which corresponded to a reduction in drug concentration due to drug precipitation, may be an artefact of the *in vitro* dissolution model, particularly in the absence of an absorption sink. The initial dissolution phase was correlated with the deconvoluted *in-vivo* plasma profile and then re-convoluted to generate a predicted plasma profile.

The IVIVR generated for the Type IV transfer model revealed significant limitations of the model; the MAE was 16.02 % for C_{max} and 15.55 % for AUC and a large prediction error for the Lipantil Supra® C_{max} of 31.82 % was noted (more than double the FDA approved error limit of 15% for an individual formulation). This error can be attributed to the raw dissolution data for the Lipantil Supra®, specifically the

concentration of fenofibrate at the fourth and fifth time point. This reduction (dip) in the release profile, while not statistically significant ($p > 0.5$) did significantly affected the *in vitro/in vivo* correlation simulated by the Gastroplus™ software. This sensitivity is a limitation of the current multi-step approach of deconvolution and correlation when comparing a small number of immediate release formulations. Removal of fifth time point from the analysis improved the correlation but consequently reduced the power of the Type IV FaSSIF-V2 transfer model IVIVR.

In silico modelling requires further investigation to overcome the limitations outlined above. To date, modified release formulations have proved most successful as regards development of effective IVIVR (105). Work to improve *in silico* modelling for formulations which employ supersaturation to improve the bioavailability of poorly water-soluble drugs will be of significant benefit in their development.

6.6 Conclusion

This study demonstrates that the dissolution performance of a fenofibrate mesoporous silica formulation varies depending on the dissolution apparatus and the dissolution experimental design. The findings demonstrate that a USP IV transfer dissolution model was best at forecasting *in vivo* performance. This observation is most likely due to hydrodynamic differences between the two apparatus and the ability of the transfer model to better simulate GI transit. This is advantageous in forecasting *in vivo* behaviour for formulations which promote drug supersaturation and as a result are prone to precipitation. As this drug supersaturation/precipitation process is complex and depends on both formulation and physiological variables, studies which relate *in vitro* to *in vivo* data can help optimise *in vitro* models used in formulation development. *In silico* modelling has the potential to assist in this process. However, further development is required to overcome the limitations outlined in this study for solubility enhancing formulations.

Chapter 7: Discussion

7.1. Introduction

This thesis investigated the mechanism of drug dissolution from mesoporous silica carriers by examining factors influencing drug adsorption, release and retention on the silica surface. In this chapter, the thesis, as a complete body of work, is discussed and the overall findings are interpreted. Following this, the overall strengths and limitations of the thesis will be described. Finally, recommendations for future work will be provided.

7.2. Interpretation and Implications of Findings

Mesoporous silica formulations continue to be the focus of much research as novel oral drug delivery systems (230, 260, 330-332). The principal contribution of this thesis is the enhancement of knowledge concerning the mechanism of drug adsorption and release from these materials. Incomplete release from these systems had been reported but not addressed in several studies (54, 55, 116). This thesis considered the rationale behind this incomplete release profile by systematically addressing factors influencing drug adsorption and dissolution from these formulations. The findings of this thesis should be of use to researchers designing *in vitro* dissolution studies involving mesoporous silica formulations to ensure they are conducting appropriate experiments for these systems. This should ultimately help in the development and success of these formulations as they move from bench to bedside.

7.2.1. Dynamic Equilibrium between Drug Adsorption on Silica and Free Drug in Solution

This thesis is the first to explore, in detail, passive drug adsorption onto mesoporous silica. While adsorption and retention of certain organic molecules on the silica surface had been considered in the literature, the potential implications for drug dissolution from novel mesoporous silica formulations had not been investigated to date (118, 119). The frequency of observed incomplete release from mesoporous silica systems was discussed in detail in Chapter 2. The investigation of factors influencing this incomplete release became one of the central themes of this thesis.

Adsorption isotherms were utilized extensively to aid in understanding the role of drug adsorption onto the silica surface (Chapters 3, 4 and 5). The Langmuir and Freundlich isotherm models have been successfully applied to explain drug adsorption onto the silica surface in the literature and also proved a good fit for the data in this work (118, 151). The adsorption isotherms generated provided evidence of an equilibrium between drug passively adsorbed on the silica surface and free drug existing in solution. This was first observed under sink conditions in Chapters 3 and 4. As mesoporous silica formulations are capable of achieving drug supersaturation levels (181, 272, 333), passive adsorption under such conditions was investigated in Chapter 5 and a dynamic equilibrium between adsorbed and free drug was also demonstrated.

It was observed in Chapters 3 and 4 that organic molecules including potential formulation excipients (surfactants) and constituents of biorelevant media (bile salts and proteins) can adsorb onto the silica surface. Competitive adsorption of these

molecules reduced passive adsorption of drug on the silica. This may have implications for excipient choice as mesoporous silica formulations move from the laboratory setting to large-scale manufacture (116, 334). The concept of biological components adsorbing onto large surface area drug carriers has been reported extensively for nanocarrier drug delivery systems (335-339). However, it has not been considered for mesoporous silica materials to date and is an important finding of this thesis.

In Chapter 5, it was determined that the equilibrium between adsorbed and free drug during passive adsorption was related to the drug's activity in solution. This activity is related to the chemical potential of the drug in the system. Passive adsorption of both drugs was compared directly by converting equilibrium free concentrations to drug activity in solution (amorphous solubility was designated an activity of one). The data overlaid closely indicating the presence of a relationship between passive adsorption and activity. Similar findings have been reported in a number of older studies in the literature examining adsorption onto carbon materials (303, 304). However, this is the first study to investigate the influence of activity on drug adsorption and release from mesoporous silica formulations.

The equilibrium between adsorbed and free drug was also confirmed under supersaturating conditions during the drug dissolution process in Chapter 5. It was determined that the equilibrium was not influenced by the quantity of silica, rather the relationship between adsorbed drug and free drug. This provides further evidence that knowledge of drug activity in solution can aid in our understanding of drug release from mesoporous silica formulations.

In Chapters 3 and 4, when passive adsorption levels were compared to retention after drug dissolution, it was determined that the amount retained on the surface after dissolution was significantly higher. This was attributed to the SC-CO_2 loading method which resulted in drug loading deep in the porous network, rendering it inaccessible to the dissolution medium (88, 273). A similar finding was noted in Chapter 5 for organic solvent loaded formulations. Drug loading methods have been examined comprehensively as regards their ability to enhance drug dissolution (as discussed in Chapter 2). However, based on these findings they warrant further investigation with respect to the location of deposited drug in the porous network and their influence on the observed equilibrium between drug adsorption and release.

7.2.2. Dissolution Experimental Set-Up for Mesoporous Silica Formulations

The second major contribution of this thesis is to provide insight into the design of more appropriate *in vitro* dissolution experiments for oral mesoporous silica drug delivery systems. To date, most dissolution studies involving these formulations are conducted in USP Type II dissolution apparatus, using simple traditional buffers as dissolution media (0.1M HCl and phosphate buffer pH 6.8) (88-92). Throughout this thesis, evidence is presented revealing these are not the most suitable conditions to investigate drug release from mesoporous silica formulations.

In Chapter 3, it was demonstrated that the addition of a surfactant (sodium dodecyl sulphate) to 0.1M HCl medium significantly enhanced drug dissolution. This increase

in drug release was not the result of enhanced drug solubility in the surfactant micelles but rather the reduced surface tension of the media, resulting in improved wetting of the silica surface. Mesoporous silica materials possess a wide range of pore sizes (2 – 50 nm) and their porous architecture was identified as a significant factor influencing the extent of drug release. This had previously been reported in a study conducted by Mellaerts *et al* who compared dissolution profiles of silica materials with a range of pore sizes (181). However, they did not consider the impact of the porous network on incomplete release or the significance of the role of dissolution media additives in the release process. As described in Section 1.3.1, during the drug loading process, solvents can access areas deep in the porous network to deposit drug as a result of their superior wetting characteristics. These areas are subsequently inaccessible to traditional aqueous buffers used in dissolution due to their high surface tension (measured in Chapter 4). As dissolution media components which improve the wettability of the silica surface can enhance drug release, their addition to dissolution media needs to be considered in the design of future dissolution experiments involving mesoporous silica formulations. These findings also suggest that accessible surface area rather than specific surface area of mesoporous silica is as an important parameter in drug loading and dissolution from these porous systems.

In Chapter 4, the influence of biorelevant components on drug adsorption and release from silica systems was investigated under sink conditions. It is increasingly recommended in the literature that biorelevant media should be utilized in dissolution studies involving formulations capable of achieving supersaturation levels (78, 230, 231). However, in this study, it was demonstrated that components of

biorelevant media can also have a significant effect on drug release from mesoporous silica systems under sink conditions due to their reduced surface tension characteristics. This echoes the observations in Chapter 3 describing the importance of dissolution medium wettability of the silica surface under sink conditions. These findings are novel in the field of mesoporous silica drug delivery. They provide strong evidence that biorelevant media can influence drug release in ways other than via promotion of drug supersaturation. As a result of these observations, the use of biorelevant media should be considered in all future dissolution studies under sink conditions involving these systems.

Chapter 6 investigated the apparatus utilized in dissolution studies to determine which is most appropriate to predict *in vivo* performance. Experiments in this Chapter were conducted under drug supersaturating conditions using biorelevant media (simulated gastric fluid (SGF) and fasted state simulated intestinal media (FaSSIF-V2)). In this chapter, the USP Type II (paddle) apparatus was compared to USP Type IV (flow-through cell) apparatus and a transfer model (using the flow-through cell equipment). It has been proposed that the Type IV apparatus is a better simulator of *in vivo* hydrodynamics than the paddle apparatus (101). Incorporating a transfer from SGF to FaSSIF-V2 media during the experiment results in conditions that more closely reflect the pH gradient associated with transit through the GI tract which, in theory, should lead to better *in vivo* simulation (305). However, as discussed in Chapter 6 the number of studies which utilise these models are limited and published data with regards to the superiority of the Type IV flow-through cell over the Type II apparatus is not in agreement (103, 104).

This study demonstrated that the *in vitro* dissolution performance of a mesoporous silica fenofibrate formulation varied depending on dissolution apparatus and experiment design. The findings provide evidence that a USP IV dissolution method incorporating an SGF to FaSSIF-V2 media transfer is the best predictor of *in vivo* oral bioavailability in a pig model. The findings build on previously published work detailing the advantages of using a transfer model to investigate formulation approaches which promote drug supersaturation and are therefore prone to precipitation (78, 322, 323). However, this was the first time the transfer model had been investigated for a mesoporous silica system. The results provide evidence that the transfer model should be the model of choice for *in vitro* studies used in the prediction of *in vivo* performance for mesoporous silica formulations.

7.3. Strengths and Limitations

The individual research chapters of this thesis were based on the findings of a comprehensive review of the literature (presented in Chapter 2). Throughout this extensive review, the current state of the art regarding oral mesoporous silica drug delivery systems was presented. It also identified gaps in the knowledge regarding the mechanism of drug release from these formulations which provided the basis for the hypothesis and aims of this thesis.

A key strength of this thesis is the approach taken to systematically investigate drug dissolution from mesoporous silica formulations. Individual research chapters examined the influence of potential excipients (surfactants), dissolution medium composition, supersaturation conditions and dissolution apparatus on drug release

from silica carriers. A robust experimental approach was adopted throughout this work involving a comprehensive range of experiments including adsorption isotherms, dissolution studies and advanced spectroscopic techniques. This facilitated the generation of valuable insights into numerous aspects of the dissolution process from mesoporous silica systems resulting in recommendations for the design of future *in vitro* studies involving these systems.

This thesis is the first to examine the role of drug adsorption onto the silica surface during the drug release process from mesoporous silica formulations. The literature review identified that passive drug adsorption onto these carriers was recognised in other fields, including environmental science. However, its influence on drug release had not been investigated to date. Drug adsorption on the silica surface was examined directly in three of the research chapters. The results generated provide enhanced understanding of the relationship between drug adsorption and release for these formulations which could aid in the future development of these formulations.

Another novel aspect of this thesis was the enhanced understanding of the role biorelevant media can play in drug release from mesoporous silica carriers. It has been recommended to use biorelevant media to conduct dissolution studies of formulations which promote supersaturation. In this work, it was demonstrated that biorelevant media should also be utilized for dissolution experiments involving mesoporous silica drug delivery systems under sink conditions as the reduced surface tension of the media can enhance release compared to simple traditional buffer media.

A major contribution of this thesis is the finding that drug activity can potentially influence the equilibrium between drug adsorbed on the silica surface and free drug in solution. It had been demonstrated in the literature that an equilibrium between adsorbed and free drug exists for these systems but the factors underpinning this process were not understood. This thesis provides evidence that the drug's activity in solution, which is related to the drug's chemical potential, plays a role in this relationship.

As the first *in vivo* studies begin to be published involving mesoporous silica formulations, this thesis examined a range of *in vitro* dissolution studies to investigate which is the best predictor of *in vivo* performance. It was determined that the Type IV apparatus incorporating a transfer model was the superior choice. This will aid in future development of oral mesoporous silica drug delivery systems.

The quality of the research conducted as part of this doctoral thesis is evidenced in the number of peer-reviewed academic publications and conference presentations achieved. This highlights that this research is of scientific merit, interesting to academic colleagues and of sufficient quality and rigour.

While there are numerous strengths associated with this research, certain limitations must also be acknowledged. The results presented are based on a small pool of model drugs and silica materials. Both weakly acidic and neutral drugs were investigated but it would be of benefit to repeat experiments in this thesis using a wider range of compounds with a variety of physicochemical characteristics to assess the universal nature of the findings. The same is true for silica materials with diverse porous architectures.

Spectroscopic techniques were employed very successfully in Chapter 5 to describe drug adsorption onto the silica surface. It is a limitation of the thesis that they were not also applied in Chapters 3 and 4 to provide further evidence of drug-silica interactions.

Drug supersaturation was dosed at amorphous solubility levels in Chapter 5 which was completed after Chapter 6 (which examined various dissolution models). It would be been preferable to conduct studies in Chapter 6 at amorphous solubility to attempt to draw parallels between the two chapters.

7.4. Recommendations for Future Work

This thesis provides many new insights into the mechanism of drug dissolution from mesoporous silica systems. In particular, the investigation of the role of adsorption during drug release from these materials was a novel concept. It therefore provides an ideal starting point for future research in the area of oral mesoporous silica formulation development. Future work should focus on the following areas:

I. Further exploration of the location of drug in the silica porous network following drug loading using organic solvents and SC-CO_2.
II. Generation of adsorption isotherms for drug adsorption onto mesoporous silica in loading solvent. Compare passive drug loading to drug retention following dissolution studies.
III. Exploration of the exact nature of surfactant-silica interactions using advanced spectroscopic techniques and microscopy.

IV. Further investigation of the role of drug adsorption on the silica surface (particularly the impact of drug activity on the dynamic equilibrium between adsorbed and free drug) using a wider variety of drug molecules with a range of physicochemical characteristics.

V. Improvement of *in silico* methods to describe *in vitro/in vivo* correlations for immediate release formulations.

7.5. Conclusions

The overall aim of this thesis was to investigate factors influencing drug adsorption and release from mesoporous silica formulations to gain an enhanced understanding of the mechanism of drug release from these systems. This aim was devised based on the findings of a comprehensive review of the literature which identified unexplained incomplete release from these carriers. Passive drug adsorption onto the silica surface had been recognised in other fields of research but its influence on drug release from oral mesoporous silica formulations had not been considered.

The first major contribution of this thesis was to describe the equilibrium between drug adsorbed on the silica surface and free drug in solution using a robust experimental approach involving adsorption isotherms, competitive adsorption and spectroscopic techniques. Of particular novelty, is the finding that equilibrium drug adsorption can be related to the drug's activity in solution. Further evidence for the role of activity was provided in dissolution experiments which demonstrate drug release was not a function of the quantity of silica but rather the relationship between adsorbed and free drug in the system.

This work also demonstrated the ability of non-biological and biological components to adsorb on the silica surface during the drug release process. These constituents were observed to competitively adsorb on the silica surface and displace drug during adsorption isotherm studies.

A second significant contribution was the generation of novel insights into the dissolution process from mesoporous silica formulations which can aid in the design of more appropriate dissolution experiments for these systems. It was demonstrated

that dissolution media additives with reduced surface tension could enhance drug release from silica carriers under sink conditions, due to superior wetting of the silica material. Of particular interest, was the finding that biorelevant media can influence drug release from mesoporous silica in ways other than via promotion of drug supersaturation. Future mesoporous silica dissolution studies conducted under sink conditions should incorporate a biorelevant approach. Furthermore, it was demonstrated that choice of dissolution apparatus is critical when performing studies to predict *in vivo* bioavailability. The Type IV apparatus featuring a transfer model component was significantly better at simulating *in vivo* conditions due to its ability to model potential drug supersaturation and precipitation during transit in the GI tract.

This thesis contributes substantially to the present literature, through the provision of comprehensive, novel data on drug dissolution from mesoporous silica materials. The value of this research is that it provides recommendations for the design of future dissolution studies involving these formulations while opening up exciting new avenues for research as a result of interesting findings concerning the dynamic equilibrium between drug adsorbed on the silica surface and free drug in solution.

References

1. Lennernäs H, Abrahamsson B. The use of biopharmaceutic classification of drugs in drug discovery and development: current status and future extension. Journal of Pharmacy and Pharmacology. 2005;57(3):273-85.
2. Hörter D, Dressman JB. Influence of physicochemical properties on dissolution of drugs in the gastrointestinal tract. Advanced Drug Delivery Reviews. 2001;46(1):75-87.
3. Lipinski CA. Drug-like properties and the causes of poor solubility and poor permeability. Journal of pharmacological and toxicological methods. 2000;44(1):235-49.
4. Lipinski CA, Lombardo F, Dominy BW, Feeney PJ. Experimental and computational approaches to estimate solubility and permeability in drug discovery and development settings. Advanced Drug Delivery Reviews. 2012;64:4-17.
5. Di L, Fish PV, Mano T. Bridging solubility between drug discovery and development. Drug Discovery Today. 2012;17(9):486-95.
6. Wong M, McAllister M. Lead Identification/Optimization. Oral Formulation Roadmap from Early Drug Discovery to Development. 2017.
7. Amidon GL, Lennernäs H, Shah VP, Crison JR. A Theoretical Basis for a Biopharmaceutic Drug Classification: The Correlation of in Vitro Drug Product Dissolution and in Vivo Bioavailability. Pharmaceutical Research. 1995;12(3):413-20.
8. Dahan A, Miller JM, Amidon GL. Prediction of Solubility and Permeability Class Membership: Provisional BCS Classification of the World's Top Oral Drugs. The AAPS Journal. 2009;11(4):740-6.
9. Lipinski CA. Poor aqueous solubility—an industry wide problem in drug discovery. American Pharmaceutical Review. 2002;5(3):82-5.
10. Smith BT. Remington Education: Physical Pharmacy: Pharmaceutical Press; 2015.
11. Pouton CW. Formulation of poorly water-soluble drugs for oral administration: Physicochemical and physiological issues and the lipid formulation classification system. European Journal of Pharmaceutical Sciences. 2006;29(3–4):278-87.
12. Moynihan H, Crean A. Physicochemical Basis of Pharmaceuticals: Oxford University Press; 2009.
13. Baird JA, Taylor LS. Evaluation of amorphous solid dispersion properties using thermal analysis techniques. Advanced Drug Delivery Reviews. 2012;64(5):396-421.
14. Siepmann J, Siepmann F. Mathematical modeling of drug dissolution. International Journal of Pharmaceutics. 2013;453(1):12-24.
15. Sugano K. Aqueous Boundary Layers Related to Oral Absorption of a Drug: From Dissolution of a Drug to Carrier Mediated Transport and Intestinal Wall Metabolism. Molecular Pharmaceutics. 2010;7(5):1362-73.
16. Noyes AA, Whitney WR. The rate of solution of solid substances in their own solutions. Journal of the American Chemical Society. 1897;19(12):930-4.
17. Nernst W. Theorie der Reaktionsgeschwindigkeit in heterogenen Systemen. Zeitschrift für Physikalische Chemie. 1904;47(1):52-5.
18. Brunner E. Reaktionsgeschwindigkeit in heterogenen Systemen. Zeitschrift für Physikalische Chemie. 1904;47(1):56-102.
19. Bates TR, Gibaldi M, Kanig JL. Rate of dissolution of griseofulvin and hexoestrol in bile salt solutions. Nature. 1966;210(5043):1331.
20. Vogt M, Kunath K, Dressman JB. Dissolution enhancement of fenofibrate by micronization, cogrinding and spray-drying: Comparison with commercial preparations. European Journal of Pharmaceutics and Biopharmaceutics. 2008;68(2):283-8.
21. Vasconcelos T, Sarmento B, Costa P. Solid dispersions as strategy to improve oral bioavailability of poor water soluble drugs. Drug Discovery Today. 2007;12(23):1068-75.

22. Lopez V, Kennedy A. Flux-assisted wetting and spreading of Al on TiC. Journal of Colloid and Interface Science. 2006;298(1):356-62.
23. Kumar G, Prabhu KN. Review of non-reactive and reactive wetting of liquids on surfaces. Advances in Colloid and Interface Science. 2007;133(2):61-89.
24. Young T. III. An essay on the cohesion of fluids. Philosophical Transactions of the Royal Society of London. 1805;95:65-87.
25. Šikalo Š, Marengo M, Tropea C, Ganić E. Analysis of impact of droplets on horizontal surfaces. Experimental Thermal and Fluid Science. 2002;25(7):503-10.
26. Williams HD, Trevaskis NL, Charman SA, Shanker RM, Charman WN, Pouton CW, et al. Strategies to Address Low Drug Solubility in Discovery and Development. Pharmacological Reviews. 2013;65(1):315-499.
27. Leuner C, Dressman J. Improving drug solubility for oral delivery using solid dispersions. European Journal of Pharmaceutics and Biopharmaceutics. 2000;50(1):47-60.
28. Van Speybroeck M, Mols R, Mellaerts R, Thi TD, Martens JA, Humbeeck JV, et al. Combined use of ordered mesoporous silica and precipitation inhibitors for improved oral absorption of the poorly soluble weak base itraconazole. European Journal of Pharmaceutics and Biopharmaceutics. 2010;75(3):354-65.
29. Perrut M, Jung J, Leboeuf F. Enhancement of dissolution rate of poorly-soluble active ingredients by supercritical fluid processes: Part I: Micronization of neat particles. International Journal of Pharmaceutics. 2005;288(1):3-10.
30. Rasenack N, Müller BW. Dissolution Rate Enhancement by in Situ Micronization of Poorly Water-Soluble Drugs. Pharmaceutical Research. 2002;19(12):1894-900.
31. Kocbek P, Baumgartner S, Kristl J. Preparation and evaluation of nanosuspensions for enhancing the dissolution of poorly soluble drugs. International Journal of Pharmaceutics. 2006;312(1):179-86.
32. Rabinow BE. Nanosuspensions in drug delivery. Nature Reviews Drug Discovery. 2004;3:785.
33. Murdande SB, Shah DA, Dave RH. Impact of Nanosizing on Solubility and Dissolution Rate of Poorly Soluble Pharmaceuticals. Journal of Pharmaceutical Sciences. 2015;104(6):2094-102.
34. Kobayashi Y, Ito S, Itai S, Yamamoto K. Physicochemical properties and bioavailability of carbamazepine polymorphs and dihydrate. International Journal of Pharmaceutics. 2000;193(2):137-46.
35. Blagden N, de Matas M, Gavan PT, York P. Crystal engineering of active pharmaceutical ingredients to improve solubility and dissolution rates. Advanced Drug Delivery Reviews. 2007;59(7):617-30.
36. Singhal D, Curatolo W. Drug polymorphism and dosage form design: a practical perspective. Advanced Drug Delivery Reviews. 2004;56(3):335-47.
37. Duggirala NK, Perry ML, Almarsson Ö, Zaworotko MJ. Pharmaceutical cocrystals: along the path to improved medicines. Chemical Communications. 2016;52(4):640-55.
38. Kuminek G, Cao F, da Rocha ABdO, Cardoso SG, Rodríguez-Hornedo N. Cocrystals to facilitate delivery of poorly soluble compounds beyond-rule-of-5. Advanced Drug Delivery Reviews. 2016;101:143-66.
39. Serrano DR, O'connell P, Paluch KJ, Walsh D, Healy AM. Cocrystal habit engineering to improve drug dissolution and alter derived powder properties. Journal of Pharmacy and Pharmacology. 2016;68(5):665-77.
40. Park S-H, Choi H-K. The effects of surfactants on the dissolution profiles of poorly water-soluble acidic drugs. International Journal of Pharmaceutics. 2006;321(1–2):35-41.
41. Balakrishnan A, Rege BD, Amidon GL, Polli JE. Surfactant-mediated dissolution: Contributions of solubility enhancement and relatively low micelle diffusivity. Journal of Pharmaceutical Sciences. 2004;93(8):2064-75.

42. Sheng JJ, Kasim NA, Chandrasekharan R, Amidon GL. Solubilization and dissolution of insoluble weak acid, ketoprofen: Effects of pH combined with surfactant. European Journal of Pharmaceutical Sciences. 2006;29(3):306-14.
43. Challa R, Ahuja A, Ali J, Khar RK. Cyclodextrins in drug delivery: An updated review. AAPS PharmSciTech. 2005;6(2):E329-E57.
44. I. CO, T. SC. Mechanism of drug dissolution rate enhancement from β-cyclodextrin-drug systems. Journal of Pharmacy and Pharmacology. 1982;34(10):621-6.
45. Zylberberg C, Matosevic S. Pharmaceutical liposomal drug delivery: a review of new delivery systems and a look at the regulatory landscape. Drug Delivery. 2016;23(9):3319-29.
46. Torchilin VP. Recent advances with liposomes as pharmaceutical carriers. Nature Reviews Drug discovery. 2005;4(2):145.
47. Feeney OM, Crum MF, McEvoy CL, Trevaskis NL, Williams HD, Pouton CW, et al. 50 years of oral lipid-based formulations: provenance, progress and future perspectives. Advanced Drug Delivery Reviews. 2016;101:167-94.
48. Rezhdo O, Speciner L, Carrier R. Lipid-associated oral delivery: Mechanisms and analysis of oral absorption enhancement. Journal of Controlled Release. 2016;240:544-60.
49. Baghel S, Cathcart H, O'Reilly NJ. Polymeric Amorphous Solid Dispersions: A Review of Amorphization, Crystallization, Stabilization, Solid-State Characterization, and Aqueous Solubilization of Biopharmaceutical Classification System Class II Drugs. Journal of Pharmaceutical Sciences. 2016;105(9):2527-44.
50. Knopp MM, Olesen NE, Holm P, Langguth P, Holm R, Rades T. Influence of Polymer Molecular Weight on Drug-Polymer Solubility: A Comparison between Experimentally Determined Solubility in PVP and Prediction Derived from Solubility in Monomer. Journal of Pharmaceutical Sciences. 2015;104(9):2905-12.
51. Sarode AL, Sandhu H, Shah N, Malick W, Zia H. Hot melt extrusion (HME) for amorphous solid dispersions: Predictive tools for processing and impact of drug–polymer interactions on supersaturation. European Journal of Pharmaceutical Sciences. 2013;48(3):371-84.
52. Watanabe T, Wakiyama N, Usui F, Ikeda M, Isobe T, Senna M. Stability of amorphous indomethacin compounded with silica. International Journal of Pharmaceutics. 2001;226(1):81-91.
53. Friedrich H, Fussnegger B, Kolter K, Bodmeier R. Dissolution rate improvement of poorly water-soluble drugs obtained by adsorbing solutions of drugs in hydrophilic solvents onto high surface area carriers. European Journal of Pharmaceutics and Biopharmaceutics. 2006;62(2):171-7.
54. Ahern RJ, Hanrahan JP, Tobin JM, Ryan KB, Crean AM. Comparison of fenofibrate–mesoporous silica drug-loading processes for enhanced drug delivery. European Journal of Pharmaceutical Sciences. 2013;50(3–4):400-9.
55. Van Speybroeck M, Barillaro V, Thi TD, Mellaerts R, Martens J, Van Humbeeck J, et al. Ordered mesoporous silica material SBA-15: A broad-spectrum formulation platform for poorly soluble drugs. Journal of Pharmaceutical Sciences. 2009;98(8):2648-58.
56. Bukara K, Schueller L, Rosier J, Daems T, Verheyden L, Eelen S, et al. In Vivo Performance of Fenofibrate Formulated With Ordered Mesoporous Silica Versus 2-Marketed Formulations: A Comparative Bioavailability Study in Beagle Dogs. Journal of Pharmaceutical Sciences. 2016;105(8):2381-5.
57. Stella VJ, Nti-Addae KW. Prodrug strategies to overcome poor water solubility. Advanced Drug Delivery Reviews. 2007;59(7):677-94.
58. Rautio J, Kumpulainen H, Heimbach T, Oliyai R, Oh D, Järvinen T, et al. Prodrugs: design and clinical applications. Nature Reviews Drug Discovery. 2008;7:255.
59. Guzman HR, Tawa M, Zhang Z, Ratanabanangkoon P, Shaw P, Gardner CR, et al. Combined use of crystalline salt forms and precipitation inhibitors to improve oral absorption

of celecoxib from solid oral formulations. Journal of Pharmaceutical Sciences. 2007;96(10):2686-702.
60. Morris KR, Fakes MG, Thakur AB, Newman AW, Singh AK, Venit JJ, et al. An integrated approach to the selection of optimal salt form for a new drug candidate. International Journal of Pharmaceutics. 1994;105(3):209-17.
61. Taylor LS, Zografi G. Spectroscopic characterization of interactions between PVP and indomethacin in amorphous molecular dispersions. Pharmaceutical Research. 1997;14(12):1691-8.
62. Roos YH. Water activity and glass transition. Water Activity in Foods: Fundamentals and Applications: Blackwell Publishing, Ames, IA; 2007. p. 29-45.
63. Caron V, Tajber L, Corrigan OI, Healy AM. A Comparison of Spray Drying and Milling in the Production of Amorphous Dispersions of Sulfathiazole/Polyvinylpyrrolidone and Sulfadimidine/Polyvinylpyrrolidone. Molecular Pharmaceutics. 2011;8(2):532-42.
64. Patterson JE, James MB, Forster AH, Lancaster RW, Butler JM, Rades T. Preparation of glass solutions of three poorly water soluble drugs by spray drying, melt extrusion and ball milling. International journal of pharmaceutics. 2007;336(1):22-34.
65. Jawad R, Elleman C, Vermeer L, Drake AF, Woodhead B, Martin GP, et al. The measurement of the β/α anomer composition within amorphous lactose prepared by spray and freeze drying using a simple 1 H-NMR method. Pharmaceutical research. 2012;29(2):511-24.
66. Alonzo DE, Gao Y, Zhou D, Mo H, Zhang GGZ, Taylor LS. Dissolution and Precipitation Behavior of Amorphous Solid Dispersions. Journal of Pharmaceutical Sciences. 2011;100(8):3316-31.
67. Abu-Diak OA, Jones DS, Andrews GP. An Investigation into the Dissolution Properties of Celecoxib Melt Extrudates: Understanding the Role of Polymer Type and Concentration in Stabilizing Supersaturated Drug Concentrations. Molecular Pharmaceutics. 2011;8(4):1362-71.
68. Abu-Diak OA, Jones DS, Andrews GP. Understanding the Performance of Melt-Extruded Poly(ethylene oxide)–Bicalutamide Solid Dispersions: Characterisation of Microstructural Properties Using Thermal, Spectroscopic and Drug Release Methods. Journal of Pharmaceutical Sciences. 2012;101(1):200-13.
69. Ilevbare GA, Liu H, Edgar KJ, Taylor LS. Maintaining Supersaturation in Aqueous Drug Solutions: Impact of Different Polymers on Induction Times. Crystal Growth & Design. 2013;13(2):740-51.
70. Alonzo DE, Zhang GGZ, Zhou D, Gao Y, Taylor LS. Understanding the Behavior of Amorphous Pharmaceutical Systems during Dissolution. Pharmaceutical Research. 2010;27(4):608-18.
71. Mellaerts R, Mols R, Kayaert P, Annaert P, Van Humbeeck J, Van den Mooter G, et al. Ordered mesoporous silica induces pH-independent supersaturation of the basic low solubility compound itraconazole resulting in enhanced transepithelial transport. International Journal of Pharmaceutics. 2008;357(1–2):169-79.
72. Vallet-Regi M, Ramila A, Del Real R, Perez-Pariente J. A new property of MCM-41: drug delivery system. Chemistry of Materials. 2001;13(2):308-11.
73. Xu W, Riikonen J, Lehto V-P. Mesoporous systems for poorly soluble drugs. International Journal of Pharmaceutics. 2013;453(1):181-97.
74. Kresge C, Leonowicz M, Roth W, Vartuli J, Beck J. Ordered mesoporous molecular sieves synthesized by a liquid-crystal template mechanism. Nature. 1992;359(6397):710-2.
75. Shen SC, Ng WK, Chia L, Dong YC, Tan RB. Stabilized amorphous state of ibuprofen by co-spray drying with mesoporous SBA-15 to enhance dissolution properties. Journal of Pharmaceutical Sciences. 2010;99(4):1997-2007.

76. Mellaerts R, Houthoofd K, Elen K, Chen H, Van Speybroeck M, Van Humbeeck J, et al. Aging behavior of pharmaceutical formulations of itraconazole on SBA-15 ordered mesoporous silica carrier material. Microporous and Mesoporous Materials. 2010;130(1):154-61.
77. Pednekar PP, Godiyal SC, Jadhav KR, Kadam VJ. Chapter 23 - Mesoporous silica nanoparticles: a promising multifunctional drug delivery system. In: Ficai A, Grumezescu AM, editors. Nanostructures for Cancer Therapy: Elsevier; 2017. p. 593-621.
78. Bevernage J, Brouwers J, Brewster ME, Augustijns P. Evaluation of gastrointestinal drug supersaturation and precipitation: strategies and issues. International journal of pharmaceutics. 2013;453(1):25-35.
79. Brouwers J, Brewster ME, Augustijns P. Supersaturating drug delivery systems: The answer to solubility-limited oral bioavailability? Journal of Pharmaceutical Sciences. 2009;98(8):2549-72.
80. Kostewicz ES, Abrahamsson B, Brewster M, Brouwers J, Butler J, Carlert S, et al. In vitro models for the prediction of in vivo performance of oral dosage forms. European Journal of Pharmaceutical Sciences. 2014;57:342-66.
81. Siewert M, Dressman J, Brown CK, Shah VP, Aiache J-M, Aoyagi N, et al. FIP/AAPS guidelines to dissolution/in vitro release testing of novel/special dosage forms. Aaps PharmSciTech. 2003;4(1):43-52.
82. Cohen JL, Hubert BB, Leeson LJ, Rhodes CT, Robinson JR, Roseman TJ, et al. The development of USP dissolution and drug release standards. Pharmaceutical Research. 1990;7(10):983-7.
83. Dressman JB, Amidon GL, Reppas C, Shah VP. Dissolution testing as a prognostic tool for oral drug absorption: immediate release dosage forms. Pharmaceutical Research. 1998;15(1):11-22.
84. Gibaldi M, Feldman S. Establishment of sink conditions in dissolution rate determinations. Theoretical considerations and application to nondisintegrating dosage forms. Journal of Pharmaceutical Sciences. 1967;56(10):1238-42.
85. Augustijns P, Brewster ME. Supersaturating drug delivery systems: Fast is not necessarily good enough. Journal of Pharmaceutical Sciences. 2012;101(1):7-9.
86. Klein S. The Use of Biorelevant Dissolution Media to Forecast the In Vivo Performance of a Drug. The AAPS Journal. 2010;12(3):397-406.
87. Kostewicz ES, Brauns U, Becker R, Dressman JB. Forecasting the oral absorption behavior of poorly soluble weak bases using solubility and dissolution studies in biorelevant media. Pharmaceutical Research. 2002;19(3):345-9.
88. Ahern RJ, Crean AM, Ryan KB. The influence of supercritical carbon dioxide (SC-CO2) processing conditions on drug loading and physicochemical properties. International Journal of Pharmaceutics. 2012;439(1):92-9.
89. Guo Z, Liu X-M, Ma L, Li J, Zhang H, Gao Y-P, et al. Effects of particle morphology, pore size and surface coating of mesoporous silica on Naproxen dissolution rate enhancement. Colloids and Surfaces B: Biointerfaces. 2013;101(0):228-35.
90. Kinnari P, Mäkilä E, Heikkilä T, Salonen J, Hirvonen J, Santos HA. Comparison of mesoporous silicon and non-ordered mesoporous silica materials as drug carriers for itraconazole. International Journal of Pharmaceutics. 2011;414(1–2):148-56.
91. Kumar D, Sailaja Chirravuri SV, Shastri NR. Impact of surface area of silica particles on dissolution rate and oral bioavailability of poorly water soluble drugs: A case study with aceclofenac. International Journal of Pharmaceutics. 2014;461(1–2):459-68.
92. Yoncheva K, Popova M, Szegedi A, Mihaly J, Tzankov B, Lambov N, et al. Functionalized mesoporous silica nanoparticles for oral delivery of budesonide. Journal of Solid State Chemistry. 2014;211:154-61.

93. Zoeller T, Klein S. Simplified biorelevant media for screening dissolution performance of poorly soluble drugs. Dissolution Technologies. 2007;14(4):8-13.
94. Kleberg K, Jacobsen J, Müllertz A. Characterising the behaviour of poorly water soluble drugs in the intestine: application of biorelevant media for solubility, dissolution and transport studies. Journal of Pharmacy and Pharmacology. 2010;62(11):1656-68.
95. Jantratid E, Dressman J. Biorelevant dissolution media simulating the proximal human gastrointestinal tract: an update. Dissolution Technologies. 2009;16(3):21-5.
96. Schiller C, Frohlich CP, Giessmann T, Siegmund W, MÖNnikes H, Hosten N, et al. Intestinal fluid volumes and transit of dosage forms as assessed by magnetic resonance imaging. Alimentary Pharmacology & Therapeutics. 2005;22(10):971-9.
97. D'Arcy DM, Corrigan OI, Healy AM. Evaluation of hydrodynamics in the basket dissolution apparatus using computational fluid dynamics—dissolution rate implications. European Journal of Pharmaceutical Sciences. 2006;27(2-3):259-67.
98. Bai G, Armenante PM, Plank RV, Gentzler M, Ford K, Harmon P. Hydrodynamic investigation of USP dissolution test apparatus II. Journal of Pharmaceutical Sciences. 2007;96(9):2327-49.
99. Qiu Y. CY, Zhang GGZ, Liu L., Porter W. Developing Solid Oral Dosage Forms; Pharmaceutical Theory & Practice. Academic Press Inc., London; 2009.
100. Fotaki N, Reppas C. The flow through cell methodology in the evaluation of intralumenal drug release characteristics. Dissolution Technologies. 2005;12(2):17-21.
101. Sunesen VH, Pedersen BL, Kristensen HG, Müllertz A. In vivo in vitro correlations for a poorly soluble drug, danazol, using the flow-through dissolution method with biorelevant dissolution media. European Journal of Pharmaceutical Sciences. 2005;24(4):305-13.
102. D'Arcy DM, Liu B, Corrigan OI. Investigating the effect of solubility and density gradients on local hydrodynamics and drug dissolution in the USP 4 dissolution apparatus. International Journal of Pharmaceutics. 2011;419(1–2):175-85.
103. Fotaki N, Aivaliotis A, Butler J, Dressman J, Fischbach M, Hempenstall J, et al. A comparative study of different release apparatus in generating in vitro–in vivo correlations for extended release formulations. European Journal of Pharmaceutics and Biopharmaceutics. 2009;73(1):115-20.
104. Okumu A, DiMaso M, Löbenberg R. Dynamic Dissolution Testing To Establish In Vitro/In Vivo Correlations for Montelukast Sodium, a Poorly Soluble Drug. Pharmaceutical Research. 2008;25(12):2778-85.
105. Sjögren E, Abrahamsson B, Augustijns P, Becker D, Bolger MB, Brewster M, et al. In vivo methods for drug absorption – Comparative physiologies, model selection, correlations with in vitro methods (IVIVC), and applications for formulation/API/excipient characterization including food effects. European Journal of Pharmaceutical Sciences. 2014;57:99-151.
106. Polli JE. IVIVR versus IVIVC. Dissolution Technologies. 2000;7(3):6-9.
107. Somasundaran P, Krishnakumar S. Adsorption of surfactants and polymers at the solid-liquid interface. Colloids and Surfaces A: Physicochemical and Engineering Aspects. 1997;123-124:491-513.
108. Adamson AW, Gast AP. Physical chemistry of surfaces. 1967.
109. Parfitt G.D RC. Adsorption from Solution at the Solid/Liquid Interface: Academic Press; 1983.
110. Zangwill A. Physics at surfaces: Cambridge university press; 1988.
111. Malek A, Farooq S. Comparison of isotherm models for hydrocarbon adsorption on activated carbon. AIChE Journal. 1996;42(11):3191-201.
112. Vijayaraghavan K, Padmesh T, Palanivelu K, Velan M. Biosorption of nickel (II) ions onto Sargassum wightii: application of two-parameter and three-parameter isotherm models. Journal of Hazardous Materials. 2006;133(1-3):304-8.

113. Kundu S, Gupta AK. Arsenic adsorption onto iron oxide-coated cement (IOCC): Regression analysis of equilibrium data with several isotherm models and their optimization. Chemical Engineering Journal. 2006;122(1):93-106.
114. Allen SJ, McKay G, Porter JF. Adsorption isotherm models for basic dye adsorption by peat in single and binary component systems. Journal of Colloid and Interface Science. 2004;280(2):322-33.
115. Adams A, Gast A. Physical chemistry of surfaces. John Wiley and Sons, New York; 1997.
116. Limnell T, Santos HA, Mäkilä E, Heikkilä T, Salonen J, Murzin DY, et al. Drug delivery formulations of ordered and nonordered mesoporous silica: comparison of three drug loading methods. Journal of Pharmaceutical Sciences. 2011;100(8):3294-306.
117. Xue JM, Shi M. PLGA/mesoporous silica hybrid structure for controlled drug release. Journal of Controlled Release. 2004;98(2):209-17.
118. Bui TX, Choi H. Adsorptive removal of selected pharmaceuticals by mesoporous silica SBA-15. Journal of Hazardous Materials. 2009;168(2):602-8.
119. Parida SK, Dash S, Patel S, Mishra BK. Adsorption of organic molecules on silica surface. Advances in Colloid and Interface Science. 2006;121(1):77-110.
120. Monkhouse DC, Lach JL. Use of adsorbents in enhancement of drug dissolution I. Journal of Pharmaceutical Sciences. 1972;61(9):1430-5.
121. Unger K, Rupprecht H, Valentin B, Kircher W. The use of porous and surface modified silicas as drug delivery and stabilizing agents. Drug Development and Industrial Pharmacy. 1983;9(1-2):69-91.
122. Mellaerts R, Aerts CA, Humbeeck JV, Augustijns P, den Mooter GV, Martens JA. Enhanced release of itraconazole from ordered mesoporous SBA-15 silica materials. Chemical Communications. 2007(13):1375-7.
123. Heikkilä T, Salonen J, Tuura J, Hamdy MS, Mul G, Kumar N, et al. Mesoporous silica material TUD-1 as a drug delivery system. International Journal of Pharmaceutics. 2007;331(1):133-8.
124. Salonen J, Kaukonen AM, Hirvonen J, Lehto VP. Mesoporous Silicon in Drug Delivery Applications. Journal of Pharmaceutical Sciences. 2008;97(2):632-53.
125. Bley H, Fussnegger B, Bodmeier R. Characterization and stability of solid dispersions based on PEG/polymer blends. International Journal of Pharmaceutics. 2010;390(2):165-73.
126. U.S. Food and Drug Administration. Inactive Ingredient Search for Approved Drug Products 2015 [Available from: http://www.accessdata.fda.gov/scripts/cder/iig/getiigWEB.cfm.
127. Fu C, Liu T, Li L, Liu H, Chen D, Tang F. The absorption, distribution, excretion and toxicity of mesoporous silica nanoparticles in mice following different exposure routes. Biomaterials. 2013;34(10):2565-75.
128. Hudson SP, Padera RF, Langer R, Kohane DS. The biocompatibility of mesoporous silicates. Biomaterials. 2008;29(30):4045-55.
129. Cao X, Deng W, Fu M, Zhu Y, Liu H, Wang L, et al. Seventy-two-hour release formulation of the poorly soluble drug silybin based on porous silica nanoparticles: in vitro release kinetics and in vitro/in vivo correlations in beagle dogs. European Journal of Pharmaceutical Sciences. 2013;48(1):64-71.
130. Kiekens F, Eelen S, Verheyden L, Daems T, Martens J, Den Mooter GV. Use of ordered mesoporous silica to enhance the oral bioavailability of ezetimibe in dogs. Journal of Pharmaceutical Sciences. 2012;101(3):1136-44.
131. Manzano M, Colilla M, Vallet-Regí M. Drug delivery from ordered mesoporous matrices. Expert Opinion on Drug Delivery. 2009;6(12):1383-400.
132. Jaganathan H, Godin B. Biocompatibility assessment of Si-based nano- and micro-particles. Advanced Drug Delivery Reviews. 2012;64(15):1800-19.

133. Bend Research. Spray-Dried NanoAdsorbate (SDNA) Technology 2014 [Available from: http://www.bendresearch.com/drug-delivery-technologies/spray-dried-composite-sdc-technology.
134. Rowe RC, Sheskey PJ, Owen SC, Association AP. Handbook of Pharmaceutical Excipients: Pharmaceutical press London; 2006.
135. Kim J. Synthesis of MCM-48 single crystals. Chemical Communications. 1998(2):259-60.
136. Izquierdo-Barba I, Martinez Á, Doadrio AL, Pérez-Pariente J, Vallet-Regí M. Release evaluation of drugs from ordered three-dimensional silica structures. European Journal of Pharmaceutical Sciences. 2005;26(5):365-73.
137. Zhao D, Feng J, Huo Q, Melosh N, Fredrickson GH, Chmelka BF, et al. Triblock copolymer syntheses of mesoporous silica with periodic 50 to 300 angstrom pores. Science. 1998;279(5350):548-52.
138. Inagaki S, Koiwai A, Suzuki N, Fukushima Y, Kuroda K. Syntheses of Highly Ordered Mesoporous Materials, FSM-16, Derived from Kanemite. Bulletin of the Chemical Society of Japan. 1996;69(5):1449-57.
139. Jansen J, Shan Z, Marchese L, Zhou W, vd Puil N, Maschmeyer T. A new templating method for three-dimensional mesopore networks. Chemical Communications. 2001(8):713-4.
140. Takeuchi H, Nagira S, Yamamoto H, Kawashima Y. Solid dispersion particles of amorphous indomethacin with fine porous silica particles by using spray-drying method. International Journal of Pharmaceutics. 2005;293(1–2):155-64.
141. Azaïs T, Tourné-Péteilh C, Aussenac F, Baccile N, Coelho C, Devoisselle J-M, et al. Solid-state NMR study of ibuprofen confined in MCM-41 material. Chemistry of Materials. 2006;18(26):6382-90.
142. Charnay C, Bégu S, Tourné-Péteilh C, Nicole L, Lerner DA, Devoisselle JM. Inclusion of ibuprofen in mesoporous templated silica: drug loading and release property. European Journal of Pharmaceutics and Biopharmaceutics. 2004;57(3):533-40.
143. Hong S, Shen S, Tan DCT, Ng WK, Liu X, Chia LS, et al. High drug load, stable, manufacturable and bioavailable fenofibrate formulations in mesoporous silica: a comparison of spray drying versus solvent impregnation methods. Drug Delivery. 2014(0):1-12.
144. Sliwinska-Bartkowiak M, Dudziak G, Gras R, Sikorski R, Radhakrishnan R, Gubbins KE. Freezing behavior in porous glasses and MCM-41. Colloids and Surfaces A: Physicochemical and Engineering Aspects. 2001;187:523-9.
145. Brás AR, Fonseca IM, Dionísio M, Schönhals A, Affouard F, Correia NT. Influence of nanoscale confinement on the molecular mobility of ibuprofen. The Journal of Physical Chemistry C. 2014;118(25):13857-68.
146. FUJI SILYSIA CHEMICAL LTD. SYLYSIA 2015 [Available from: http://www.fujisilysia.com/products/sylysia/.
147. W. R. Grace & Co.-Conn. Syloid Silica Excipients for Pharmaceutical Applications [Available from: https://grace.com/pharma-and-biotech/en-us/Documents/Syloid/B561b_SYLOID_8.5x11VERSION_9-18-14_FINAL.pdf.
148. Gumaste SG, Pawlak SA, Dalrymple DM, Nider CJ, Trombetta LD, Serajuddin AT. Development of solid SEDDS, IV: effect of adsorbed lipid and surfactant on tableting properties and surface structures of different silicates. Pharmaceutical Research. 2013;30(12):3170-85.
149. Galarneau A, Nader M, Guenneau F, Di Renzo F, Gedeon A. Understanding the stability in water of mesoporous SBA-15 and MCM-41. The Journal of Physical Chemistry C. 2007;111(23):8268-77.

150. Merck Millipore Introduces Parteck® SLC, Silica-based Excipient for Enhanced Drug Solubility and Bioavailability [press release]. 2013.
151. Andersson J, Rosenholm J, Areva S, Lindén M. Influences of material characteristics on ibuprofen drug loading and release profiles from ordered micro-and mesoporous silica matrices. Chemistry of Materials. 2004;16(21):4160-7.
152. Singh A, Worku ZA, Van den Mooter G. Oral formulation strategies to improve solubility of poorly water-soluble drugs. Expert Opinion on Drug Delivery. 2011;8(10):1361-78.
153. Prestidge CA, Barnes TJ, Lau C-H, Barnett C, Loni A, Canham L. Mesoporous silicon: a platform for the delivery of therapeutics. 2007.
154. Mellaerts R, Jammaer JAG, Van Speybroeck M, Chen H, Van Humbeeck J, Augustijns P, et al. Physical state of poorly water soluble therapeutic molecules loaded into SBA-15 ordered mesoporous silica carriers: A case study with itraconazole and ibuprofen. Langmuir. 2008;24(16):8651-9.
155. Waters LJ, Bedford S, Parkes GM. Controlled microwave processing applied to the pharmaceutical formulation of ibuprofen. AAPS PharmSciTech. 2011;12(4):1038-43.
156. Waters LJ, Hussain T, Parkes G, Hanrahan JP, Tobin JM. Inclusion of fenofibrate in a series of mesoporous silicas using microwave irradiation. European Journal of Pharmaceutics and Biopharmaceutics. 2013;85(3):936-41.
157. Qu F, Zhu G, Lin H, Zhang W, Sun J, Li S, et al. A controlled release of ibuprofen by systematically tailoring the morphology of mesoporous silica materials. Journal of Solid State Chemistry. 2006;179(7):2027-35.
158. Ambrogi V, Perioli L, Pagano C, Latterini L, Marmottini F, Ricci M, et al. MCM-41 for furosemide dissolution improvement. Microporous and Mesoporous Materials. 2012;147(1):343-9.
159. Qian K, Wurster D, Bogner R. Spontaneous Crystalline-to-Amorphous Phase Transformation of Organic or Medicinal Compounds in the Presence of Porous Media, Part 3: Effect of Moisture. Pharmaceutical Research. 2012;29(10):2698-709.
160. IMPURITIES: GUIDELINE FOR RESIDUAL SOLVENTS Q3C(R5)
161. Hata H, Saeki S, Kimura T, Sugahara Y, Kuroda K. Adsorption of taxol into ordered mesoporous silicas with various pore diameters. Chemistry of Materials. 1999;11(4):1110-9.
162. Heikkilä T, Salonen J, Tuura J, Kumar N, Salmi T, Murzin DY, et al. Evaluation of mesoporous TCPSi, MCM-41, SBA-15, and TUD-1 materials as API carriers for oral drug delivery. Drug Delivery. 2007;14(6):337-47.
163. Lehto V, Riikonen J, Santos H. Drug loading and characterization of porous silicon materials. Porous Silicon for Biomedical Applications. 2014:337.
164. van Speybroeck M, Mellaerts R, Thi TD, Martens JA, Van Humbeeck J, Annaert P, et al. Preventing release in the acidic environment of the stomach via occlusion in ordered mesoporous silica enhances the absorption of poorly soluble weakly acidic drugs. Journal of Pharmaceutical Sciences. 2011;100(11):4864-76.
165. Kruk M, Jaroniec M, Ko CH, Ryoo R. Characterization of the Porous Structure of SBA-15. Chemistry of Materials. 2000;12(7):1961-8.
166. Vetere A. A short-cut method to predict the solubilities of solids in supercritical carbon dioxide. Fluid Phase Equilibria. 1998;148(1–2):83-93.
167. Gignone A, Manna L, Ronchetti S, Banchero M, Onida B. Incorporation of clotrimazole in Ordered Mesoporous Silica by supercritical CO2. Microporous and Mesoporous Materials. 2014;200(0):291-6.
168. Bahl D, Hudak J, Bogner RH. Comparison of the ability of various pharmaceutical silicates to amorphize and enhance dissolution of indomethacin upon co-grinding. Pharmaceutical Development and Technology. 2008;13(3):255-69.

169. Aerts CA, Verraedt E, Mellaerts R, Depla A, Augustijns P, Van Humbeeck J, et al. Tunability of pore diameter and particle size of amorphous microporous silica for diffusive controlled release of drug compounds. The Journal of Physical Chemistry C. 2007;111(36):13404-9.
170. Horcajada P, Ramila A, Perez-Pariente J, Vallet-Regı M. Influence of pore size of MCM-41 matrices on drug delivery rate. Microporous and Mesoporous Materials. 2004;68(1):105-9.
171. Tozuka Y, Wongmekiat A, Kimura K, Moribe K, Yamamura S, Yamamoto K. Effect of pore size of FSM-16 on the entrapment of flurbiprofen in mesoporous structures. Chemical and Pharmaceutical Bulletin. 2005;53(8):974-7.
172. Ukmar T, Maver U, Planinšek O, Kaučič V, Gaberšček M, Godec A. Understanding controlled drug release from mesoporous silicates: theory and experiment. Journal of Controlled Release. 2011;155(3):409-17.
173. Gao L, Sun J, Zhang L, Wang J, Ren B. Influence of different structured channels of mesoporous silicate on the controlled ibuprofen delivery. Materials Chemistry and Physics. 2012;135(2–3):786-97.
174. Zhu Y-F, Shi J-l, Li Y-S, Chen H-r, Shen W-H, Dong X-p. Hollow mesoporous spheres with cubic pore network as a potential carrier for drug storage and its in vitro release kinetics. Journal of Materials Research. 2005;20(01):54-61.
175. Zhang Y, Zhi Z, Jiang T, Zhang J, Wang Z, Wang S. Spherical mesoporous silica nanoparticles for loading and release of the poorly water-soluble drug telmisartan. Journal of Controlled Release. 2010;145(3):257-63.
176. Rengarajan G, Enke D, Steinhart M, Beiner M. Stabilization of the amorphous state of pharmaceuticals in nanopores. Journal of Materials Chemistry. 2008;18(22):2537-9.
177. Jia LJ, Shen JY, Li ZY, Zhang DR, Zhang Q, Duan CX, et al. Successfully tailoring the pore size of mesoporous silica nanoparticles: Exploitation of delivery systems for poorly water-soluble drugs. International Journal of Pharmaceutics. 2012;439(1-2):81-91.
178. Shen S-C, Ng WK, Chia L, Hu J, Tan RBH. Physical state and dissolution of ibuprofen formulated by co-spray drying with mesoporous silica: Effect of pore and particle size. International Journal of Pharmaceutics. 2011;410(1–2):188-95.
179. Hu Y, Wang J, Zhi Z, Jiang T, Wang S. Facile synthesis of 3D cubic mesoporous silica microspheres with a controllable pore size and their application for improved delivery of a water-insoluble drug. Journal of Colloid and Interface Science. 2011;363(1):410-7.
180. Miura H, Kanebako M, Shirai H, Nakao H, Inagi T, Terada K. Stability of amorphous drug, 2-benzyl-5-(4-chlorophenyl)-6-[4-(methylthio)phenyl]-2H-pyridazin-3-one, in silica mesopores and measurement of its molecular mobility by solid-state 13C NMR spectroscopy. International Journal of Pharmaceutics. 2011;410(1–2):61-7.
181. Van Speybroeck M, Mellaerts R, Mols R, Thi TD, Martens JA, Van Humbeeck J, et al. Enhanced absorption of the poorly soluble drug fenofibrate by tuning its release rate from ordered mesoporous silica. European Journal of Pharmaceutical Sciences. 2010;41(5):623-30.
182. Qi L, Ma J, Cheng H, Zhao Z. Micrometer-sized mesoporous silica spheres grown under static conditions. Chemistry of Materials. 1998;10(6):1623-6.
183. Slowing II, Vivero-Escoto JL, Wu C-W, Lin VSY. Mesoporous silica nanoparticles as controlled release drug delivery and gene transfection carriers. Advanced Drug Delivery Reviews. 2008;60(11):1278-88.
184. Qu F, Zhu G, Huang S, Li S, Sun J, Zhang D, et al. Controlled release of Captopril by regulating the pore size and morphology of ordered mesoporous silica. Microporous and Mesoporous Materials. 2006;92(1–3):1-9.

185. Manzano M, Aina V, Areán CO, Balas F, Cauda V, Colilla M, et al. Studies on MCM-41 mesoporous silica for drug delivery: Effect of particle morphology and amine functionalization. Chemical Engineering Journal. 2008;137(1):30-7.
186. Hu J, Rogers TL, Brown J, Young T, Johnston KP, Williams Iii RO. Improvement of dissolution rates of poorly water soluble APIs using novel spray freezing into liquid technology. Pharmaceutical Research. 2002;19(9):1278-84.
187. Song SW, Hidajat K, Kawi S. Functionalized SBA-15 Materials as Carriers for Controlled Drug Delivery: Influence of Surface Properties on Matrix−Drug Interactions. Langmuir. 2005;21(21):9568-75.
188. Balas F, Manzano M, Horcajada P, Vallet-Regí M. Confinement and Controlled Release of Bisphosphonates on Ordered Mesoporous Silica-Based Materials. Journal of the American Chemical Society. 2006;128(25):8116-7.
189. Doadrio JC, Sousa EM, Izquierdo-Barba I, Doadrio AL, Perez-Pariente J, Vallet-Regí M. Functionalization of mesoporous materials with long alkyl chains as a strategy for controlling drug delivery pattern. Journal of Materials Chemistry. 2006;16(5):462-6.
190. Qu F, Zhu G, Huang S, Li S, Qiu S. Effective Controlled Release of Captopril by Silylation of Mesoporous MCM-41. ChemPhysChem. 2006;7(2):400-6.
191. Tang Q, Yao X, Dong W, Sun Y, Wang J, Jun X, et al. Studies on a new carrier of trimethylsilyl-modified mesoporous material for controlled drug delivery. Journal of Controlled Release. 2006;114(1):41-6.
192. Moritz M, Łaniecki M. SBA-15 mesoporous material modified with APTES as the carrier for 2-(3-benzoylphenyl) propionic acid. Applied Surface Science. 2012;258(19):7523-9.
193. Nastase S, Bajenaru L, Matei C, Mitran RA, Berger D. Ordered mesoporous silica and aluminosilicate-type matrix for amikacin delivery systems. Microporous and Mesoporous Materials. 2013;182(0):32-9.
194. Carmona D, Balas F, Santamaria J. Pore ordering and surface properties of FDU-12 and SBA-15 mesoporous materials and their relation to drug loading and release in aqueous environments. Materials Research Bulletin. 2014;59:311-22.
195. Jambhrunkar S, Qu Z, Popat A, Karmakar S, Xu C, Yu C. Modulating in vitro release and solubility of griseofulvin using functionalized mesoporous silica nanoparticles. Journal of Colloid and Interface Science. 2014;434(0):218-25.
196. Hancock BC, Zografi G. Characteristics and significance of the amorphous state in pharmaceutical systems. Journal of Pharmaceutical Sciences. 1997;86(1):1-12.
197. Morris KR, Griesser UJ, Eckhardt CJ, Stowell JG. Theoretical approaches to physical transformations of active pharmaceutical ingredients during manufacturing processes. Advanced Drug Delivery Reviews. 2001;48(1):91-114.
198. Limnell T, Riikonen J, Salonen J, Kaukonen AM, Laitinen L, Hirvonen J, et al. Surface chemistry and pore size affect carrier properties of mesoporous silicon microparticles. International Journal of Pharmaceutics. 2007;343(1–2):141-7.
199. Limnell T, Heikkilä T, Santos HA, Sistonen S, Hellstén S, Laaksonen T, et al. Physicochemical stability of high indomethacin payload ordered mesoporous silica MCM-41 and SBA-15 microparticles. International Journal of Pharmaceutics. 2011;416(1):242-51.
200. Hailu SA, Bogner RH. Complex effects of drug/silicate ratio, solid-state equivalent pH, and moisture on chemical stability of amorphous quinapril hydrochloride coground with silicates. Journal of Pharmaceutical Sciences. 2011;100(4):1503-15.
201. Pan X, Julian T, Augsburger L. Increasing the Dissolution Rate of a Low-Solubility Drug Through a Crystalline-Amorphous Transition: A Case Study with Indomethicin. Drug Development and Industrial Pharmacy. 2008;34(2):221-31.

202. Bahl D, Bogner R. Amorphization of Indomethacin by Co-Grinding with Neusilin US2: Amorphization Kinetics, Physical Stability and Mechanism. Pharmaceutical Research. 2006;23(10):2317-25.
203. Mellaerts R, Roeffaers MBJ, Houthoofd K, Van Speybroeck M, De Cremer G, Jammaer JAG, et al. Molecular organization of hydrophobic molecules and co-adsorbed water in SBA-15 ordered mesoporous silica material. Phys Chem Chem Phys. 2011;13(7):2706-13.
204. Shalaev EY, Zografi G. How does residual water affect the solid-state degradation of drugs in the amorphous state? Journal of Pharmaceutical Sciences. 1996;85(11):1137-41.
205. Byrn SR, Xu W, Newman AW. Chemical reactivity in solid-state pharmaceuticals: formulation implications. Advanced Drug Delivery Reviews. 2001;48(1):115-36.
206. Vialpando M, Martens JA, Van den Mooter G. Potential of ordered mesoporous silica for oral delivery of poorly soluble drugs. Therapeutic Delivery. 2011;2(8):1079-91.
207. Wang S. Ordered mesoporous materials for drug delivery. Microporous and Mesoporous Materials. 2009;117(1):1-9.
208. Turku I, Sainio T, Paatero E. Thermodynamics of tetracycline adsorption on silica. Environ Chem Lett. 2007;5(4):225-8.
209. Ahern RJ. Application of Mesoporous Silica for the Oral Delivery of Poorly Water Soluble Drugs [PhD Thesis]. Ireland: University College Cork; 2013.
210. Atkin R, Craig VSJ, Wanless EJ, Biggs S. Mechanism of cationic surfactant adsorption at the solid–aqueous interface. Advances in Colloid and Interface Science. 2003;103(3):219-304.
211. Vandecruys R, Peeters J, Verreck G, Brewster ME. Use of a screening method to determine excipients which optimize the extent and stability of supersaturated drug solutions and application of this system to solid formulation design. International Journal of Pharmaceutics. 2007;342(1):168-75.
212. Miriyala N, Ouyang D, Perrie Y, Lowry D, Kirby DJ. Activated carbon as a carrier for amorphous drug delivery: Effect of drug characteristics and carrier wettability. European Journal of Pharmaceutics and Biopharmaceutics. 2017;115:197-205.
213. Singla P, Chabba S, Mahajan RK. A systematic physicochemical investigation on solubilization and in vitro release of poorly water soluble oxcarbazepine drug in pluronic micelles. Colloids and Surfaces A: Physicochemical and Engineering Aspects. 2016;504:479-88.
214. Li M, Lopez N, Bilgili E. A study of the impact of polymer–surfactant in drug nanoparticle coated pharmatose composites on dissolution performance. Advanced Powder Technology. 2016;27(4):1625-36.
215. U.S. Food and Drug Administration. Dissolution Methods 2017 [Available from: http://www.accessdata.fda.gov/scripts/cder/dissolution/.
216. Swearingen RA, Chen X, Petersen JS, Riley KS, Wang D, Zhorov E. Determination of the binding parameter constants of Renagel® capsules and tablets utilizing the Langmuir approximation at various pH by ion chromatography. Journal of Pharmaceutical and Biomedical Analysis. 2002;29(1):195-201.
217. García-Calzón JA, Díaz-García ME. Characterization of binding sites in molecularly imprinted polymers. Sensors and Actuators B: Chemical. 2007;123(2):1180-94.
218. Ding S, Chen J, Jiang H, He J, Shi W, Zhao W, et al. Application of Quantum Dot−Antibody Conjugates for Detection of Sulfamethazine Residue in Chicken Muscle Tissue. Journal of Agricultural and Food Chemistry. 2006;54(17):6139-42.
219. Im SH, Ryoo JJ. Characterization of sodium laureth sulfate by reversed-phase liquid chromatography with evaporative light scattering detection and 1H nuclear magnetic resonance spectroscopy. Journal of Chromatography A. 2009;1216(12):2339-44.

220. Barrett EP, Joyner LG, Halenda PP. The determination of pore volume and area distributions in porous substances. I. Computations from nitrogen isotherms. Journal of the American Chemical Society. 1951;73(1):373-80.
221. Rangel-Yagui CO, Pessoa Jr A, Tavares LC. Micellar solubilization of drugs. Journal of Pharmaceutical Sciences. 2005;8(2):147-63.
222. McCarthy CA, Ahern RJ, Dontireddy R, Ryan KB, Crean AM. Mesoporous silica formulation strategies for drug dissolution enhancement: a review. Expert Opinion on Drug Delivery. 2016;13(1):93-108.
223. Smirnova I, Mamic J, Arlt W. Adsorption of drugs on silica aerogels. Langmuir. 2003;19(20):8521-5.
224. Umpleby RJ, Baxter SC, Chen Y, Shah RN, Shimizu KD. Characterization of molecularly imprinted polymers with the Langmuir− Freundlich isotherm. Analytical Chemistry. 2001;73(19):4584-91.
225. Umpleby II RJ, Baxter SC, Bode M, Berch Jr JK, Shah RN, Shimizu KD. Application of the Freundlich adsorption isotherm in the characterization of molecularly imprinted polymers. Analytica Chimica Acta. 2001;435(1):35-42.
226. Kosmulski M. Positive Electrokinetic Charge of Silica in the Presence of Chlorides. Journal of Colloid and Interface Science. 1998;208(2):543-5.
227. Gao Y, Du J, Gu T. Hemimicelle formation of cationic surfactants at the silica gel–water interface. Journal of the Chemical Society, Faraday Transactions 1: Physical Chemistry in Condensed Phases. 1987;83(8):2671-9.
228. Vigil G, Xu Z, Steinberg S, Israelachvili J. Interactions of Silica Surfaces. Journal of Colloid and Interface Science. 1994;165(2):367-85.
229. Rosen MJ, Kunjappu JT. Surfactants and Interfacial Phenomena: John Wiley & Sons; 2012.
230. O'shea JP, Nagarsekar K, Wieber A, Witt V, Herbert E, O'driscoll CM, et al. Mesoporous silica-based dosage forms improve bioavailability of poorly soluble drugs in pigs: case example fenofibrate. Journal of Pharmacy and Pharmacology. 2017;69(10):1284-92.
231. Dressman JB, Herbert E, Wieber A, Birk G, Saal C, Lubda D. Mesoporous silica-based dosage forms improve release characteristics of poorly soluble drugs: case example fenofibrate. Journal of Pharmacy and Pharmacology. 2016;68(5):634-45.
232. McCarthy CA, Faisal W, O'Shea JP, Murphy C, Ahern RJ, Ryan KB, et al. In vitro dissolution models for the prediction of in vivo performance of an oral mesoporous silica formulation. Journal of Controlled Release. 2017;250:86-95.
233. Jantratid E, Janssen N, Reppas C, Dressman JB. Dissolution Media Simulating Conditions in the Proximal Human Gastrointestinal Tract: An Update. Pharmaceutical Research. 2008;25(7):1663-76.
234. The United States Pharmacopeial Convention Inc. The United States Pharmacopeia 26, The National Formulary 21. Canada: Webcom Ltd.; 2003.
235. Enright EF, Joyce SA, Gahan CGM, Griffin BT. Impact of Gut Microbiota-Mediated Bile Acid Metabolism on the Solubilization Capacity of Bile Salt Micelles and Drug Solubility. Molecular Pharmaceutics. 2017;14(4):1251-63.
236. Tso J, Aga DS. Wrong-Way-Round Ionization of Sulfonamides and Tetracyclines Enables Simultaneous Analysis with Free and Conjugated Estrogens by Liquid Chromatography Tandem Mass Spectrometry. Analytical Chemistry. 2011;83(1):269-77.
237. Boreen AL, Arnold WA, McNeill K. Photochemical Fate of Sulfa Drugs in the Aquatic Environment: Sulfa Drugs Containing Five-Membered Heterocyclic Groups. Environmental Science & Technology. 2004;38(14):3933-40.
238. Belyakova LA, Besarab LN, Roik NV, Lyashenko DY, Vlasova NN, Golovkova LP, et al. Designing of the centers for adsorption of bile acids on a silica surface. Journal of Colloid and Interface Science. 2006;294(1):11-20.

239. Vertzoni M, Dressman J, Butler J, Hempenstall J, Reppas C. Simulation of fasting gastric conditions and its importance for the in vivo dissolution of lipophilic compounds. European Journal of Pharmaceutics and Biopharmaceutics. 2005;60(3):413-7.
240. Shi B, Shin YK, Hassanali AA, Singer SJ. DNA Binding to the Silica Surface. The Journal of Physical Chemistry B. 2015;119(34):11030-40.
241. Valle-Delgado J, Molina-Bolivar J, Galisteo-Gonzalez F, Galvez-Ruiz M, Feiler A, Rutland MW. Hydration forces between silica surfaces: Experimental data and predictions from different theories. The Journal of chemical physics. 2005;123(3):034708.
242. Dishon M, Zohar O, Sivan U. From Repulsion to Attraction and Back to Repulsion: The Effect of NaCl, KCl, and CsCl on the Force between Silica Surfaces in Aqueous Solution. Langmuir. 2009;25(5):2831-6.
243. Carey MC, Small DM. Micelle formation by bile salts: physical-chemical and thermodynamic considerations. Archives of Internal Medicine. 1972;130(4):506-27.
244. Dokoumetzidis A, Macheras P. A century of dissolution research: from Noyes and Whitney to the biopharmaceutics classification system. International journal of pharmaceutics. 2006;321(1-2):1-11.
245. Bevernage J, Hens B, Brouwers J, Tack J, Annaert P, Augustijns P. Supersaturation in human gastric fluids. European Journal of Pharmaceutics and Biopharmaceutics. 2012;81(1):184-9.
246. Rabe M, Verdes D, Seeger S. Understanding protein adsorption phenomena at solid surfaces. Advances in Colloid and Interface Science. 2011;162(1):87-106.
247. Bremer MGEG, Duval J, Norde W, Lyklema J. Electrostatic interactions between immunoglobulin (IgG) molecules and a charged sorbent. Colloids and Surfaces A: Physicochemical and Engineering Aspects. 2004;250(1):29-42.
248. Demaneche S, Chapel JP, Monrozier LJ, Quiquampoix H. Dissimilar pH-dependent adsorption features of bovine serum albumin and alpha-chymotrypsin on mica probed by AFM. Colloids and surfaces B, Biointerfaces. 2009;70(2):226-31.
249. Van Speybroeck M, Barillaro V, Do Thi T, Mellaerts R, Martens J, Van Humbeeck J, et al. Ordered mesoporous silica material SBA-15: a broad-spectrum formulation platform for poorly soluble drugs. Journal of pharmaceutical sciences. 2009;98(8):2648-58.
250. Charnay C, Bégu S, Tourné-Péteilh C, Nicole L, Lerner D, Devoisselle J-M. Inclusion of ibuprofen in mesoporous templated silica: drug loading and release property. European Journal of Pharmaceutics and Biopharmaceutics. 2004;57(3):533-40.
251. Tang S, Huang X, Chen X, Zheng N. Hollow Mesoporous Zirconia Nanocapsules for Drug Delivery. Advanced Functional Materials. 2010;20(15):2442-7.
252. Yang P, Gai S, Lin J. Functionalized mesoporous silica materials for controlled drug delivery. Chemical Society Reviews. 2012;41(9):3679-98.
253. Vallet-Regí M, Balas F, Arcos D. Mesoporous Materials for Drug Delivery. Angewandte Chemie International Edition. 2007;46(40):7548-58.
254. Rosenholm JM, Lindén M. Towards establishing structure–activity relationships for mesoporous silica in drug delivery applications. Journal of Controlled Release. 2008;128(2):157-64.
255. Wang J, Somasundaran P. Adsorption and conformation of carboxymethyl cellulose at solid–liquid interfaces using spectroscopic, AFM and allied techniques. Journal of Colloid and Interface Science. 2005;291(1):75-83.
256. Ilevbare GA, Liu H, Edgar KJ, Taylor LS. Impact of Polymers on Crystal Growth Rate of Structurally Diverse Compounds from Aqueous Solution. Molecular Pharmaceutics. 2013;10(6):2381-93.
257. Mellaerts R, Mols R, Kayaert P, Annaert P, Van Humbeeck J, Van den Mooter G, et al. Ordered mesoporous silica induces pH-independent supersaturation of the basic low

solubility compound itraconazole resulting in enhanced transepithelial transport. International journal of pharmaceutics. 2008;357(1-2):169-79.
258. Van Speybroeck M, Mellaerts R, Mols R, Do Thi T, Martens JA, Van Humbeeck J, et al. Enhanced absorption of the poorly soluble drug fenofibrate by tuning its release rate from ordered mesoporous silica. European Journal of Pharmaceutical Sciences. 2010;41(5):623-30.
259. Lainé A-L, Price D, Davis J, Roberts D, Hudson R, Back K, et al. Enhanced oral delivery of celecoxib via the development of a supersaturable amorphous formulation utilising mesoporous silica and co-loaded HPMCAS. International journal of pharmaceutics. 2016;512(1):118-25.
260. Maleki A, Kettiger H, Schoubben A, Rosenholm JM, Ambrogi V, Hamidi M. Mesoporous silica materials: From physico-chemical properties to enhanced dissolution of poorly water-soluble drugs. Journal of Controlled Release. 2017;262:329-47.
261. Almeida e Sousa L, Reutzel-Edens SM, Stephenson GA, Taylor LS. Assessment of the Amorphous "Solubility" of a Group of Diverse Drugs Using New Experimental and Theoretical Approaches. Molecular Pharmaceutics. 2015;12(2):484-95.
262. Taylor LS, Zhang GGZ. Physical chemistry of supersaturated solutions and implications for oral absorption. Advanced Drug Delivery Reviews. 2016;101:122-42.
263. Mosquera-Giraldo LI, Taylor LS. Glass–liquid phase separation in highly supersaturated aqueous solutions of telaprevir. Molecular pharmaceutics. 2015;12(2):496-503.
264. Jackson MJ, Kestur US, Hussain MA, Taylor LS. Dissolution of danazol amorphous solid dispersions: supersaturation and phase behavior as a function of drug loading and polymer type. Molecular pharmaceutics. 2015;13(1):223-31.
265. Ilevbare GA, Liu H, Pereira J, Edgar KJ, Taylor LS. Influence of Additives on the Properties of Nanodroplets Formed in Highly Supersaturated Aqueous Solutions of Ritonavir. Molecular Pharmaceutics. 2013;10(9):3392-403.
266. Alonzo DE, Gao Y, Zhou D, Mo H, Zhang GG, Taylor LS. Dissolution and precipitation behavior of amorphous solid dispersions. Journal of pharmaceutical sciences. 2011;100(8):3316-31.
267. Tung H-H, Paul EL, Midler M, McCauley JA. Crystallization of organic compounds: an industrial perspective: John Wiley & Sons; 2009.
268. Trasi NS, Purohit HS, Wen H, Sun DD, Taylor LS. Non-sink dissolution behavior and solubility limit of commercial tacrolimus amorphous formulations. Journal of pharmaceutical sciences. 2017;106(1):264-72.
269. Xie T, Taylor LS. Dissolution performance of high drug loading celecoxib amorphous solid dispersions formulated with polymer combinations. Pharmaceutical research. 2016;33(3):739-50.
270. Raina SA, Alonzo DE, Zhang GG, Gao Y, Taylor LS. Using environment-sensitive fluorescent probes to characterize liquid-liquid phase separation in supersaturated solutions of poorly water soluble compounds. Pharmaceutical research. 2015;32(11):3660-73.
271. Que C, Gao Y, Raina SA, Zhang GG, Taylor LS. Paclitaxel Crystal Seeds with Different Intrinsic Properties and Their Impact on Dissolution of Paclitaxel-HPMCAS Amorphous Solid Dispersions. Crystal Growth & Design. 2018;18(3):1548-59.
272. Dening TJ, Taylor LS. Supersaturation Potential of Ordered Mesoporous Silica Delivery Systems. Part 1: Dissolution Performance and Drug Membrane Transport Rates. Molecular Pharmaceutics. 2018;15(8):3489-501.
273. Hillerström A, Andersson M, Samuelsson J, van Stam J. Solvent strategies for loading and release in mesoporous silica. Colloid and Interface Science Communications. 2014;3:5-8.

274. Waranusantigul P, Pokethitiyook P, Kruatrachue M, Upatham ES. Kinetics of basic dye (methylene blue) biosorption by giant duckweed (Spirodela polyrrhiza). Environmental Pollution. 2003;125(3):385-92.
275. Liu Y. Some consideration on the Langmuir isotherm equation. Colloids and Surfaces A: Physicochemical and Engineering Aspects. 2006;274(1):34-6.
276. Jain AK, Gupta VK, Bhatnagar A, Suhas. Utilization of industrial waste products as adsorbents for the removal of dyes. Journal of Hazardous Materials. 2003;101(1):31-42.
277. Chen SG, Yang RT. Theoretical Basis for the Potential Theory Adsorption Isotherms. The Dubinin-Radushkevich and Dubinin-Astakhov Equations. Langmuir. 1994;10(11):4244-9.
278. Kanô F, Abe I, Kamaya H, Ueda I. Fractal model for adsorption on activated carbon surfaces: Langmuir and Freundlich adsorption. Surface Science. 2000;467(1):131-8.
279. Trask AV, Shan N, Jones W, Motherwell WS. Indomethacin methyl ester. Acta Crystallographica Section E: Structure Reports Online. 2004;60(4):o508-o9.
280. McIlvaine T. A buffer solution for colorimetric comparison. Journal of Biological Chemistry. 1921;49(1):183-6.
281. Hobza P, Sauer J, Morgeneyer C, Hurych J, Zahradnik R. Bonding ability of surface sites on silica and their effect on hydrogen bonds. A quantum-chemical and statistical thermodynamic treatment. The Journal of Physical Chemistry. 1981;85(26):4061-7.
282. Nash T, Allison A, Harington J. Physico-chemical properties of silica in relation to its toxicity. Nature. 1966;210(5033):259.
283. Sahai N, Rosso KM. Chapter 13 - Computational Molecular Basis for Improved Silica Surface Complexation Models. In: Lützenkirchen J, editor. Interface Science and Technology. 11: Elsevier; 2006. p. 359-96.
284. Winnik FM, Winnik MA, Tazuke S. Interaction of hydroxypropylcellulose with aqueous surfactants: fluorescence probe studies and a look at pyrene-labeled polymer. The Journal of Physical Chemistry. 1987;91(3):594-7.
285. Kalyanasundaram K, Thomas JK. Environmental effects on vibronic band intensities in pyrene monomer fluorescence and their application in studies of micellar systems. Journal of the American Chemical Society. 1977;99(7):2039-44.
286. Goddard ED, Turro NJ, Kuo PL, Ananthapadmanabhan KP. Fluorescence probes for critical micelle concentration determination. Langmuir. 1985;1(3):352-5.
287. Ilevbare GA, Taylor LS. Liquid–Liquid Phase Separation in Highly Supersaturated Aqueous Solutions of Poorly Water-Soluble Drugs: Implications for Solubility Enhancing Formulations. Crystal Growth & Design. 2013;13(4):1497-509.
288. Mellaerts R, Jammaer JA, Van Speybroeck M, Chen H, Humbeeck JV, Augustijns P, et al. Physical state of poorly water soluble therapeutic molecules loaded into SBA-15 ordered mesoporous silica carriers: a case study with itraconazole and ibuprofen. Langmuir. 2008;24(16):8651-9.
289. Yoshioka M, Hancock BC, Zografi G. Crystallization of indomethacin from the amorphous state below and above its glass transition temperature. Journal of pharmaceutical sciences. 1994;83(12):1700-5.
290. Součková M, Klomfar J, Pátek J. Measurement and Correlation of the Surface Tension−Temperature Relation for Methanol. Journal of Chemical & Engineering Data. 2008;53(9):2233-6.
291. Nawrocki J. Silica surface controversies, strong adsorption sites, their blockage and removal. Part I. Chromatographia. 1991;31(3):177-92.
292. Dijkstra TW, Duchateau R, van Santen RA, Meetsma A, Yap GPA. Silsesquioxane Models for Geminal Silica Surface Silanol Sites. A Spectroscopic Investigation of Different Types of Silanols. Journal of the American Chemical Society. 2002;124(33):9856-64.
293. Delle Piane M, Corno M, Ugliengo P. Chapter 9 - Ab Initio Modeling of Hydrogen Bond Interaction at Silica Surfaces With Focus on Silica/Drugs Systems. In: Catlow CRA, Van

Speybroeck V, van Santen RA, editors. Modelling and Simulation in the Science of Micro- and Meso-Porous Materials: Elsevier; 2018. p. 297-328.
294. Nawrocki J. The silanol group and its role in liquid chromatography. Journal of Chromatography A. 1997;779(1):29-71.
295. Mellaerts R, Fayad EJ, Van den Mooter G, Augustijns P, Rivallan M, Thibault-Starzyk F, et al. In Situ FT-IR Investigation of Etravirine Speciation in Pores of SBA-15 Ordered Mesoporous Silica Material upon Contact with Water. Molecular Pharmaceutics. 2013;10(2):567-73.
296. Ambrogi V, Perioli L, Marmottini F, Accorsi O, Pagano C, Ricci M, et al. Role of mesoporous silicates on carbamazepine dissolution rate enhancement. Microporous Mesoporous Mater. 2008;113(1):445-52.
297. Van Speybroeck M, Barillaro V, Thi TD, Mellaerts R, Martens J, Van Humbeeck J, et al. Ordered mesoporous silica material SBA-15: A broad-spectrum formulation platform for poorly soluble drugs. J Pharm Sci. 2009;98(8):2648-58.
298. Martin YC. Exploring QSAR: Hydrophobic, Electronic, and Steric Constants C. Hansch, A. Leo, and D. Hoekman. American Chemical Society, Washington, DC. 1995. Xix + 348 pp. 22 × 28.5 cm. Exploring QSAR: Fundamentals and Applications in Chemistry and Biology. C. Hansch and A. Leo. American Chemical Society, Washington, DC. 1995. Xvii + 557 pp. 18.5 × 26 cm. ISBN 0-8412-2993-7 (set). $99.95 (set). Journal of Medicinal Chemistry. 1996;39(5):1189-90.
299. Ahern RJ, Hanrahan JP, Tobin JM, Ryan KB, Crean AM. Comparison of fenofibrate–mesoporous silica drug-loading processes for enhanced drug delivery. European Journal of Pharmaceutical Sciences. 2013;50(3-4):400-9.
300. Pillai C. Textbook of Organic Chemistry: Universities Press; 2012.
301. Nokhodchi A, Javadzadeh Y, Siahi-Shadbad MR, Barzegar-Jalali M. The effect of type and concentration of vehicles on the dissolution rate of a poorly soluble drug (indomethacin) from liquisolid compacts. J Pharm Pharm Sci. 2005;8(1):18-25.
302. Rouquerol J, Rouquerol F, Llewellyn P, Maurin G, Sing KS. Adsorption by powders and porous solids: principles, methodology and applications: Academic press; 2013.
303. Hansen RS, Craig RP. The adsorption of aliphatic alcohols and acids from aqueous solutions by non-porous carbons. The Journal of Physical Chemistry. 1954;58(3):211-5.
304. Wurster DE, Alkhamis KA, Matheson LE. Prediction of the adsorption of diazepam by activated carbon in aqueous media. Journal of pharmaceutical sciences. 2003;92(10):2008-16.
305. Perng C-Y, Kearney AS, Palepu NR, Smith BR, Azzarano LM. Assessment of oral bioavailability enhancing approaches for SB-247083 using flow-through cell dissolution testing as one of the screens. International Journal of Pharmaceutics. 2003;250(1):147-56.
306. Junghanns J-UA, Müller RH. Nanocrystal technology, drug delivery and clinical applications. International journal of nanomedicine. 2008;3(3):295.
307. Jantratid E, De Maio V, Ronda E, Mattavelli V, Vertzoni M, Dressman JB. Application of biorelevant dissolution tests to the prediction of in vivo performance of diclofenac sodium from an oral modified-release pellet dosage form. European Journal of Pharmaceutical Sciences. 2009;37(3–4):434-41.
308. Juenemann D, Jantratid E, Wagner C, Reppas C, Vertzoni M, Dressman JB. Biorelevant in vitro dissolution testing of products containing micronized or nanosized fenofibrate with a view to predicting plasma profiles. European journal of pharmaceutics and biopharmaceutics : official journal of Arbeitsgemeinschaft fur Pharmazeutische Verfahrenstechnik eV. 2011;77(2):257-64.
309. O'Shea JP, Faisal W, Ruane-O'Hora T, Devine KJ, Kostewicz ES, O'Driscoll CM, et al. Lipidic dispersion to reduce food dependent oral bioavailability of fenofibrate: In vitro, in

vivo and in silico assessments. European Journal of Pharmaceutics and Biopharmaceutics. 2015;96:207-16.
310. Griffin BT, Kuentz M, Vertzoni M, Kostewicz ES, Fei Y, Faisal W, et al. Comparison of in vitro tests at various levels of complexity for the prediction of in vivo performance of lipid-based formulations: case studies with fenofibrate. European Journal of Pharmaceutics and Biopharmaceutics. 2014;86(3):427-37.
311. Faisal W, Ruane-O'Hora T, O'Driscoll CM, Griffin BT. A novel lipid-based solid dispersion for enhancing oral bioavailability of Lycopene – In vivo evaluation using a pig model. International Journal of Pharmaceutics. 2013;453(2):307-14.
312. FDA Guidance for Industry Extended Release Oral Dosage Forms: Development, Evaluation, and Application of In Vitro/In vivo Correlations (1997).
313. Vallet-Regí M, Balas F, Arcos D. Mesoporous materials for drug delivery. Angewandte Chemie International Edition. 2007;46(40):7548-58.
314. Granero GE, Ramachandran C, Amidon GL. Dissolution and solubility behavior of fenofibrate in sodium lauryl sulfate solutions. Drug development and industrial pharmacy. 2005;31(9):917-22.
315. Jamzad S, Fassihi R. Role of surfactant and pH on dissolution properties of fenofibrate and glipizide—a technical note. Aaps Pharmscitech. 2006;7(2):E17-E22.
316. Hirtz J. The gastrointestinal absorption of drugs in man: a review of current concepts and methods of investigation. British journal of clinical pharmacology. 1985;19(S2):77S-83S.
317. Riegelman S, Loo J, Rowland M. Shortcomings in pharmacokinetic analysis by conceiving the body to exhibit properties of a single compartment. Journal of pharmaceutical sciences. 1968;57(1):117-23.
318. Loo J, Riegelman S. New method for calculating the intrinsic absorption rate of drugs. Journal of pharmaceutical sciences. 1968;57(6):918-28.
319. McCarthy LG, Kosiol C, Healy AM, Bradley G, Sexton JC, Corrigan OI. Simulating the hydrodynamic conditions in the united states pharmacopeia paddle dissolution apparatus. AAPS PharmSciTech. 2003;4(2):83-98.
320. Baxter JL, Kukura J, Muzzio FJ. Hydrodynamics-induced variability in the USP apparatus II dissolution test. International Journal of Pharmaceutics. 2005;292(1–2):17-28.
321. D'Arcy DM, Corrigan OI, Healy AM. Hydrodynamic simulation (computational fluid dynamics) of asymmetrically positioned tablets in the paddle dissolution apparatus: impact on dissolution rate and variability. Journal of Pharmacy and Pharmacology. 2005;57(10):1243-50.
322. Kostewicz ES, Wunderlich M, Brauns U, Becker R, Bock T, Dressman JB. Predicting the precipitation of poorly soluble weak bases upon entry in the small intestine. Journal of Pharmacy and Pharmacology. 2004;56(1):43-51.
323. Carlert S, Pålsson A, Hanisch G, von Corswant C, Nilsson C, Lindfors L, et al. Predicting Intestinal Precipitation—A Case Example for a Basic BCS Class II Drug. Pharmaceutical Research. 2010;27(10):2119-30.
324. Hens B, Brouwers J, Corsetti M, Augustijns P. Supersaturation and precipitation of posaconazole upon entry in the upper small intestine in humans. Journal of pharmaceutical sciences. 2016.
325. Psachoulias D, Vertzoni M, Goumas K, Kalioras V, Beato S, Butler J, et al. Precipitation in and Supersaturation of Contents of the Upper Small Intestine After Administration of Two Weak Bases to Fasted Adults. Pharmaceutical Research. 2011;28(12):3145-58.
326. Butler JM, Dressman JB. The developability classification system: application of biopharmaceutics concepts to formulation development. Journal of pharmaceutical sciences. 2010;99(12):4940-54.

327. Custodio JM, Wu C-Y, Benet LZ. Predicting drug disposition, absorption/elimination/transporter interplay and the role of food on drug absorption. Advanced drug delivery reviews. 2008;60(6):717-33.
328. Fei Y, Kostewicz ES, Sheu M-T, Dressman JB. Analysis of the enhanced oral bioavailability of fenofibrate lipid formulations in fasted humans using an in vitro–in silico–in vivo approach. European Journal of Pharmaceutics and Biopharmaceutics. 2013;85(3, Part B):1274-84.
329. Sauron R, Wilkins M, Jessent V, Dubois A, Maillot C, Weil A. Absence of a food effect with a 145 mg nanoparticle fenofibrate tablet formulation. International Journal of Clinical Pharmacology & Therapeutics. 2006;44(2).
330. Wang Y, Cui Y, Zhao Y, Zhao Q, He B, Zhang Q, et al. Effects of surface modification and size on oral drug delivery of mesoporous silica formulation. Journal of colloid and interface science. 2018;513:736-47.
331. Biswas N. Modified mesoporous silica nanoparticles for enhancing oral bioavailability and antihypertensive activity of poorly water soluble valsartan. European Journal of Pharmaceutical Sciences. 2017;99:152-60.
332. Sun W-J, Aburub A, Sun CC. A mesoporous silica based platform to enable tablet formulations of low dose drugs by direct compression. International journal of pharmaceutics. 2018;539(1):184-9.
333. Mellaerts R, Mols R, Jammaer JAG, Aerts CA, Annaert P, Van Humbeeck J, et al. Increasing the oral bioavailability of the poorly water soluble drug itraconazole with ordered mesoporous silica. European Journal of Pharmaceutics and Biopharmaceutics. 2008;69(1):223-30.
334. Vialpando M, Backhuijs F, Martens JA, Van den Mooter G. Risk assessment of premature drug release during wet granulation of ordered mesoporous silica loaded with poorly soluble compounds itraconazole, fenofibrate, naproxen, and ibuprofen. European Journal of Pharmaceutics and Biopharmaceutics. 2012;81(1):190-8.
335. Oh JY, Kim HS, Palanikumar L, Go EM, Jana B, Park SA, et al. Cloaking nanoparticles with protein corona shield for targeted drug delivery. Nature communications. 2018;9(1):4548.
336. Angioletti-Uberti S, Ballauff M, Dzubiella J. Competitive adsorption of multiple proteins to nanoparticles: the Vroman effect revisited. Molecular Physics. 2018:1-10.
337. Zhang H, Wu T, Yu W, Ruan S, He Q, Gao H. Ligand Size and Conformation Affect the Behavior of Nanoparticles Coated with in Vitro and in Vivo Protein Corona. ACS applied materials & interfaces. 2018;10(10):9094-103.
338. Lee YK, Choi E-J, Webster TJ, Kim S-H, Khang D. Effect of the protein corona on nanoparticles for modulating cytotoxicity and immunotoxicity. International journal of nanomedicine. 2015;10:97.
339. Corbo C, Molinaro R, Parodi A, Toledano Furman NE, Salvatore F, Tasciotti E. The impact of nanoparticle protein corona on cytotoxicity, immunotoxicity and target drug delivery. Nanomedicine. 2016;11(1):81-100.